A story of recombination

Lettier, Gaëlle

Publication date:
2007

Document Version
Publisher's PDF, also known as Version of record

A story of Recombination

PhD thesis by Gaëlle Lettier
March 2007

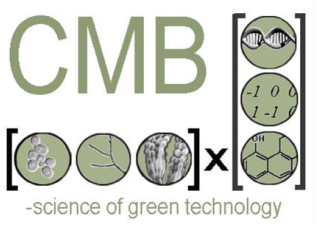

Center for Microbial Biotechnology
BioCentrum-DTU
Technical University of Denmark
DK-2800 Kgs. Lyngby
Denmark

This thesis is typeset in LaTeX.

Acknowledgements

This thesis describes the results obtained during my PhD project carried out at the Center for Microbial Biotechnology (CMB), BioCentrum, at the Technical University of Denmark (DTU). This project was supported by a grant co-financed by DTU, FOBI (Forskerskole for Bioteknologi) and IVC (Ingeniør-Videnskabelige Centre) and for this I am grateful.

I would like to thank my supervisor, Associate Professor Uffe H. Mortensen, for his support, his guidance and his help during this project. His enthusiasm and his passion for the field of DNA repair has made my PhD project an exciting and unforgettable experience. Moreover, I thank him for teaching me all that I know about yeast, for the many hours of good scientific discussions and for spending time on proof-reading this thesis.

Many thanks also go to the members of the DNA repair group for many lively discussion during our weekly group meetings, for always helping out in the lab and for the many good times outside the lab! More than just excellent colleagues, they have also become really good friends. Very special thanks go to postdoc Michael L. Nielsen and PhD student Jakob B. Nielsen for introducing me to the magical world of filamentous fungi, for fruitful collaborations and for the hours they spent on proof-reading this thesis. It has been a great pleasure to work with you both. Special thanks also go to lab technician Lene Christensen for all the excellent help she provided with lab work, specially in the last stressing months of this project, and for the many kilometers we ran together! I also thank my office mates, Iben, Kiran, Jakob and Line for making each day at work much more fun!

I would also like to thank all the students that I have had the pleasure of supervising during this project. Svetlana, Halfdan, Louise, Lara, Els and Lene, the results of this project would never be what they are if it was not for all the efforts that you have put in your work and for that I am extremely grateful.

Very special thanks go to my colleague and friend, PhD student Mikael Rørdam, for his support during this project and for his patience while helping me to understand the mysteries of LateX.

Of course, I would like to thank all my former and present colleagues at CMB for making this center the dynamic work place that it is. Thank you to all the technical and administrative staff for always being available and very helpful.

I thank friends and family for supporting me during this project.

Mum, dad, thanks for living on paradise island, i really appreciated the vacation! Special thanks go to my Danish family who have made Denmark to the place I now call "home-sweet-home".

Finally, I would like to thank Christoffer for his incredible support throughout this whole project. Thank you for your delicious cooking, your permanent good mood and most of all for always being there for me during the hard times.

Gaëlle Lettier
March 2007
Kgs. Lyngby, Denmark

Summary

Homologous recombination (HR) is involved in several important biological processes, e.g. generation of genetic diversity, DNA repair and maintenance of genomic stability. Most of our knowledge of this process comes from studies in meiotic cells where HR occurs at high rates, triggered by the programmed formation of many DNA double-strand breaks (DSBs). Less studied is its mitotic counterpart which, although rare, can lead to severe health threatening events such as genomic instability and loss of heterozygosity, two of the many factors that are believed to be involved in tumorigenesis. Furthermore, mitotic HR is the mechanism that permits gene targeting, a process that allows precise site-directed genome modifications to be made in organisms of interest. For these reasons, obtaining a full understanding of the molecular events behind spontaneous mitotic HR is of interest at a scientific, medical and industrial level.

By analogy to meiotic HR, it is commonly believed that spontaneous mitotic HR arises from the repair of DNA DSBs, which accidentally occur during mitotic growth. However, this remains purely speculative and the nature of the lesion(s) triggering mitotic HR remains unknown. In the yeast, *Saccharomyces cerevisiae*, Rad52 is a key protein involved in DNA double strand break (DSB) repair and homologous recombination (HR), making it a good candidate to study these processes in details. In 2002, we have identified a group of *rad52* mutant strains (class C mutants), which are unable to repair DNA DSBs, but are proficient for mitotic HR. This paradox suggests that DNA lesions, different from DSBs, trigger most spontaneous HR in mitotic yeast cells. Chapter 4 of this thesis presents a detailed characterization of the separation-of-function phenotype of these *rad52* mutants. Using these mutants as a diagnostic tool, we provide the first direct evidence that most spontaneous mitotic HR in *S. cerevisiae* is initiated by DNA lesions other than DNA DSBs such as DNA nicks and single-stranded gaps.

The fact that the functions of Rad52 in DNA DSB repair and HR can be separated in the *rad52* class C mutants suggests that this protein may play different roles in these processes. For this reason, understanding why these mutants are unable to repair DNA DSBs will shed light not only on the mechanisms of mitotic HR but also on the different functions of the Rad52 protein. In Chapter 5 of this thesis, further analyses of the *rad52* class C mutants are presented. Because the *rad52* class C mutations are situated in the putative DNA binding groove of Rad52, we speculate that DNA binding/annealing activity of Rad52 is

impaired in these mutants. In this study, we show that efficient DNA binding through the Rad52 N-terminal binding domain does not seem to be required for the re-localization of Rad52 to sites of DNA damage, for the recruitment of the RecA homolog, Rad51, to these sites and for strand invasion. Based on these results, we suggest that, due to its inability to bind/anneal DNA, the class C Rad52 mutant protein is unable to promote second strand capture, thus proposing an essential role for DNA binding by Rad52 in this step. Moreover, we show that deletion of the gene encoding the Srs2 helicase suppresses the *rad52* class C mutants' sensitivity to DNA damaging agents. Based on these results, we propose a model where Rad52 and Srs2 antagonize each other during the second strand capture step of the DNA DSB repair process.

As mentioned above, mitotic HR is the process allowing gene targeting. In higher eukaryotes, this process is highly ineffective as the main DSB repair pathway is non-homologous end-joining (NHEJ). This is a problem as it poses limitations on the gene targeting possibilities in mouse and plants and for its use in human gene therapy. Other organisms where the predominance of NHEJ hinders gene targeting are filamentous fungi, among which many industrially relevant species are found. For these reasons, the development of new strategies to increase gene targeting in these organisms has both medical and industrial relevance. After a short introduction of the filamentous fungi *Aspergillus nidulans*, Chapter 6 of this thesis describes an efficient gene targeting method developed in this organism. As a proof-of-concept of this method, a deletion strain of the *Aspergillus nidulans radC*, a homolog of the *S. cerevisiae* DSB repair gene RAD52, was created.

Studies of Rad52 in higher eukaryotes have shown that the importance of this protein seems to have decreased from yeast to human, most likely because additional repair pathways have evolved. To investigate the role of Rad52 in filamentous fungi and understand how the role of this protein has changed with time, we performed an initial characterization of a deletion strain of the *A. nidulans radC*, a homolog of the *S. cerevisiae* DSB repair gene *RAD52*. This study is presented in Chapter 7 of this thesis. Interestingly, the phenotype of this deletion strain appears to be intermediate between that of yeast and that of human cells and we propose that *A. nidulans* may serve as an interesting model system to investigate how new repair pathways have developed in higher eukaryotes.

Dansk sammenfatning

Homolog rekombination (HR) indgår i adskillige væsentlige biologiske processer og bidrager både til at vedligeholde en celles arvemateriale og til udvikling af en arts genetiske diversitet. Det meste af vores viden om denne reparationsproces stammer fra studie lavet i meiotiske celler hvor HR sker tit, udløst af den programmerede dannelse af mange DNA dobbeltstrengsbrud (DSB). Undersøgt i mindre grad er dens mitoiske modvægt, som sker mere sjældent, men kan føre til hændelser med alvorlig helbredstrussel, fx i form af genomisk ustabilitet og tab af heterozygositet, to af mange faktorer som tilskrives at indgå i tumordannelse. Yderligere er mitotisk HR den mekanisme der tillader "gene targeting", en proces som tillader at man kan lave specifikke ændringer i udvalgte organismes DNA. Af disse årsager er det på et forskningsmæssigt, medicinsk såvel som industrielt niveau væsentligt at opnå fuld indsigt i de molekylære hændelser der ligger til grund for spontan mitotisk HR.

Ved at analogisere udefra meiotisk HR, er det den almindelige opfattelse at spontan mitotisk HR initieres af DNA DSB, som optræder tilfældigt under mitotisk vækst. Denne synsvinkel er dog rent spekulativ - og selve karakteren af de(n) læsion(er) der udløser mitotisk HR er fortsat ukendt. I gærarten, *Saccharomyces cerevisiae*, er Rad52 et centralt protein involveret i reparation af DNA DSB og i HR, som gør proteinet til en velegnet kandidat til studiet af disse processer i detaljer. Vi har i 2002, identificeret en gruppe *rad52* mutanter (klasse C mutanter) som ikke er i stand til at reparere DNA DSB, men kan udføre mitotisk HR på samme niveau som vildtypen. Denne paradoks indikerer at DNA læsioner, ikke at forveksle med DSBs, er de hyppigste udløsere af spontan HR i mitotiske gærceller. Kapitel 4 i nærværende afhandling, giver en detaljeret karakterisering af "separation-of-function" phenotypen af *rad52* mutanterne. Under anvendelse af disse mutanter som et diagnostisk værktøj fremfører vi den første direkte evidens for at hyppigste spontane mitotiske HR i *S. cerevisiae* initieres ved andre DNA læsioner end DNA DSBs, fx i form af DNA enkeltstrengsbrud og enkeltstrenget DNA spalter. Det faktum at betydningen af Rad52 i DNA DSB reparation og HR kan isoleres i *rad52* klasse C mutanterne, kunne indikere at dette protein kunne spille forskellige roller i disse processer. På grund af dette, vil erkendelsen af, at disse mutanter ikke er i stand til at reparere DNA DSBs, kunne kaste lys over ikke bare de mitotiske HR mekanismer, men også Rad52 proteinets forskellige egenskaber. I kapitel 5 i nærværende afhandling findes yderligere analyse af *rad52* klasse

C mutanterne. Idet *rad52* klasse C mutationerne er lokaliseret i den forventede Rad52 DNA bindningsdomæne, overvejer vi om denne lokalisation er grunden til den manglende Rad52 bindning/annealing aktivitet i disse mutanter. I dette studie demonstreres, at den effektive DNA bindning via Rad52 N-terminal bindningsdomæne hverken forekommer nødvendig for relokalisering af Rad52 til områder med DNA skade, eller for tiltrækningen af RecA homologen Rad51 til disse områder eller for "strand invasion". Baseret på disse resultater, antyder vi - på grund af klasse C Rad52 mutant proteins manglende evne til at binde/anneal DNA - at klasse C Rad52 mutant protein ikke er i stand til at fremme "second strand capture", og således antyde en væsentlig funktion for DNA bindningen med Rad52 i dette trin. Yderligere viser vi at deletion af genet der koder Srs2 helicasen undertrykker *rad52* klasse C mutanternes følsomhed overfor DNA beskadigende stoffer. Byggende på disse resultater, foreslår vi en model hvor Rad52 og Srs2 antagoniserer hinanden under "second strand capture" trinet af DNA DSB reparationsprocessen.

Som anført ovenfor er mitotisk HR en proces der tillader "gene targeting". I højere eukaryoter er denne proces meget ineffektiv, idet den væsentligste måde til reparation af DSB er non-homologous endjoining (NHEJ). Dette forhold indeholder et problem, idet det stiller begrænsninger for mulighederne for "gene targeting" hos mus og planter samt for dets anvendelighed i human gen terapi. Andre organismer hvor prædominansen af NHEJ er hindrende for gene targeting er skimmelsvampe, hvoriblandt mange industrielt relevante arter findes. Af disse årsager har udviklingen af nye metoder til at fremme gene targeting i disse organismer både en medicinsk og industriel relevans. Efter en kort introduktion af skimmelsvampen, Aspergillus nidulans, beskrives der i denne afhandlings kapitel 6 en effektiv "gene targeting" metode udviklet i denne organisme. Som et "proof of concept" på denne metodes holdbarhed udvikledes en stamme af *Aspergillus nidulans* hvor *radC* genet, en homolog til *S. cerevisiae* DSB reparationsgen *RAD52*, er deleteret.

Studier af Rad52 hos højere eukaryoter, har vist at vigtigheden af dette protein forekommer at være reduceret for humane i forhold til gærceller, formodentlig fordi nye reparationsmekanismer er opstået gennem evolution. For at undersøge Rad52's rolle i skimmelsvamp, og samtidig forstå hvordan betydningen af dette protein har skiftet med tiden, karakteriserede vi en deletion stamme af *A. nidulans radC* genet, en homolog til *S. cerevisiae* DSB reparationsgen *RAD52*. Dette studie beskrives i kapitel 7 i denne afhandling. Ret interessant viser det sig at denne stammes phenotype er en mellemting mellem den til gærcellen hørende og den til humane celler hørende. Vi foreslår at *A. nidulans* kunne tjene som interessant forsøgsmodel til videre undersøgelse af hvorledes nye reparationsmekanismer har udviklet sig hos højere eukaryoter.

Contents

List of Figures

List of Tables

Abbreviations

AP Apurinic/apyrimidinic

BER Base excision repair

BIR Break-induced replication

CPD Cyclobutane-pyrimidine dimer

CFP Cyan fluorescent protein

DNA Deoxyribonucleic acid

DSB Double-strand break

dsDNA Double-stranded DNA

GCR Gross chromosomal rearrangement

hDNA Heteroduplex DNA

HJ Holliday junction

HR Homologous recombination

IR Ionizing radiation

LOH Loss of heterozygosity

MMR Mismatch repair

MMS Methyl methanesulfonate

NER Nucleotide excision repair

NHEJ Non-homologous end-joining

RDR Recombination-dependent replication

RFP Red fluorescent protein

RNA Ribonucleic acid

RNS Reactive nitrogen species

ROS Reactive oxygen species

SDSA Synthesis-dependant strand annealing

SSA Single-strand annealing

SSB Single-strand break

ssDNA Single-stranded DNA

TLS Translesion synthesis

UV Ultraviolet

YFP Yellow fluorescent protein

Chapter 1

Introduction

1.1 Why study homologous recombination?

Homologous recombination (HR) occurs in all life forms where it is involved in several important biological processes. In meiotic cells, HR insures the correct pairing and segregation of homologous chromosomes in meiosis I, thus securing an orderly distribution of chromosomes through meiosis. In mitotic cells, HR is involved in the repair of DNA DSBs thereby assuring the maintenance of genomic stability. Failure to perform these functions is detrimental to any organism. In higher eukaryotes, a mistuning of this system is often accompanied by a high tendency to develop cancer, accelerated ageing or developmental abnormalities.

Ironically, although HR acts as a genomic caretaker, this process can contribute to tumorigenesis. Indeed, recombination between two heteroalleles can result in loss of heterozygosity (LOH), an event that can lead to tumorigenesis if the alleles in questions are tumor-suppressor genes. In general, cells that carry an inherited mutated allele of a tumor-suppressor gene also carry a non-mutated copy of this allele, thus the mutated allele has no effect. However, if HR converts the "healthy" allele into a mutated one, this may initiate a cascade of events that can lead to tumorigenesis. Accordingly, individuals that carry a germline mutation in a tumor-suppressor gene are predisposed to develop cancer. This is for example the case for individuals carrying a mutation in the *BRCA1* or *BRCA2* genes, who are predisposed to breast and ovarian cancer (for recent review see Jasin (2002)). Interestingly, results from several studies suggest a role of both *BRCA1* and *BRCA2* in DSB repair in mammalian cells (reviewed by Pierce et al. (2001). Defects in HR have also been shown to lead to severe genetic diseases. For example, Fanconi anaemia is believed to be due to a failure to repair DNA lesions such as interstrand DNA crosslinks that can stall replication forks. Accordingly cells from Fanconi anaemia patients are sensitive to DNA crosslinking agents and present chromosomal instability (reviewed by Kennedy & D'Andrea (2005)). Similar phenotypes are observed in cells from Bloom's syndrome patients, a disease believed to arise from mutations in the RecQ helicase, BLM, which is known to

participate in HR in mammalian cells (reviewed by (Hickson, 2003)). Because of their consequences on genome stability, these diseases are highly cancer-prone.

Another important aspect of HR is that it is the mechanism permitting gene targeting, a process by which modifications can be specifically introduced in the genome of an organism of choice. This process can be used as a tool in genetic engineering, thus has both industrial and medical applications. In organisms such as yeast and filamentous fungi, which are used for the production of many products relevant to man like antibiotics and enzymes, gene targeting can be used to create strains with improved production yields or even strains producing novel compounds of interest (for review see Timberlake & Marshall (1989)). Gene targeting in higher eukaryotes such as mice, can permit to create model systems of human diseases that can be essential in the development of drugs and treatments. Ultimately, gene targeting could permit gene therapy in humans (for review see Parekh-Olmedo et al. (2005)).

For these reasons, understanding the mechanisms underlying HR as well as the role of the different proteins involved in this process is of great scientific, medical and industrial importance. Fortunately, the mechanisms of HR are conserved from bacteria to human and many proteins involved in these processes have homologs in bacteria and lower eukaryotes such as yeast. These organisms have therefore been extensively used as model to study the mechanisms of HR and the roles of HR proteins in vivo. However, many aspects of this complex process remain to be understood.

1.2 Outline of the thesis

This thesis summarizes the work that was carried out during my PhD project and is divided in seven chapters. The first two chapters as well as the beginning of Chapter 6 present background information while the rest of the thesis describes results obtained in the form of original publications and manuscripts.

Chapter 2 introduces the reader to the different types and sources of DNA damage, their consequences and the different repair pathways that the cell has evolved to protect the integrity of its genome. In Chapter 3, the HR repair pathway is presented in details. Specifically, models of the mechanisms by which HR is believed to occur and the main proteins involved in this pathway are described.

The following chapters present the results obtained during this PhD project. Chapter 4 consists of the original version of the article "The Role of DNA double-strand breaks in spontaneous homologous recombination in *S. cerevisiae*" published in PLoS GENETICS in 2006, where the role of DNA DSBs as triggering lesions for mitotic HR is discussed. In Chapter 5, the role of an important HR protein in *S.cerevisiae*, Rad52, is investigated. Specifically, the question of the biological relevance of DNA binding/annealing through the N-terminal binding domain of Rad52 is discussed in the context of the DNA DSB repair

process. The results obtained in this study will be published soon and for this reason this chapter is written in manuscript form.

During this PhD project, the role of HR in filamentous fungi was also investigated. This was done using the model organism *Aspergillus nidulans* which is shortly presented at the beginning of Chapter 6. Later in this chapter, the relation between HR and gene targeting is described and the problematic of low gene targeting efficiency in higher eukaryotes is discussed. Lastly, the original version of the article "Efficient PCR-based gene targeting with a recyclable marker for *Aspergillus nidulans*" published in Fungal Genetics and Biology in 2006, concludes Chapter 6 with a description of the gene targeting method developed by our laboratory. Moreover, this article presents the construction of the deletion strain of the *A. nidulans radC*, a homolog of the *S. cerevisiae* DSB repair gene *RAD52*. An initial characterization of this strain is presented in Chapter 7 where the evolution of the role of Rad52 from yeast to human is also discussed. As the results obtained in this study will be published soon, this chapter is also written in manuscript form.

Chapter 2

DNA damage and repair

The aim of this chapter is to provide a general overview on how DNA damage can be handled by the cell. First, the different causes of DNA damage and their consequences for the cell are presented. Then, several mechanisms involved in DNA repair are described. In this section, the repair of DNA double-strand breaks by homologous recombination is purposely only briefly mentioned as it is described in detail in Chapter 3.

During their lifetime, all living organisms are constantly subjected to DNA damaging agents that create a large variety of DNA lesions in their genome. The nature of these damaging agents is diverse; some arise from the external environment, e.g. ultraviolet (UV) radiation, chemicals, toxins from other organisms, others are the results of the cell's own metabolism, e.g. oxygen radicals, errors of the DNA replication or proof-reading machineries, etc... Various types of DNA lesions are produced affecting the DNA bases and/or the DNA backbone (Figure 2.2). If left unrepaired these lesions can lead to mutations, genomic instability or even, in the case of DNA double-strand breaks (DSBs), be lethal. For these reasons, cells have evolved many complex mechanisms that continuously detect and repair DNA lesions thus dramatically reducing their harmful effects.

2.1 DNA damaging agents: types of damage and consequences

2.1.1 Exogenous sources of DNA damage

Solar UV radiations are one of the most common environment-related DNA damaging agents. Their effects on human health are various going from sunburns to skin cancer, the latter being the most diagnosed cancer world-wide today (Godar, 2005). The spectrum of ultraviolet light ranges from 100 to 400 nm and is divided into UV-A (320-400 nm), UV-B (280-320 nm) and UV-C (<280 nm).Only UV-A and UV-B reach the earth's surface, as UV-C is completely absorbed by the

atmosphere. UV-A indirectly forms DNA lesions by inducing the formation of reactive oxygen species (ROS). UV-B is directly absorbed by the DNA inducing mainly two types of lesions, cyclobutane-pyrimidine dimers (CPDs) (Figure 2.1) and 6-4 photoproducts (6-4PPs). Both types of lesions distort the DNA helix and inhibit the progression of the DNA and RNA polymerases thus interfering with replication and transcription (Sinha & Hader, 2002). Indeed, when the replication machinery collides these DNA adducts during S-phase, replication forks may stall and their reactivation by specialized restart pathways is crucial as it ensures that DNA replication is completed faithfully (Heller & Marians, 2006).

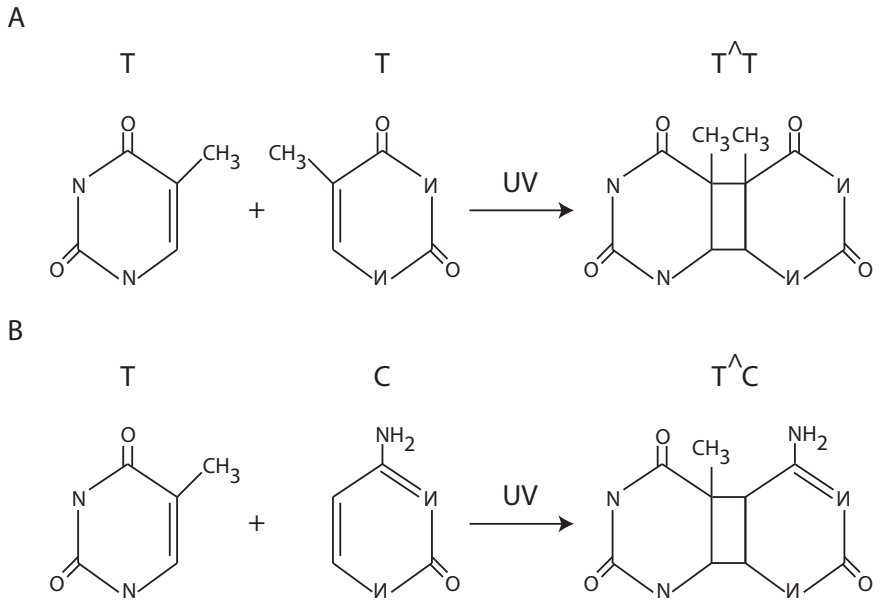

Figure 2.1. Formation of cyclobutane-pyrimidine dimers by UV irradiation. (A) Thymine(T)-thymine(T) cylcobutane-pyrimidine dimer and (B) thymine(T)-cytosine(C) dimer. Figure adapted from Sinha & Hader (2002).

Ionizing radiations such as gamma and x-rays produce many different DNA lesions including several types of base damage, single-stranded breaks (SSBs), DSBs, DNA-DNA and DNA-protein crosslinks (Ward, 2000; Jenner et al., 2001; Bjelland & Seeberg, 2003; Cadet et al., 2004). Based on the estimation that approximately 35-40 DSBs are induced by a dose of 1 Gy in a mammalian cell (Rothkamm & Lobrich, 2003), these lesions are believed to be the main cause of cell death after irradiation. Moreover, ionizing radiation also results in clusters of individual DNA lesions localized in 0-20 bp regions of the DNA that make simultaneous repair of these lesions a tedious task for the cell (Dianov et al., 2001). Indeed, the repair of closely located lesions or of lesions situated on opposite DNA strands will often lead to the formation of the life threatening DNA DSBs even though the original lesions were not necessarily deadly. When cells are irradiated, ionizations will also occur in the molecules surrounding the DNA. Irradiation of water, for example, will produce highly reactive hydroxyl radicals ($OH^{\bullet}$), which are known

to be the source of several types of DNA damage as discussed below (see Section 2.1.2).

Alkylating agents add alkyl groups to the DNA bases. As opposed to UV lesions, alkylated bases do not significantly alter the DNA helix conformation; however, they can lead to base mispairing and block DNA synthesis thus inducing cell death (Beranek, 1990; Kupiec, 2000). A widely used alkylating agent is methyl methanesulfonate (MMS) which forms heat-labile methylated DNA products such as 7-methylguanine (7MeG) and 3-methyladenine (3MeA) (Lundin et al., 2005). Crosslinking agents form intra-strand and inter-strand DNA crosslinks. These crosslinks can prevent the DNA strands from separating thus blocking DNA replication and eventually leading to cell death. Because of their high cell killing efficiency, both ionizing radiations as well as alkylating and crosslinking agents are widely used tools in cancer radio- and chemotherapy.

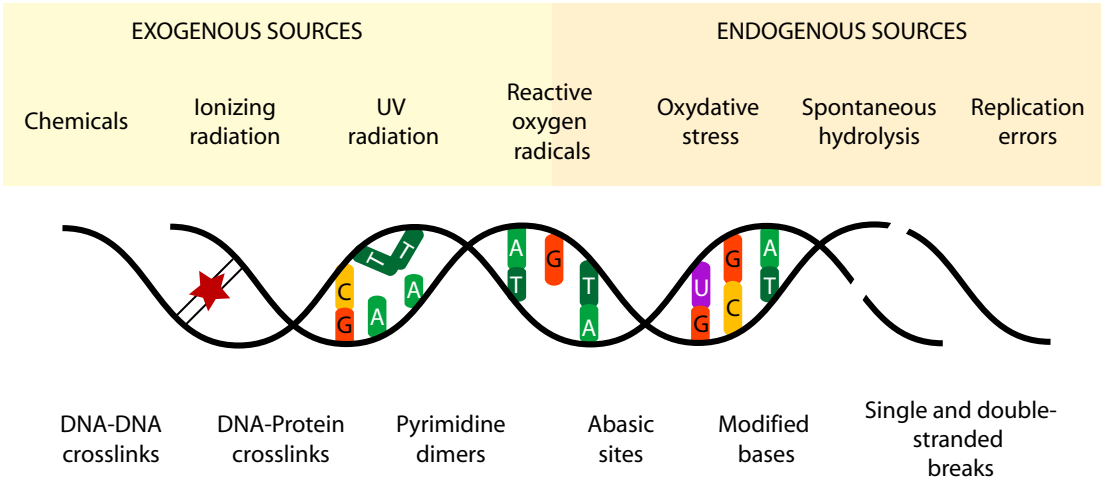

Figure 2.2. Different exogenous and endogenous sources of DNA damage and examples of their consequences at the level of DNA.

2.1.2 Endogenous sources of DNA damage

As described above, the environment is responsible for a great share of the damage inflicted to the DNA of living organisms. However, the cellular metabolism itself is also a major source of DNA damage and spontaneous decay of the cellular DNA is believed to be one of the main sources of mutagenesis, tumorigenesis and ageing (Lindahl, 1993; Slupphaug et al., 2003; Halliwell, 2007).

Oxidative stress resulting from the cellular oxidative metabolism is primarily due to reactive oxygen species (ROS) and reactive nitrogen species (RNS). For example, oxygen radicals such as superoxide ($O_2^{\bullet -}$), hydroxyl ($OH^{\bullet}$) and peroxyl ($RO_2^{\bullet}$) are common ROS while nitric oxide radical ($NO^{\bullet}$) and nitrogen dioxide radical ($NO_2^{\bullet}$), are some of the species under the term RNS. Amongst these, $OH^{\bullet}$ is the most "reactive" intermediate as it can act rapidly and directly on the DNA and

create several different products from all four DNA bases (reviewed by Halliwell (2007)). Both ROS and RNS are believed to contribute to the initiation of cancer as they induce severe alterations in the DNA such as base changes, strand breaks, rearrangements, deletions, etc... For example, conversion of guanine to 8-hydroxyguanine (8-OHG) is a common base lesion produced by ROS. This chemical modification changes the hydrogen bonding specificity of the DNA base causing 8-OHG to base-pair preferentially with adenine instead of cytosine thus eventually generating transversion mutations after replication (Kasai & Nishimura, 1984; Shibutani et al., 1991). Moreover, this lesion has been shown to alter the enzyme-catalyzed methylation of adjacent cytosines (Weitzman et al., 1994), a process otherwise known to be important for regulation of gene expression. Accordingly, ROS could be a source of altered methylation observed during carcinogenesis (Weitzman et al., 1994).

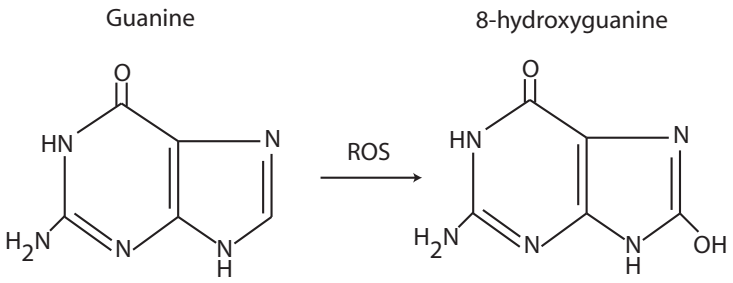

Figure 2.3. Conversion of guanine to 8-hydroxyguanine by reactive oxygen species (ROS).

Base modifications can occur when the relatively unstable primary amino groups of nucleic acid bases are converted to keto groups, transforming bases such as cytosine into uracil. As uracil is not a normal DNA base, this type of deamination reaction is easily detected and the uracil replaced by cytosine. However, deamination of 5-methylcytosine into thymine is not detected as an erroneous base thus eventually leading to the persistence of the mutation created if not repaired. This is believed to explain why CpG sites, which when methylated form 5-methylcytosine, are rare in eukaryotic genomes (Walsh & Xu, 2006).

Apurinic/apyrimidinic (AP) sites, also known as abasic sites, are a very common type of DNA lesion as they can occur spontaneously through the hydrolysis of the labile *N*-glycosylic bond linking DNA bases with deoxyribose. This phenomenon is considered to be frequent and has been suggested to be responsible for the loss of approximately 10^4 bases per day per mammalian cell (Lindahl & Nyberg, 1972). Interestingly, AP sites are also created when *N*-glycosylases remove damaged or inappropriate bases such as the ones formed by alkylating agents, deamination or ROS (Boiteux & Guillet, 2004). In addition to being mutagenic, AP sites can block DNA replication and transcription and are therefore potentially lethal lesions. Their removal by AP endonucleases or DNA N-glycosylases/AP lyases leads to the formation of SSBs

with 3' or 5' blocked ends. As these ends are inaccessible for further processing by polymerases or ligases, they remain unrepaired and are eventually converted to DNA DSBs by the replication machinery (Boiteux & Guillet, 2004).

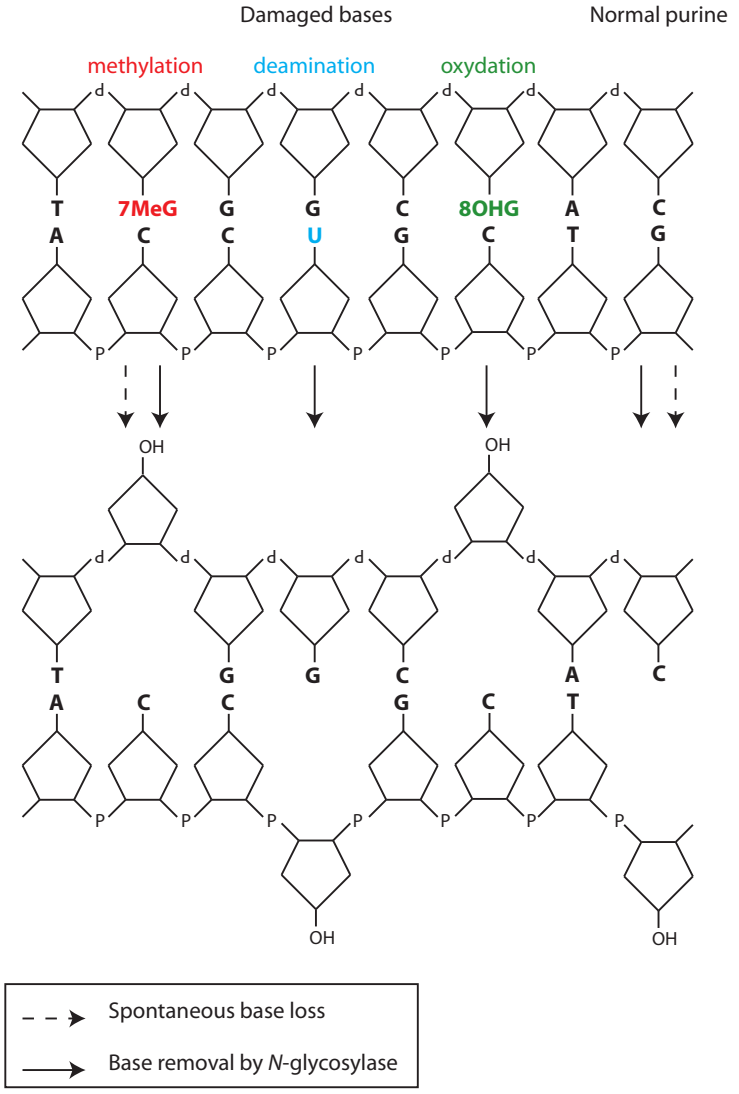

Figure 2.4. Origin of apurinic (AP) sites in DNA. AP sites are generated when normal purines or damaged bases are removed by the spontaneous hydrolysis of the *N*-glycosylic bond or by excision of normal purines, damaged or inappropriate bases by DNA *N*-glycosylases. 7MeG: 7-methylguanine, 8OHG: 8-hydroxyguanine. Figure adapted from Boiteux & Guillet (2004).

DNA replication itself is a source of DNA damage. The high-fidelity DNA polymerases in charge of accurately replicating the genome are not flawless and sometimes incorporate mismatches and induce small deletions or insertions. As mentioned above, active replication forks sometimes collide with unrepaired DNA damage which blocks their progression thus leading to stalled replication forks. Moreover, collapsed replication forks can occur when a SSB is converted to a DSB by replication. If not restarted or repaired, stalled and collapsed repli-

cation forks can be detrimental to the cell. Indeed, recent studies in yeast showed that deletion strains of *mus81*, *mms4*, *slx1*, *slx4*, *slx5* and *slx8*, all genes known to be involved in processing of stalled replication forks in *S. cerevisiae*, had elevated levels of spontaneous gross chromosomal rearrangements (GCRs) (Zhang et al., 2005). In fission yeast, site-specific GCRs were also observed in strains where replication forks blockage was induced at a specific euchromatic site (Lambert et al., 2005). GCRs include translocations, large interstitial deletions and loss of a chromosome arm, in other words, events that can have severe consequences for genome stability. For this reason, cells have evolved several pathways to enable reactivation and repair of stalled and collapsed forks (see below).

DNA damage can occur in many different ways both as a results of environmental factors such as radiation or chemicals but also from the cell's own metabolism. Moreover, repair of these lesions itself can sometimes lead to the formation of new and more severe types of DNA damage that also need to be repaired. Indeed, unrepaired lesions will most generally result in mutagenesis, carcinogenesis and ageing. For these reasons, it is not surprising that cells have developed a plethora of DNA repair systems and pathways to detect and repair DNA damage and to protect the integrity and the stability of their genome.

2.2 DNA repair pathways

As presented in the previous section, many types of DNA damage exist going from chemically modified or lost bases, DNA-DNA or DNA-protein crosslinks to DNA SSBs and DSBs. Repair pathways that are specific to each type of lesions have therefore evolved, providing the cell with a powerful DNA repair arsenal. The following section will give a general introduction to these pathways. As most of the work in this thesis was done in the yeast *S.cerevisiae*, the proteins involved in the different pathways described are named using the yeast nomenclature. When relevant, the human nomenclature is given in parenthesis.

2.2.1 Direct reversal of damage

When the reaction that led to DNA damage is reversible, direct reversal of the lesion is a simple and efficient repair mechanism. One example is photoreversion of UV-induced CPDs by the CPD photolyase, also know as photoreactivation (Sancar, 2000). During this process, the photolyase restores pyrimidine dimers to monomers by cleavage of carbon-carbon bonds, a reaction that requires visible light. This pathway has been thoroughly studied particularly in *S.cerevisiae* as no CPD photolyases have been found in mammals. Another example of direct damage reversal is the sealing of DNA nicks by DNA ligases. Indeed, if the nicks to be sealed contain compatible 5'-phosphates and 3'-hydroxyl ends, no additional processing of these ends is required.

2.2.2 Excision and replacement of damage

The fact that DNA is a double-stranded molecule presents certain advantages when DNA lesions need to be removed. Indeed, if damage is present only on one of the DNA strands it can be excised and specifically replaced by DNA synthesis using the undamaged strand as a template. Three well-characterized excision repair pathways are mismatch repair (MMR), base excision repair (BER) and nucleotide excision repair (NER).

Mismatch repair

As reviewed by Kolodner & Marsischky (1999) and more recently by Modrich (2006), MMR in yeast requires two different heterodimeric protein complexes: MSH2-MSH3 (MutS*beta*) and MSH2-MSH6 (MutS*alpha*). Current models suggest that the MutS*alpha* is responsible for the recognition of base:base mispairs as well as small insertion/deletion loops while larger insertion/deletion mispairs are recognized by MutS*beta*. Another heterodimeric complex involved in MMR is the MLH1-PMS1 complex (MutL*alpha*) which introduces nicks around the mismatch thus providing the 5'termini necessary for 5' to 3' hydrolysis of the mismatch-containing DNA strand by exonuclease I (Kadyrov et al., 2006). The resulting gap is filled by DNA polymerase delta, and the final nick is sealed by DNA ligase I, as in normal DNA replication.

Base excision repair

This pathway removes incorrect or damaged bases using damage-specific DNA *N*-glycosylase. In agreement with the fact that many different types of damage exist, a large number of N-glycosylases have been identified (Slupphaug et al., 2003). In yeast, BER is the main pathway used for the repair of AP sites. In most cases, the AP site is primarily recognized and cleaved on the 5' side by an AP endonuclease, Apn1. This generates a SSB with a 5'-deoxyribosephosphate (5'-dRP) end that is removed by the specific 5'-flap endonuclease Rad27 (Fen1). This process is known as long-patch BER. In higher eukaryotes, the 5'-dRP is released by the 5'-dRPase activity of DNA polymerase β in a process known as short-patch BER (Boiteux & Guillet, 2004). However, in *S. cerevisiae*, no DNA polymerase is known to have such an activity thus short-patch BER does not seem to take place in this organism. The created gap is filled by DNA polymerase ε and ligated by the Cdc9 ligase (Boiteux & Guillet, 2004). In Apn1-deficient cells, AP sites are mostly cleaved on the 3' side by AP lyases such as Ntg1 and Ntg2, resulting in a SSB with a 3'-α,β-unsaturated aldehydic end (3'-dRP). Such ends can be processed by the 3'-phosphodiesterase activity of the AP endonuclease Apn2 or by the 3'-flap endonuclease activity of the Rad1-Rad10 heterodimer. In both cases, DNA polymerase ε and DNA ligase Cdc9 finish to fill the SSB formed (Boiteux & Guillet, 2004).

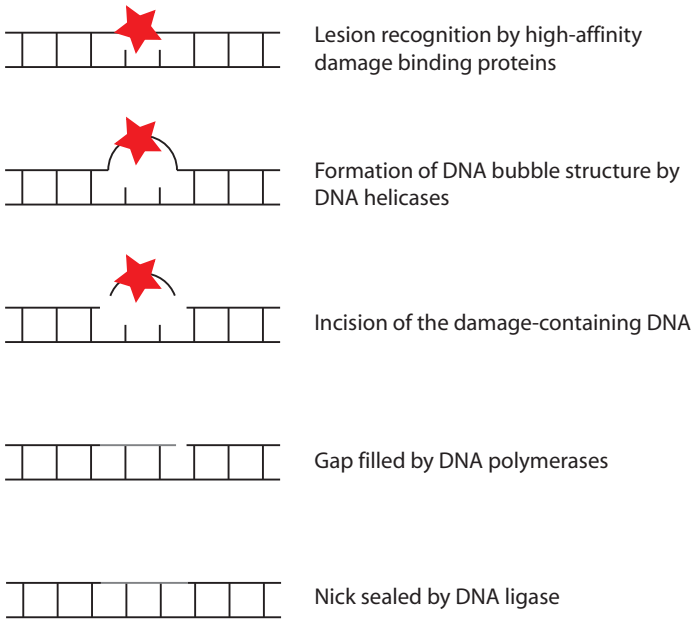

Figure 2.5. Nucleotide excision repair pathway. The DNA damage, represented as a red star, is recognized, excised and the single-stranded gap created in filled using the undamaged DNA strand as a template.

Nucleotide excision repair

Because it is a more flexible DNA damage repair mechanism, NER is often described as a backup repair pathway of BER. In NER, damaged DNA regions are recognized based on their abnormal structure or chemistry, excised and replaced (Figure 2.5). NER can act on a variety of different lesions including those creating distortion of the DNA helix such as UV-induced damage (see Section 2.1.1). Specifically, damage is first recognized by high-affinity damage binding proteins such as Rad14 (XPA), RPA, the Rad4-Rad23 (XPC-HR23B) and Rad7-Rad16 complexes. Once damage is localized, a DNA bubble structure is formed by the 5' to 3' DNA helicase Rad3 (XPD) and the 3' to 5' DNA helicase Rad25 (XPB). Once unwinded, the damage-containing DNA is incised both on the 5' side of the lesion by the Rad1-Rad10 (XPF-ERCC1) complex and on the 3'side of the lesion by Rad2 (XPG). The resulting gap can then be filled and ligated (Prakash & Prakash, 2000).

2.2.3 DNA DSB break repair

In contrast to the "excisable" damage presented above, DNA DSBs affect both DNA strands and are therefore extremely severe lesions for the cell. Two different mechanisms are in charge of repairing DNA DSBs in living organisms. One of them, non-homologous end-joining (NHEJ) brings the two ends of a broken DNA molecule together and ligates them without the need for extensive sequence homology between them (Figure 2.6). This pathway is potentially error-prone as resection of the DNA ends prior to ligation will result in loss of genetic information

and, in the scenario where a cell contains more than one DNA DSB, ligation of two DNA ends can potentially lead to chromosomal translocations. The second pathway, homologous recombination (HR), repairs the break by copying information from a homologous sequence within the genome such as the sister chromatid or the homologous chromosome. This pathway is theoretically error-free as the broken sequence is faithfully replaced by information copied from a homologous sequence.

In *S.cerevisiae*, HR is the main DNA repair pathway and NHEJ is mostly only required when HR is defective. In contrast, both HR and NHEJ are active DNA repair pathways in higher eukaryotes where they are differentially regulated depending on cell-cycle phases or developmental stages. Indeed, studies in both chicken and mouse showed that HR and NHEJ are differentially involved in the repair of γ-ray induced DNA DSBs. Specifically, HR deficient mice are hypersensitive to IR at the embryonic but not at the adult stage (Essers et al., 2000). In chicken cells, NHEJ was found to be the preferred repair pathway during G1-early S phase whereas HR took over in late S-G2 phase (Takata et al., 1998). Moreover, HR was also shown to be the DNA DSB repair pathway of choice during S-phase in human cells (Saleh-Gohari & Helleday, 2004). In meiosis, several DNA DSBs are specifically induced in a process involving the topoisomerase type II-like protein, Spo11 (for recent review see Keeney & Neale (2006)) and ligation of these breaks by NHEJ could lead to chromosomal rearrangements with severe consequences for the cell. Accordingly, Goedecke et al. (1999) showed that, in early meiotic prophase, Ku70, which is essential for NHEJ (see below), could not be detected thus permitting DNA DSB repair by the meiotic HR pathway.

As most of the results obtained during this PhD project shed light on the mechanisms of DNA DSB repair by HR as well as on the role of some of the key proteins in this pathway, a whole chapter (Chapter 3) has been dedicated to described this pathway in detail. For this reason, HR is not described further in this section.

Non-homologous end joining

The NHEJ pathway is globally conserved from yeast to higher eukaryotes and the central proteins involved in NHEJ can be found in all eukaryotic cells. As reviewed recently by Hefferin & Tomkinson (2005), repair by end-joining is initiated by the recruitment of the yKU70/yKU80 heterodimer to the DNA ends of the break. Then, the MRX complex, composed of the Mre11, Rad50 and Xrs2 (Nbs1) proteins, is recruited to the ends. This complex is believed to act as a bridging factor that holds the DNA ends together during repair (Chen et al., 2001). If the ends have ligatable termini, the repair process will be ended by simple ligation by a DNA ligase. However, this is rarely the case and the DNA ends need to be processed before they can be ligated. This processing step involves the alignment of the ends using microhomology (1 to 4 nucleotides) within the sequences close to the break site. This alignment step can result in the formations of gaps or overhangs. The following

step is the recruitment of the NHEJ-specific DNA ligase, Dnl4 (DNA ligase IV) complexed with Lif1 (XRCC4). This promotes the processing and gap-filling of the ends by Rad27 and Pol4, respectively, which will result in the formation of ligation-compatible ends. Because of its nuclease activity, Mre11 is also believed to be involved in end-processing. The ligase Dnl4 is then in charge of ligating the compatible DNA ends thus closing the break (Figure 2.6).

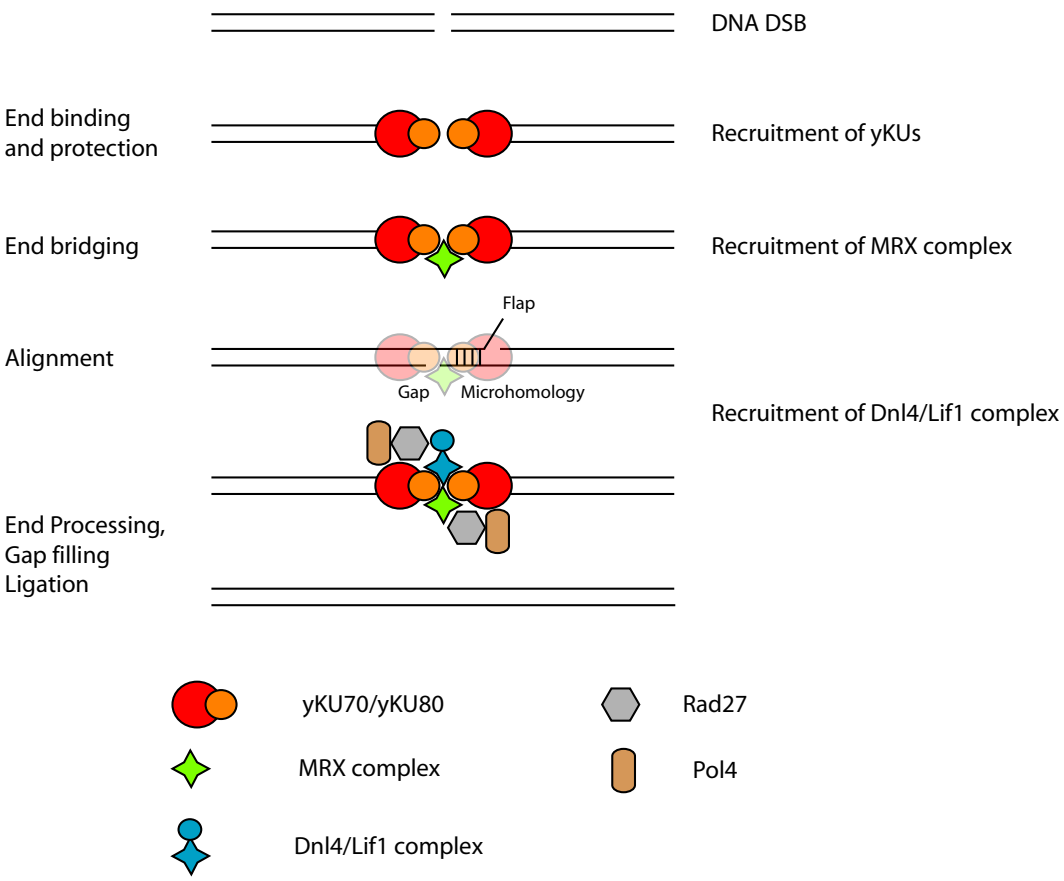

Figure 2.6. Model of NHEJ is *S.cerevisiae*. Figure adapted from Hefferin & Tomkinson (2005).

2.2.4 Replication fork restart

As mentioned previously, stalled and collapsed replication fork arise from the collision of the replication machinery with unrepaired DNA damage. As these lesions prevent further DNA polymerization, they are a threat to genome integrity and stability. For this reason, cells have evolved several pathways to enable reactivation of replication. As recently reviewed by Heller & Marians (2006), all restart pathways are composed of three basic steps:

- First, the stalled replication fork needs to be processed by specific enzymes into DNA structures that can be used by the replication

restart mechanisms.

- Second, the replication machinery must be reloaded on the DNA at places that are usually not origins of replication

- Finally, the damage that caused the replication blockage must be removed. This can be done at the replication fork during the restart process or after replication restart using lesion bypass (see below).

One of the mechanisms believed to be involved in replication fork restart is recombination-dependent replication (RDR) (Figure 2.7). Several models of how this mechanism takes place have been proposed (for review, see McGlynn & Lloyd (2002)). Common to these models is the formation of a D-loop recombination structure when the DNA end produced by fork regression invades a homologous template (see Figure 2.7). This results in the formation of a Holliday junction(s) believed to be resolved by the RuvABC complex in *E.coli*. Furthermore, in *E.coli*, D-loop structures have been shown to be targeted by the PriA helicase, which catalyzes the reloading of the replisome on the DNA thus allowing replication restart.

In some cases, removal of the DNA lesion is delayed and carried out after the passage of the replication fork. In fact, letting replication proceed through the damaged DNA can be seen as an advantage as it will provide a sister chromatid that can be used as template for subsequent repair of the lesion by HR. The mechanism by which replication is allowed to proceed through a DNA lesion is referred to as lesion or damage bypass.

2.2.5 Damage bypass

To allow the replication machinery to proceed through a DNA lesion, the high-fidelity replicative polymerase needs to be substituted. Recently, a new family of DNA polymerases (Y-family) has been defined that can act specifically on damaged templates (Goodman, 2002; Yang, 2003). Because of their low-fidelity, these enzymes can introduce errors if recruited to undamaged templates and they have been named "error prone". However, as they can act on DNA substrates which would normally block the classical high-fidelity polymerases, they can be the only way to avoid cell death (Rattray & Strathern, 2003). For this reason, these polymerases are also called translesion polymerases. In *S.cerevisiae*, the RAD6 epistasis group represents the family of proteins responsible for damage bypass. Rad6 exists as a complex with Rad18, a single-stranded DNA (ssDNA) binding protein that is believed to target Rad6 to regions of ssDNA created at stalled replication forks (Bailly et al., 1994, 1997). The fact that Δ*rad6* strains are deficient for replication bypass show that this pathway is totally dependent on the ubiquitylation activity of this enzyme. One target of Rad6 is PCNA, which is mono-ubiquitinated by Rad6 on its lysine 164 (Ulrich, 2005).

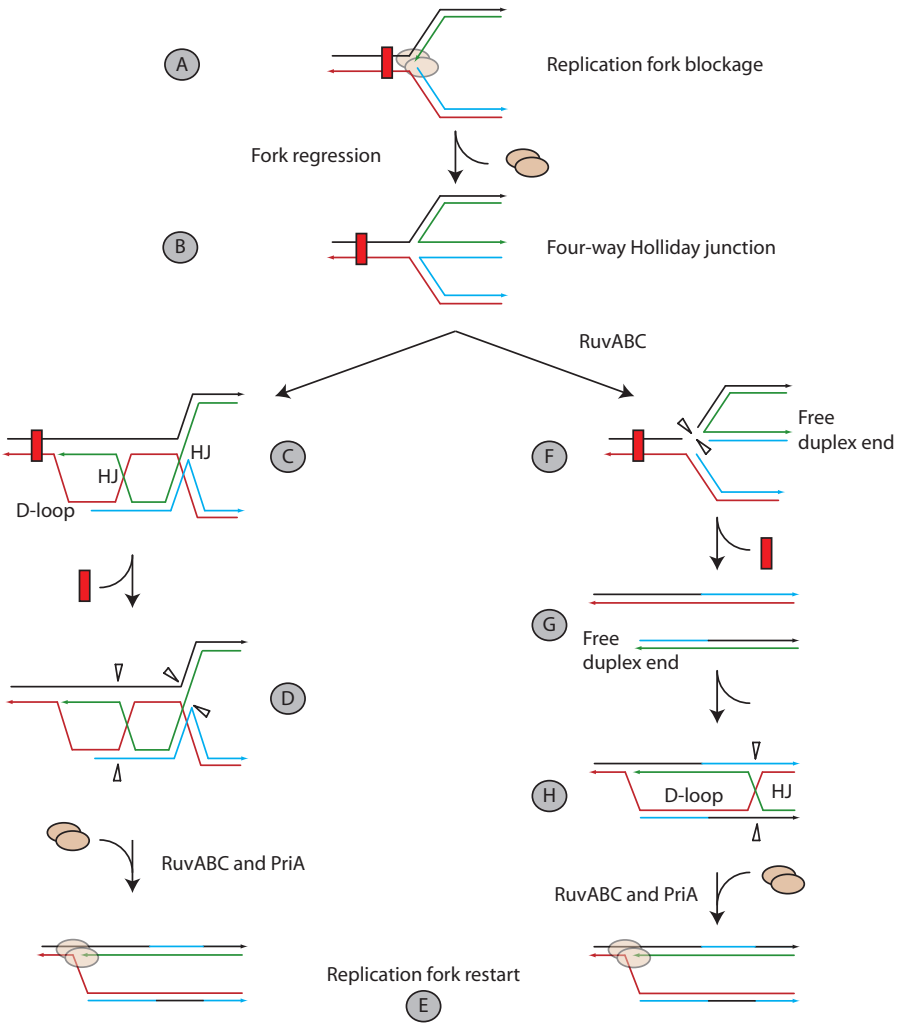

Figure 2.7. Models of replication fork restart by junction cleavage. (A) The replication machinery (beige ovales) stalls at a DNA lesion (red rectangle). (B) Fork regression into a four-way Holliday junction (HJ). (C) In this model, a D-loop recombination structure is formed when the DNA end produced by fork regression invades a homologous template. This creates a second HJ at the D-loop. (D) After removal of the lesion, both HJs are believed to be resolved by the RuvABC complex (white triangles represent cleavage sites). (E) PriA catalyzes the reloading of the replication machinery thus restarting DNA replication. (F) In this model, RuvABC cleaves the HJ created by fork regression before recombination occurs thus releasing a double-stranded DNA end. (G + H) After removal of the lesion, the released end can recombine with a homologous template thus creating a D-loop and a HJ. Cleavage of this HJ by the RuvABC complex and reloading of the replication machinery by PriA permits replication restart (E). 3'-ends of DNA strands are shown with arrowheads. Figure adapted from McGlynn & Lloyd (2002).

This initial monoubiquitylation of PCNA by Rad6 assists PCNA in interacting with the different bypass polymerases of translesion synthesis (Prakash et al., 2005). In yeast, polymerase zeta (Polζ) and polymerase eta (Polη) are the main polymerases involved in translesion bypass. These enzymes have low binding affinity to DNA and disso-

ciate from the DNA after inserting a single nucleotide at the site of damage. However, this is sufficient to allow the replication machinery to pass the damaged region. At that point, normal DNA synthesis by the traditional high fidelity polymerase and other replication proteins can resume while other repair mechanisms can remove the DNA lesion behind the fork.

Chapter 3

Double-strand break repair by homologous recombination

DNA DSB are serious lesions that if left unrepaired can lead to genomic instability and cell death. In *S.cerevisiae*, the main pathway used to repair DNA DSBs is homologous recombination (HR). This and the fact that yeast can be easily genetically manipulated has made *S.cerevisiae* a model organism of choice to study HR both at the molecular and at the biochemical level. This chapter presents a detailed description of the different mechanisms of HR together with their currently accepted models as well as the role of the main proteins involved in HR. As most of the work performed during this PhD study has been dedicated to the understanding of the mechanisms of mitotic HR and of the role of Rad52 in this process, the results obtained are included as part of the "state of the art" knowledge available on this subject today. The experiments and results backing up these findings are presented in detail in Chapters 4 and 5.

3.1 Mechanisms of HR

Many models have been proposed to explain the repair of DSB in mitotic yeast cells. In this section, the most common models are presented: HR through gene conversion with the DNA DSB repair and the synthesis-dependant strand annealing (SDSA) models, HR by single-strand annealing (SSA) and finally HR by break-induced replication (BIR).

3.1.1 Gene conversion

In yeast, gene conversion occurs both in meiotic and mitotic cells albeit at different rates. Meiotic recombination is very frequent and ensures genetic diversity and accurate segregation of homologous chromosomes during the first meiotic division. This process is essential and its occurrence is not random. Indeed, meiotic recombination is a well-programmed event of the meiotic cell cycle, initiated genome-wide by DSB formation at chromosomal hot spots probably made by the

topoisomerase type II protein Spo11 (reviewed recently by Keeney & Neale (2006)). For these reasons, meiotic recombination has been extensively studied and most of the knowledge on recombination available today is derived from studies in meiotic cells. Early studies by Fogel and colleagues have shown that meiotic recombination results from two types of events: gene conversion and crossing over. Gene conversion is a non-reciprocal event where genetic information is transferred from one homologous sequence to another. In meiotic yeast cells, this phenomenon is directly observable when analyzing tetrads as it results in a non-mendelian 3:1 segregation pattern instead of the 2:2 segregation pattern expected for a heterozygous site. In a study of gene conversion at 3 separate heteroallelic sites in 1611 unselected tetrads, Fogel & Mortimer (1969) concluded that approximately 2% of a haploid genome is gene-converted in each meiosis and that the major source of aberrant tetrads stemmed from gene conversion and from reciprocal recombination (crossover) between the parental alleles. They also observed that the gene conversion frequency was locus specific going from 0.1% to as much as 20%. Later, they showed that gene conversion and crossover are often associated events and that this is the case in about 50% of the time (Hurst et al., 1972). Taking this into account, several models of recombination were proposed in which differential resolutions of the Holliday junction (HJ) can lead to both crossover and non-crossover outcomes (Holliday, 1964; Meselson & Radding, 1975; Resnick & Martin, 1976; Szostak et al., 1983; Sun et al., 1991). Among these, the DNA DSB repair model proposed by Szostak et al. (1983) is one of the most referred to today. Indeed, supporting this model are data from the Kleckner laboratory that provided physical evidence that double Holliday junctions (dHJs) are intermediates of meiotic recombination (Schwacha & Kleckner, 1994, 1995, 1997). This model is presented in Figure 3.1 and described in details below.

In the DNA DSB repair model, recombination is initiated by the formation of a DNA DSB. This is followed by the 5' to 3' resection of the ends of the break creating 3' single-stranded DNA (ssDNA) tails that can invade and anneal to a homologous template. Invasion of the homologous template results in the formation of a D-loop structure which is able to pair with the non-invading 3' tail on the other side of the break. This permits extension of both ends of the break by DNA synthesis. Subsequent gap filling and ligation result in a double HJ intermediate: a dynamic 4-stranded heteroduplex DNA structure between the broken chromosome and the chromosome serving as repair template. This structure can be resolved in two ways leading to crossover or non-crossover products as shown in Figure 3.1. Indeed, if both HJs are cut in the same way (both at the crossed strands or at the non-crossed strands) gene conversion will not be associated with crossover. On the other hand, if the HJs are cleaved in different ways (one at the crossed strands and one at the non crossed strands, or opposite), the outcome will be a gene conversion event associated with a crossover. The resolvase responsible for this step has not yet been de-

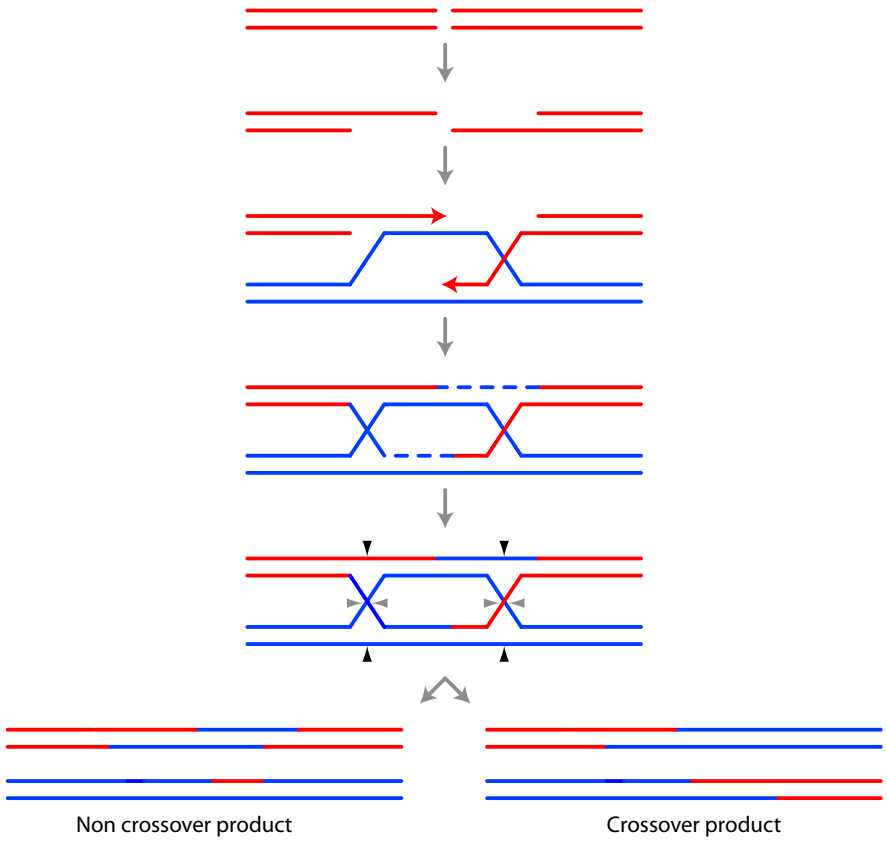

Figure 3.1. DNA DSB repair model by (Szostak et al., 1983). The repair process results in both crossover and non-crossover products depending on how the two Holliday junction structures are resolved as illustrated by the black (cutting of the non-crossed strands) and grey (cutting of the crossed strands) arrows.

scribed but if resolution of this structure is random, one would expect an equal amount of crossover and non-crossover products. In any case, this repair pathway is semi-conservative as newly synthesized DNA is present in both the donor and the recipient molecules.

Gene conversion also occurs spontaneously in mitotic cells yet at lower rates compared to that observed in meiotic cells. A classical way of analyzing this type of event has been the use of sectored colonies or by selection of prototrophs often resulting from a gene conversion event between two heteroalleles of an auxotrophic marker (see Paques & Haber (1999) for a review of existing genetic assays). As opposed to its meiotic counterpart, mitotic gene conversion is not a pre-programmed event and is believed to arise from the repair DNA damage arising sporadically during the cell-cycle. In agreement with this view, Roman & Fabre (1983) showed that mitotic gene conversion occurs both in the G1 and the G2 phase of the cell cycle. Another difference between meiotic and mitotic gene conversion is that mitotic events are not strongly associated with crossing overs. Indeed, when measured after selection for prototrophs, gene conversion between heteroalleles on homologous chromosomes show crossover frequencies of 10 to 20% (Esposito, 1978;

Haber & Hearn, 1985; Kupiec & Petes, 1988). In *S.cerevisiae* mating-type switching, a mitotic gene conversion event initiated by DSB formation at the MAT locus by the HO endonuclease, is rarely associated with crossovers (Strathern et al., 1982; Kostriken et al., 1983). However, this result may be specific to this event as crossovers accompanying mating-type switching would result in lethal chromosome deletions. In order to account for the uncoupling of mitotic gene conversion and crossover events, new models of gene conversion that mainly result in non-crossover products were proposed (reviewed by Paques & Haber (1999)). Among these, the synthesis-dependent strand annealing (SDSA) model (Nassif et al., 1994) is the most commonly described (Figure 3.2).

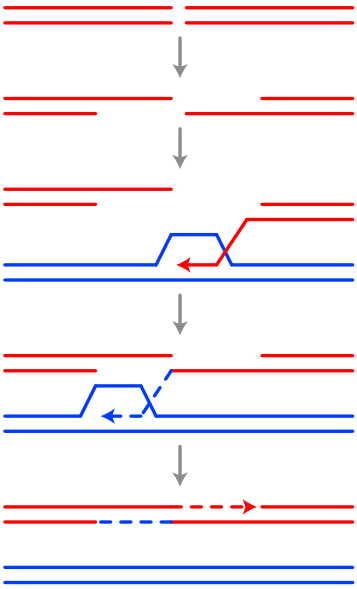

Figure 3.2. The SDSA repair model. This repair model yields non-crossover gene conversion products exclusively.

The main difference between the SDSA model and the DNA DSB repair model (Figure 3.1) is that, in the SDSA model, the newly synthesized DNA strand is displaced back to the broken DNA molecule after DNA synthesis has taken place thus no dHJ intermediate is formed. In this model, DNA synthesis is conservative as all the newly synthesized DNA is situated on the DNA molecule that was broken while the repair template is left unmodified. Recently, using in vivo metabolic labeling, Ira et al. (2006) showed that the newly synthesized DNA strands created during gene conversion at the MAT locus are found at the repaired locus thus leaving the donor sequence unchanged. These results suggest that SDSA is the main pathway used to repair DNA DSBs induced at the MAT locus in *S.cerevisiae*.

3.1.2 Crossover or no crossover: helicases regulate the outcome of HR

As mentioned above, few gene conversion events are associated with crossovers in mitotic cells, suggesting that these events are regulated. One reason for this can be the fact that crossovers can lead to loss of heterozygosity (LOH) (Figure 3.3) and chromosomal translocations which are both believed to be involved in cancer development.

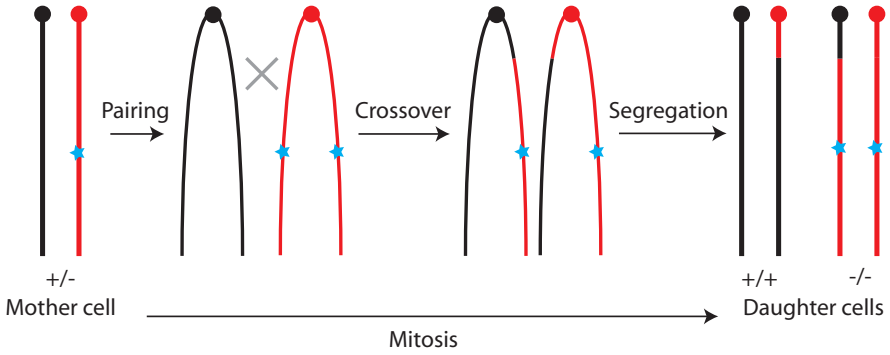

Figure 3.3. Crossover can lead to loss of heterozygosity. The mother cell is heterozygous for a mutation (represented by the blue star). Crossover between non-sister chromatids leads to the transfer of the mutation. Random segregation of the chromatids will lead to the formation of a daughter cell, homozygous for the mutation in 50% of the cases. For simplicity, only one chromatid is represented for chromosomes in the mother and daughter cells.

Proteins believed to act as suppressors of crossover formation are the RecQ helicase, Sgs1 (BLM helicase in human) and the Srs2 helicase. *srs2*Δ and *sgs1*Δ cells show 2 to 3 fold increase in crossover rates compared to wild-type , showing that both proteins prevents some HR intermediates from becoming crossovers. As mentioned above and shown in Figures 3.1 and 3.2, the DNA DSB repair model and the SDSA model are similar until the invasion step suggesting that, up to this step, the outcome of HR is still undecided. As Srs2 has been shown to disrupt the Rad51 nucleoprotein filament necessary for strand invasion (Krejci et al., 2003; Veaute et al., 2003) (described in more details later in this section), one hypothesis is that Srs2 facilitates the displacement of the invading strand by removing Rad51, thus promoting SDSA (Ira et al., 2003) (Figure 3.4, A). Another possibility is that Srs2 removes the Rad51 filament from the non-invading strand of the break thus preventing second end invasion and formation of the double Holliday structure that characterizes the DNA DSB repair pathway. Either way, Srs2 appears to specifically promote SDSA thus HR events with non-crossover outcomes.

In contrast to Srs2, Sgs1 is believed to act directly on the resolution of the dHJ structures of the DNA DSB repair pathway. In collaboration with topoisomerase III (Top3), Sgs1 is believed to push the two HJs of the paired duplex towards each other in a process called reverse branch migration (Wu & Hickson, 2003; Ralf et al., 2006; Raynard et al., 2006;

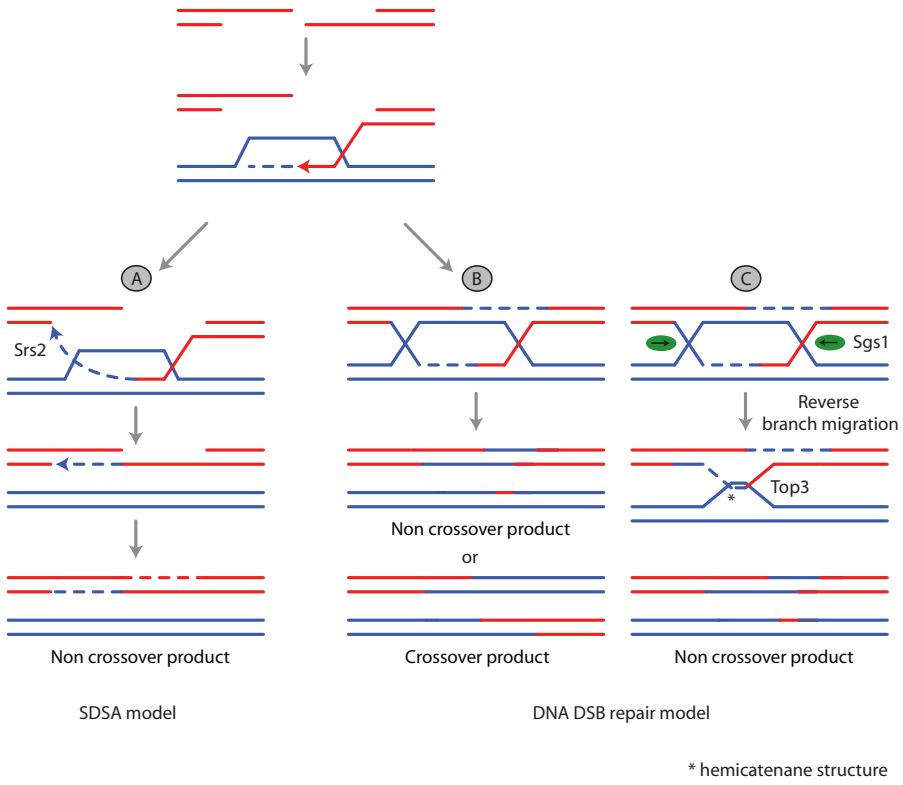

Figure 3.4. Model of crossover suppression by Srs2 and Sgs1. (A) Srs2 specifically promotes SDSA by facilitating the displacement of the invading strand back towards the non-invading end of the DSB. (B) Classical DNA DSB repair model. (C) Sgs1 (green circles) and Top3 promote the resolution of the dHJ structure into non-crossover products. Figure adapted from Ira et al. (2003).

Wu et al., 2006a). This results in the formation of a hemicatenane structure that is believed to be resolved by Top3 into non-crossover products (Raynard et al., 2006; Wu et al., 2006a) (Figure 3.4, C). If this true, one can envision that reverse branch migration would reduce the length of the gene conversion tract thus associating non crossover products with short conversion tracts. Reciprocally, crossover events should then be associated with long conversion tracts. In fact, when studying intrachromosomal recombination in yeast, Aguilera & Klein (1989) observed that long conversion tracts were often associated with crossovers. Moreover, Lo et al. (2006) recently showed that allelic crossovers and gene conversion tract lengths are increased in *sgs1*Δ *S. cerevisiae* strains. The same study also showed the Sgs1 helicase activity was not required for suppression of crossovers thus arguing against a role of Sgs1 in reverse branch migration. The authors therefore proposed that the two HJs converge passively towards each other and that Sgs1 acts to stimulate resolution of the hemicatenane by Top3 (Lo et al., 2006).

In the sections above, the two main models of DSB-induced HR and their regulation have been presented. However, in cases where a DNA DSB was induced between direct repeats or when only one end of the break was available for HR, the outcome of HR observed experimentally

could not be explained using these models. Accordingly, other models of HR have been proposed to account for these events and these models are presented below.

3.1.3 Single-strand annealing

Single-strand annealing (SSA) was first described as a potentially important repair pathway for the repair of lesions in genomes containing many repeated sequences such as those of higher eukaryotes (Lin et al., 1984). Indeed, in yeast, this pathway has been shown to be involved in the repair of a DNA DSB induced between two directly repeated homologous regions (Fishman-Lobell et al., 1992). This results in the deletion of one of the repeats and of the intervening sequence (Figure 3.5) (Sugawara & Haber, 1992). Efficient repair by SSA has been shown to require a minimum homology length of approximately 90 bp under which the repair efficiency is greatly reduced (Sugawara & Haber, 1992). After DSB formation, extensive resection of the 5' ends on each side of the break eventually results in the exposure of the 3' single-stranded complementary repeated sequences which can then anneal. The non-homologous 3' tails are excised by nucleases, a step requiring the NER genes *RAD1* and *RAD10* (Fishman-Lobell et al., 1992; Ivanov & Haber, 1995), and repair is ended by DNA synthesis and ligation.

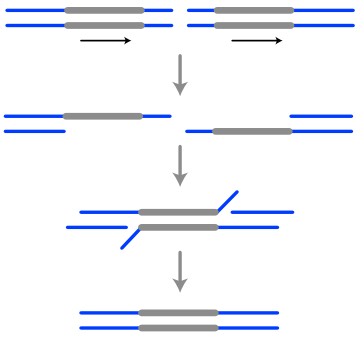

Figure 3.5. Repair of a DNA DSB between two direct repeats by SSA. The repair process results in the loss of one repeat and of the inter-repeat region. The black arrows indicate the orientation of the repeats.

As opposed to gene conversion, strand invasion does not occur in SSA thus avoiding the formation and resolution of Holliday structures. In yeast, SSA has been shown to be reduced in the absence of Rad52 (Fishman-Lobell et al., 1992; Sugawara & Haber, 1992). This probably reflects the need for Rad52's DNA binding/annealing activity to promote the annealing of the exposed repeated sequences (Mortensen et al., 1996; Smith & Rothstein, 1999). Supporting this hypothesis, we have recently shown that HO-induced SSA between leu2 heteroalleles is impaired in *rad52* mutant strains in which the DNA-binding activity of Rad52 by its N-terminal domain is impaired (Chapter 4). Based on these results, we concluded that this activity is required for SSA. Moreover, deletion of *RAD51*, *RAD54*, *RAD55* and *RAD57* has

no negative effect on SSA (Ivanov & Haber, 1995), again suggesting that Rad52 is the key protein of this process. The fact that SSA is not totally impaired in *rad52*Δ strains suggests that annealing of the repeated sequences can occur spontaneously. This is in agreement with the finding that the efficiency of Rad52-independent SSA is increased when the amount of homology between the recombining sequences is increased (Ozenberger & Roeder, 1991).

3.1.4 Break-induced replication

BIR is characterized by the fact that only one end of the DSB participates in the repair reaction (Figure 3.6). This can be due to the fact that the other end has been lost or is unavailable for invasion of a homologous template. This one-ended recombination event is very efficient in acting on ends of broken chromosomes in cases such as broken replication forks or the maintenance of telomeres in the absence of telomerase. The particularity of these events is that they often require extensive DNA synthesis down the chromosome arm in order to reestablish a full length chromosome (Golin & Esposito, 1984; Voelkel-Meiman & Roeder, 1990; Bosco & Haber, 1998). Morrow et al. (1997) and later Davis & Symington (2004) showed that an entirely new chromosome could be created when transforming yeast cells with a linear DNA fragment containing an origin of replication, a centromere and ends with homology to specific chromosomal sequences. These ends enable pairing to the homologous template and BIR to the end of the chromosome thus adding telomeres and generating a stable chromosomal fragment.

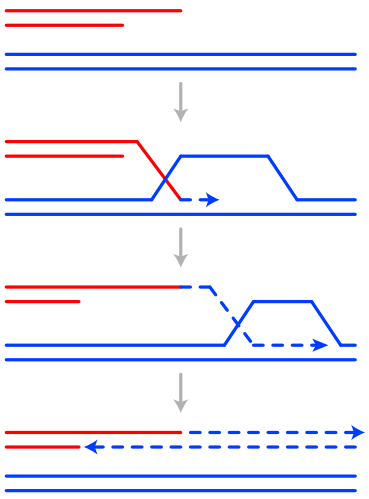

Figure 3.6. A classical representation of BIR. One-ended invasion by the only available 3'end of the DNA DSB initiates replication that proceeds to the end of the chromosomal template. After this new strand is double-stranded, an intact chromosome is reestablished.

BIR has been unanimously shown to be Rad52-dependent (Malkova et al., 1996; Bosco & Haber, 1998; Davis & Symington, 2004). On the other hand, the question of the implication of Rad51 in BIR has been

more controversial. In a study using HO-induced DNA DSBs at the mating-type locus in *S.cerevisiae*, Malkova et al. (1996) showed that a broken chromosome was lost in 99% of the time in Δ*rad52* strains while it was repaired in 35% of the time in Δ*rad51* cells. These observations led them to conclude that repair could occur by BIR in a Rad51-independent fashion. Using the same assay, Signon et al. (2001) later showed that a broken chromosome could be repaired by BIR in Δ*rad54*, Δ*rad55* and Δ*rad57* mutant strains showing that these proteins were not required for BIR. Importantly, in this assay, Rad51-independent BIR was shown to be initiated more than 13 kb from the DSB and to depend on a 200-bp BIR facilitator sequence (Malkova et al., 2001). Further characterization of this Rad51-independent pathway by Ira & Haber (2002) showed that it is dependent on Rad52, Rad59, Rad50, Tid1 and Srs2 and that it is mainly involved in recombination between short repeats. Indeed, in the absence of Rad51, much less homology (app. 30 bp compared to 100 bp required in the Rad51-dependent pathway) was required for recombination. In fact, this study showed that Rad51 impairs recombination with short homology (Ira & Haber, 2002).

Using a chromosome fragmentation assay, Davis & Symington (2004) showed that *RAD51* was required for more than 95% of BIR events involving a single-end invasion and was essential when two BIR events were required for generation of a chromosome fragment. Moreover, they showed that *RAD54*, *RAD55* and *RAD57* were required for repair by BIR and that deletion of *RAD50* and *RAD59* in their assay had no effect neither on Rad51-dependent nor Rad51-independent BIR.

In conclusion, BIR occurs through two different pathways: a Rad51-dependent and a Rad51-independent pathway. Rad51-dependent BIR is dependent on Rad51, Rad52, Rad54, Rad55 and Rad57 but not on Rad50 or Rad59. On the other hand, Rad51-independent BIR is dependent on Rad52, Rad59 and Rad50 but not on Rad54, Rad55 or Rad57. Interestingly, these two pathways are the ones used in yeast to maintain telomeres in the absence of telomerase (Le et al., 1999; Chen et al., 2001).

3.1.5 Instigators of HR in mitotic cells

As mentioned above, most of our knowledge of HR is derived from the studies of the meiotic system where specifically induced DNA DSBs are the known initiators of the recombination process. For this reason, most recombination models include the formation of a DNA DSB as a first step and it is generally accepted that spontaneous DNA DSBs initiate mitotic recombination in vegetative cells. However, the exact nature of the lesion(s) that triggers mitotic HR is still unknown. Although it is undeniable that DNA DSB induce HR in mitotic cells, some studies show that it is not the only (and probably not the main) lesion that triggers mitotic HR. One example is the finding that the synthetic lethality in *srs2 sgs1* mutant strains occurs randomly and is dependent on the

ability of these cells to perform mitotic HR (Gangloff et al., 2000). One hypothesis is that Sgs1 and Srs2 are involved in the processing of recombinogenic DNA lesions as part of the HR pathway. By removing HR, these lesions can be channeled to other repair pathways thus restoring cell viability. If these lesions are DNA DSBs, removing the pathways responsible for DNA DSB repair (HR and NHEJ) should induce cell death in these mutants. However, Fabre et al. (2002) showed that *srs2 sgs1 rad52 lig4* mutant strains are viable and therefore concluded that DNA DSBs are not the major lesions initiating mitotic recombination events. In another study, Mortensen et al. (2002) identified a group of *rad52* mutants (Class C mutants) which show null-like phenotypes after γ-irradiation but wild-type or hyper-rec phenotype when considering mitotic HR rates. Further analysis of these mutants showed that a single endonuclease-induced DNA DSB causes high mortality thus confirming the separation of function phenotype of the *rad52* Class C mutants (Lettier et al., 2006). From this study, it is clear that mitotic HR can occur without prior formation of DNA DSBs. Following the thoughts of Fabre and colleagues, the authors consider nicks and/or single-stranded gaps as possible triggers of mitotic HR. This work is presented in its integrity in Chapter 4. Interestingly, the concept of nicks and single-stranded gaps being the principal initiators of mitotic HR has also recently been proposed in studies involving mammalian cell systems (Lee et al., 2004; Saleh-Gohari et al., 2005). In fact, in the early HR models proposed by Holliday (1964), Meselson & Radding (1975) and later by Radding (1982), HR was initiated by DNA nicks (Smith, 2004).

3.2 Roles of the *RAD52* epistasis group

The repair of a DNA DSB by HR is a complex multi-step reaction involving many different but specific proteins in a coordinated manner. The proteins encoded by the *RAD52* epistasis group genes: *RAD50*, *RAD51*, *RAD52*, *RAD54*, *RAD55*, *RAD57*, *RAD59*, *RDH54*, *MRE11* and *XRS2*, are key players involved in all the steps of the repair process by HR. This section describes the role of these proteins following the chronology of the HR process presented previously (see Section 3.1.1).

3.2.1 Preparing the ends: the MRX complex

The MRX complex has the particularity of being involved in both the HR and the NHEJ DNA repair pathways. As the similarities between these pathways are limited, one can imagine that the MRX complex is involved at the very beginning of these processes in steps such as DSB formation and initial processing of these ends. MRX is a stable trimeric complex composed of Mre11, Rad50 and Xrs2 (Nbs1 or Nibrin) (Johzuka & Ogawa, 1995; Usui et al., 1998). In yeast, null mutations of each of the genes encoding these proteins result in similar phenotypes: poor growth, extreme sensitivity to IR and MMS and meiotic defects

(Game & Mortimer, 1974; Ivanov et al., 1992; Ajimura et al., 1993; Bressan et al., 1999). Interestingly, mutants of *MRE11* and *RAD50* show reduced rates of 5'-3' resection of both meiotic-specific and HO-induced DNA DSB ends (Sugawara & Haber, 1992; Ivanov et al., 1994; Tsubouchi & Ogawa, 1998). This suggests that the MRX complex is involved in the processing of the DSB ends into 3' ssDNA tails prior to invasion. However, biochemical studies of both human and yeast Mre11 showed that this protein forms a dimer that has ssDNA endonuclease as well as 3'-5' exonuclease activity (Johzuka & Ogawa, 1995; Furuse et al., 1998; Paull & Gellert, 1998; Trujillo et al., 1998; Usui et al., 1998; Moreau et al., 2001; Trujillo & Sung, 2001) which is, at first view, in contradiction with its involvement in the 5'-3' resection step. One proposed hypothesis is that MRX can, using the ssDNA endonuclease activity of Mre11, cleave the ssDNA secondary structures formed when DNA at the break is unwound by a helicase thus forming the 3' DNA overhang (Paques & Haber, 1999; Krogh & Symington, 2004). Rad50 has structural similarities with the structural maintenance of chromosomes (SMC) family of proteins as it is composed of a N-terminal Walker A and a C-terminal Walker B motif separated by two coiled-coil regions. Between these regions, a small non-coiled hinge region is present that is characterized by a Cys-X-X-Cys motif (Alani et al., 1989; Hopfner et al., 2002). Studies suggest that the Rad50 molecule can bend at its hinge domain thus bringing the two catalytic Walker regions together to form a catalytic ATPase/DNA binding domain while the coiled-coil region protrudes from the globular part of the structure. (Anderson et al., 2001; de Jager et al., 2001). A Mre11 dimer is able to bind at the base of the coiled-coil region close to the Rad50 DNA-binding interface creating the Rad50/Mre11 DNA-binding domain (Hopfner et al., 2001) and could act as an intramolecular link holding the Rad50 dimer together. Moreover, the hinge region appears as a hook structure at the summit of the coiled-coil domain and permits the interaction and formation of $Rad50_2/Mre11_2$ hetero-tetramers. One hypothesis is that two globular $Rad50_2/Mre11_2$ cores can be connected through their coiled-coil "arms" when these are linked to each other by their interlocking molecular zinc-hooks (Figure 3.7). If the DNA-binding cores are sitting on two different sister chromatids or at the ends of a DNA DSB, one can imagine that this structure could be used as a tether to avoid broken ends to move apart from each other or to keep a homologous repair template in place until invasion of the intact template by one of the broken ends has occurred (de Jager et al., 2001; Hopfner et al., 2002).

In *S. cerevisiae*, diploids homozygous for *mre11*, *rad50* or *xrs2* are unable to form meiosis-specific DSBs leading to the formation of inviable spores (Johzuka & Ogawa, 1995; Alani et al., 1990). This shows that the MRX complex is involved in DSB formation during meiosis and evidence tends to point towards the implication of the complex in the removal of the DSB-forming Spo11 from the DSB ends after DSB formation. This hypothesis is strongly backed up by the results

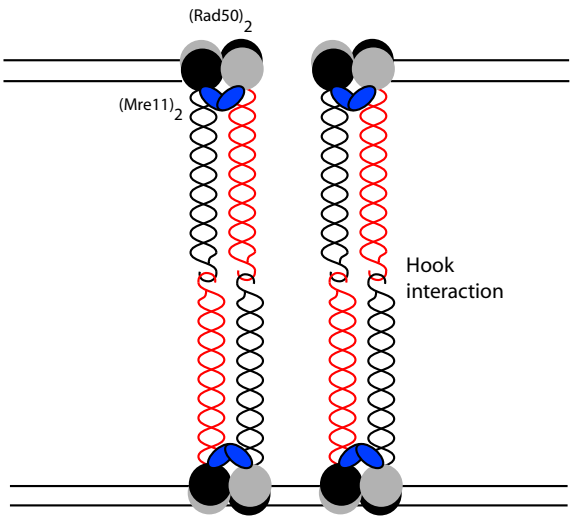

Figure 3.7. Representation of how the $Rad50_2/Mre11_2$ tetramer could act as a tether keeping the two ends of a DSB in the vicinity of the sister chromatid or another homologous template. In this figure, the Walker A and B motifs are represented as black and grey circles, respectively. Figure adapted from (Krogh & Symington, 2004).

of Keeney et al. (1997) showing that Spo11 remains bound to the 5' ends of the break in *rad50S* mutants. Interestingly, while *mre11*, *rad50* and *xrs2* diploids are severely impaired in meiotic recombination, they are hyper-rec (10-fold) for spontaneous mitotic recombination (Bressan et al., 1999), again demonstrating that these processes are intrinsically different. Moreover, HO-induced DSBs are also repaired in these mutants albeit with some delay probably due to the reduced rates of 5'-3' resection observed in these mutants as mentioned above. These results suggest that the requirements for the MRX complex depend on the type and the state of the DSB ends. One hypothesis is that in the meiotic context, removal of protein-DNA adducts is a crucial step that specifically requires the action of the MRX complex. On the other hand, HO-induced or spontaneous mitotic breaks could be "cleaner" substrates that can be processed by other less effective nucleases in case the MRX complex is absent. One possible candidate for this is Exo1, a 5'-3' endonuclease which can suppress *mre11*, *rad50* and *xrs2* mitotic defects when overexpressed (Fiorentini et al., 1997; Lewis et al., 2002).

In conclusion, the MRX complex appears to act at the very first steps of DNA DSB repair. As this complex is most likely involved in initiating 5' to 3' resection of the ends of the break, one can hypothesize that it is responsible for committing these ends to repair by HR. This commitment can be due to the fact that resected ends are unsuitable for direct ligation by NHEJ and/or that MRX will subsequently recruit the Tel1 checkpoint kinase, resulting in cell-cycle checkpoints activation and recruitment of other HR proteins (Lisby et al., 2004).

3.2.2 Activating the ends: the Rad51 filament

After 5'-3' resection of the DSB ends, the resulting 3' single-stranded DNA tails engage in the repair process by invading a homologous template and priming for DNA synthesis. This requires covering of the ssDNA tails by an active nucleoprotein filament of Rad51.

Structure of the Rad51 protein

ScRad51 is a highly conserved 43-kDa protein that not only shares homology with the bacterial RecA protein but also forms flexible right-handed helical filaments on double-stranded (ds) and single-stranded (ss) DNA, similar to those formed by its bacterial homologue (Aboussekhra et al., 1992; Basile et al., 1992; Shinohara et al., 1992; Ogawa et al., 1993; Conway et al., 2004). The very N-terminal of HsRad51, conserved in eukaryotes but missing in RecA, has been shown to mediate DNA-binding and protein-protein interactions (Aihara et al., 1999; Krejci et al., 2001; Zhang et al., 2005). Crystal structure and electron microscopy analysis of Rad51 suggest that the protein forms ring structures in its inactive or storage form. These structures are believed to be dissolved and reassembled as a filament on ssDNA when Rad51 activity is required (Figure 3.8) (Yang et al., 2001; Shin et al., 2003; Sauvageau et al., 2005).

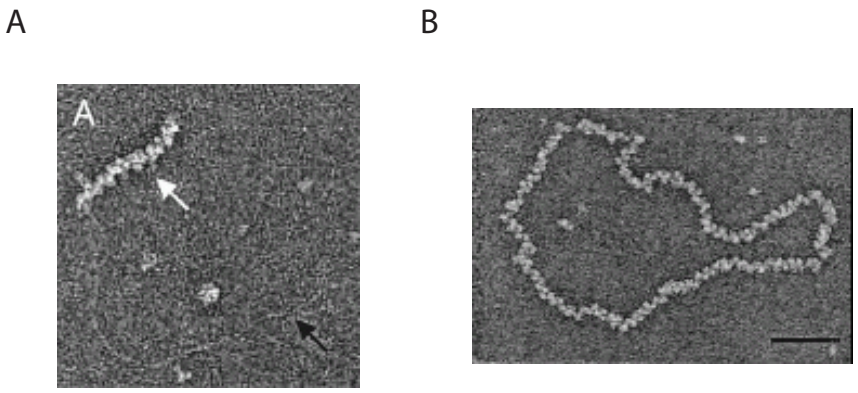

Figure 3.8. Electron microscopy visualization of fission yeast Rad51 on ssDNA. (A) Electron micrograph showing the binding of Rad51 to a linear duplex containing a single-stranded tail. The bound ssDNA tail is indicated by the white arrow, while the black arrow indicates unbound dsDNA. (B) Electron microscopic visualization of Rad51 bound to ΦX174 ssDNA. Pictures from (Sauvageau et al., 2005).

Rad51 nucleoprotein filament formation

The Rad51 filament formation onto ssDNA is stimulated in the presence of RPA which is believed to remove secondary structures from the ssDNA tails thus permitting a continuous Rad51 filament to be formed (Sung & Robberson, 1995). If this is the case, one would expect RPA to

bind ssDNA before Rad51 in vivo. Surprisingly, in vitro studies showed that the efficiency of the strand exchange reaction is greatly increased when RPA is added after the Rad51 nucleation step, while it is severely reduced when RPA is bound to ssDNA prior to the addition of Rad51 (Sung, 1997b). Thus, RPA acts as a inhibitor of the Rad51 filament formation in vitro. Further studies using different strand exchange assays later showed that the inhibitory effect of RPA is alleviated when mediator proteins such as Rad52 and the Rad55-Rad57 heterodimer are added to the reaction (Sung, 1997b,a; Benson et al., 1998; New et al., 1998; Shinohara & Ogawa, 1998). These results and the fact that Rad52 is able to bind both RPA and Rad51 led to the hypothesis that Rad52 mediates Rad51 filament assembly by removing RPA from the ssDNA while simultaneously replacing it by Rad51 (Song & Sung, 2000; Sugiyama & Kowalczykowski, 2002). In agreement with this view, it has been shown that Rad52 is essential for the formation of Rad51 foci at the site of DSB in *S. cerevisiae* (Gasior et al., 1998; Miyazaki et al., 2004; Lisby et al., 2004). This is however not the case in mammalian cells (van Veelen et al., 2005). ssDNA binding by Rad51 requires Rad52 which, in combination with Rad55-57, is thought to promote the formation and/or the stabilization of the Rad51 nucleoprotein filament (Sugawara et al., 2003; Wolner et al., 2003). Rad55 and Rad57 are indeed believed to be involved in the stabilization of the Rad51 filament based on the results of Fortin & Symington (2002) showing that the requirements for Rad55 and Rad57 can be suppressed by the Rad51-I345T mutant which has increased DNA binding abilities. Moreover, *RAD51* overexpression suppresses the DNA repair defects in *rad55* and *rad57* strains (Hays et al., 1995; Johnson & Symington, 1995). Another protein shown to stabilize the Rad51 filament is the chromatin remodeling protein Rad54, that directly binds to the Rad51-ssDNA complex (Mazin et al., 2003; Alexeev et al., 2003; Wolner et al., 2003). Wether these mediator proteins (Rad52, Rad55, Rad57 and Rad54) are required for the formation of the Rad51 filament onto the ssDNA, for the strand exchange reaction itself or for both remains unclear but there is no doubt that these two processes are intrinsically linked. The Rad51 nucleoprotein filament is a functional entity which is believed to be involved in the genome-wide search for sequences homologous to the DNA DSB site as well as in one of the key steps of the recombination process, strand exchange.

Anti-recombinase activity of Srs2

The role of the Srs2 helicase in recombination was first described when mutations in *srs2* were found to suppress the severe UV sensitivity induced by *rad6* and *rad18* mutations that affect post-replication repair (PRR) (Lawrence & Christensen, 1979; Aboussekhra et al., 1989; Schiestl et al., 1990; Rong et al., 1991). As this suppression was found to be *RAD52*-dependent, it was proposed that, in the absence of Srs2, some DNA lesions are channeled from the PRR pathway to HR (Aboussekhra et al., 1989; Schiestl et al., 1990; Rong et al., 1991). Accordingly, one

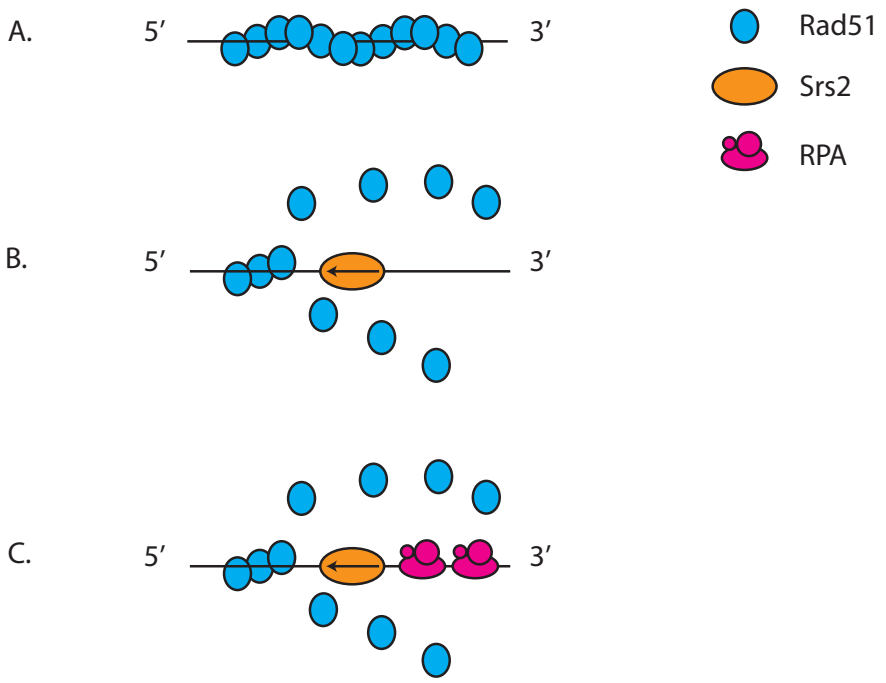

Figure 3.9. Anti-recombinase activity of Srs2. (A) In the absence of Srs2, Rad51 forms a filament on ssDNA. (B) Srs2 disrupts the Rad51 filament and releases the ssDNA. (C) RPA binds the Srs2-released ssDNA to avoid re-nucleation of Rad51. Figure adapted from Macris & Sung (2005), based on results by Krejci et al. (2003) and Veaute et al. (2003).

of the roles of Srs2 in the cell is to ensure that such lesions do not enter the DSB repair pathway. Studies of *srs2* diploids showed that they are sensitive to DNA damage induced by methyl methanesulfonate (MMS) and search for suppressors of this sensitivity revealed several *rad51* alleles (Aboussekhra et al., 1992). Interestingly, all the *rad51* alleles isolated from this screen were semidominant suggesting that suppression of the MMS sensitivity in *srs2* mutant strains requires decreased but not abolished HR activity (Aboussekhra et al., 1992). Supporting the idea of a role of Srs2 in HR, studies by (Milne et al., 1995) and (Schild, 1995) showed that the MMS sensitivity of a number of *rad52* mutations could be suppressed by deletion of *srs2*. Interestingly, most of these *rad52* mutations were found to map in or lack the C-terminal region of the protein, which contains the Rad51 binding domain. Accordingly, these mutations were also shown to be suppressed by overexpression of *RAD51*, suggesting that deleting *srs2* could have an influence on the amounts of Rad51 in the cell (Milne et al., 1995; Schild, 1995). However, in 2003, Srs2 was shown to physically interact with Rad51 and to act as a negative regulator of HR by disrupting the Rad51 nucleoprotein filament (Krejci et al., 2003; Veaute et al., 2003). Using biochemical analyses and electron microscopy, these groups showed that Srs2 displaces Rad51 thus releasing ssDNA that is immediately covered by RPA to avoid re-nulceation of Rad51 (Figure 3.9, B and C). Furthermore, us-

ing Srs2 variants that lack ATPase activity, Krejci et al. (2004) showed that this process requires ATP hydrolysis. Accordingly, Srs2 appears to act as a negative regulator of HR by displacing Rad51 from the presynaptic filament. By this process, Srs2 is believed to prevent initiation of untimely recombination events that can occur if the Rad51 nucleoprotein filament is formed on ssDNA intermediates that are not destined to HR . This has been proposed to be the case for ssDNA gaps formed at stalled replication forks (Fabre et al., 2002). Accordingly, the observed recruitment of Srs2 to stalled replication forks could prevent the formation of Rad51 filament on the ssDNA gaps produced at this type of lesions (Papouli et al., 2005; Pfander et al., 2005).

In chapter 5 of this thesis, I present data that suggest a novel role of Srs2 in the second strand capture step of the DNA DSB repair process.

Homology search and strand exchange: a close Rad51/Rad54 collaboration

Consistent with the classical DSB repair model by HR where resected ends of the break invade a homologous template, Mazin et al. (2000) showed that Rad51's preferred DNA substrate consists of dsDNA with ssDNA tails. In *S. cerevisiae*, Rad51 binding to ssDNA and strand exchange require ATP consistent with the fact that the Rad51 ATPase activity is DNA-dependent (De Zutter & Knight, 1999; Sung, 1994). How the search for a homologous sequence through the entire genome is performed has not been well studied in higher eukaryotes but studies of the Rad51 bacterial homologue RecA propose models where homology search is rapid and involves random collision with and unwinding of the target duplex DNA together with local strand exchange (Cunningham et al., 1979; Shibata et al., 1979; Honigberg et al., 1986; Pinsince & Griffith, 1992; Rould et al., 1992; Ellouze et al., 1997; Adzuma, 1998; Cai et al., 2001; Sagi et al., 2006). Specifically, this has been proposed to occur in two ways. One hypothesis is the formation of a "triple helix" intermediate by non-Watson-Crick bonding between the RecA-bound ssDNA and dsDNA (Hsieh et al., 1990; Rao & Radding, 1993). Another hypothesis is a "base-flipping" model where the complex between ss- and ds-DNA is formed by rotation of bases (Adzuma, 1992; Nishinaka et al., 1998). Once homology has been located, strand exchange occurs between the nucleoprotein filament and the homologous repair template. Using a D-loop assay, where a D-loop structure is produced when a single-stranded molecule invades circular dsDNA, Petukhova et al. (1998, 2000) showed that D-loop formation by the Rad51 filament is strongly promoted by the addition of Rad54. Other studies describe what seems to appear as a close collaboration between the Rad51 filament and Rad54. Indeed, Rad54 dynamically remodels and unwinds dsDNA, a reaction requiring ATP, in order to facilitate the access of Rad51 to the DNA and promote pairing (Petukhova et al., 1999b; Mazin et al., 2000; Petukhova et al., 2000; Sigurdsson et al., 2002). Remodeling of dsDNA by Rad54's ATPase activity has also been shown to be stimulated by the Rad51-ssDNA complex (Van Komen et al., 2000).

In agreement with this, Alexeev et al. (2003) showed that Rad54 catalyzes the redistribution of nucleosomes by sliding them along DNA and that this reaction is stimulated by the Rad51 filament. Finally, Rad54 has been shown to promote the extension of heteroduplex DNA after the Rad51 filament has primed to a homologous repair sequence (Solinger et al., 2001; Solinger & Heyer, 2001). Rad54 is also involved in ending the strand invasion reaction by preferentially binding to the end of the dsDNA heteroduplex-Rad51 filament complex and removing Rad51 from the DNA strands (Kiianitsa et al., 2002; Solinger et al., 2002; Kiianitsa et al., 2006).

3.2.3 In charge of annealing: Rad52

In *S. cerevisiae*, deletion of *RAD52* leads to the most severe phenotype of all the *RAD52* epistasis group deletion mutant strains. *rad52* mutant strains are extremely sensitive to DNA damaging agents as they are severely impaired in their ability to repair DNA DSBs by gene conversion, BIR and SSA. This shows that Rad52 is a key protein involved in all homologous recombination processes in *S. cerevisiae*.

Structure of the Rad52 protein

RAD52 encodes a 504 amino acid-long protein (Adzuma et al., 1984). However, it has recently been shown that perfectly functional Rad52 protein species are formed when translation is initiated from either of the last three of the five putative start sites of *RAD52* (Antunez de Mayolo et al., 2006). If the third putative start codon is considered, Rad52 is a 471 amino acid protein with a predicted molecular weight of 52 kDa (Shinohara et al., 1998). When observed on sodium dodecyl sulfate (SDS)-polyacrylamide gel electrophoresis, purified Rad52 has an apparent molecular weight of 56 kDa (Shinohara et al., 1998). HsRad52 molecules can self-associate via a self-association domain mapped between amino acid 65 and 165 of the N-terminal domain of the protein (Shen et al., 1996b). This self-association domain has not been mapped in yeast but as the N-terminal of Rad52 is well conserved from yeast to human, it is generally accepted that ScRad52 self-association also occurs through its N-terminal domain. Using electron microscopy, Shinohara et al. (1998), Van Dyck et al. (1998), Ranatunga et al. (2001) and Stasiak et al. (2000) showed that both yeast and human Rad52 proteins are multimers that form ring-like structures. Stasiak et al. (2000) also showed that the rings formed by HsRad52 were heptameric with a large central channel. Based on their results, Ranatunga et al. (2001) proposed the existence of a second self-association domain situated in the C-terminal part of Rad52. They therefore concluded that Rad52 must have two modes of self-association: the assembly of Rad52 monomers into rings driven by the N-terminus of Rad52 and the assembly of these rings into higher-order multimers carried out by the C-terminus of the protein. Kagawa et al. (2002) and Singleton et al. (2002) resolved the crystal structure of the HsRad52 N-terminus and

discovered an undecameric ring with a mushroom-like structure (see Figure 3.10). The stem, composed of highly conserved hydrophobic residues, is crowned by a domed cap with an underlying positively charged groove. Some amino acids in this groove were shown to be essential for ss- and ds-DNA binding (Kagawa et al., 2002).

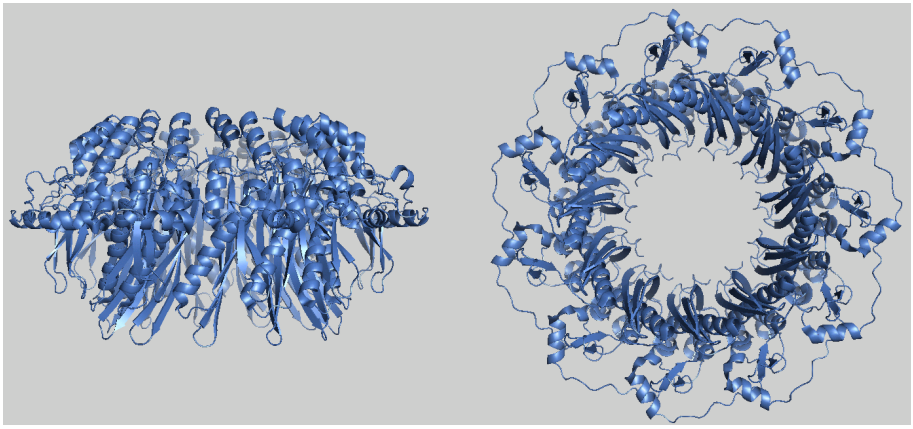

Figure 3.10. Side and bottom views of the predicted undecameric structure of the N-terminal of Rad52. These pictures were made using the PyMOL freeware and the Protein Data Bank (PDB) file "1KN0" deposited by Kagawa et al. (2002). The PDB file was retrieved from http://www.rcsb.org/pdb/home/home.do

DNA-binding and annealing

The Rad52 DNA-binding domain resides in the evolutionary conserved N-terminal part of the molecule (Mortensen et al., 1996). A study of mutations located in this domain that impair DNA binding as well as a discussion on when DNA binding by Rad52 N-terminal is required during DNA DSB repair is presented in Chapter 5. Rad52 binds both ds and ssDNA, with a higher affinity for the latter, and promotes annealing between complementary ssDNA molecules in vitro (Mortensen et al., 1996; Reddy et al., 1997; Shinohara et al., 1998; Kagawa et al., 2001). Under the electron microscope, the structure formed between ssDNA and Rad52 has been described as having a "beads on a string" appearance with Rad52 molecules distributed along the DNA (Van Dyck et al., 1998) (see Figure 3.11). Using the same technique, Van Dyck et al. (2001) directly visualized Rad52 bound to resected DNA tails and how Rad52 can anneal complementary tails to form large heteroduplex DNA-protein complexes. Rad52-mediated annealing can be enhanced by RPA which is known to avoid the formation of secondary structures in ssDNA but also interacts with Rad52 in a species-specific manner suggesting a more complex role of RPA in the annealing reaction (Shinohara et al., 1998; Sugiyama et al., 1998).

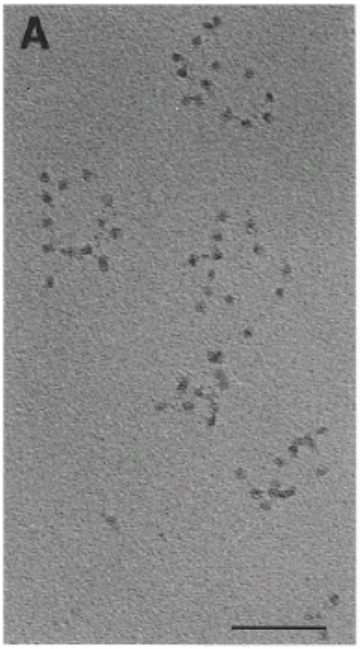

Figure 3.11. Human Rad52 bound to ssDNA as observed under the electron microscope by Van Dyck et al. (1998). As mentioned by the authors, the Rad52 molecules appear as beads along the ssDNA string. Picture from Van Dyck et al. (1998).

Strand exchange mediator

As mentioned previously, Rad52 stimulates the Rad51-mediated strand exchange reaction by removing RPA from ssDNA while simultaneously replacing it by Rad51. A less studied function of Rad52 is its recombinase activities. Kumar & Gupta (2004) show that HsRad52 itself is able to promote a strand exchange reaction among oligonucleotide substrates. Similar results were obtained by Bi et al. (2004) for both human and yeast Rad52 who also showed that this activity was promoted by amino acids 1 to 273 of the N-terminal of HsRad52.

Protein Partners of Rad52

As mentioned above, Rad52 is believed to mediate Rad51 filament assembly by removing RPA from the ssDNA while simultaneously replacing it by Rad51. Such hypothesis is further strengthened by the fact that the Rad52 physically interacts with both Rad51 and RPA.

Rad52 interacts with Rad51 through its C-terminal domain (Milne & Weaver, 1993; Shen et al., 1996a; Shinohara & Ogawa, 1998). In ScRad52, amino acids 409 to 420 have been shown to be indispensable for interaction with Rad51 and a Rad52 mutant lacking four amino acids within this region (409 to 412) was shown to be unable to bind Rad51 (Krejci et al., 2002). Interestingly, while it behaved as wild-type Rad52 in DNA binding and RPA interaction assays, the Rad52-Δ409-412 mutant protein lacked mediator function in strand exchange assays. Accordingly, strains carrying this deletion show a 4-fold reduction in in-

terchromosomal heteroallelic recombination compared to wild-type and are sensitive to γ-ray irradiation. This sensitivity can be complemented by Rad51 overexpression which underlines the physiological importance of the Rad51-Rad52 interaction during DNA DSB repair. On the other hand, meiotic processes seem unaffected by the lack of Rad51-Rad52 interaction in this mutant showing that this is not a requirement for completion of meiosis in *S. cerevisiae* (Krejci et al., 2002).

Rad52 also interacts physically with RPA in both human and yeast (Park et al., 1996; Hays et al., 1998; Shinohara et al., 1998). RPA is a protein complex composed of three subunits of 70, 34 and 14 kDa, encoded by *RFA1*, *RFA2* and *RFA3*, respectively. Deletion of each one of these genes is lethal in *S. cerevisiae* as RPA is essential for DNA replication (Heyer et al., 1990; Brill & Stillman, 1991). By two-hybrid analysis, Hays et al. (1998) showed that ScRad52 interacts with all the RPA subunits and that interaction with the large subunit of RPA, but not with the medium-sized subunit, was mediated by the N-terminal region of Rad52. In contrast, HsRad52 has been shown to interact directly with RPA's 34-kDa subunit and Park et al. (1996) pinpointed the central 221-280 amino acid domain of HsRad52 as being responsible for mediating this interaction. Moreover, this group also demonstrated that this interaction was physiologically relevant as cells expressing Rad52 proteins lacking the RPA-interaction domain failed to induce homologous recombination.

Rad59 is a 26-kDa protein which is often structurally described as a truncated version of Rad52. It's N-terminal domain resembles the one of Rad52 but it lacks the C-terminal domain (Bai & Symington, 1996). Physical interaction between Rad59 and Rad52 has been shown by yeast two-hybrid and co-immunoprecipitation, suggesting the possible formation of heteromeric Rad52-Rad59 ring structures (Davis & Symington, 2001). Based on several observations, it was proposed that Rad52 and Rad59 could have similar or overlapping functions. Indeed, like Rad52, Rad59 has been shown to binds both ss and dsDNA as well as to promote annealing of complementary ssDNA (Petukhova et al., 1999a; Davis & Symington, 2001). Rad59-mediated annealing of ssDNA is however not enhanced by RPA (Petukhova et al., 1999a). Recently, Wu et al. (2006a) showed that ScRad52 and ScRad59 bind and protect dsDNA ends and internal sequences equally well which suggests that they both act at similar steps of the DSB repair process, possibly after DSB end processing. In *S. cerevisiae*, deletion of *RAD59* only results in a mild recombination phenotype that can be rescued by *RAD52* overexpression (Bai & Symington, 1996). Interestingly, some *rad52* mutations (*rad52*-R70K, *rad52* Class E mutants) have been shown to only present a phenotype in the absence of Rad59, suggesting that the two proteins do have overlapping functions and that Rad59 can substitute Rad52 in some cases (Bai et al., 1999; Feng et al., 2007).

However, despite their similarities, Rad59 is unable to substitute for Rad52 in cases such as Rad51-independent recombination or interchromosomal heteroallelic recombination (Bai & Symington, 1996;

Davis & Symington, 2001; Lettier et al., 2006). Importantly, Rad59-YFP fails to localize to the nucleus in the absence of Rad52 showing that Rad52 is required for the nuclear transport of Rad59 (Lisby et al., 2004). Recently, in a study using chimeras of Rad52 and Rad59, Feng et al. (2007) showed that the N-terminal domain of Rad52 possesses functions that cannot be fulfilled by Rad59. This could for example be the Rad52 DNA-binding activity as overexpression of Rad59 has no effect on the MMS sensitivity of *rad52* mutants impaired in this activity (see Chapter 5). Recently, Wu et al. (2006b) showed that although Rad52 and Rad59 are both able to bind ssDNA, Rad59 is unable to bind an RPA-ssDNA complex. The DNA annealing abilities of Rad59 are also different of those of Rad52 as Rad59-promoted DNA annealing follows first-order reaction kinetics (second-order reaction kinetics for Rad52-promoted annealing).

Rad59 has been shown to be important for SSA especially when the length of homology between the repeats was limited (Bai et al., 1999; Sugawara et al., 2000). Later, Spell & Jinks-Robertson (2003) observed that deletion of *RAD59* led to a larger increase in homeologous recombination than in homologous recombination and suggested that this was due to the fact that Rad59-dependent repair required shorter regions of homology than for example Rad51-dependent repair. These results suggest that Rad59 could act as a helper of Rad52 when its annealing activity is required during the DNA DSB repair process. This is in agreement with the fact that both proteins have been shown to interact physically and that the Rad52-Rad59 complex can interact with Rad51 and RPA (Davis & Symington, 2001, 2003; Cortes-Ledesma et al., 2004). Finally, Rad59 has been shown to enhance Rad52-mediated DNA annealing, both in the absence and in the presence of RPA (Wu et al., 2006b).

Chapter 4

The Role of DNA double-strand breaks in spontaneous homologous recombination in *S. cerevisiae*

This chapter includes the original article "The Role of DNA double-strand breaks in spontaneous homologous recombination in *S. cerevisiae*" published in PLoS GENETICS in 2006. Supplementary information (Figures S1 and S2, Table S1 and Protocols) can be found at the end of the chapter.

The Role of DNA Double-Strand Breaks in Spontaneous Homologous Recombination in *S. cerevisiae*

Gaëlle Lettier[1], Qi Feng[2☯], Adriana Antúnez de Mayolo[2☯], Naz Erdeniz[2], Robert J. D. Reid[2], Michael Lisby[3], Uffe H. Mortensen[1*], Rodney Rothstein[2]

1 Center for Microbial Biotechnology, BioCentrum-DTU, Technical University of Denmark, Lyngby, Denmark, **2** Department of Genetics and Development, Columbia University Medical Center, New York, New York, United States of America, **3** Department of Genetics, Institute of Molecular Biology and Physiology, University of Copenhagen, Copenhagen, Denmark

Homologous recombination (HR) is a source of genomic instability and the loss of heterozygosity in mitotic cells. Since these events pose a severe health risk, it is important to understand the molecular events that cause spontaneous HR. In eukaryotes, high levels of HR are a normal feature of meiosis and result from the induction of a large number of DNA double-strand breaks (DSBs). By analogy, it is generally believed that the rare spontaneous mitotic HR events are due to repair of DNA DSBs that accidentally occur during mitotic growth. Here we provide the first direct evidence that most spontaneous mitotic HR in *Saccharomyces cerevisiae* is initiated by DNA lesions other than DSBs. Specifically, we describe a class of *rad52* mutants that are fully proficient in inter- and intra-chromosomal mitotic HR, yet at the same time fail to repair DNA DSBs. The conclusions are drawn from genetic analyses, evaluation of the consequences of DSB repair failure at the DNA level, and examination of the cellular re-localization of Rad51 and mutant Rad52 proteins after introduction of specific DSBs. In further support of our conclusions, we show that, as in wild-type strains, UV-irradiation induces HR in these *rad52* mutants, supporting the view that DNA nicks and single-stranded gaps, rather than DSBs, are major sources of spontaneous HR in mitotic yeast cells.

Citation: Lettier G, Feng Q, Antúnez de Mayolo A, Erdeniz N, Reid RJD, et al. (2006) The role of DNA double-strand breaks in spontaneous homologous recombination in *S. cerevisiae*. PLoS Genet 2(11): e194. doi:10.1371/journal.pgen.0020194

Introduction

Spontaneous mitotic homologous recombination (HR) plays an important role in securing the integrity of the genome [1–3]. On the other hand, this process may lead to loss of heterozygosity, which plays a major role in tumorigenesis in higher eukaryotes. For these reasons, it is important to understand how spontaneous mitotic HR is initiated. Much of our understanding of how HR is initiated comes from meiotic studies. Here, the high level of HR is due to the programmed formation of a large number of DNA double-strand breaks (DSBs) [4]. These breaks are produced in early prophase by the coordinated action of a number of proteins including Spo11, which is believed to be directly responsible for strand cleavage [5–7]. Likewise, DSBs have been shown to promote HR in mitotic cells. For example, the well-characterized ability of haploid *Saccharomyces cerevisiae* cells to switch mating type is the result of an HR event that is initiated by a DSB produced by the HO-endonuclease [8]. More generally, γ-irradiation, which induces DSBs in the genome, increases the frequency of HR [3], and linear DNA molecules transformed into a cell may integrate into the genome via HR [9,10]. Importantly, both DSB repair and spontaneous HR are dependent on the activities encoded by the genes in the *RAD52* epistasis group [3], which strongly indicates that the two processes have a common biochemistry. It has therefore generally been assumed that the source of spontaneous HR is a DSB that occurs accidentally during the cell cycle. However, this assumption remains speculative as spontaneous HR is rare and the triggering lesion has never been identified [1]. It is known that repair of other types of lesions may result in HR. For example, HR is stimulated by UV-irradiation that mostly produces pyrimidine dimers [11,12]. Moreover, in *Escherichia coli* it has been demonstrated that single-stranded gaps are potent substrates for HR [13–16]. Although many different lesions have been shown to trigger HR, the nature of the molecular event(s) that causes most spontaneous mitotic HR remains unclear.

Rad52 is important for DSB repair and all types of HR in *S. cerevisiae*, and to understand the role of Rad52 in these processes we have previously performed a comprehensive alanine scan mutation study. This plasmid-based screen identified a class of nine *rad52* mutants (class C mutants) that are sensitive to γ-irradiation, yet maintain wild-type levels of mitotic HR [17]. This result suggests that the role of

Editor: James E. Haber, Brandeis University, United States of America

Received February 3, 2006; **Accepted** October 4, 2006; **Published** November 10, 2006

A previous version of this article appeared as an Early Online Release on October 5, 2006 (doi:10.1371/journal.pgen.0020194.eor).

Abbreviations: BIR, break-induced replication; CFP, cyan fluorescent protein; DSB, double-strand break; HR, homologous recombination; NHEJ, non-homologous end-joining; SSA, single-strand annealing; YFP, yellow fluorescent protein

* To whom correspondence should be addressed. E-mail: um@biocentrum.dtu.dk

☯ These authors contributed equally to this work.

Synopsis

The genome of any organism is constantly damaged as an inevitable result of its own metabolism and exposure to irradiation. For that reason all organisms have developed many DNA repair systems to cope with the different types of DNA damage that challenge the stability of their genomes during daily life. One of these repair mechanisms is based on homologous recombination (HR), which, as a side effect, may result in loss of heterozygosity. For example, if a diploid organism harbors one functional and one dysfunctional copy of an important gene, DNA repair by HR may lead to a cell where both copies are defective. Since loss of heterozygosity plays a major role in tumorigenesis in higher eukaryotes, it is important to understand what types of DNA damage trigger HR most efficiently. In this paper, the authors have used a yeast-based system to investigate this topic, and based on mutations that separate the functions of Rad52 (a protein that is essential for HR) they conclude that DNA double-strand breaks are not the lesions that initiate most HR, but rather it is due to DNA nicks and single-stranded DNA regions.

Rad52 in DSB repair and spontaneous HR can be separated. To investigate this possibility, we have introduced each of the nine separation-of-function *rad52* mutations into the genome of *S. cerevisiae* for further characterization. By analyzing the repair of different types of defined DSBs we have shown that *rad52* class C mutants indeed are defective in DSB repair and that repair is blocked at a stage after the recruitment of both Rad51 and mutant Rad52 to the break. In contrast, all class C mutants perform mitotic HR at wild-type or higher levels and this activity is independent of the presence of Rad59, a Rad52 paralog in *S. cerevisiae*. Interestingly, mitotic HR is efficiently induced by UV-irradiation in the *rad52* class C mutant strains. Together our results are consistent with a view that DNA nicks and single-stranded gaps, rather than DSBs, are major sources of spontaneous HR in mitotic yeast cells.

Results

Initial Characterization of *rad52* Separation-of-Function Mutants

Initially, we addressed the possibility that the *rad52* separation-of-function phenotype identified in our previous screen [17] was caused by the fact that all mutant Rad52 species were ectopically expressed from a plasmid. Therefore, we replaced the endogenous *RAD52* gene by each of the nine *rad52* class C alleles and the resulting strains were individually tested for their ability to repair γ-ray-induced DNA damage and to perform mitotic heteroallelic HR. First, we confirmed that all *rad52* class C mutant strains are γ-ray sensitive (Figure 1 and Table 1). In fact, most *rad52* class C mutant strains display sensitivities comparable to that measured for *rad52*Δ strains. Next, we confirmed that spontaneous HR occurs at a high rate in all *rad52* class C mutant strains. Hence, all diploid *rad52* class C mutant strains display high interchromosomal-heteroallelic HR rates (Table 2). In fact, four strains, *rad52-Y66A, -R70A, -W84A,* and -R*156A* are significantly hyper-recombinogenic (3- to 4-fold). Moreover, we measured the rate of HR between two directly repeated *leu2* heteroalleles, *leu2*-Δ*Eco*RI and *leu2*-Δ*Bst*EII in haploid strains (Table 2). In this assay, two *rad52* class C mutant strains, *rad52-R85A* and -*R156A,* produced HR rates identical to that obtained with wild-type strains. The remaining *rad52* class C mutant strains were slightly hypo-recombinogenic and the largest decrease, 3-fold, was observed for *rad52-C180A*. Importantly, even with *rad52-C180A* strains, the direct-repeat HR rate is 10-fold higher than that observed for *rad52*Δ strains. Taken together we have confirmed the separation of Rad52 functions in HR and γ-ray damage repair in strains where the *rad52* class C mutations are integrated at the *RAD52* locus.

The *rad52* Class C Mutant Phenotype Is Not Caused by Reduced Rad52 Protein Levels

The separation-of-function phenotype of *rad52* class C mutants could potentially be related to instability of the mutant proteins. For example, it could be argued that repair of γ-ray-induced damage requires more Rad52 protein compared to the amount required to maintain rare mitotic HR events. However, protein blot analysis showed that the Rad52 levels are slightly reduced, but none of these reductions are statistically different from the protein level found for wild-type strains (Table 2). Moreover, we have previously shown that γ-ray survival is reduced only 2- to 3-fold and HR 4-fold in strains, which produce 25% of the wild-type level of Rad52 protein [18]. Thus, the separation-of-function phenotype of *rad52* class C mutations cannot be explained by slightly lowered Rad52 protein concentrations.

Mitotic Recombination in *rad52* Class C Mutants Does Not Depend on Rad59

S. cerevisiae contains a truncated Rad52 paralog, Rad59. A mutation in *RAD52 (rad52-R70K)* has previously been described to cause a synthetic defect with *rad59*Δ suggesting that the two proteins have overlapping functions [19,20]. All of the *rad52* class C mutations are located in a region of Rad52 that is homologous to Rad59. Thus, we investigated whether the ability of the *rad52* class C mutants to perform HR was due to the ability of Rad59 to substitute for an impaired Rad52 function. However, the rates of interchromosomal heteroallelic HR obtained for wild-type and all the *rad52* class C mutant strains in the absence of Rad59 are mostly indistinguishable from the rates obtained in its presence (Table 2). In fact, three strains, *RAD52, rad52-Y66A,* and *rad52-W84A* show small, 1.5- to 2-fold, but significant, increases of the HR rate in the absence of Rad59.

rad52 Class C Mutant Strains Fail to Repair Defined DNA DSBs

It is generally assumed that the lethality of *rad52*Δ strains after exposure to γ-rays is the consequence of unrepaired DSBs. However, besides DSBs, γ-irradiation causes a variety of DNA modifications such as clustered base-modifications, abasic sites, and nicks, as well as DNA-DNA and DNA-protein crosslinks [21–24]. Repair of such lesions may rely on Rad52 functions that differ from those required for efficient DSB repair. It is therefore possible that *rad52* class C mutant strains are capable of repairing DSBs, but die after γ-irradiation because of their inability to repair other types of lesions. Assuming that a DSB is required to initiate HR, this scenario would explain why *rad52* class C mutants can be γ-ray sensitive yet at the same time be HR-proficient. To explore this possibility, *rad52* class C mutant strains were investigated for their ability to repair and survive a single well-defined DSB. First, the ability of *rad52* class C mutants to

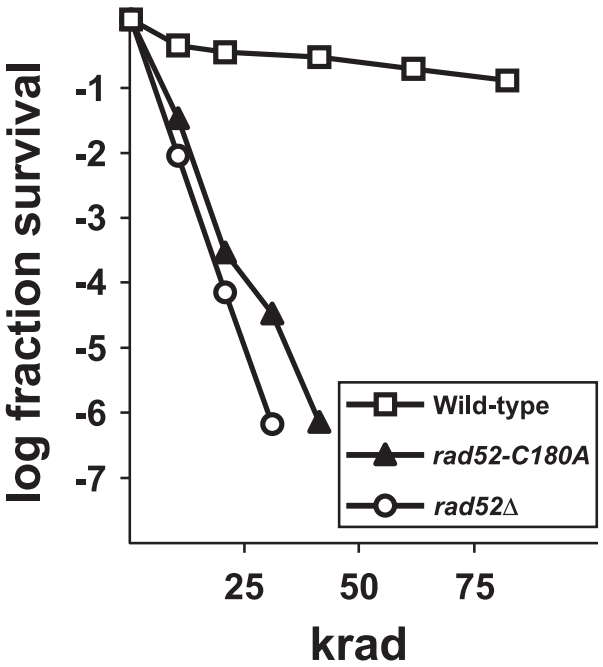

Figure 1. γ-Ray Sensitivity of *rad52-C180A, rad52*Δ, and Wild-Type Strains
doi:10.1371/journal.pgen.0020194.g001

catalyze plasmid gap repair was determined (Figure 2A). In wild-type strains, all transformants tested (20 out of 20, see Table 3) contained a plasmid that was sealed by HR using the genomic *trp1–1* allele as template (ten are shown in Figure 2B). In contrast, with *rad52* class C and *rad52*Δ mutant strains, the repair frequencies are reduced 10–100- and 250-fold, respectively, compared to the efficiency obtained with wild-type strains, indicating that plasmid re-circularization occurs inefficiently in these strains. The low repair frequencies in *rad52* class C and *rad52*Δ mutants are likely due to their inability to close a gapped plasmid by HR. Indeed, with the exception of *rad52-R70A,* the majority of the transformants tested contained plasmids that were generated by non-homologous end-joining (NHEJ) rather than by HR (Table 3). In addition, we obtained a few aberrant transformants with *rad52*Δ and *rad52* class C mutant strains that were not formed as the result of plasmid repair by simple NHEJ or plasmid-gap repair (Table 3). For these events, the PCR analysis produced either a band of a size that is significantly different from that expected if the two plasmid ends simply joined; hence, indicating a larger deletion/rearrangement event had taken place, or no PCR fragment could be recovered. For one mutant strain, *rad52-Y96A,* this class constitutes the major type of events.

Table 1. Effect of γ-Irradiation on *rad52* Mutant Strains

Allele	γ-Ray Sensitivity (LD37)[a]	% Cells Containing γ-Ray-Induced Rad52-Foci[b]	
		G1	S/G2/M
RAD52	52 ± 4	69	85
*rad52*Δ	1.9 ± 0.07	—	—
Y66A	4.9 ± 0.2	3	72
R70A	3.3 ± 0.09	6	73
W84A	2.3 ± 0.06	11	74
R85A	2.4 ± 0.17	7	50
Y96A	2.3 ± 0.19	11	76
R156A	5.3 ± 0.07	7	56
T163A	2.6 ± 0.19	8	60
C180A	2.4 ± 0.11	11	49
F186A	2.6 ± 0.14	2	67

[a]LD37 in krad, see Materials and Methods.
[b]Cells were exposed to 80 krad prior to microscopy.
doi:10.1371/journal.pgen.0020194.t001

We next investigated the ability of the *rad52* class C mutants to repair a single chromosomal DSB induced by the HO-endonuclease at the mating-type locus. To survive, a cell must repair the break by gene conversion using either *HML*α or *HMR***a** as template [25]. We measured the ability of all *rad52* class C mutants to survive and switch mating type after transient induction of the HO-endonuclease (Table 3). After this treatment, essentially all wild-type cells survive and approximately half of them switch mating type. In contrast, significant amounts of all *rad52*Δ and *rad52* class C mutant cells (20%–40%) die after HO-endonuclease induction indicating that they suffered a DNA DSB, which failed to be repaired. The surviving cells likely failed to produce a DSB at the *MAT* locus after induction as none of the *rad52*Δ survivors and only few 1% *(rad52-Y96A* and *rad52-C180A)* to 9% *(rad52-W84A)* of the *rad52* class C mutant survivors switched mating type. Thus, even a single DSB is inefficiently repaired in *rad52* class C mutant strains. We also compared the ability of wild-type, *rad52*Δ, and one of the *rad52* class C mutant strains, *rad52-C180A,* to survive sustained expression of the HO-endonuclease in a spot assay. For wild-type strains, continuous expression of the HO-endonuclease caused a 10-fold reduction in viability. In contrast, the viability of *rad52*-C180A and *rad52*Δ strains was reduced an additional three orders of magnitude (Figure S1).

We also investigated the ability of *rad52* class C mutants to repair a DSB induced by the HO-endonuclease between two directly repeated sequences (Figure 3A). In wild-type strains, such a DSB is preferentially and efficiently repaired via the single-strand-annealing (SSA) pathway where the break is sealed at the expense of the intervening sequence [26]. In agreement with this, most of the wild-type cells survive induction of the HO-endonuclease and 70% of the survivors lose the sequence between the two repeats indicating successful repair by SSA (Table 3). In contrast, the viability of all *rad52* class C mutant strains was reduced to a level similar to that obtained for *rad52*Δ strains (Table 3) and among the survivors only a few of the cells contained a deletion event (6%–12%). This result suggests that *rad52* class C mutants are defective in SSA. To investigate this possibility in more detail, the fate of the HO-induced break was determined at the DNA level for all *rad52* class C mutant strains. Specifically, genomic blot analysis was used to measure three different DNA species: intact DNA, cut DNA, and the repair product. Consistent with an earlier study [27], we observed that the cut DNA is efficiently repaired in more than 80% of the wild-type cells within 5 h. In contrast, *rad52*Δ strains repaired less than 3% of the cleaved DNA in a similar time span. This explains the high lethality in the absence of Rad52. By performing the same analysis for the *rad52* class C mutant strains, we find that they all fail to produce wild-type

Table 2. Effects of *rad52* Mutations on Rad52 Protein Levels, Inter- and Intrachromosomal Recombination, and Rad52 Focus Formation in Mitotic Cells

Allele	Protein Levels (% of Wild-Type)			Heteroallelic Recombination (Rate × 10^{-8})						Direct Repeat Recombination (Rate × 10^{-6})			Spontaneous Rad52 Focus (% Cells)	
				RAD59			*rad59*						G1	S/G2/M
RAD52	100	±	30	110	±	30[b]	220	±	27[d]	46	±	12[b]	0	14
rad52Δ		—		0.6	±	0.3[c]	1.8	±	0.5	1.5	±	0.4[c]	—	—
Y66A	83	±	15[a]	290	±	50[b,c]	350	±	30[d]	30	±	9.2[b,c]	4	59
R70A	48	±	14[a]	370	±	60[b,c]	340	±	60	20	±	6.8[b,c]	0	56
W84A	60	±	11[a]	330	±	40[b,c]	410	±	50[d]	20	±	5.6[b,c]	8	71
R85A	37	±	13[a]	130	±	30[b]	130	±	70	44	±	12[b]	0	66
Y96A	42	±	11[a]	150	±	40[b]	190	±	60	23	±	7.1[b,c]	4	75
R156A	62	±	1[a]	430	±	110[b,c]	410	±	40	32	±	8.6[b]	9	65
T163A	40	±	6[a]	120	±	20[b]	140	±	40	17	±	3.6[b,c]	6	62
C180A	71	±	1[a]	190	±	40[b]	150	±	30	14	±	3.2[b,c]	15	55
F186A	60	±	22[a]	240	±	100[b]	250	±	50	19	±	3.9[b]	2	56

[a] $p > 0.05$ *rad52* mutants versus wild-type.
[b] $p < 0.05$ wild-type or *rad52* class C mutant versus *rad52Δ*.
[c] $p < 0.05$ *rad52* mutants versus wild-type.
[d] $p < 0.05$ *RAD52* allele *RAD59* versus *RAD52* allele *rad59*.
doi:10.1371/journal.pgen.0020194.t002

levels of repaired DNA (Figure 3B and Table 3). In strains *rad52-Y66A, -R70A, -W84A, -R85A, -R156A,* and *-F186A* approximately 25% of the breaks are sealed to form a product, whereas in *rad52-Y96A, -T163A,* and *-C180A* approximately 10% of the breaks are repaired. Accordingly, most of the *rad52* class C mutant cells die after induction of the break, simply because they fail to join the resulting two ends. In addition, as is the case with *rad52*Δ strains, we note that cut DNA disappears as a function of time in *rad52* class C mutant strains despite the fact that no corresponding amount of product is being formed (Figure 3 and unpublished data). In *rad52*Δ strains, this phenomenon is due to the continuous degradation of the 5′-strand at the breaks. Eventually the single-stranded region expands to include the restriction enzyme, *Spe*I, cut site, which is used to liberate the detectable fragment for the genomic blot analysis. Accordingly, this fragment is shifted in the gel [26–28].

rad52 Class C Mutant Strains Are Sensitive to Camptothecin

A lesion similar to a DSB may also be formed if a cell replicates a nicked template since a free DNA end is formed when a replication fork collapses at a nick. The replication fork can be restored if the free DNA end invades a homologous sequence in a process that involves recombination. Unlike repair of a DSB, this event only involves single-end invasion [29,30]. To test whether this type of DNA lesion could account for the HR observed in *rad52* class C mutant strains, we determined their ability to survive exposure to the anti-tumor drug camptothecin. This drug stabilizes the covalent DNA-Top1 intermediate that forms during the catalytic DNA nicking-closing cycle of Top1 [31,32]. Accordingly, addition of camptothecin leads to the formation of stable nicks in the genome that may be converted into recombinogenic DNA ends when the genome is replicated [33]. At 0.5 μg/ml camptothecin, the viability of *rad52* class C and *rad52*Δ mutant strains is reduced 10- to 1,000-fold and 1,000-fold, respectively, compared to wild-type strains (Figure 4A, and unpublished data). Similar stable DNA nicks are generated in strains expressing *top1-T722A* since the nicking-closing equilibrium of this mutant is shifted towards nicking [34]. To substantiate the results obtained by exposing *rad52* class C mutants to camptothecin, we tested the ability of *rad52* class C mutant strains to survive expression of the *top1-T722A* mutant (Figure 4B). Plasmid-borne copies of *TOP1, top1-T722A,* or a vector control were transferred into haploid *RAD52, rad52*Δ, and *rad52* class C mutant strains by plasmoduction (see Materials and Methods). All strains tested were competent for plasmoduction as they took up the vector control and *TOP1* expression plasmids as indicated by growth on the selective media (Figure 4B). Consistent with previous results, the *top1-T722A*-containing plasmid could be transferred to wild-type strains, but not to *rad52*Δ strains [35], showing that *rad52*Δ strains do not survive DNA damage created by expression of the *top1-T722A* allele. As with *rad52*Δ strains, the *top1-T722A* plasmid failed to transfer to the *rad52* class C mutant strains as indicated by lack of growth on the selection plates (Figure 4B). Taken together, these data suggest that *rad52* class C mutant strains are deficient in repair of single-ended DSBs generated by a progressing replication fork.

rad52 Class C Mutant Strains Perform Break-Induced Replication with Reduced Efficiency

We also investigated the possibility that a selected *rad52* class C mutant, *rad52-C180A,* could rescue a linearized plasmid by a reaction that involves break-induced replication (BIR), by using a chromosome fragmentation assay. In this assay, one end of the plasmid contains TG_{1-3} repeats, which will be rescued by de novo telomere addition, the other end is rescued in a BIR event that involves one-ended invasion at the D8B region of Chromosome III [36,37]. Davis and Symington found that the efficiency of BIR in this assay is reduced at least 4,000-fold in *rad52*Δ strains, and in agreement with this we did not recover any transformants that result from BIR in the absence of Rad52. On the other hand,

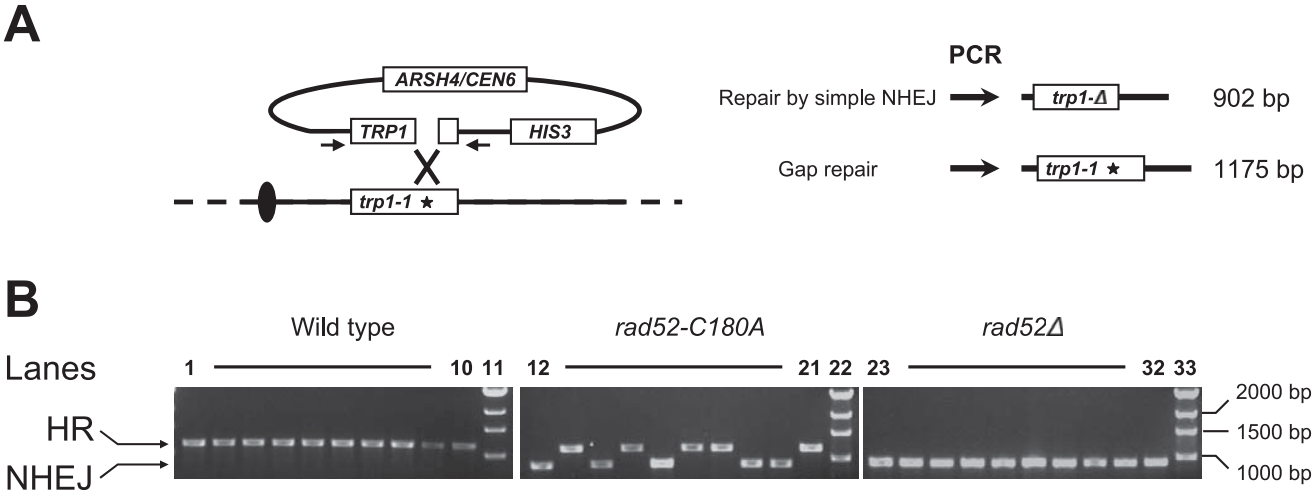

Figure 2. Gap Repair Is Impaired in *rad52* Class C Mutant Strains

(A) Graphical representation of the assay used to address the nature of gap closure events. Gapped pRS413-TRP1 repaired by HR. This event results in transfer of the *trp1–1* mutation in the genome to the plasmid. The position of the *trp1–1* mutation relative to the gapped *TRP1* plasmid-borne sequence is indicated by an asterisk. Repair by simple NHEJ (without any further rearrangement/deletion of plasmid DNA) results in a 273-bp deletion in *TRP1*. The two types of events were distinguished by PCR using a plasmid specific primer pair, indicated as small arrows. The PCR product sizes expected from transformants resulting from a gapped plasmid that has been repaired by HR and from one that has been closed by NHEJ are shown.

(B) Gel electrophoresis analysis of PCR fragments obtained from strains transformed with gapped pRS413-TRP1. Arrows point to the band sizes expected if the gapped plasmid has been repaired by HR or by NHEJ. Representative analyses of ten transformants obtained with wild-type strains (lanes 1–10), ten with *rad52-C180A* strains (lanes 12–21), and ten with *rad52*Δ strains (lanes 23–32). Sizes of relevant bands in the DNA marker (lane 11, 22, and 33) are indicated.

doi:10.1371/journal.pgen.0020194.g002

with *rad52-C180A* strains, we find that the BIR efficiency is only 2.7-fold reduced compared to wild-type indicating that the efficiency of a one-ended invasion is only mildly affected in class C mutants.

Rad52 Class C Mutant Protein Forms Spontaneous Foci during the Mitotic Cell Cycle

We have previously used a biologically functional Rad52-YFP (yellow fluorescent protein) fusion protein to monitor DNA repair in individual wild-type cells. This is possible as Rad52-YFP accumulates to form a bright focus at a lesion during S/G2/M-phase [38,39]. Like wild-type strains, a subset of S/G2/M-phase cells expressing class C mutant Rad52-YFP contains a spontaneous focus. This is consistent with *rad52* class C mutants being proficient for spontaneous HR (Table 2 and Figure 5A). In fact, the number of cells containing a repair focus is typically 5- to 6-fold higher than for wild-type strains. This phenomenon could be due to either more cells on average forming foci or to foci lasting longer in *rad52* class C mutant strains. To distinguish between these possibilities,

Table 3. Effects of *rad52* Mutations on the Repair Efficiency of Defined DNA DSBs

Allele	Re-Circularization of Linear Plasmid[a]																								
	Repair Frequency[b]	Mechanism[c]							Mating-Type Switching						*HO*-Induced SSA										
									Viability (%)			Efficiency (%)			Viability (%)			Deletions[d] (%)			Repair[e] (%)				
	(% of Wild-Type)	HR:NHEJ:A / Total																							
RAD52	100	20	:	0	:	0	/	20	98	±	4	45	±	2	87	±	13	70	±	10	84	±	4		
*rad52*Δ	0.4	0	:	16	:	1	/	17	69	±	6	0			26	±	8	5	±	2	3	±	1		
Y66A	10.4	7	:	9	:	4	/	20	66	±	1	4	±	0.3	40	±	5	10	±	1	24	±	8		
R70A	2.0	16	:	2	:	2	/	20	79	±	19	7	±	2	34	±	5	11	±	4	25	±	6		
W84A	3.5	5	:	14	:	1	/	20	59	±	16	9	±	3	29	±	4	8	±	2	24	±	10		
R85A	0.7	6	:	11	:	3	/	20	66	±	13	2	±	1	17	±	6	12	±	5	28	±	6		
Y96A	2.1	0	:	3	:	7	/	10	50	±	11	1	±	1	32	±	11	7	±	2	11	±	2		
R156A	10.4	3	:	15	:	2	/	20	63	±	10	9	±	3	29	±	11	10	±	2	23	±	6		
T163A	1.1	3	:	15	:	1	/	20	72	±	24	2	±	1	22	±	7	8	±	1	8	±	2		
C180A	1.7	8	:	11	:	1	/	20	63	±	9	1	±	0.4	20	±	7	7	±	2	12	±	2		
F186A	5.0	1	:	17	:	2	/	20	41	±	3	3	±	0.7	28	±	8	6	±	1	26	±	12		

[a]Transformation with gapped pRS413-TRP1.
[b]Transformation efficiency normalized to wild-type.
[c]Number of independent transformants generated by HR, NHEJ, or an aberrant event A/Total number of transformants analyzed.
[d]A comparison of the number of Ura^- cells present 60 min after *HO* induction with the number of Trp^+ cells present at the zero time point.
[e]The repair % was determined five h after *HO* induction by genomic blot analyses like those presented in Figure 3.

doi:10.1371/journal.pgen.0020194.t003

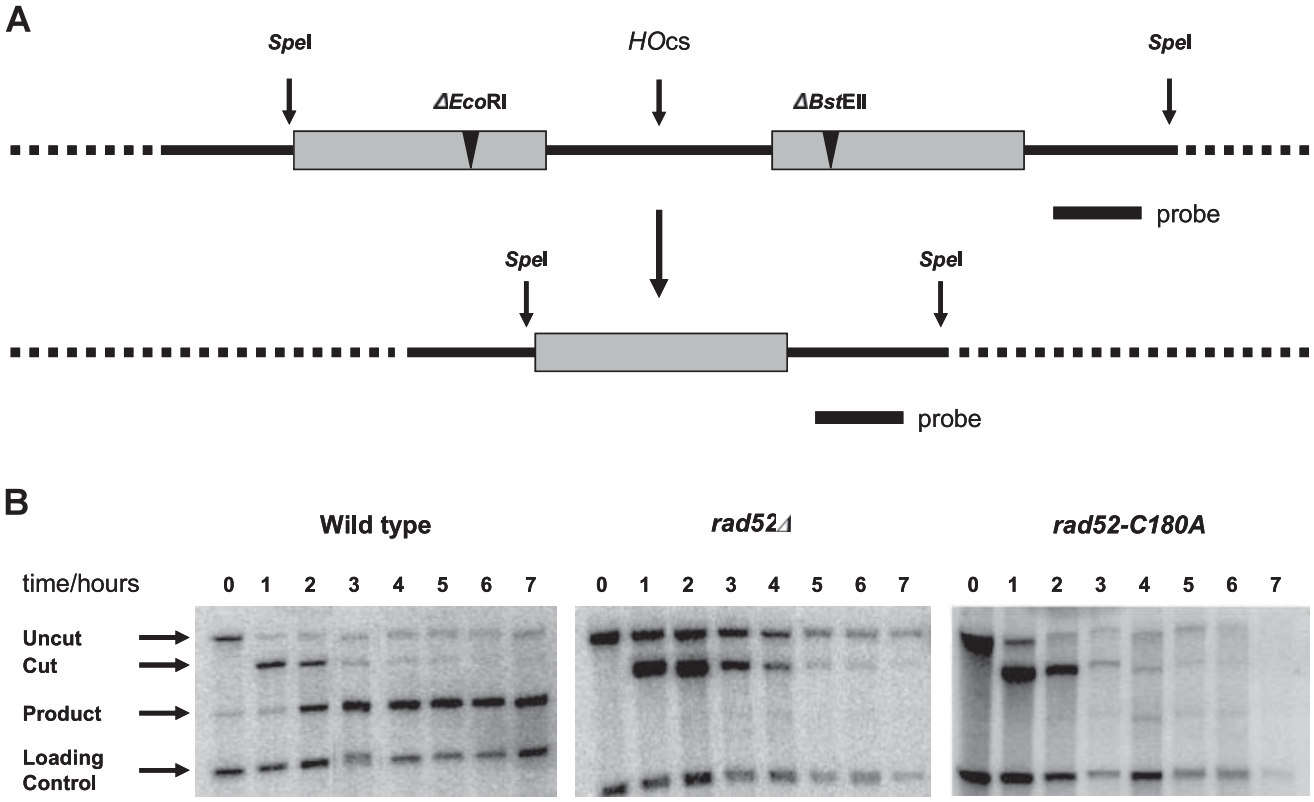

Figure 3. Kinetics of the Repair of a DSB Produced between Directly Repeated *leu2* Heteroalleles

(A) Graphical representation of the assay used to follow HO-endonuclease-induced direct-repeat HR. The positions of the *leu2*-Δ*Bst*EII and *leu2*-Δ*Eco*RI heteroalleles are indicated by black wedges. The position of the *HO* cut-site, *HO*cs, is indicated by an arrow. The product resulting from DSB repair by SSA is shown below the direct-repeat assay. Note that the product is given as a wild-type sequence, but it could also contain any combination of the *leu2*-Δ*Bst*EII and *leu2*-Δ*Eco*RI alleles, as the analysis performed here does not discriminate between these possibilities. Arrows labeled *Spe*I indicate the positions of the *Spe*I cut-sites used to release the region from its chromosomal context for genomic blot analysis. Horizontal bars represent the location of the probe used for genomic blot analysis.

(B) The DSB was produced by induction of the HO-endonuclease and repair was analyzed in three different strain backgrounds, wild-type, *rad52*Δ, and *rad52-C180A,* as indicated. In each strain, the kinetics of three DNA species in the process was followed: uncut DNA, cut DNA, and product. The positions of these species are indicated by arrows. A DNA fragment serving as loading control (see Materials and Methods) is also visualized. The number above each lane indicates the time point after induction of the HO-endonuclease in hours.

doi:10.1371/journal.pgen.0020194.g003

rad52-C180A-YFP was analyzed in more detail by time-lapse microscopy (Figure 5B). The results from this analysis suggest that repair in the *rad52-C180A-YFP* mutant strain is slower than in wild-type strains. Specifically, 50% of all repair foci are processed within 10 min in wild-type cells and 90% within 1 h. In comparison, *rad52-C180A-YFP* cells need approximately 1 and 6 h to process 50% and 90% of all repair foci, respectively. The longer duration of Rad52-C180A-YFP foci likely reflects slow repair. In most cells, Rad52-C180A-YFP foci eventually disappear and cell division proceeds as normal indicating that the spontaneous Rad52-C180A-CFP foci represent active repair of spontaneous DNA lesions and not inactive Rad52 aggregates. Overall, the percentage of cells forming foci per cell cycle is higher in *rad52-C180A* strains (76%) compared to wild-type strains (53%) indicating that the number of lesions is slightly increased in *rad52-C180A* strains or that some foci in wild-type cells are too short-lived to be registered in the analysis. Finally, unlike wild-type strains most of the *rad52* class C mutant strains (seven out of nine) contain Rad52-YFP foci at a low frequency in G1 cells. Since yeast has been shown to adapt to the DNA damage checkpoint at G2/M [40,41] such foci are likely the result of long-lasting Rad52 foci being transmitted into G1 cells after adaptation to the G2/M checkpoint.

A Rad52 Class C Mutant Protein and Rad51 Co-Localize at a Defined DNA DSB

The failure of *rad52* class C mutant strains to repair γ-ray-induced damage as well as defined DSBs could be explained if these lesions were never recognized by the mutant Rad52 species. To test this possibility, all class C *rad52-YFP* mutant strains were γ-irradiated with a dose of 80 krad to investigate whether this would induce class C Rad52-YFP focus formation (Table 1). As previously observed, un-irradiated wild-type G1 cells rarely, if ever, form repair foci. However, after irradiation, 69% of wild-type G1 cells display one or more bright foci [38]. This may represent an abnormal stress situation where the system that normally prevents Rad52-dependent DNA repair to occur in G1 is overwhelmed or bypassed. Interestingly, γ-irradiation did not increase the number of *rad52* class C mutant G1 cells containing a class C Rad52-YFP focus. In S/G2/M cells, which represent the population of cells where Rad52 dependent repair normally occurs, the number of wild-type cells that contain at least one

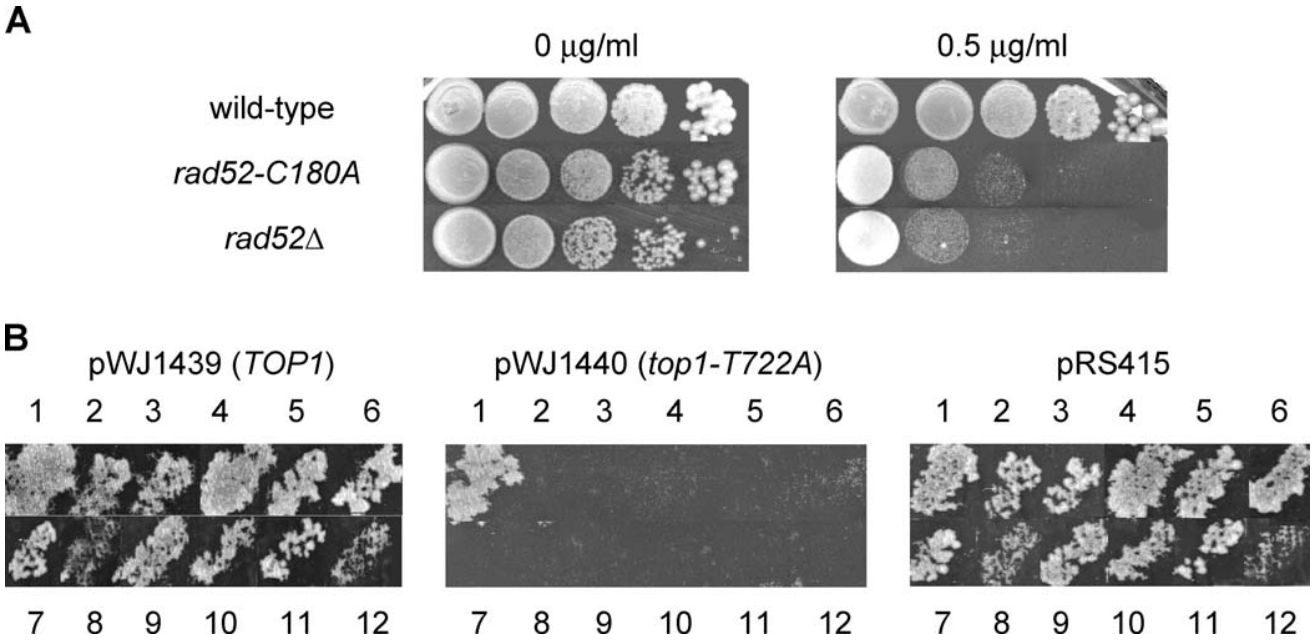

Figure 4. *rad52* Class C Mutant Strains Are Sensitive to Stable Topoisomerase-Induced DNA Nicks

(A) Serial 10-fold dilutions of wild-type, *rad52-C180A,* and *rad52* null strains were spotted on solid medium containing no camptothecin or 0.5 μg/ml camptothecin as indicated.

(B) pWJ1439 *(TOP1),* pWJ1440 *(top1-T722A),* and pRS415 were transferred to wild-type, *rad52*Δ, and all *rad52* class C mutant strains by plasmoduction as described in Materials and Methods. The positions of wild-type, *rad52*Δ, *rad52-Y66A, -R70A, -W84A, -R85A, -Y96A, -R156A, -T163A, -C180A,* and *-F186A* strains on selective plates are indicated by numbers: 1, (2 and 3), 4, 5, 6, 7, 8, 9, 10, 11, and 12, respectively.

doi:10.1371/journal.pgen.0020194.g004

Rad52-YFP focus increases 6-fold after γ-irradiation. In contrast, no significant increase is observed with *rad52* class C mutant cells (compare Tables 1 and 2). These results suggest that class C mutant Rad52-YFP proteins are not recruited to γ-ray-induced DSBs. However, this conclusion may be flawed because the majority of *rad52* class C mutant S/G2/M cells already contain a repair focus before irradiation making it hard to determine whether any additional foci were formed. We therefore decided to investigate whether a selected Rad52 class C mutant protein, Rad52-C180A-CFP (cyan fluorescent protein), is recruited to an HO-inducible cut-site. In strains expressing the lac-repressor fused to YFP, this *HO* cut-site is marked by a yellow dot in the nucleus as it is adjacent to an array of 256 copies of *lacO* (Figure 6A). This allows a Rad52 focus formed at the induced DSB to be distinguished from a focus at a spontaneous lesion. With wild-type cells, approximately 60% of the cells contain a Rad52 focus. This number roughly represents the induction efficiency, i.e., the fraction of cells where a DNA DSB was induced, as spontaneous foci are rare in a population of wild-type cells. Of the cells that contained a Rad52 focus after induction, 90% contained a Rad52 focus that co-localized with the induced DNA DSB. This confirms our previous observation that Rad52 is efficiently recruited to this break [39]. With *rad52-C180A-CFP* strains, Rad52-C180A-CFP foci co-localized with the labeled DNA DSB in 55% of the cases, showing that Rad52-C180A is also recruited to a defined DNA DSB. At first glance, it may seem that the recruitment efficiency of Rad52-C180A-CFP is somewhat reduced compared to wild-type Rad52-CFP. However, it is important to note that, unlike in wild-type, many *rad52-C180A-CFP* cells already contain a spontaneous focus before induction. If the DSB induction efficiency in the mutant is similar to that in wild-type (60%), a significant number of *rad52-C180A-CFP* cells containing a spontaneous focus may in fact not have received a DSB during induction. We therefore believe that 55% is an underestimate of the recruitment efficiency as these cells contribute to increase the total number of cells containing a focus after induction. As previously shown for wild-type strains, fortuitous co-localization of Rad52-C180A-CFP and the HO-induced break is less than 5% in control cells that do not express the HO-endonuclease and in cells where the HO-inducible DSB and the *lacO* array are placed on different chromosomes (Figure 6B and 6C).

Next, we investigated whether Rad51, which is required in the subsequent steps of the repair pathway, is also recruited to a specific DNA DSB in *rad52-C180A* strains. Specifically, co-localization of Rad52-C180A-YFP and Rad51-CFP was determined at a specific DNA DSB induced by the I-*Sce*I endonuclease. In a strain expressing the tetI-repressor fused to RFP (red fluorescent protein), this I-*Sce*I cut-site is marked by a red dot in the nucleus as it is adjacent to an array of 336 copies of *tetO* (Figure 7). Similar to above, approximately 55% of the wild-type cells contained a Rad52-YFP focus after induction. Of these cells, 95% contain a Rad52 focus that co-localized with the marked I-*Sce*I cut-site. Previously, Rad51 and Rad52 have been shown to co-localize at an HO-induced DSB at the *MAT* locus [42]. In agreement with this, we observed that the Rad52 foci that co-localized with an I-*Sce*I cut-site also co-localized with a Rad51-CFP focus in 95% of the cases (Figure 7), demonstrating the presence of both the repair proteins at the I-*Sce*I-induced DSB. Of the 56% *rad52-*

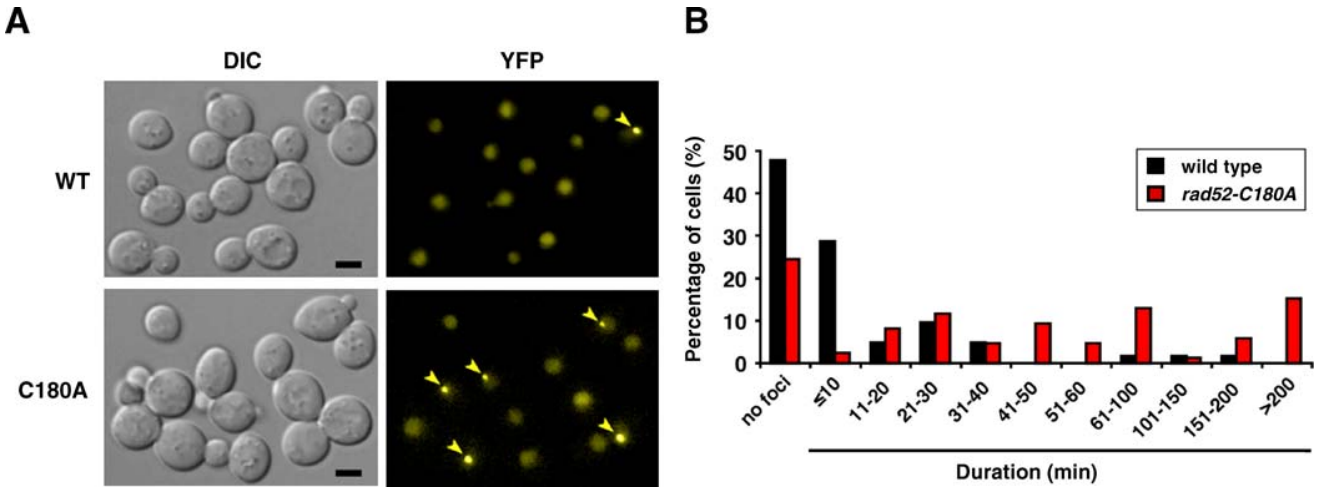

Figure 5. Duration of Spontaneous Rad52-YFP and Rad52-C180A-YFP Foci

(A) Rad52-YFP and Rad52-C180A-YFP foci are formed in small-budded cells in mitotically growing cultures. Arrowheads point to Rad52-YFP foci. Scale bar, 3 μm.

(B) The percentage of cells that do not develop a Rad52 focus during a cell cycle is shown in the left side of the histogram. The percentage of cells that do form a Rad52 focus is shown in the right side of the histogram as a distribution arranged according to the duration of the Rad52 focus observed in individual cells. Each column represents the percentage of cells that have turned the Rad52 focus over in the time frame indicated. Results from *RAD52* and *rad52-C180A* strains are shown as indicated. Median duration of Rad52 foci is 8 min for the wild-type and 57 min for *rad52-C180A*.

doi:10.1371/journal.pgen.0020194.g005

C180A-YFP cells that contained a Rad52-C180A-YFP focus, 46% of these foci co-localized with the I-*Sce*I cut-site. Similar to wild-type cells, 94% of the observed Rad52-C180A-YFP foci that co-localized with an I-*Sce*I cut-site also co-localized with a Rad51-CFP focus. These results show that Rad51 is efficiently recruited to a repair focus at a defined DNA DSB in a *rad52-C180A* strain.

Homologous Recombination Is Efficiently Induced by UV-Irradiation in *rad52* Class C Mutant Strains

The fact that *rad52* class C mutant strains fail to repair DSBs, yet efficiently produce recombinants by HR, prompted us to look for another type of lesion that could induce HR in these mutants. It is well known that HR is stimulated by UV-irradiation [11], which produces DNA lesions that mostly consist of pyrimidine dimers and pyrimidine adducts [12]. To investigate whether UV-rays can induce HR in *rad52* class C mutant strains, the mutants were irradiated by a dose that resulted in 91% viability for wild-type and 15% for *rad52*Δ strains (Table 4). Although rare, DSBs may form as the result of bi-stranded and clustered UV-ray-induced damage [43] and the higher lethality observed for *rad52*Δ strains compared to wild-type strains may be due to the failure of *rad52*Δ strains to repair these DSBs. In agreement with this view, the UV sensitivities measured for *rad52* class C mutant strains, which also fail to repair DSBs, are similar to that obtained for *rad52*Δ cells. At this UV dose, the frequency of heteroallelic interchromosomal HR is increased 410-fold in wild-type strains compared to the spontaneous HR rate (Table 4). Similar stimulations of HR, 230-fold *(rad52-R70A)* to 800-fold *(rad52-T163A),* relative to the spontaneous rates of HR, were observed for all *rad52* class C mutant strains. Importantly, the absolute HR frequencies obtained for most of the *rad52* class C mutant strains after UV irradiation are higher (3.4-fold in the case of *rad52-Y66A*) than the HR frequency obtained with wild-type strains (Table 4). We note that prototroph formation is also strongly stimulated in *rad52*Δ strains. Such prototrophs, which are formed independently of Rad52, do not contribute significantly to the number of prototrophs obtained in wild-type and in class C mutant strains, as they occur at a frequency that is more than 100-fold lower than in these strains (Table 4). Rad52 independent prototroph formation has previously been observed in *rad52*Δ strains designed to detect heteroallelic HR [44]. However, in that study they were accounted for as being generated by UV-induced mutation rather than by HR. Since *rad52* is a known mutator [45], we investigated the ability of diploid wild-type, *rad52-C180A,* and *rad52*Δ strains, which are homozygous for either *leu2-*Δ*BstE*II or *leu2-*Δ*Eco*RI, for their ability to revert and form prototrophs after UV-irradiation. In all cases, no prototrophs were obtained when similar numbers of cells were plated. Hence, in the case of wild-type and *rad52-C180A,* reversion rates are at least three orders of magnitude lower than the rates of prototroph formation found for hetero-alleles. For *rad52*Δ strains it is at least 6-fold reduced. Hence, prototrophs obtained from heterozygous *leu2-*Δ*BstE*II/*leu2-*Δ*Eco*RI strains after UV irradiation are likely true recombinants. Together, these results show that some UV-induced DNA lesions are substrates for Rad52 class C mutant species in a process that yields viable recombinants at wild-type levels.

Discussion

In this study we have thoroughly characterized *rad52* class C mutants, which were originally identified in a plasmid-based screen as being γ-ray sensitive but proficient for HR [17]. First, we confirmed this separation-of-function phenotype in strains where the mutations were integrated into the *RAD52* locus. Next, we examined the separation-of-function pheno-

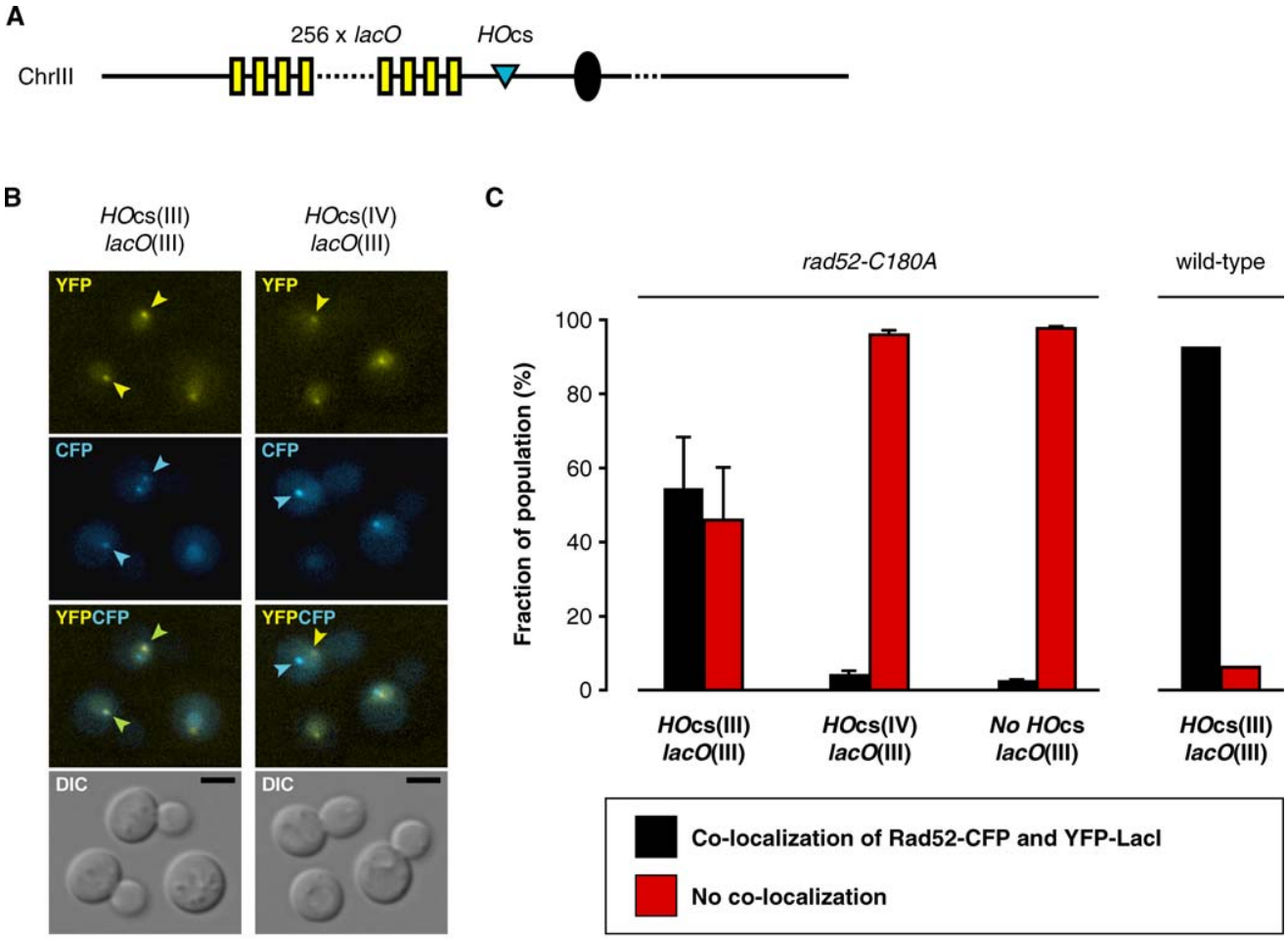

Figure 6. Rad52-C180A-CFP Is Recruited to a Specific DNA Double-Strand Break

(A) Assay in Chromosome III for visualizing an HO-endonuclease inducible DSB. Yellow boxes: *lacO* sites. Cyan triangle: HO cut-site (HOcs). Solid circle: centromere.

(B) Localization of a Rad52–CFP focus to an HO-endonuclease-induced DSB. The panels show YFP, CFP, CFP/YFP-merged, and DIC images of representative cells of a strain expressing Rad52-C180A-CFP in a strain with a *lacO* tandem array next to an HOcs on Chromosome III (left, strain W4021-20A) and in a strain with an HOcs on Chromosome III and a *lacO* tandem array on Chromosome IV (right, strain W4341-16A). The *lacO* tandem array is visualized by LacI-YFP as a yellow focus. The marked foci (arrowheads) in the left panels are examples of Rad52/LacI co-localization and the arrowheads in the example on the right indicate the absence of co-localization when the *lacO* elements and the HOcs are on different chromosomes. Scale bar, 3 μm.

(C) Quantitative analysis of co-localization between Rad52-CFP and YFP-LacI foci. Chromosomal locations of the HOcs and the *lacO* tandem array are given below the histogram columns. As a control, strain W4341-6D with no HOcs was analyzed. The wild-type dataset shown for comparison is from [39].

doi:10.1371/journal.pgen.0020194.g006

type in more detail. With respect to HR, we showed that the mitotic HR observed in *rad52* class C mutants is not due to a compensatory effect of Rad59. With respect to the inability of *rad52* class C mutants to repair DNA DSBs, we analyzed them in three different types of DSB repair assays, one measuring repair by SSA (direct-repeat recombination assay) and two measuring repair by gene conversion (mating-type switching and plasmid gap-repair assays) and firmly established that these mutants are defective in DSB repair by HR. Indeed, the repair efficiencies of the three different types of DSBs in the *rad52* class C mutants resemble that obtained in the absence of Rad52. Moreover, the results obtained with the plasmid gap-repair assay, where the individual contributions of HR and NHEJ to DSB repair can be evaluated, show that a gapped plasmid is repaired preferentially by NHEJ in *rad52* class C mutant strains rather than by HR as in wild-type strains. Thus, we conclude that *rad52* class C mutants fail to repair endonuclease-induced DSBs via mechanisms that require strand invasion of an intact homologous sequence as well as via a more simple mechanism where the ends can be joined by annealing.

Several of the Rad52 functions in DNA DSB repair could potentially be impaired by the *rad52* class C mutations as Rad52-mediated DNA DSB repair is a multi-step reaction that involves many activities, including binding to Rad51, Rad59, RP-A, and DNA [46–50]. All nine *rad52* class C mutations are situated in the evolutionarily conserved N-terminus of Rad52, which contains a DNA-binding domain, domains responsible for Rad52 self-association, and Rad59 binding [50–53]. However, an inspection of the three-dimen-

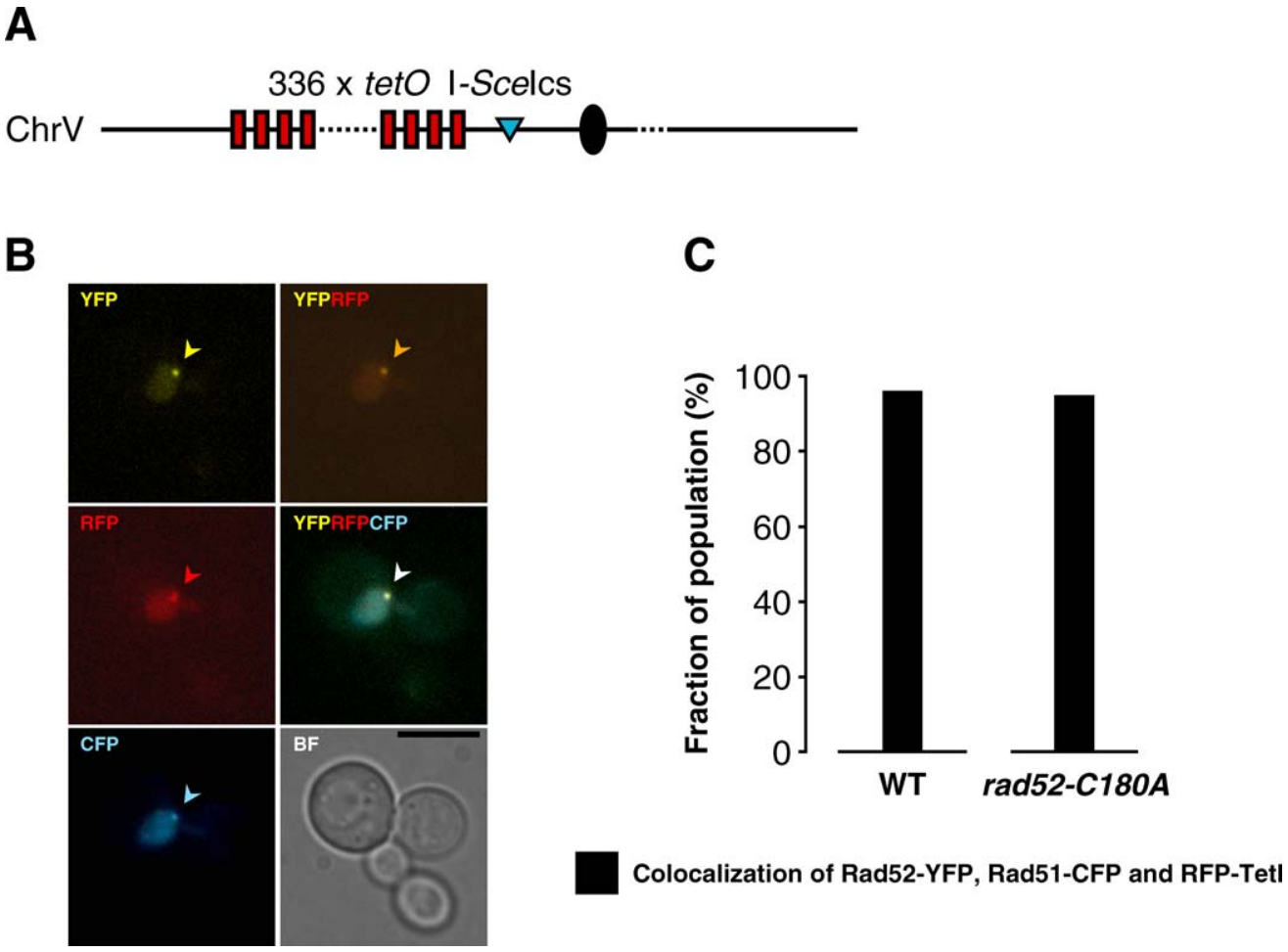

Figure 7. Rad51-CFP and Rad52-C180A-YFP Are Recruited to a Specific DNA DSB

(A) Assay in Chromosome V for visualizing an I-*Sce*I-endonuclease inducible DSB. Red boxes: *tetO* sites. Cyan triangle: I-*Sce*I cut-site (I-*Sce*Ics). Solid circle: centromere.

(B) Localization of Rad51-CFP and Rad52-C180A-YFP foci to an I-*Sce*I-endonuclease-induced DSB. The panels show YFP, CFP, RFP, RFP/YFP-merged, and CFP/RFP/YFP-merged, as well as a bright field image of representative cells containing Rad51-CFP and Rad52-C180A-YFP in a strain with a *tetO* tandem array next to an I-*Sce*Ics on Chromosome V. The *tetO* tandem array is visualized by TetI-RFP as a red focus. The Rad51-CFP, Rad52-YFP, and TetI-RFP foci are marked by arrowheads. Scale bar, 3 μm.

(C) Quantitative analysis of co-localization between Rad52-C180A-YFP/RFP–TetI foci and Rad51-CFP foci. The wild-type dataset is shown for comparison.

doi:10.1371/journal.pgen.0020194.g007

sional crystal structure of an N-terminal fragment of human Rad52 [52,54] showed that eight of the corresponding amino acid residues in the human Rad52 structure are located in, or close to, the putative DNA-binding groove (see Figure S2). The remaining amino acid residue, HsRad52-Y81 (ScRad52-Y96A) is buried beneath this groove. Moreover, four of the corresponding human Rad52 mutant species: HsRad52-Y51A (ScY66A), HsRad52-R55A (ScR70A), HsRad52-R70A (ScR85A), and HsRad52-Y81A (ScY96A) have been purified, and the three latter species show decreased affinity for single-stranded DNA [52,55]. Hence, the failure of Rad52 class C mutants to perform efficient DSB repair may likely be a consequence of impaired DNA-binding activity.

Defective DNA-binding of Rad52 may affect several stages of the DNA repair process, e.g., resection, homology search, strand invasion, and second-strand capture. The genomic blot analyses indicate that the nucleolytic processing of DSB ends is intact in *rad52* class C mutant strains. This is not surprising, as most models for DSB repair predict that the single-stranded DNA tails at the break are covered by RP-A before Rad52 is recruited [56–59]. In agreement with this view, we have previously shown that RP-A is recruited to a DSB in the absence of Rad52 [60]. In fact, if Rad52 class C mutants are defective in DNA binding, the inability to repair DNA DSBs could simply be explained by the failure of the mutant proteins to recognize and bind to these lesions. In contradiction to this view, we observed in two independent experiments that Rad52-C180A was recruited to defined DNA DSBs, one induced by the HO-endonuclease on Chromosome III and one induced by I-*Sce*I on Chromosome V. These results indicate that the DNA-binding domain in the Rad52 N-terminus is not required for Rad52 recruitment to the DNA lesion. This recruitment is then most easily explained by a scenario where Rad52 is attracted to the DNA lesion via its

Table 4. UV-Ray Survival and Induction of Mitotic Heteroallelic Inter-Chromosomal Recombination in *rad52* Mutant Strains

Allele	Survival (%)	Heteroallelic Recombination		
		Frequency $\times 10^{-5}$	Relative Fold-Up[a]	Fold Induction[b]
RAD52	91	41	1	410
rad52Δ	15	0.27	0.0066	450
Y66A	28	140	3.4	483
R70A	24	85	2.1	230
W84A	24	120	2.9	364
R85A	9	73	1.8	563
Y96A	37	40	0.98	267
R156A	28	100	2.4	233
T163A	12	96	2.3	800
C180A	11	100	2.4	526
F186A	14	110	2.7	458

[a]Frequency of UV-induced HR in a given strain relative to the frequency of UV-induced HR in wild-type strains.
[b]UV-induced recombination frequency relative to the corresponding rate of spontaneous recombination (see Table 2).
doi:10.1371/journal.pgen.0020194.t004

ability to interact with RP-A when the latter has formed a complex with single-stranded DNA at the DSB. This view is supported by the observation that Rad52-C180A, like wild-type Rad52, physically interacts with Rfa1 in a two-hybrid assay (unpublished data) and that no wild-type Rad52 focus is formed at a lesion in the absence of RP-A [60]. Accordingly, *rad52* class C mutations affect a function in Rad52 that is downstream of damage recognition. In fact, we have shown that the reaction is blocked after Rad51 has been recruited to the DNA DSB. However, our experiments do not show whether Rad51 or Rad52 are bound to the damaged DNA in the repair center. The possibility exists that they are just attracted to the lesion via protein-protein interactions. In this case, the failure of Rad52 class C mutants to efficiently bind DNA could result in its inability to mediate the replacement of RP-A by Rad51, thus impairing repair. If, on the other hand, a Rad51 filament is formed at the lesion in *rad52* class C mutant cells, we speculate that the DSB remains unrepaired either because the defective Rad52 DNA-binding activity impairs a Rad52-catalyzed homology search important for strand invasion or an annealing step important for second-strand capture. The latter view may explain the observation that the BIR efficiency is reduced only 3-fold in *rad52-C180A* strains as second-strand capture is not required in BIR.

It is generally believed that DSBs are the lesions that initiate spontaneous HR. However, here we show that nine *rad52* class C mutants are proficient for spontaneous inter- and intrachromosomal heteroallelic HR, but fail to repair different types of DSBs. Since Rad52 forms spontaneous repair foci during S-, but not during the G1-phase of the cell cycle [38], an alternative source of spontaneous HR could be recombinogenic DNA ends generated when a migrating replication fork converts a nick into a DSB. Such ends may be easier to repair than those induced by γ-irradiation and endonucleases as they require only a one-ended invasion of the intact strand to restore the replication fork. However, *rad52* class C mutant strains are sensitive to camptothecin and Top1-T722A expression. If the replication-induced ends in these experiments are equivalent to the DNA end rescued in the BIR experiment, these results may appear surprising as BIR is reduced only 3-fold in *rad52*-C180A compared to wild-type. However, unlike in the BIR experiment, multiple lesions are likely produced when Top1-T722A is expressed and in the presence of camptothecin, and strains with a weakened, but not abolished, ability to repair such lesions may die. The possibility therefore still remains that one-ended DNA breaks contribute to spontaneous HR. However, if this contribution was large, one would expect that even a small, but significant, reduction of the efficiency of one-ended DNA break repair should be reflected as reduced HR levels. Since this is not the case in the *rad52* class C mutants, replication-induced breaks are likely to initiate only a minor fraction of the spontaneous recombination events.

Based on the above, we find it unlikely that DSBs contribute substantially to the spontaneous HR observed for *rad52* class C mutant strains, since mutant cells only rarely survive even a single DSB. This view is supported by work from Fabre and colleagues based on their studies of *srs2* and *sgs1* strains [61]. They argued that *srs2 sgs1* synthetic lethality is due to a toxic recombination intermediate. If this intermediate were initiated by spontaneous DSBs, they must occur at a sufficiently high frequency to prevent propagation of *srs2 sgs1* strains. However, since *rad52 null lig4* as well as *rad52 null lig4 srs2 sgs1* strains, which cannot repair DSBs (i.e., no HR and no NHEJ), are viable, they conclude that DSBs cannot be initiating the frequent recombination intermediates that kill *srs2 sgs1* strains. In this context, it is important to note that around 75% of *rad52-C180A* cells spontaneously develop a Rad52-C180A focus during the cell cycle. If these foci solely represent attempts to repair DSBs in the genome, then *rad52-C180A* strains should be inviable due to their inability to repair DSBs. Moreover, we observe that Rad52-C180A foci are turned over before cell division, albeit at a slow rate, suggesting that repair of the spontaneous lesions is in fact completed.

We also note that some of the *rad52* class C mutants are hyperrecombinogenic. This behavior is similar to mutations in proteins of the Mre11-Rad50-Xrs2 complex (MRX), which act at an early stage of both HR and NHEJ [3], and also produce a hyper-recombination phenotype [62]. The high HR rate in these MRX mutants is thought to be due to a shift in the preferred repair template from the sister chromatid to the homologous chromosome, hence increasing the number of scorable recombinants [63]. We find that the median

lifetime of a Rad52 class C mutant repair focus is seven times longer than a wild-type Rad52 focus. This longer time frame of repair may increase the frequency of genetic exchange with the homolog. Alternatively, more recombinational lesions may be formed in *rad52* class C mutant strains. In fact, we observe that a larger number of cells spontaneously form Rad52 repair foci during the cell cycle in *rad52* class C mutant cells than in wild-type cells.

If only a minor fraction of spontaneous HR is initiated by DSBs, alternative lesions need to be considered as triggers for HR. In many of the original models for HR, DNA nicks and single-stranded gaps were proposed to initiate HR [64–66]. In the present study, we find that UV-irradiation leads to a dramatic increase in interchromosomal heteroallelic HR in *rad52* class C mutant strains. This is similar to what has been observed for wild-type strains. UV-rays mostly produce pyrimidine dimmers, and in the dark, the majority of these lesions are repaired by the nucleotide excision and base excision repair pathways. This type of repair produces nicks and single-stranded DNA gaps that could be recombinogenic. Moreover un-repaired pyrimidine dimers may lead to stalled replication forks and expose regions of single-stranded DNA. Single-stranded gaps are potent substrates for recombination in *E. coli* via the RecFOR pathway [13–16], and it is interesting to note that both the RecFOR complex and Rad52 mediate replacement of a single-strand binding protein, SSB and RP-A, respectively, to allow access of a protein with a strand invasion activity, RecA and Rad51, respectively, during DNA repair [16,56,57,59,67–69]. In addition, a stalled replication fork may produce a DNA substrate suitable for HR, if the fork is regressed into a "chicken foot" structure and the resulting DNA end processed by nucleases to produce a stretch of single-stranded DNA [30]. Considering that Rad52 repair foci form during DNA replication, such lesions are attractive candidates as substrates that elicit spontaneous HR.

Recently, it was demonstrated that nicked intermediates produced by mutant RAG proteins during V(D)J recombination can be channeled into HR [70]. Furthermore, the spectrum of spontaneous recombinants obtained in an assay that measures direct-repeat gene conversion and unequal sister-chromatid exchange in a mammalian cell line is similar to the spectrum obtained after addition of camptothecin, but different from the spectrum obtained after induction of recombination by the endonuclease I-*Sce*I [71]. Accordingly, lesions other than DSBs may also play a significant role in spontaneous HR in higher eukaryotes.

Materials and Methods

Genetic methods, strains, and plasmids. All media were prepared as described previously [72] with minor modifications as the synthetic medium contains twice the amount of leucine (60 mg/L). Standard genetic techniques were used to manipulate yeast strains [73] and transformations were performed according to [74]. All strains are derivatives of W303 [75] except that they are *RAD5* [76,77] and are listed in Table S1. Plasmids pJH283 [78] and pJH132 contain a GAL10::*HO* fusion in a *CEN4 ARS1*-based vector as well as a *TRP1* and a *URA3* marker for selection, respectively, and were kindly provided by J. Haber. For construction of pRS413-*TRP1,* a replicative *ARSH4/CEN6*-based plasmid, see Protocol S1. The plasmid CFV/D8B-tg was a kind gift from Dr. L. Symington.

Viability after γ- and UV-irradiation, HO-endonuclease induction, and exposure to camptothecin sensitivity. HO-endonuclease induction and γ- and UV-irradiation was performed as previously described [27,79], except UV-irradiation was performed by using a Stratalinker 2400 UV Crosslinker from Stratagene (La Jolla, California, United States) and cells were exposed to a dose of 50 J/m^2 at 254 nm. The dose rate of the γ-irradiator was 2.1 krad/min. The slope (α) of the resulting straight line can be used to calculate an LD37 value -ln(1/0.37)/lnα. The LD37 value represents the dose in krad necessary to induce a mean of one lethal hit per cell and was used to quantitatively compare survival of different strains. For details see Protocol S1. Camptothecin sensitivity was assayed by growing cells overnight to mid-log phase. A 10-fold serial dilution for each culture was made and spotted on two individual YPD plates containing 0 and 0.5 μg camptothecin, respectively. The ability of each strain to form colonies on each plate was evaluated after 3 d incubation at 30 °C.

Determination of spontaneous and induced mitotic recombination rates. Spontaneous mitotic HR between *leu2*-Δ*Eco*RI and *leu2*-Δ*Bst*EII heteroalleles was measured in diploid strains (interchromosomal HR) or in haploid strains (intrachromosomal HR) as previously described [27,79]. The intrachromosomal HR assay used contains the *leu2*-heteroalleles in the proximal configuration. HO-endonuclease-induced intrachromosomal direct-repeat HR was performed as previously described [27,79]. UV-induced interchromosomal *leu2*-Δ*Eco*RI/*leu2*-Δ*Bst*EII heteroallelic HR experiments were made in triplicates for each strain analyzed. The HR frequency after UV-irradiation was determined by dividing the total number of recombinants in the culture by the total corresponding number of surviving cells following irradiation.

Determination of BIR efficiency. The ability of selected strains to perform BIR was evaluated by a chromosome fragmentation assay [36,37] . Specifically, 1 μg of either intact or *Sna*BI linearized CFV/D8B-tg plasmid was transformed into relevant *ura3–1, ade2–1* strains. The BIR efficiency for each strain was determined as the number of BIR transformants obtained by linearized CFV/D8B-tg divided by the number of transformants obtained by uncut CFV/D8B-tg. BIR transformants were identified as Ura+ transformants with a low rate of red sectoring, in contrast to transformants resulting from plasmids that had simply re-circularized, which were characterized by a very high rate of red sectoring. For further details, see [36].

Plasmoduction. Details of the plasmoduction protocol for transferring plasmids into haploid strains by mating will be published elsewhere (RJDR and RR, unpublished data). In brief, the *MAT*α plasmid donor strain J1361 was transformed with pWJ1439 *(TOP1),* pWJ1440 *(top1-T722A),* or pRS415 (vector), and crossed to the *MAT***a** *rad52* class C mutants using a mating reaction that predominantly produces heterokaryons rather than diploids. Plasmid transfer into the recipient nucleus is selected for, while counter-selection is applied to the donor nucleus using 5-FOA and galactose. The selection plates were photographed after 3 d incubation at 30 °C to measure the growth of the recipient *MAT***a** strains containing the plasmids.

Gap-repair assay. To evaluate the gap-repair frequency, strains were transformed with circular and linear pRS413-*TRP1*. The linear substrate was made by cutting the *TRP1* marker in pRS413-*TRP1* with *Bsg*I and *Mfe*I. The resulting gap spans the region that harbors the *trp1–1* amber stop-codon mutation [80] in the genome. Transformants containing a plasmid sealed by HR or by NHEJ is therefore His+ Trp-. The repair frequency was calculated by dividing the number of His+ Trp- transformants with the number of transformants obtained in a parallel experiment using circular pRS413-*TRP1*. To determine whether the plasmid was sealed by NHEJ or by HR, a PCR assay using plasmid specific primers, T3 and T7 (5′-AATTAACCCTCACTAAAGGG-3′ and 5′-TAATACGACTCACTA-TAGGG-3′) was employed. Events generated by NHEJ and HR produces PCR fragments of approximately 902 bp and 1,175 bp, respectively. If the 1,175-bp fragment is generated by HR it contains *trp1–1*. This was verified by demonstrating the absence of a *Bsu36I* site in the 1,175-bp fragment.

Determination of Rad52 concentrations in RAD52 and *rad52* strains. Western blot analysis and subsequent quantification of band intensities were performed as previously described [50] except for minor modifications (see Protocol S1).

Yeast live cell imaging and fluorescence microscopy. Cells from liquid cultures were imaged by fluorescence microscopy as described previously [38,60]. Image acquisition times for Rad52-CFP and Rad52-YFP were 750 ms and 1,000 ms, respectively. Induction of Rad52-CFP and Rad52-YFP foci by γ-irradiation was done after the cells received a dose of 80 krad followed by 30 min of recovery in liquid SC medium at 23 °C. The fluorescently marked (YFP-LacI) chromosomal *HO* cut-site, the fluorescently marked (RFP-TetI) chromosomal I-*Sce*I cut-site, and induction of DSBs at these sequences by the HO- and I-*Sce*I endonucleases, respectively, were described previously [39]. The red fluorophore used in this study is the monomeric version of DsRed (mRFP1; [81]). The yellow- and blue-shifted enhanced variants of the

GFP gene and the DNA sequence encoding the monomeric version of DsRed (mRFP1) were generous gifts from R. Tsien (University of California, San Diego, California, United States).

Statistical methods. A Student's *t*-test was used to determine the significance of differences among the mutants versus wild-type and *rad52*Δ strains when comparing protein levels and mitotic and direct-repeat HR rates. For replacement events, the test of significance was determined using a *chi*-square analysis.

Supporting Information

Figure S1. Induced Mating-Type Switching Is Lethal in *rad52* Class C Mutant Strains

Found at doi:10.1371/journal.pgen.0020194.sg001 (392 KB DOC).

Figure S2. *rad52* Class C Mutations Are Located at the DNA-Binding Site of Rad52

Found at doi:10.1371/journal.pgen.0020194.sg002 (4.2 MB DOC).

Protocol S1. Supporting Protocol

Found at doi:10.1371/journal.pgen.0020194.sd001 (48 KB DOC).

Table S1. Strains Used in This Study

Found at doi:10.1371/journal.pgen.0020194.st001 (84 KB DOC).

Acknowledgments

Author contributions. GL, RJDR, ML, UHM, and RR conceived and designed the experiments. GL, QF, AAdM, NE, RJDR, ML, and UHM performed the experiments. GL, QF, AAdM, NE, RJDR, ML, and UHM analyzed the data. GL, QF, AAdM, and UHM contributed reagents/materials/analysis tools. GL, QF, ML, UHM, and RR wrote the paper.

Funding. This work was supported by the Danish Research Council for Technology and Production Sciences (UHM), the Alfred Benzon Foundation (UHM), the Hartmann Foundation (UHM), the Danish Biotech Research Academy, Forskerskole for Bioteknologi, the Technical University of Denmark for PhD grant (GL), the Danish Natural Science Research Council (ML), the Villum Kann Rasmussen Foundation (ML), and National Institutes of Health grants GM50237, GM67055, and HG02614 (RR).

Competing interests. The authors have declared that no competing interests exist.

References

1. Paques F, Haber JE (1999) Multiple pathways of recombination induced by double-strand breaks in *Saccharomyces cerevisiae*. Microbiol Mol Biol Rev 63: 349–404.
2. Thompson LH, Schild D (2002) Recombinational DNA repair and human disease. Mutat Res 509: 49–78.
3. Symington LS (2002) Role of RAD52 epistasis group genes in homologous recombination and double-strand break repair. Microbiol Mol Biol Rev 66: 630–670.
4. Sun H, Treco D, Schultes NP, Szostak JW (1989) Double-strand breaks at an initiation site for meiotic gene conversion. Nature 338: 87–90.
5. Keeney S, Giroux CN, Kleckner N (1997) Meiosis-specific DNA double-strand breaks are catalyzed by Spo11, a member of a widely conserved protein family. Cell 88: 375–384.
6. Bergerat A, de Massy B, Gadelle D, Varoutas PC, Nicolas A, et al. (1997) An atypical topoisomerase II from *Archaea* with implications for meiotic recombination. Nature 386: 414–417.
7. Keeney S (2001) Mechanism and control of meiotic recombination initiation. Curr Top Dev Biol 52: 1–53.
8. Haber JE (1992) Mating-type gene switching in *Saccharomyces cerevisiae*. Trends Genet 8: 446–452.
9. Rothstein RJ (1983) One-step gene disruption in yeast. In: Wu R, Grossman L, Moldave K, editors. Methods in enzymology. New York: Academic Press. pp. 202–211.
10. Orr-Weaver TL, Szostak JW, Rothstein RJ (1981) Yeast transformation: A model system for the study of recombination. Proc Natl Acad Sci U S A 78: 6354–6368.
11. Friedberg EC, Walker GC, Siede W (1995) DNA repair and mutagenesis. Washington (D. C.): American Society for Microbiology.
12. Sinha RP, Hader DP (2002) UV-induced DNA damage and repair: A review. Photochem Photobiol Sci 1: 225–236.
13. Grompone G, Sanchez N, Dusko ES, Michel B (2004) Requirement for RecFOR-mediated recombination in priA mutant. Mol Microbiol 52: 551–562.
14. Kuzminov A (1999) Recombinational repair of DNA damage in *Escherichia coli* and bacteriophage lambda. Microbiol Mol Biol Rev 63: 751–813.
15. Tseng YC, Hung JL, Wang TC (1994) Involvement of RecF pathway recombination genes in postreplication repair in UV-irradiated *Escherichia coli* cells. Mutat Res 315: 1–9.
16. Morimatsu K, Kowalczykowski SC (2003) RecFOR proteins load RecA protein onto gapped DNA to accelerate DNA strand exchange: A universal step of recombinational repair. Mol Cell 11: 1337–1347.
17. Mortensen UH, Erdeniz N, Feng Q, Rothstein R (2002) A molecular genetic dissection of the evolutionarily conserved N terminus of yeast Rad52. Genetics 161: 549–562.
18. Antunez de MA, Lisby M, Erdeniz N, Thybo T, Mortensen UH, et al. (2006) Multiple start codons and phosphorylation result in discrete Rad52 protein species. *Nuc Acids Res* 34: 2587–2597.
19. Bai Y, Davis AP, Symington LS (1999) A novel allele of *RAD52* that causes severe DNA repair and recombination deficiencies only in the absence of *RAD51* or *RAD59*. Genetics 153: 1117–1130.
20. Bai Y, Symington LS (1996) A Rad52 homolog is required for *RAD51*-independent mitotic recombination in *Saccharomyces cerevisiae*. Genes Dev 10: 2025–2037.
21. Bjelland S, Seeberg E (2003) Mutagenicity, toxicity, and repair of DNA base damage induced by oxidation. Mutat Res 531: 37–80.
22. Cadet J, Bellon S, Douki T, Frelon S, Gasparutto D, et al. (2004) Radiation-induced DNA damage: Formation, measurement, and biochemical features. J Environ Pathol Toxicol Oncol 23: 33–43.
23. Breen AP, Murphy JA (1995) Reactions of oxyl radicals with DNA. Free Radic Biol Med 18: 1033–1077.
24. Jenner TJ, Fulford J, O'Neill P (2001) Contribution of base lesions to radiation-induced clustered DNA damage: Implication for models of radiation response. Radiat Res 156: 590–593.
25. Moore JK, Haber JE (1996) Cell cycle and genetic requirements of two pathways of nonhomologous end-joining repair of double-strand breaks in *Saccharomyces cerevisiae*. Mol Cell Biol 16: 2164–2173.
26. Sugawara N, Haber JE (1992) Characterization of double-strand break-induced recombination: Homology requirements and single-stranded DNA formation. Mol Cell Biol 12: 563–575.
27. Smith J, Rothstein R (1999) An allele of RFA1 suppresses RAD52-dependent double-strand break repair in *Saccharomyces cerevisiae*. Genetics 151: 447–458.
28. White CI, Haber JE (1990) Intermediates of recombination during mating type switching in *Saccharomyces cerevisiae*. EMBO J 9: 663–673.
29. Michel B, Grompone G, Flores MJ, Bidnenko V (2004) Multiple pathways process stalled replication forks. Proc Natl Acad Sci U S A 101: 12783–12788.
30. McGlynn P, Lloyd RG (2002) Recombinational repair and restart of damaged replication forks. Nat Rev Mol Cell Biol 3: 859–870.
31. Hsiang YH, Hertzberg R, Hecht S, Liu LF (1985) Camptothecin induces protein-linked DNA breaks via mammalian DNA topoisomerase I. J Biol Chem 260: 14873–14878.
32. Hsiang YH, Liu LF (1988) Identification of mammalian DNA topoisomerase I as an intracellular target of the anticancer drug camptothecin. Cancer Res 48: 1722–1726.
33. Hsiang YH, Lihou MG, Liu LF (1989) Arrest of replication forks by drug-stabilized topoisomerase I-DNA cleavable complexes as a mechanism of cell killing by camptothecin. Cancer Res 49: 5077–5082.
34. Megonigal MD, Fertala J, Bjornsti MA (1997) Alterations in the catalytic activity of yeast DNA topoisomerase I result in cell cycle arrest and cell death. J Biol Chem 272: 12801–12808.
35. Reid RJ, Fiorani P, Sugawara M, Bjornsti MA (1999) CDC45 and DPB11 are required for processive DNA replication and resistance to DNA topoisomerase I-mediated DNA damage. Proc Natl Acad Sci U S A 96: 11440–11445.
36. Davis AP, Symington LS (2004) RAD51-dependent break-induced replication in yeast. Mol Cell Biol 24: 2344–2351.
37. Morrow DM, Connelly C, Hieter P (1997) "Break copy" duplication: A model for chromosome fragment formation in *Saccharomyces cerevisiae*. Genetics 147: 371–382.
38. Lisby M, Rothstein R, Mortensen UH (2001) Rad52 forms DNA repair and recombination centers during S phase. Proc Natl Acad Sci U S A 98: 8276–8282.
39. Lisby M, Mortensen UH, Rothstein R (2003) Colocalization of multiple DNA double-strand breaks at a single Rad52 repair center. Nat Cell Biol 5: 572–577.
40. Sandell LL, Zakian VA (1993) Loss of a yeast telomere: Arrest, recovery, and chromosome loss. Cell 75: 729–739.
41. Lee SE, Moore JK, Holmes A, Umezu K, Kolodner RD, et al. (1998) *Saccharomyces* Ku70, mre11/rad50, and RPA proteins regulate adaptation to G2/M arrest after DNA damage. Cell 94: 399–409.
42. Miyazaki T, Bressan DA, Shinohara M, Haber JE, Shinohara A (2004) In vivo assembly and disassembly of Rad51 and Rad52 complexes during double-strand break repair. EMBO J 23: 939–949.
43. Rapp A, Greulich KO (2004) After double-strand break induction by UV-A, homologous recombination and nonhomologous end joining cooperate at the same DSB if both systems are available. J Cell Sci 117: 4935–4945.
44. Prakash S, Prakash L, Burke W, Montelone BA (1980) Effects of the *RAD52* gene on recombination in *Saccharomyces cerevisiae*. Genetics 94: 31–50.

45. von Borstel RC, Cain KT, Steinberg CM (1971) Inheritance of spontaneous mutability in yeast. Genetics 69: 17–27.
46. Davis AP, Symington LS (2001) The yeast recombinational repair protein Rad59 interacts with Rad52 and stimulates single-strand annealing. Genetics 159: 515–525.
47. Milne GT, Weaver DT (1993) Dominant-negative alleles of *RAD52* reveal a DNA repair/recombination complex including Rad51 and Rad52. Genes Dev 7: 1755–1765.
48. Shinohara A, Ogawa H, Ogawa T (1992) Rad51 protein involved in repair and recombination in *S. cerevisiae* is a RecA-like protein. Cell 69: 457–470.
49. Hays SL, Firmenich AA, Massey P, Banerjee R, Berg P (1998) Studies of the interaction between Rad52 protein and the yeast single-stranded DNA binding protein RPA. Mol Cell Biol 18: 4400–4406.
50. Mortensen UH, Bendixen C, Sunjevaric I, Rothstein R (1996) DNA strand annealing is promoted by the yeast Rad52 protein. Proc Natl Acad Sci U S A 93: 10729–10734.
51. Shen Z, Peterson SR, Comeaux JC, Zastrow D, Moyzis RK, et al. (1996) Self-association of human *RAD52* protein. Mutat Res 364: 81–89.
52. Kagawa W, Kurumizaka H, Ishitani R, Fukai S, Nureki O, et al. (2002) Crystal structure of the homologous-pairing domain from the human Rad52 recombinase in the undecameric form. Mol Cell 10: 359–371.
53. Cortes-Ledesma F, Malagon F, Aguilera A (2004) A novel yeast mutation, rad52-L89F, causes a specific defect in Rad51-independent recombination that correlates with a reduced ability of Rad52-L89F to interact with Rad59. Genetics 168: 553–557.
54. Singleton MR, Wentzell LM, Liu Y, West SC, Wigley DB (2002) Structure of the single-strand annealing domain of human RAD52 protein. Proc Natl Acad Sci U S A 99: 13492–13497.
55. Lloyd JA, McGrew DA, Knight KL (2005) Identification of residues important for DNA binding in the full-length human Rad52 protein. J Mol Biol 345: 239–249.
56. Sung P (1997) Function of yeast Rad52 protein as a mediator between replication protein A and the Rad51 recombinase. J Biol Chem 272: 28194–28197.
57. New JH, Sugiyama T, Zaitseva E, Kowalczykowski SC (1998) Rad52 protein stimulates DNA strand exchange by Rad51 and replication protein A. Nature 391: 407–410.
58. Krogh BO, Symington LS (2004) Recombination proteins in yeast. Annu Rev Genet 38: 233–271.
59. Shinohara A, Ogawa T (1998) Stimulation by Rad52 of yeast Rad51-mediated recombination. Nature 391: 404–407.
60. Lisby M, Barlow JH, Burgess RC, Rothstein R (2004) Choreography of the DNA damage response: Spatiotemporal relationships among checkpoint and repair proteins. Cell 118: 699–713.
61. Fabre F, Chan A, Heyer WD, Gangloff S (2002) Alternate pathways involving Sgs1/Top3, Mus81/Mms4, and Srs2 prevent formation of toxic recombination intermediates from single-stranded gaps created by DNA replication. Proc Natl Acad Sci U S A 26: 16887–16892.
62. Ajimura M, Leem SH, Ogawa H (1993) Identification of new genes required for meiotic recombination in *Saccharomyces cerevisiae*. Genetics 133: 51–66.
63. Bressan DA, Baxter BK, Petrini JH (1999) The Mre11-Rad50-Xrs2 protein complex facilitates homologous recombination-based double-strand break repair in *Saccharomyces cerevisiae*. Mol Cell Biol 19: 7681–7687.
64. Holliday R (1964) A mechanism for gene conversion in fungi. Genet Res 5: 282–304.
65. Meselson MJ, Radding CM (1975) A general model for genetic recombination. Proc Natl Acad Sci U S A 72: 359–361.
66. Radding C (1982) Homologous pairing and strand exchange in genetic recombination. Annu Rev Genet 16: 405–437.
67. Benson FE, Baumann P, West SC (1998) Synergistic actions of Rad51 and Rad52 in recombination and DNA repair. Nature 391: 401–404.
68. Shinohara A, Shinohara M, Ohta T, Matsuda S, Ogawa T (1998) Rad52 forms ring structures and co-operates with RPA in single-strand DNA annealing. Genes Cells 3: 145–156.
69. Song B, Sung P (2000) Functional interactions among yeast Rad51 recombinase, Rad52 mediator, and replication protein A in DNA strand exchange. J Biol Chem 275: 15895–15904.
70. Lee GS, Neiditch MB, Salus SS, Roth DB (2004) RAG proteins shepherd double-strand breaks to a specific pathway, suppressing error-prone repair, but RAG nicking initiates homologous recombination. Cell 117: 171–184.
71. Saleh-Gohari N, Bryant HE, Schultz N, Parker KM, Cassel TN, et al. (2005) Spontaneous homologous recombination is induced by collapsed replication forks that are caused by endogenous DNA single-strand breaks. Mol Cell Biol 25: 7158–7169.
72. Sherman F, Fink GR, Hicks JB (1986) Methods in yeast genetics. Cold Spring Harbor (New York): Cold Spring Harbor Laboratory Press. 205 p.
73. Gietz D, St Jean A, Woods RA, Schiestl RH (1992) Improved method for high efficiency transformation of intact yeast cells. Nucleic Acids Res 20: 1425.
74. Thomas BJ, Rothstein R (1989) Elevated recombination rates in transcriptionally active DNA. Cell 56: 619–630.
75. Fan HY, Cheng KK, Klein HL (1996) Mutations in the RNA polymerase II transcription machinery suppress the hyperrecombination mutant hpr1 delta of *Saccharomyces cerevisiae*. Genetics 142: 749–759.
76. Zou H, Rothstein R (1997) Holliday junctions accumulate in replication mutants via a RecA homolog-independent mechanism. Cell 90: 87–96.
77. Jensen RE, Herskowitz I (1984) Directionality and regulation of cassette substitution in yeast. Cold Spring Harbor Symposia on Quantitative Biology 49: 97–104.
78. Smith J, Rothstein R (1995) A mutation in the gene encoding the *Saccharomyces cerevisiae* single-stranded DNA-binding protein Rfa1 stimulates a *RAD52*-independent pathway for direct-repeat recombination. Mol Cell Biol 15: 1632–1641.
79. McDonald JP, Levine AS, Woodgate R (1997) The *Saccharomyces cerevisiae* RAD30 gene, a homolog of *Escherichia coli* dinB and umuC, is DNA damage inducible and functions in a novel error-free postreplication repair mechanism. Genetics 147: 1557–1568.
80. Campbell RE, Tour O, Palmer AE, Steinbach PA, Baird GS, et al. (2002) A monomeric red fluorescent protein. Proc Natl Acad Sci U S A 99: 7877–7882.

Supporting Information

Supporting Figures

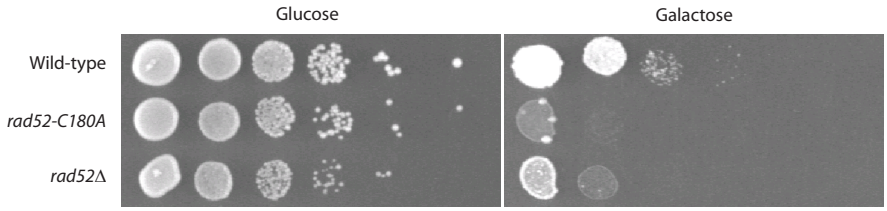

Figure S.1. Induced mating-type switching is lethal in *rad52* class C mutant strains. Strains were transformed with a plasmid that allowed galactose induced expression of the HO-endonuclease. A spot assay was performed to evaluate the sensitivity of *rad52* strains to expression of the HO-endonuclease. Serial 10-fold dilutions of wild-type, *rad52-C180A* and *rad52*Δ strains were spotted on solid repressive medium, SC-Ura + 2% glucose and solid inductive medium, SC-Ura + 2% galactose as indicated.

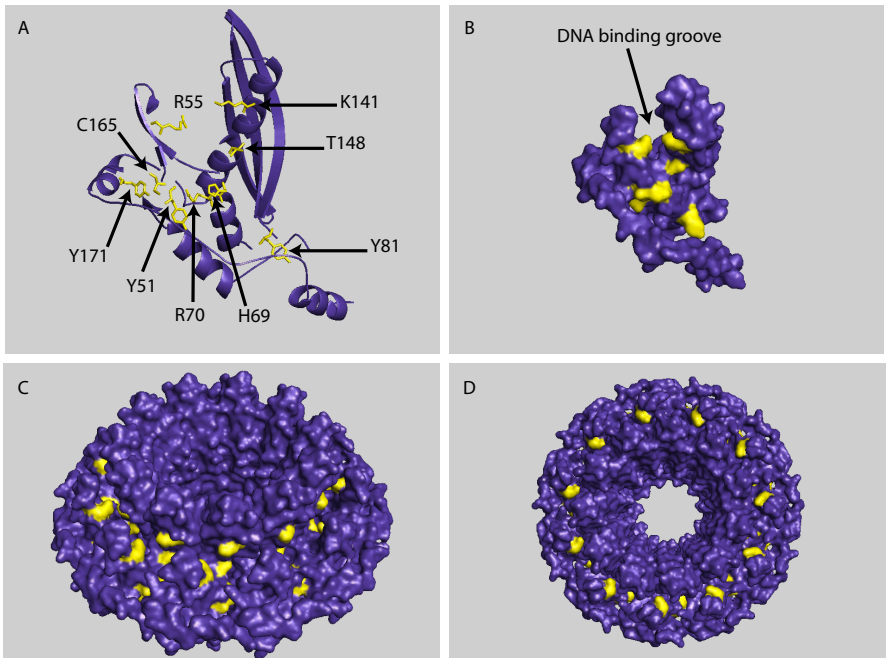

Figure S.2. *rad52* class C mutations are located at the DNA binding site of Rad52. A single subunit of the human Rad52 N-terminal fragment (amino acid residues 1-212) is shown in the upper panels (A and B). The positions of amino acid residues corresponding to mutated residues in *S. cerevisiae* class C *rad52* mutations are presented in yellow and indicated with arrows. Representations of Rad52 subunits (N-terminal fragments) in an undecameric ring are given in the lower panels (C and D). Rad52 coordinates are from Kagawa et al. (2002) and Singleton et al. (2002).

Supporting Table

Table S1. Strains used in this study. All strains are made in this study with the exception of the strains marked by footnotes

Strain[a]	Genotype
W1588-4C[b]	*MAT***a** *ade2-1 can1-100 his3-11,15 leu2-3,112 trp1-1 ura3-1*
J787	*MAT***a** *rad52-Y66A ade2-1 can1-100 his3-11,15 leu2-3,112 trp1-1 ura3-1*
J788	*MAT***a** *rad52-R70A ade2-1 can1-100 his3-11,15 leu2-3,112 trp1-1 ura3-1*
J774	*MAT***a** *rad52-W84A ade2-1 can1-100 his3-11,15 leu2-3,112 trp1-1 ura3-1*
J738	*MAT***a** *rad52-R85A ade2-1 can1-100 his3-11,15 leu2-3,112 trp1-1 ura3-1*
J765-1	*MAT***a** *rad52-Y96A ade2-1 can1-100 his3-11,15 leu2-3,112 trp1-1 ura3-1*
J771	*MAT***a** *rad52-R156A ade2-1 can1-100 his3-11,15 leu2-3,112 trp1-1 ura3-1*
J783	*MAT***a** *rad52-T163A ade2-1 can1-100 his3-11,15 leu2-3,112 trp1-1 ura3-1*
J786	*MAT***a** *rad52-C180A ade2-1 can1-100 his3-11,15 leu2-3,112 trp1-1 ura3-1*
J777	*MAT***a** *rad52-F186A ade2-1 can1-100 his3-11,15 leu2-3,112 trp1-1 ura3-1*
W3749-14C[c]	*MAT***a** *RAD52-YFP ADE2 bar1::LEU2 can1-100 his3-11,15 leu2-3,112 trp1-1 ura3-1*
J1207	*MAT***a** *rad52-Y66A-YFP ADE2 bar1::LEU2 can1-100 his3-11,15 leu2-3,112 trp1-1 ura3-1*
W3840-15D	*MAT***a** *rad52-R70A-YFP ADE2 bar1::LEU2 can1-100 his3-11,15 leu2-3,112 trp1-1 ura3-1*
UM190-6B	*MAT***a** *rad52-W84A-YFP ADE2 bar1::LEU2 can1-100 his3-11,15 leu2-3,112 trp1-1 ura3-1*
W3734-8B	*MAT***a** *rad52-R85A-YFP ADE2 bar1::LEU2 can1-100 his3-11,15 leu2-3,112 trp1-1 ura3-1*
UM140-2A	*MAT***a** *rad52-Y96A-YFP ADE2 bar1::LEU2 can1-100 his3-11,15 leu2-3,112 trp1-1 ura3-1*
W3167-5A	*MAT***a** *rad52-R156A-YFP ADE2 bar1::LEU2 can1-100 his3-11,15 leu2-3,112 trp1-1 ura3-1*
W4024-1B	*MAT***a** *rad52-T163A-YFP ADE2 bar1::LEU2 can1-100 his3-11,15 leu2-3,112 trp1-1 ura3-1*
W2594-4A	*MAT***a** *rad52-C180A-8ALA-YFP ADE2 bar1::LEU2 can1-100 his3-11,15 leu2-3,112 trp1-1 ura3-1*
UM31-1D	*MAT***a** *rad52-F186A-YFP ADE2 bar1::LEU2 can1-100 his3-11,15 leu2-3,112 trp1-1 ura3-1*
W2282-2C	*Mat::HIS3 rad52::HIS5 leu2-ΔEcoRI::URA3-HO::leu2-ΔBstEII trp1-1*
W2158-1C	*Mat::HIS3 Rad52 leu2-ΔEcoRI::URA3-HO::leu2-ΔBstEII trp1-1*
J822	*Mat::HIS3 rad52-Y66A leu2-ΔEcoRI::URA3-HO::leu2-ΔBstEII trp1-1*
W4158-3D	*Mat::HIS3 rad52-R70A leu2-ΔEcoRI::URA3-HO::leu2-ΔBstEII trp1-1*
W4159-6C	*Mat::HIS3 rad52-W84A leu2-ΔEcoRI::URA3-HO::leu2-ΔBstEII trp1-1*
W2158-16B	*Mat::HIS3 rad52-R85A leu2-ΔEcoRI::URA3-HO::leu2-ΔBstEII trp1-1*
W2177-15D	*Mat::HIS3 rad52-Y96A leu2-ΔEcoRI::URA3-HO::leu2-ΔBstEII trp1-1*
W4157-5A	*Mat::HIS3 rad52-R156A leu2-ΔEcoRI::URA3-HO::leu2-ΔBstEII trp1-1*
W2180-3A	*Mat::HIS3 rad52-T163A leu2-ΔEcoRI::URA3-HO::leu2-ΔBstEII trp1-1*
W2181-8A	*Mat::HIS3 rad52-C180A leu2-ΔEcoRI::URA3-HO::leu2-ΔBstEII trp1-1*
W2179-16A	*Mat::HIS3 rad52-F186A leu2-ΔEcoRI::URA3-HO::leu2-ΔBstEII trp1-1*
J1361	*Mat***a** *16X Gal-CEN - K.lactis URA3 ADE2+ kar1Δ15 rho+*
W4021-20A	*Mat::HIS3 ADE2 bar1::LEU2 trp1-1 LYS2 RAD52-C180A-CFP HO-iYCL018W his3-11,15::YFP-LacI::his3-x leu2-3,112::LacO::LEU2*
W4341-6D	*Mat::HIS3 ADE2 bar1::LEU2 trp1-1 LYS2 RAD52-C180A-CFP his3-11,15::YFP-LacI::his3-x leu2-3,112::LacO::LEU2*
W4341-16A	*Mat::HIS3 ADE2 bar1::LEU2 trp1-1 LYS2 RAD52-C180A-CFP HO-iYDR010C his3-11,15::YFP-LacI::his3-x leu2-3,112::LacO::LEU2*
UM214-60B	*Mat***a** *ade2-1 bar1::LEU2 trp1-1 LYS2 RAD52-YFP RAD51-CFP ura::3xURA3-tetOx112 I-SceI-iYEL023C TetI-mRFP1*
UM215-22B	*Mat***a** *ade2-1 bar1::LEU2 trp1-1 LYS2 RAD52-C180A-YFP RAD51-CFP ura::3xURA3-tetOx112 I-SceI-iYEL023C TetI-mRFP1*

UM157	*MAT***a** *ade2-1 can1-100 his3-11,15 leu2ΔBstEII lys2 TRP1 ura3-1*
	MATα ade2-1 can1-100 his3-11,15 leu2ΔEcoRI LYS2 trp1-1 ura3-1
UM158	*MAT***a** *rad59Δ ade2-1 can1-100 his3-11,15 leu2ΔBstEII lys2 TRP1 ura3-1*
	MATα rad59Δ ade2-1 can1-100 his3-11,15 leu2ΔEcoRI LYS2 trp1-1 ura3-1
UM159	*MAT***a** *rad52::HIS5 rad59Δ ade2-1 can1-100 his3-11,15 leu2ΔBstEII lys2 TRP1 ura3-1*
	MATα rad52::HIS5 rad59Δ ade2-1 can1-100 his3-11,15 leu2ΔEcoRI LYS2 trp1-1 ura3-1
UM160	*MAT***a** *rad52-R70A ade2-1 can1-100 his3-11,15 leu2ΔBstEII lys2 TRP1 ura3-1*
	MATα rad52-R70A ade2-1 can1-100 his3-11,15 leu2ΔEcoRI LYS2 trp1-1 ura3-1
UM161	*MAT***a** *rad52-W84A ade2-1 can1-100 his3-11,15 leu2ΔBstEII lys2 TRP1 ura3-1*
	MATα rad52-W84A ade2-1 can1-100 his3-11,15 leu2ΔEcoRI LYS2 trp1-1 ura3-1
UM162	*MAT***a** *rad52-R85A ade2-1 can1-100 his3-11,15 leu2ΔBstEII lys2 TRP1 ura3-1*
	MATα rad52-R85A ade2-1 can1-100 his3-11,15 leu2ΔEcoRI LYS2 trp1-1 ura3-1
UM163	*MAT***a** *rad52-Y96A ade2-1 can1-100 his3-11,15 leu2ΔBstEII lys2 TRP1 ura3-1*
	MATα rad52-Y96A ade2-1 can1-100 his3-11,15 leu2ΔEcoRI LYS2 trp1-1 ura3-1
UM164	*MAT***a** *rad52- R156A ade2-1 can1-100 his3-11,15 leu2ΔBstEII lys2 TRP1 ura3-1*
	MATα rad52-R156A ade2-1 can1-100 his3-11,15 leu2ΔEcoRI LYS2 trp1-1 ura3-1
UM165	*MAT***a** *rad52-T163A ade2-1 can1-100 his3-11,15 leu2ΔBstEII lys2 TRP1 ura3-1*
	MATα rad52-T163A ade2-1 can1-100 his3-11,15 leu2ΔEcoRI LYS2 trp1-1 ura3-1
UM166	*MAT***a** *rad52-C180A ade2-1 can1-100 his3-11,15 leu2ΔBstEII lys2 TRP1 ura3-1*
	MATα rad52-C180A ade2-1 can1-100 his3-11,15 leu2ΔEcoRI LYS2 trp1-1 ura3-1
UM167	*MAT***a** *rad52-F186A ade2-1 can1-100 his3-11,15 leu2ΔBstEII lys2 TRP1 ura3-1*
	MATα rad52-F186A ade2-1 can1-100 his3-11,15 leu2ΔEcoRI LYS2 trp1-1 ura3-1
UM168	*MAT***a** *rad52-Y66A rad59Δ ade2-1 can1-100 his3-11,15 leu2ΔBstEII lys2 TRP1 ura3-1*
	MATα rad52-Y66A rad59Δ ade2-1 can1-100 his3-11,15 leu2ΔEcoRI LYS2 trp1-1 ura3-1
UM169	*MAT***a** *rad52-R70A rad59Δ ade2-1 can1-100 his3-11,15 leu2ΔBstEII lys2 TRP1 ura3-1*
	MATα rad52-R70A rad59Δ ade2-1 can1-100 his3-11,15 leu2ΔEcoRI LYS2 trp1-1 ura3-1
UM170	*MAT***a** *rad52-W84A rad59Δ ade2-1 can1-100 his3-11,15 leu2ΔBstEII lys2 TRP1 ura3-1*
	MATα rad52-W84A rad59Δ ade2-1 can1-100 his3-11,15 leu2ΔEcoRI LYS2 trp1-1 ura3-1
UM171	*MAT***a** *rad52-R85A rad59Δ ade2-1 can1-100 his3-11,15 leu2ΔBstEII lys2 TRP1 ura3-1*
	MATα rad52-R85A rad59Δ ade2-1 can1-100 his3-11,15 leu2ΔEcoRI LYS2 trp1-1 ura3-1
UM172	*MAT***a** *rad52-Y96A rad59Δ ade2-1 can1-100 his3-11,15 leu2ΔBstEII lys2 TRP1 ura3-1*
	MATα rad52-Y96A rad59Δ ade2-1 can1-100 his3-11,15 leu2ΔEcoRI LYS2 trp1-1 ura3-1
UM173	*MAT***a** *rad52- R156A rad59Δ ade2-1 can1-100 his3-11,15 leu2ΔBstEII lys2 TRP1 ura3-1*
	MATα rad52-R156A rad59Δ ade2-1 can1-100 his3-11,15 leu2ΔEcoRI LYS2 trp1-1 ura3-1
UM174	*MAT***a** *rad52-T163A rad59Δ ade2-1 can1-100 his3-11,15 leu2ΔBstEII lys2 TRP1 ura3-1*
	MATα rad52-T163A rad59Δ ade2-1 can1-100 his3-11,15 leu2ΔEcoRI LYS2 trp1-1 ura3-1
UM175	*MAT***a** *rad52-C180A rad59Δ ade2-1 can1-100 his3-11,15 leu2ΔBstEII lys2 TRP1 ura3-1*
	MATα rad52-C180A rad59Δ ade2-1 can1-100 his3-11,15 leu2ΔEcoRI LYS2 trp1-1 ura3-1
UM176	*MAT***a** *rad52-F186A rad59Δ ade2-1 can1-100 his3-11,15 leu2ΔBstEII lys2 TRP1 ura3-1*
	MATα rad52-F186A rad59Δ ade2-1 can1-100 his3-11,15 leu2ΔEcoRI LYS2 trp1-1 ura3-1

[a] All strains are made in the W303 background except that they are *RAD5*

[b] Zou and Rothstein (1997)

[c] Lisby et al. (2003)

Supporting Protocols

Construction of pRS413-TRP1 A PCR fragment containing the entire TRP1 gene was generated by primers SalI_TRP1_fw (TGGATGGTgtcgacGATTGTACTGAGAGTGCACC) and EcoRI_TRP1_Rv (ACCTTTACgaattcGCATAGGCAAGTGCACAAAC) using pRS414 (Sikorski & Hieter, 1989) as substrate. The resulting fragment was trimmed by digestion with *Eco*RI and *Sal*I and inserted into an *Eco*RI-*Sal*I fragment of pRS413 (Sikorski & Hieter, 1989), a *CEN4* vector that contains a *HIS3* selectable marker, to produce pRS413-*TRP1*.

Construction of strains All class C mutant alleles were transferred into the *RAD52* locus in W1588-4C from their original pWJ1086 context, see Mortensen et al. (2002) by a PCR based method (Erdeniz et al., 1997). The *rad52* sequence in all *rad52* class C mutant strains were extended in frame by the gene encoding CFP or YFP. This was done by transforming the mutant strains by plasmid pWJ1385, which is a pRS414 based plasmid that contains the structural gene of *RAD52* under the control of the *MET25* promoter and terminator. Subsequently, endogenous *rad52* mutant genes were tagged by CFP or YFP sequences according to the method described in Lisby et al. (2001).

Viability after γ- and UV-irradiation, HO-endonuclease induction and exposure to camptothecin sensitivity γ-irradiation was performed as previously described (Smith & Rothstein, 1995) using a Gammacell-220 60Co irradiator (Atomic Energy of Canada). UV irradiation was performed by using a Stratalinker 2400 UV Crosslinker from Stratagene. Cells were exposed to a dose of 30 J/m^2 at 254 nm. Triplicates were performed for all experiments and all strains were sonicated prior to plating. For each strain an appropriate number of cells were plated on YPD plates (γ-ray experiments) or SC plates (UV-ray experiments) before and after irradiation. Viability was determined after three days of incubation in the dark at 30°C by dividing the number of colony forming units in a culture after irradiation with the corresponding number obtained before irradiation. To evaluate the ability of *rad52* mutant strains to survive sustained expression of the HO-endonuclease in strains containing the native MAT locus, selected strains were transformed by the HO-endonuclease encoding plasmid pJH283. For each strain, at least two of the resulting transformants were grown overnight in SC-Ura to midlog phase and each culture spotted in ten-fold serial dilutions on two plates of solid SC-Ura medium containing either glucose or galactose as carbon source, respectively. The ability of *rad52* strains, which contain a single HOcs either at the MAT locus or in the context of a direct repeat, *leu2*-Δ*Eco*RI::*URA3*-HOcs::*leu2*-Δ*Bst*EII, to survive a brief expression of the HO-endonuclease was determined by transforming strains by pJH283 or pJH132, respectively. Strains were pre-grown in either SC-Ura 2% raffinose or SC-Trp 2% raffinose,

transferred to liquid SC-Ura, 2% galactose or SC-Trp, 2% galactose and incubated for 1 or 1.5 hours. The strains were appropriately diluted and plated on solid YPD medium before and after induction and the plates were incubated for 2 days at 30°C before the colonies were counted. In the case of surviving a cut at the MAT locus, viability was determined by dividing the number of Ura+ colonies with the number of Ura+ colonies before induction. In the case of surviving a cut between directly repeated *leu2* heteroalleles, viability was determined by dividing the number of Trp+ colonies with the number of Trp+ colonies before induction. The scheme to monitor intermediates in DSB repair of a HO-endonuclease induced break situated between *leu2* heteroalleles by Southern blot analysis was described previously [6]. DNA was visualized using phosphorImager 445 SI and quantified by ImageQuant software (Molecular Dynamics). A probe detecting the *ADE2* locus was added as a loading control. This probe was generated by the primers ADE-F: 5'-CTCACTGGCTTGTTCCACAGG and ADE-B: 5'-ATGGCTCCTTTTCCAATCCTC.

HO-endonuclease and UV induced recombination To evaluate the ability of *rad52* mutant strains to perform HO-endonuclease induced mating-type switching, the colonies on YPD plates obtained from cultures that were briefly exposed to inductive medium, see above, were replicated to SC-Ura plates and to plates containing lawns of MAT**a** (D297-4B or R113) and MATα tester strains (B3847 or R194). The mating-type switching efficiency was determined by dividing the number of Ura+ MATα colonies with the total number of Ura+ colonies. The numbers are means of five to seven individual trials for each *rad52* mutant strain. To evaluate HO-endonuclease induced direct-repeat HR, colonies on YPD plates obtained from cultures that were briefly exposed to inductive medium were replica plated to SC-Leu, SC-Ura and SC-Trp plates to detect HR events (Leu+ cells) and deletion events (Ura- cells) and to determine survival rates (Trp+ cells), see above. The numbers are means of five independent trials. In UV-induced interchromosomal *leu2*-Δ*Eco*RI/*leu2*-Δ*Bst*EII heteroallelic HR experiments, triplicates were made for each strain analyzed. An appropriate number of cells were plated onto SC and SC-Leu plates and irradiated as described above. The HR frequency after UV irradiation was determined by dividing the total number of recombinants (Leu+ cells) in the culture by the corresponding total number of surviving cells following irradiation.

Determination of Rad52 concentration in *RAD52* and *rad52* strains Three different 10 ml cultures of each strain were grown to mid-log phase. The total protein extraction was done by glass bead disruption as described in Harlow & Lane (1988). The protein was separated on sodium dodecyl sulfate (SDS)-10% polyacrylamide gel and electrically transferred to Immobilon-P membrane (Millipore). The membrane was blocked by 45 ml nonfat dry milk and probed with Rad52 antibody (Mortensen et al., 1996) that has been affinity puri-

fied using a Rad52-Sepharose column (Mortensen et al., 1996). The resulting immunocomplexes were visualized using an enhanced chemiluminescence kit (Amersham) and analyzed by ImageQuant (Molecular Dynamics). The relative protein levels (three trials for each allele) are given as percentages of the Rad52 level in wild-type strains.

Chapter 5

Rad52 DNA binding activity is required for second strand capture in DNA DSB repair

5.1 Introduction

Rad52 is a key protein involved in DNA double strand break (DSB) repair and homologous recombination (HR) in *S. cerevisiae*. Accordingly, *rad52* null strains have growth defects, fail to produce viable spores, are defective in mating-type switching and have reduced levels of meiotic and mitotic recombination (reviewed in Symington (2002)). Extensive studies of this protein in *S. cerevisiae* and other organisms have permitted to map several functional domains notably involved in the interaction of Rad52 with itself, other proteins and DNA, suggesting that Rad52 is a multi-task protein. The N-terminal domain of Rad52 is evolutionary conserved and results from several studies, e.g. its crystal structure determination and mutational analyses, are consistent with this region being involved in DNA binding (Mortensen et al., 1996; Kagawa et al., 2002; Singleton et al., 2002). Accordingly, Rad52 has been shown to bind both double-stranded (ds) and single-stranded (ss) DNA, with a higher affinity for the latter. Moreover, Rad52 promotes the annealing of complementary ssDNA molecules in vitro (Mortensen et al., 1996; Reddy et al., 1997; Shinohara et al., 1998; Van Dyck et al., 1998; Kagawa et al., 2001). Interestingly, while point mutations in the C-terminal domain of Rad52 or truncation mutations of this domain can be partially or completely suppressed by over-expression of RAD51, this is not the case for mutations situated in the Rad52 N-terminal region (Boundy-Mills & Livingston, 1993; Milne & Weaver, 1993; Schild, 1995; Asleson et al., 1999). These results suggest that the N-terminal domain of Rad52 contains a central activity of the protein, an activity that seems to have unique functions in DNA DSB repair in *S. cerevisiae*. In an effort to identify amino acid residues of the N-terminal domain of Rad52 that are important for Rad52 functions, Mortensen et al. (2002) systematically replaced 76 of the 165 amino acid residues in this domain with alanine. The mutants obtained were tested for their ability to re-

pair γ-ray induced DNA damage and to perform mitotic HR and were then divided into four classes according to their phenotypes. Among these, nine mutants (*rad52-Y66A, -R70A, -W84A, -R85A, -Y96A, -R156A, -T163A, -C180A*, and *-F186A*), defined as class C mutants, displayed a phenotype similar to that observed in one of the first *rad52* mutants identified, *rad52-2* (P64L) (Resnick et al., 1986; Malone et al., 1988; Boundy-Mills & Livingston, 1993; Kaytor & Livingston, 1994). Thus, *rad52* null strains transformed with plasmids expressing *rad52* class C alleles were shown to be sensitive to γ-irradiation but proficient for heteroallelic recombination (Mortensen et al., 2002). This phenotype was then later confirmed in a more thorough characterization study of strains where each of the nine *rad52* class C mutations had been integrated at the genomic *RAD52* locus (Lettier et al., 2006). Moreover, this study showed that these mutants were specifically deficient in the repair of defined restriction enzyme-induced DNA DSBs on a plasmid or at a genomic locus.

Why these mutants are unable to repair DNA DSBs and at which step of the repair process these mutants are blocked remains unclear. Recently, the DNA DSB repair process was dissected by studying the recruitment and colocalization of fluorescently tagged proteins to the site of DNA damage. In this study, Lisby et al. (2004) show that Rad52 is recruited to sites of DNA damage in the S and G2 phases of the cell cycle and that this recruitment is dependent on Rad52's interaction with Rfa1. Recruitment of another important DSB repair protein, Rad51, is believed to occur after Rad52 has been recruited as Rad51 foci form at the site of DNA damage in a Rad52-dependent manner (Gasior et al., 1998; Miyazaki et al., 2004; Lisby et al., 2004). This is consistent with the idea that Rad52 mediates Rad51 filament assembly by removing RPA from ssDNA while simultaneously replacing it by Rad51 (Sung, 1997a; Benson et al., 1998; New et al., 1998; Shinohara & Ogawa, 1998; Song & Sung, 2000; Sugiyama & Kowalczykowski, 2002; Sung et al., 2003). Accordingly, we investigated whether the DNA DSB repair phenotype of the *rad52* class C mutant was due to the fact that the mutant Rad52 proteins were unable to recruit to a DNA DSB (Lettier et al., 2006). We showed that the mutant protein was not only able to recruit to the break, but that it was also able to recruit and colocalize with Rad51 at this site, thus showing that recruitment of Rad52 and Rad51 to the break is not impaired in the *rad52* class C mutants. Altogether, these results suggest that the recombination mediator activity of Rad52 is not impaired in the *rad52* class C mutants.

In addition to its recombination mediator activity, Rad52 has ssDNA binding and annealing activities (Mortensen et al., 1996). These activities may be required if Rad52 mediates the annealing of ssDNA saturated with RPA in SSA or during second strand capture (Shinohara et al., 1998; Sugiyama et al., 1998, 2006). A closer analysis of the position of each class C mutations within the N-terminal crystal structure of hsRad52 revealed that the corresponding amino acid residues in the human Rad52 structure are located in, or close to, the putative DNA-

binding groove (Lettier et al., 2006). This observation suggests that the class C mutants are deficient in DNA DSB repair because the class C Rad52 mutant proteins are unable to bind DNA in a proper manner. In agreement with this view, four of the corresponding human Rad52 mutant species: HsRad52-Y51A (ScY66A), HsRad52-R55A (ScR70A), HsRad52-R70A (ScR85A), and HsRad52-Y81A (ScY96A) have been purified, and the three latter species show decreased affinity for ssDNA in gel shift assays (Kagawa et al., 2002; Lloyd et al., 2005). Moreover, the fact that the *rad52* class C mutants are deficient in HO-induced single-strand annealing (SSA) suggest that the DNA annealing activity of Rad52 is also affected in these mutants (Lettier et al., 2006). These results and the fact that the *rad52* class C mutants cannot repair DNA DSBs suggest that these mutants are probably impaired in a step of the DNA repair process that requires intact Rad52 DNA binding and annealing activities. Going back to the classical DNA DSB repair models (Resnick & Martin, 1976; Szostak et al., 1983; Allers & Lichten, 2001; Haber et al., 2004), several steps could require these activities. Interestingly, several research groups have recently focused on describing novel Rad52 functions that are different from its well-established recombination mediator role and involve Rad52's DNA binding and annealing activities. Arai et al. (2005) have for example shown that Rad52 is still required for the Rad51-promoted formation of D-loop even in the absence of RPA. Specifically the authors suggest the existence of an active stoichiometric complex of Rad51-Rad52 (1:3 ratio) bound to ssDNA that would be required for the invasion of dsDNA to form a D-loop structure. Looking into a later step of the DSB repair process, Sugiyama et al. (2006) found that Rad52 promotes annealing of the ssDNA strand, displaced by Rad51-mediated strand exchange, to a second ssDNA strand in vitro. The authors therefore suggested that, in addition to and after its role in Rad51-mediated strand exchange, Rad52 could also be involved in promoting second strand capture of the second ssDNA tail derived from a DNA DSB via its DNA binding and annealing activities.

With the goal of understanding why the *rad52* class C mutants are unable to repair DNA DSBs and in which step of the repair process these mutants are impaired, a further characterization of the HR and DSB repair phenotypes of two representative *rad52* class C mutants, *rad52-R70A* and *rad52-C180A*, has been performed. Using a new recombination assay, we first investigated the different types of recombination events observed in these mutants to determine if the *rad52* mutations had an effect on the repair pathway used for spontaneous HR. The involvement of Rad51 in the spontaneous HR observed in the *rad52* class C mutants was also investigated using the same assay as well as by fluorescence microscopy. In our previous study of these mutants (Lettier et al., 2006), we concluded that the *rad52* class C mutants were impaired at a step of the repair process situated after Rad51 recruitment. Accordingly, using a PCR strand-invasion assay, we investigated if strand invasion occurred in our *rad52* mutants. Fi-

nally, with the goal of understanding why the *rad52* class C mutants are unable to repair DNA DSBs, we investigated if some of the previously described suppressors of *rad52* mutations could suppress the sensitivity of the *rad52* class C mutants to DNA damaging agents. Our results are presented here.

5.2 Materials and Methods

5.2.1 Strains and media

Strains used in this study are presented in Table 5.6 (Supplementary materials). All media were prepared as described by Sherman et al. (1989) with minor modifications as the synthetic medium contained twice the amount of leucine (60mg/L). All the strains used are isogenic to W303 (Thomas & Rothstein, 1989) except that they are RAD5 (Fan et al., 1996; Zou & Rothstein, 1997). Geneticin (G418) plates was made by sterile-filtering a stock solution of geneticin (Sigma) to autoclaved, 50°C warm YPD medium containing agar, to a final concentration of 300 mg/L. Nourseothricin (Nat) medium was made by sterile-filtering a stock solution of nourseothricin to autoclaved, 50°C warm YPD medium containing agar, to a final concentration of 100 mg/L. Methyl methane-sulfonate (MMS) containing medium was made by adding MMS (Sigma) to autoclaved, 50°C warm SC medium containing agar, to the final concentration desired. Galactose containing plates (YP-Gal and SC-Gal) were made by filter sterilizing a 20% (w/v) solution of galactose (Sigma) into autoclaved, 50°C warm medium containing agar, to a final concentration of 2%.

5.2.2 Construction of the heteroallelic recombination assay

To investigate the spectrum of recombination events in the *rad52* class C mutants, a heteroallelic recombination assay was constructed (Figure 5.2). This assay was built on top of the previously described *leu2* interchromosomal heteroallelic recombination assay where HR is measured between *leu2*Δ*EcoRI* and *leu2*Δ*BstEII* alleles in a diploid strain (Smith & Rothstein, 1995). As shown in Figure 5.2 and for simplicity, the chromosomes carrying the *leu2*Δ*EcoRI* and the *leu2*Δ*BstEII* alleles are named ChrIII-E and ChrIII-B, respectively. Approximately 350 bp downstream of the *leu2* heteroalleles, *ADE2* and *ade2*Δ*AatII* alleles were inserted at allelic positions on ChrIII-E and ChrIII-B, respectively (Figure 5.2). The KanMX marker was inserted upstream of the *leu2*Δ*BstEII* allele, in the non-coding intergenic region between *SPB1* and *NBS1* (Figure 5.2). The marker was amplified by PCR from plasmid pUG6 using the primers $KanR\_fw\_80adpt$ and $KanR\_rv\_80adpt$ (Figure 5.1). These primers contain 80 bp-long adaptamers, homologous to the genomic target site, which allowed the integration of the KanMX marker by gene targeting. Similarly, the

NAT1 marker was inserted downstream of the *leu2ΔBstEII* allele on the opposite arm of ChrIII-B, in the non-coding intergenic region between *TRX3* and *TUP1* (Figure 5.2). *NAT1* was amplified by PCR from plasmid pAG35 using the primers *nat*1_*fw* and *nat*1_*rv* (Figure 5.1) and this fragment was then inserted into the genome by gene targeting. A second variant of the heteroallelic recombination assay was also constructed where the KanMX and the *NAT1* markers were integrated as described above but on ChrIII-E (see Figure 5.14 in Supplementary materials).

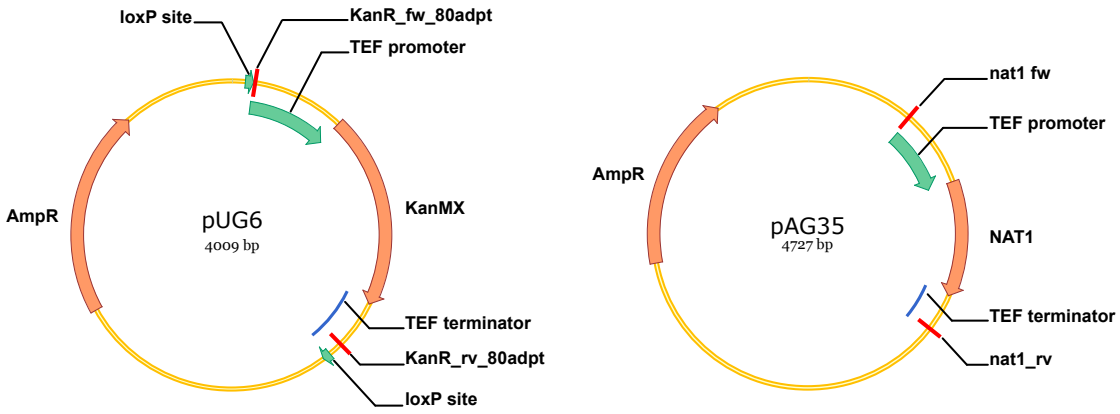

Figure 5.1. Maps representing the main features of the pUG6 and pAG35 plasmids.

5.2.3 Determination of spontaneous and induced mitotic recombination rates

Spontaneous mitotic HR between *leu2ΔEcoRI* and *leu2ΔBstEII* heteroalleles was measured in diploid strains (interchromosomal HR) as described previously (McDonald et al., 1997; Smith & Rothstein, 1999). UV-induced interchromosomal *leu2ΔEcoRI/leu2ΔBstEII* heteroallelic HR experiments were made in triplicates for each strain analyzed. The HR frequency after UV irradiation was determined by dividing the total number of recombinants in the culture by the total corresponding number of surviving cells following irradiation. The recombinants obtained on SC-Leu medium (synthetic medium lacking leucine) were replica plated on G418 and Nat plates and colonies that could not grow on these media were counted. Recombination rates and their standard deviations were calculated using the the median method as described by Lea & Coulson (1949).

5.2.4 Yeast live cell imaging and fluorescence microscopy

Cells used for fluorescence microscopy were grown in 2ml SC medium overnight to an OD_{600} of 0.3 at 23°C (to allow efficient formation of the fluorescent chromophore). Cultures were spun down, cells were

washed in fresh SC media and spun down again. 5μl of cells were immobilized on a glass slide by mixing them a 37°C solution of 1.2% (w/v) low melting agarose (NuSieve 3:1 from FMC) containing SC medium (Lisby et al., 2001). Live cell images were captured with a cooled Evolution QEi monochrome digital camera (Media Cybernetics Inc., USA) mounted on a Nikon Eclipse E1000 automated microscope (Nikon, Japan). Images were captured at 100-fold magnification using a Plan-Fluor 100x 1.3 NA objective lens. The illumination source was a 103W mercury arc lamp (Osram, Germany). Image acquisition times for Rad52-CFP and Rad52-YFP were 750 ms and 1 s, respectively, with a 12.5% neutral density filter (ND8) in place to reduce photobleaching. For each field of cells, nine to eleven fluorescent images were obtained at 0.4μm intervals along the Z-axis to allow inspection of all focal planes of each cells.

5.2.5 Strand invasion assay

The strand invasion assay was performed as previously described except that all strains used were RAD5 (Aylon et al., 2003). Wild-type strains carrying an HO cut site (cs) on chromosome V (*ura3*::HOcs) as well as the HO-endonuclease under the control of a GAL promoter integrated at *ade3* (*ade3*::GAL-HO), were a kind gift from M. Kupiec. The composition of individual primers were also obtained from M. Kupiec.

5.2.6 Spot assay

Sensitivity to MMS was tested by spotting cell suspensions on complete medium containing various concentrations of this chemical. Cells grown overnight at 30°C in 2ml appropriate medium were washed with sterile MilliQ water, spun down and resuspended in an appropriate volume of water. Six 10-fold dilutions of cell suspensions containing 10^8 cells per ml were then made and 5 μl of each dilution was spotted on MMS-containing medium. Plates were incubated at 30°C for 2 days before being examined and photographed (Prakash & Prakash, 1977).

5.2.7 Rad51 and Rad59 overexpression

For Rad51 overexpression experiments, strains were transformed with the *RAD51* overexpression plasmid, pYESS10Rad51 (Jiang et al., 1996). This plasmid contains *RAD51*, under the control of a GAL promoter, and *URA3* as a marker. Strains were also transformed with an empty plasmid for control. Transformants obtained were grown in liquid SC-Ura (synthetic medium lacking uracil) medium containing 2% galactose to a cell density of 10^7 cells/ml. Spot assay were carried out as previously described (see 5.2.6), except that the cells were spotted onto SC-Ura agar plates containing 2% galactose as a carbon source. For Rad59 overexpression experiments, strains were transformed with the 2μ-based plasmid pRS423-Rad59, which contains *RAD59* and *HIS3*

as a marker. Strains were also transformed with an empty plasmid for control. Transformants obtained were grown and spotted as in the *RAD51* overexpression experiments, except that liquid SC-HIS (synthetic medium lacking histidine) and SC-HIS agar plates were used.

5.3 Results

5.3.1 Description of the heteroallelic recombination system

We have previously shown that the *rad52* class C mutants are proficient for HR at similar or higher levels than wild-type strains (Mortensen et al., 2002; Lettier et al., 2006). These results were obtained using the previously described *leu2* heteroallelic assay which measures spontaneous interchromosomal recombination between two *leu2* heteroalleles in a diploid strain (Smith & Rothstein, 1995). However, in this assay, Leu^+ recombinants can arise via several types of events, i.e. gene conversion, gene conversion associated with a crossover, crossover between the *leu2* alleles or break induced replication (BIR). Moreover, HR events accompanied by chromosome loss can also result in viable Leu^+ recombinants as a diploid *S.cerevisiae* strain is relatively tolerant of 2n-1 monosomy. In order to further characterize the mitotic HR observed in the *rad52* class C mutant strains, we investigated if the spectrum of recombination events obtained in these strains was identical to that of wild-type strains or if this spectrum was biased towards a specific type of HR event. As the different HR events mentioned above could not easily be distinguished in the original *leu2* assay, we constructed a new assay containing a number of additional markers (Figure 5.2).

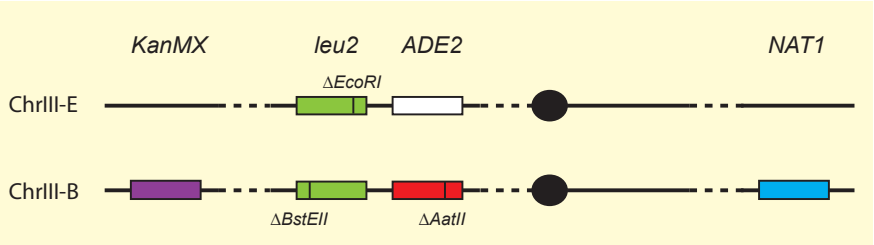

Figure 5.2. Representation the heteroallelic recombination assay used in this study. For simplicity, only one chromatid of each chromosome is represented (black line). The centromeres and the different alleles are represented as black circles and colored boxes, respectively. Mutations present in some of the alleles are represented as vertical black lines.

As shown in Figure 5.2, *ADE2*, *ade2*Δ*AatII*, KanMX and *NAT1* genes were added to the original assay (for a description of the construction of this assay see Section 5.2.2). Accordingly, the diploid cells used in this assay are Leu^-, Ade^+, resistant to G418 (Kan^R) and to nourseothricin (Nat^R). An overview of the different events that can be detected in this assay is presented below.

Simple gene conversion

Simple gene conversion of either *leu2* alleles will result in Leu$^+$ recombinants. As these events are local, they will not alter the position of the other markers thus recombinants obtained will be Kan^R and Nat^R. Accordingly, these events can be scored as colonies that can grow on SC-Leu, G418 and Nat plates.

Gene conversion associated with crossover or BIR

In order to differentiate between local gene conversion events and gene conversion associated with crossover, crossover or BIR, the dominant KanMX marker was integrated upstream of the *leu2*Δ*BstEII* allele on ChrIII-B (Figure 5.2). As shown in Figure 5.3, each of these events can lead to the loss of the KanMX marker thus resulting in Leu$^+$, Kan^S recombinants. These events can therefore be scored as colonies that can grow on SC-Leu but not on G418 plates.

Gene conversion associated with chromosome loss

Chromosome loss is rare in wild-type strains (Campbell et al., 1975; Campbell & Fogel, 1977; Haber & Hearn, 1985) but is frequently observed to accompany HR in *rad52* null strains (Haber & Hearn, 1985). As the *rad52* class C mutant strains have a close to null DNA DSB repair phenotype, it was important to verify if HR in the mutant strains was often associated with chromosome loss. Moreover, as described above, crossover events can lead to the loss of the KanMX marker that we can detect by replica plating on G418 media. However, chromosome loss events can also result in the loss of KanMX, thus scoring this event only could lead to a misinterpretation of the results. Accordingly, to distinguish between crossovers and chromosome loss events, we needed a system that could score for chromosome loss events specifically. For this reason, the *NAT1* marker was inserted downstream of the *leu2*Δ*BstEII* allele on the opposite arm of ChrIII-B (Figure 5.2). We considered that chromosome loss had occurred when Leu$^+$ recombinants that had lost both the KanMX and the NAT1 markers were recovered. These were scored as colonies that could grow on SC-Leu but not on either G418 plates or Nat plates. Moreover, the fact that the MAT locus is also situated on chromosome III allowed a second verification of chromosome loss. Indeed, loss of one homologue of chromosome III from a non-mating *MAT*a/*MAT*α diploid leads to the formation of monosomic strain expressing either *MAT*a or *MAT*α. Such cells can therefore mate with wild-type cells of the opposite mating type. Accordingly, colonies scored as Leu$^+$, Kan^S, Nat^S were tested for their ability to mate with either wild-type *MAT*a or *MAT*α strains. Leu$^+$, Kan^S, Nat^S colonies that were able to mate were interpreted as resulting from a chromosome loss event.

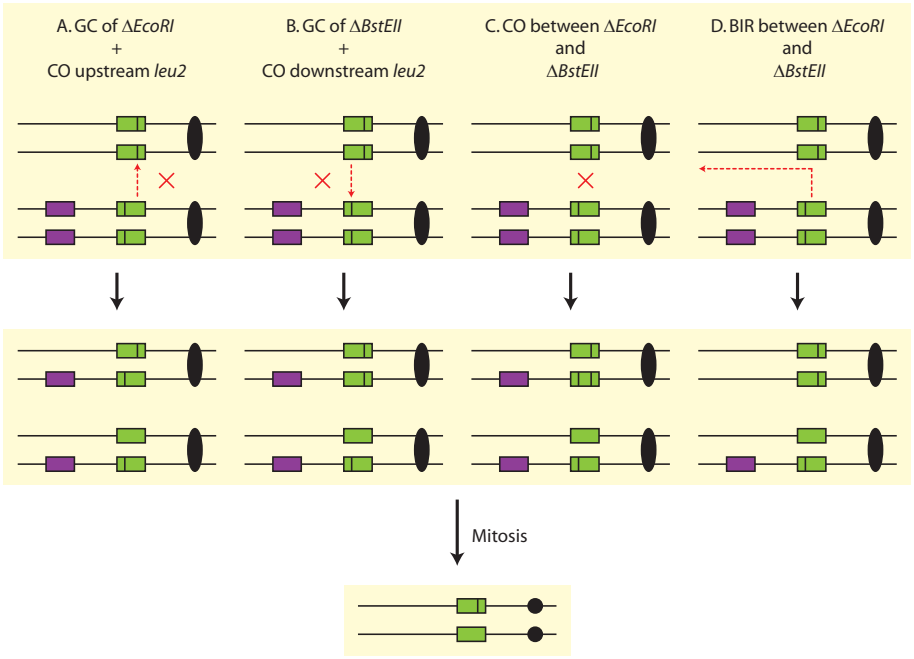

Figure 5.3. Detection of (A and B) gene conversion (GC) events associated with crossover (CO), (C) crossover (CO) between *leu2*Δ*EcoRI* and *leu2*Δ*BstEII* or (D) BIR. In the two upper panels, chromosomes are represented with two chromatids (black lines). The centromeres, the *leu2* alleles and the KanMX marker are represented as black ovales, green and purple boxes, respectively. Mutations present in the *leu2* alleles are represented as vertical black lines. Gene conversion is represented by a doted red arrow pointing from the donor sequence to the recipient sequence. Crossover is represented as a red cross. BIR is represented as a doted arrow going from the point where BIR is initiated to the end of the chromosome being copied. The lower panel represents the genotype of the diploid cells that can be detected by replica plating on G418 plates after mitosis. As all events result in the loss of the KanMX marker, these cells are Leu$^+$, Kan^S. In this panel, chromosomes are represented with only one chromatid and centromeres as black circles.

Gene conversion associated with long conversion tracts

Approximately 350 bp downstream of the *leu2* heteroalleles, *ADE2* and *ade2*Δ*AatII* alleles were inserted at allelic positions on ChrIII-E and ChrIII-B, respectively (Figure 5.2). Accordingly, the parental strain carrying ChrIII-E is Ade$^+$ and produces white colonies while the other, carrying ChrIII-B, is Ade$^-$ and produces red colonies. As shown in Figure 5.4, if the conversion tract leading to gene conversion of *leu2*Δ*EcoRI* is long, co-conversion of *ADE2* can occur. The resulting recombinants are Leu$^+$, Ade$^-$ and can be scored as red colonies on the SC-Leu plates.

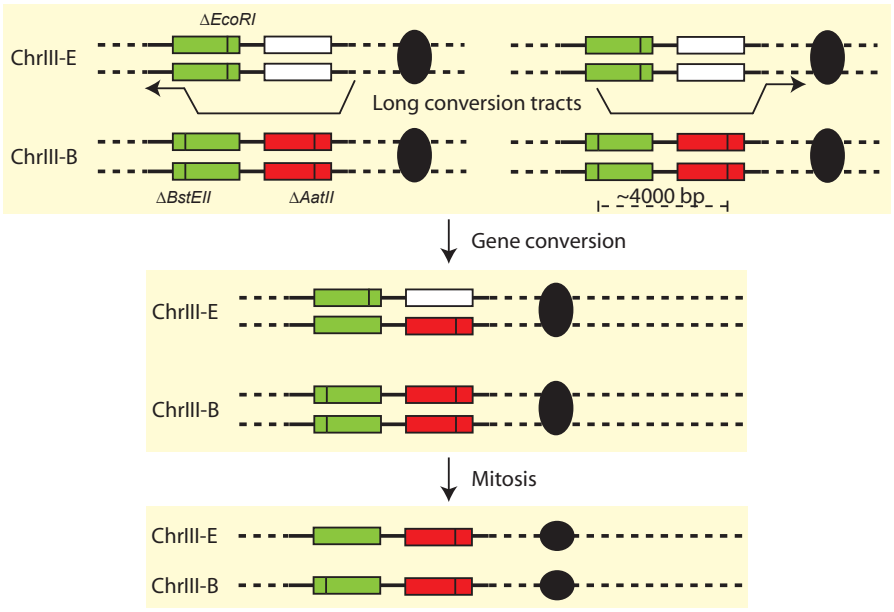

Figure 5.4. Detection of gene conversion events involving long conversion tracts in our heteroallelic assay. In the two upper panels, chromosomes are represented with two chromatids (black lines). The centromeres and the different alleles are represented as black ovales and colored boxes, respectively. Mutations present in some of the alleles are represented as vertical black lines. The lower panel represents the genotype of the diploid cells obtained after mitosis. As the long conversion tracts involved the *ade2ΔAatII* allele in the gene conversion of *leu2ΔEcoRI*, these cells are Leu^+, Ade^-. In the lower panel, chromosomes are represented with only one chromatid and centromeres as black circles.

5.3.2 Wild-type spectrum of recombination events observed in the class C mutants

Using the assay described above, we investigated the spectrum of recombination events in wild-type, *rad52Δ* and *rad52-C180A* strains. The results obtained are presented in Table 5.1 and Figure 5.6.

Table 5.1. Interchromosomal heteroallelic recombination rates of *RAD52*, *rad52-C180A* and *rad52*Δ

Allele	**Total HR** **Rate x** 10^{-8}	**GC** **Rate x** 10^{-8}	**GC+long CT** **Rate x** 10^{-8}	**GC+CO/CO/BIR** **Rate x** 10^{-8}	**Chr. loss** **Rate x** 10^{-8}
RAD52	160 ± 32	120 ± 23	22 ± 6	19 ± 5	3 ± 1.5
*rad52*Δ	6.8 ± 2.3[a]	3.1 ± 1.2	1.5 ± 0.8	1.8 ± 0.9	3.3 ± 1.4
rad52-C180A	114 ± 30[b,c]	106 ± 28	19 ± 7.2	15 ± 6.4	12 ± 5.4

a: p < 0.05 *rad52*Δ versus wild-type

b: p < 0.05 *rad52-C180A* mutant versus *rad52*Δ

c: p > 0.05 *rad52-C180A* versus wild-type

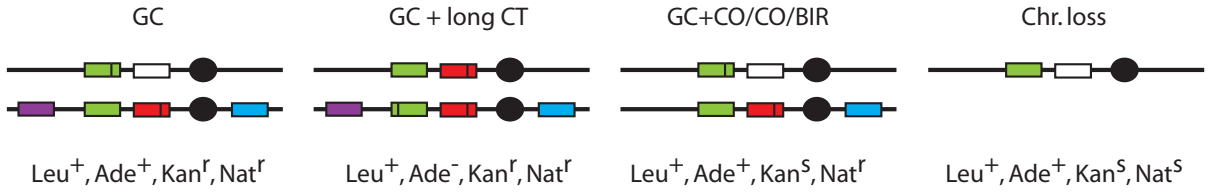

Figure 5.5. Summary of the different phenotypes obtained in this assay and their interpretation in terms of recombination events. The four phenotypes obtained in this assay are shown together with a representation of ChrIII-E and ChrIII-B showing the allele configuration for each phenotype. The events corresponding to each phenotype are also given. GC: Gene conversion, CT: conversion tract, CO: crossover, BIR: break-induced replication, Chr.: chromosome.

As shown in Figure 5.6, in the wild-type strain, most of the Leu$^+$ prototrophs resulted from a simple gene conversion event of either *leu2ΔEcoRI* or *leu2ΔBstEII*. This is in agreement with results from Haber & Hearn (1985) who showed that simple gene conversion between two *his4* heteroalleles was responsible for 74% of the recovered His$^+$ prototrophs. Other events leading to Leu$^+$ recombinants in the wild-type strain were gene conversion associated with crossover or BIR which represent 24% (12% × 2 as we only detect 50% of the total number of crossover events) of the total HR rate. Again, this is in agreement with previous results of 10 to 20% crossover frequencies obtained when mitotic gene conversion were measured after selection for prototrophs between heteroalleles on homologous chromosomes (Esposito, 1978; Haber & Hearn, 1985; Kupiec & Petes, 1988). Finally, a small amount of Leu$^+$ prototrophs arose from a process accompanied by chromosome loss.

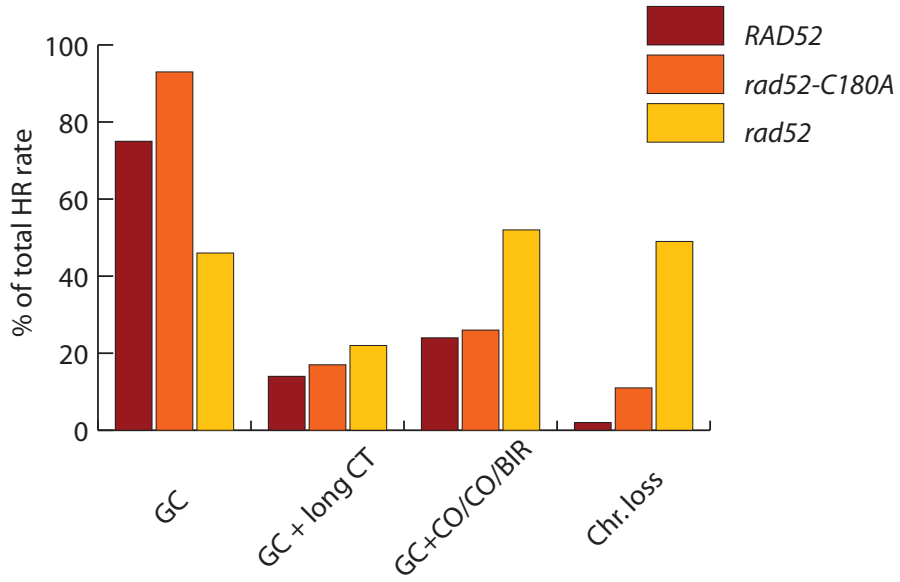

Figure 5.6. Graph representing the spectrum of recombination events observed in wild-type, *rad52-C180A* and *rad52Δ* strains as a percentage of the total HR rate. The total HR is calculated from the total amount of Leu$^+$ colonies obtained after plating on SC-Leu plates. GC: Gene conversion, CT: Conversion tract, CO: Crossover, Chr.: Chromosome.

As expected and previously shown, HR was dramatically reduced in the *rad52Δ* strain where gene conversion rates were about 4% of the rate obtained in wild-type strains (Malone & Esposito, 1980; Haber & Hearn, 1985; Mortensen et al., 2002; Lettier et al., 2006). In fact, for these strains, the main event leading to the formation of Leu$^+$ prototrophs was chromosome loss which we found to represent as much as 49% of the total recombination rate. Again, this is in agreement with the results of Haber & Hearn (1985) who observed frequent loss of an entire chromosome in *rad52Δ* strains. Finally, we also observed an increase in the percentage of gene conversion events associated with crossover in the absence of *rad52* though not to the extent described

by Haber & Hearn (1985).

The spectrum of HR events observed in the *rad52-C180A* mutant strain was very similar to that obtained for the wild-type strain with respect to gene conversion and gene conversion associated with crossover or BIR (Figure 5.6). Interestingly, we found that the chromosome loss rate was relatively high in this strain, representing up to 11% of the total recombination rate.

5.3.3 Rad52-R70A and Rad52-C180A mutant proteins colocalize with Rad51 in spontaneous foci

We have previously shown that a Rad52 Class C mutant protein and Rad51 co-localize at a defined DNA DSB induced by the I-*Sce*I or the HO endonucleases at two different loci (Lettier et al., 2006). This showed that the inability of the *rad52* class C mutants to repair DNA DSBs is not due to an inability to recruit Rad51 to the site of damage. Moreover, this suggests that the recombination mediator role of Rad52 in intact in the class C mutants. To confirm this further, we investigated if Rad52 Class C mutant proteins, Rad52-R70A and Rad52-C180A, and Rad51 co-localized in spontaneous foci. The results obtained are presented in Table 5.2.

Table 5.2. Rad52-R70A and Rad52-C180A mutant proteins colocalize with Rad51 in spontaneous foci

Allele	**Spontaneous Rad52 focus (% Cells)**		**Colocalization of Rad52 and Rad51 foci (%)**	
	G1	**S/G2/M**	**G1**	**S/G2/M**
RAD52	1(181)	18(22)	100	100
rad52-R70A	6(158)	41(133)	100	94
rad52-C180A	3(111)	32(72)	100	68

Given in parenthesis are the total number of cells counted.

In agreement with previous results, practically no spontaneous foci were observed in G1 and about 20% of the cells contained a Rad52 foci in S/G2/M. In both *rad52* class C mutant strains, a larger number of cells spontaneously formed Rad52 repair foci during the cell cycle compared to wild-type strains (Lisby et al., 2001; Lettier et al., 2006). In G1, all Rad52 foci co-localized with Rad51 foci in the *rad52* class C mutant strains. In S/G2/M, 100%, 94% and 68% co-localization between Rad52 and Rad51 foci was observed for the wild-type, *rad52-R70A* and *rad52-C180A* strains, respectively. This shows that the Rad52 class C mutant proteins are able to recruit Rad51 at the site of spontaneous DNA damage.

5.3.4 HR observed in the class C mutants is dependent on Rad51

If the spontaneous foci observed in the *rad52* class C mutant cells represent the site of on-going DNA repair by HR, the results above suggest that HR observed in the *rad52* class C mutants involves Rad51. We therefore investigated if HR in the *rad52* class C mutants was Rad51-dependent using the version of the heteroallelic assay presented in Figure 5.14 (see Supplementary materials) in strains where *rad51* had been deleted. The results obtained are presented in Table 5.3. In the absence of *rad51*, mitotic recombination rates decreased to the level observed in *rad52*Δ strains for both *RAD52* and *rad52* class C mutant strains. This shows that, using our assay, HR observed in these strains is strongly dependent on Rad51. This suggest that spontaneous HR in the *rad52* class C mutant and wild-type strains occurs by a similar mechanism that is dependent on both Rad51 and Rad52. In these experiments, very few colonies were obtained and plating of high amounts of cells was necessary to obtain a value for the total HR rate. Moreover, no colonies could be scored as resulting from events associated with crossover or chromosome loss. For this reason, only the total HR rate is given in Table 5.3.

Table 5.3. Effect of deletion of *rad51* on interchromosomal heteroallelic recombination rates of *RAD52*, *rad52-R70A* and *rad52-C180A*

Allele	**Total HR Rate x** 10^{-8}
*RAD52 rad51*Δ	1.9 ± 1.2
*rad52-R70A rad51*Δ	1.4 ± 1.0[a]
*rad52-C180A rad51*Δ	1.4 ± 1.0[a]

a: $p > 0.05$ mutants versus wild-type

5.3.5 A Rad52 class C is proficient for strand invasion

According to classical HR models (Szostak et al., 1983), transfer of genetic information between DNA strands involves strand invasion of a homologous donor sequence by one of the resected 3' ends of the DNA DSB to initiate DNA synthesis. In this step, Rad52 is believed to act as a mediator, promoting the assembly of the Rad51 nucleoprotein filament onto ssDNA (Song & Sung, 2000; Sugiyama & Kowalczykowski, 2002; Sung et al., 2003). In order to verify that this function is intact in the *rad52* class C mutants, we performed an assay originally used at the MAT locus by J. Haber and co-workers and later adapted by the Kupiec laboratory at the *URA3* locus on chromosome V (White & Haber, 1990; Aylon et al., 2003). In this assay, a specific DNA DSB is

formed by the *HO*-endonuclease in a *ura3*::HOcs allele on chromosome V. This break can be repaired by HR using the *ura3*::HOcs-inc allele inserted on chromosome II as a template. Accordingly, one of the 3' ssDNA tails of the DSB on chromosome V will invade the homologous template on chromosome II and initiate DNA synthesis. This will extended the 3' end of chromosome V by chromosome II sequences, thus creating a PCR substrate for primers situated adjacent to the homology regions on chromosome II and V, respectively (see primers P1 and P2 in Figure 5.7, Panel A).

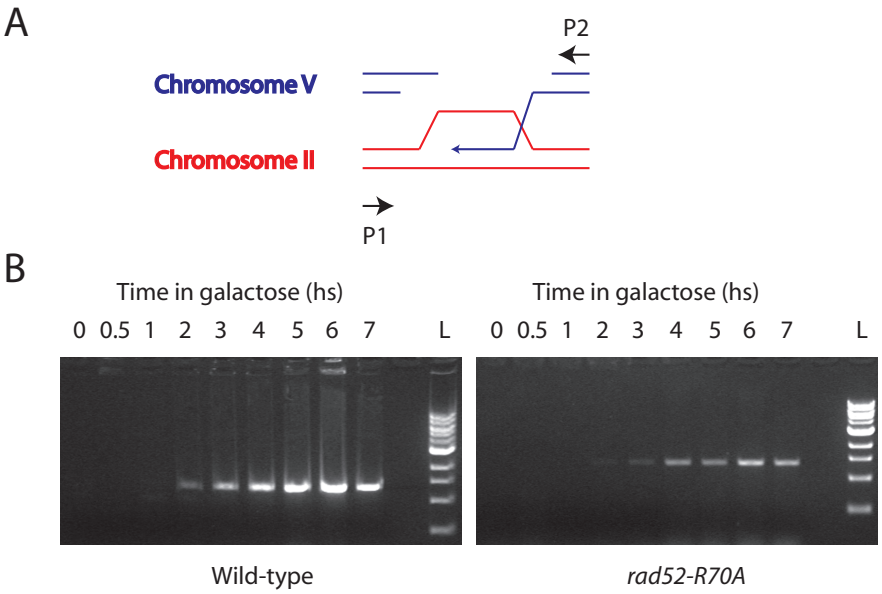

Figure 5.7. Strand invasion PCR assay. (A) Primers P1 and P2 situated on each side of the homology region on chromosome II and V, respectively, amplify the polymerized invading intermediate. (B) PCR products obtained in wild-type (left) and *rad52-R70A* mutant strains. L: 1 Kb ladder (New England Biolabs).

First, we followed the formation and repair of the HO-induced DNA DSB in wild-type and *rad52-R70A* strains. This was done both by analysis the survival of these strains on SC-Gal plates and by quantitatively measuring the amount of intact chromosome V by PCR (see Figure 5.15, Supplementary Materials). In agreement with our previous results (Lettier et al., 2006), the *rad52-R70A* mutant was unable to repair the HO-induced DSB. We then performed a PCR invasion assay to follow strand invasion as described above. As shown in Figure 5.7, Panel B, strand invasion products are detected in wild-type and *rad52-R70A* strains. Indeed, for both strains, a PCR product appeared approximately 2-3 hours after induction of the break with galactose. For the wild-type strain, this correlates with the time points where minimal levels of intact chromosome are observed (Figure 5.15, Supplementary Materials). It is important to note that, in the results described by (Aylon et al., 2003), the PCR product obtained as a result of strand invasion is not detected at the late time points and the authors con-

clude that this is because repair is completed. In our hands, a strong band can still be observed at the last time point (7 hours after induction) and the reason for this is unknown. One hypothesis is that DNA synthesis elongating the invading 3'-end can, in some cases, proceed beyond the region of homology thus copying the P1 annealing site back to chromosome V. If this occurs, both P1 and P2 primers can annealing on chromosome V even after repair has been completed. To test this hypothesis, wild-type cells were plated on YP-Gal plates and incubated for 2 days. Colonies formed on SC-Gal after this time were considered to derive form cells that repaired the HO-induced break on chromosome V thus were able to divide and form a colony. A representative number of colonies were picked, their DNA was extracted and PCR was run using primers P1 and P2. In 20% of the cases, a band was obtained showing that the transfer of the P1 annealing site from chromosome II to chromosome V does take place in about 20% of the cell population. Controls were run with cells that had not been induced on SC-Gal and no P1-P2 PCR product was ever recovered with these cells.

Although it is clear that additional experiments need to be run, we conclude that *rad52-R70A* mutant strains are proficient for strand invasion and that it is therefore not at this step of the DNA DSB repair process that these mutants are blocked.

5.3.6 Neither overexpression of RAD59 nor decreased amounts of RPA suppress the DNA DSB repair phenotype of a class C mutant

In order to understand the origin of the DNA DSB repair phenotype observed in the *rad52* class C mutants, suppressors of this phenotype were investigated.

Because of its N-terminal sequence similarity with Rad52, Rad59 is often described as a Rad52 paralog. Although Rad59 is unable to complement all the functions of Rad52, the two proteins have been shown to have some overlapping functions (Bai & Symington, 1996; Bai et al., 1999; Petukhova et al., 1999a; Davis & Symington, 2001; Wu et al., 2006a; Feng et al., 2007). Rad59 has been shown to binds both ss and dsDNA as well as to promote annealing of complementary ssDNA (Petukhova et al., 1999a; Davis & Symington, 2001). Moreover, Rad59 was found to enhance Rad52-mediated DNA annealing, both in the absence and in the presence of RPA (Wu et al., 2006b). Interestingly, some *rad52* mutations situated in the N-terminal domain of the protein (*rad52*-R70K and *rad52* Class E mutants) have been shown to have synergistic defects with *rad59*Δ (Bai et al., 1999; Feng et al., 2007). Previously, we showed that deletion of *RAD59* did not affect the hyper-rec phenotype of the *rad52* class C mutant strains thus concluding that this phenotype was not due to a helper role of Rad59 (Lettier et al., 2006). Here, we investigated if overexpression of *RAD59* could suppress the DNA DSB repair phenotype observed in the *rad52-R70A* and *rad52-C180A* mutant strains. The results obtained, presented in

Figure 5.8, showed that overexpression of *RAD59* did not suppress the sensitivity of these strains to MMS. Accordingly, the function of Rad52 that is impaired in the *rad52* class C mutants cannot be substituted by Rad59.

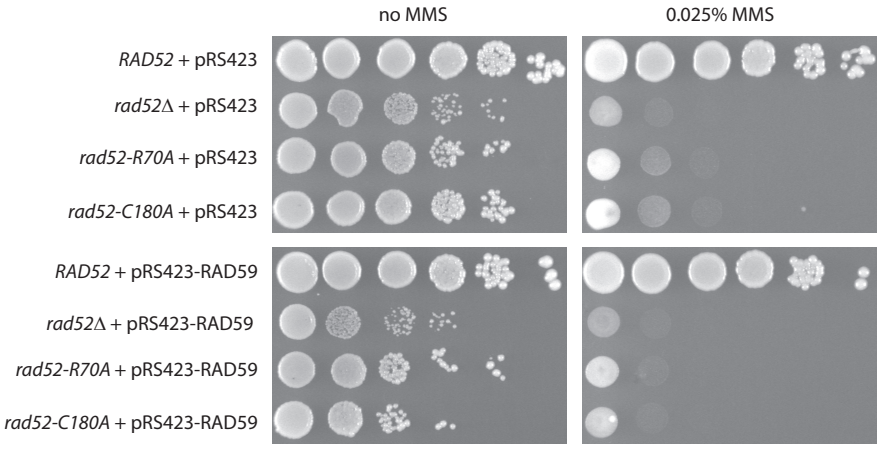

Figure 5.8. Effect of *RAD59* overexpression on the survival of *RAD52*, *rad52Δ*, *rad52-R70A* and *rad52-C180A* strains to MMS. Strains were spotted on SC-HIS medium containing the mentioned amounts of MMS.

As mentioned above, all the amino acid residues in the hsRad52 structure corresponding to *rad52* class C mutations are located in, or close to, the putative Rad52 DNA-binding groove. Moreover, four of the corresponding human Rad52 mutant species: HsRad52-Y51A (ScY66A), HsRad52-R55A (ScR70A), HsRad52-R70A (ScR85A), and HsRad52-Y81A (ScY96A) have been purified, and the three latter species show decreased affinity for ssDNA in gel shift assays (Kagawa et al., 2002; Lloyd et al., 2005). Accordingly, we speculate that it is the DNA binding and/or annealing activities of Rad52 that are impaired in our *rad52* mutants. This is in agreement with our previous findings showing that the *rad52* class C mutants are unable to repair an HO-induced DSB between two direct repeats by single strand annealing (SSA) (Lettier et al., 2006). Interestingly, an allele of *RFA1*, *rfa1-D228Y*, has been shown to partially suppress the SSA defects of rad52Δ strains (Smith & Rothstein, 1999). This is probably due to a lower amount of RPA complex in this mutant that increases spontaneous annealing of non RPA-coated ssDNA (Smith & Rothstein, 1995). Based on these results, we then investigated if *rfa1-D228Y* would increase survival of the *rad52* class C mutant strains to DNA damaging agents. However, our results show that the *rfa1-D228Y* mutation did not have any positive effect on the survival of the *rad52* class C mutants to MMS (Figure 5.9). This shows that decreasing the amount of RPA complex does not suppress the DNA DSB repair phenotype of the *rad52* class C mutants and suggests that it is not the presence of the RPA complex on ssDNA that hinders DNA DSB repair in these mutants.

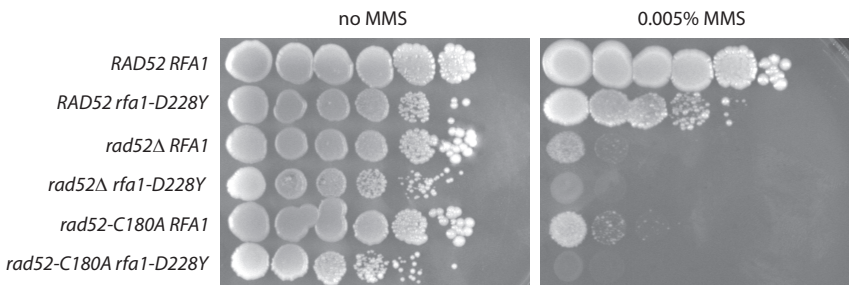

Figure 5.9. Effect of *rfa1-D228Y* mutation on the survival of *RAD52*, *rad52*Δ and *rad52-C180A* strains to MMS. Strains were spotted on YPD medium containing the mentioned amounts of MMS.

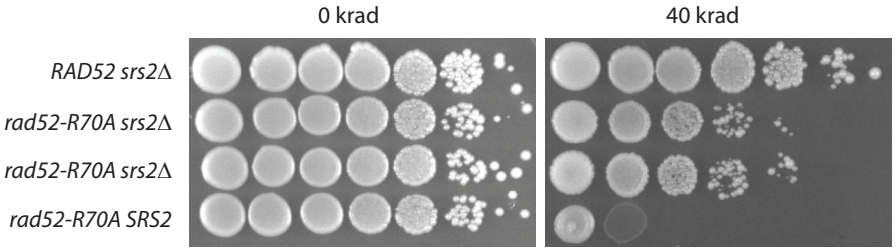

Figure 5.10. Effect of *srs2* deletion on the survival of *RAD52* and *rad52-R70A* strains to γ-irradiation. Results from two different *rad52-R70A srs2* are shown. Strains were spotted on YPD medium and irradiated at the mentioned doses.

5.3.7 Deletion of *srs2*, but not overexpression of *RAD51*, suppresses the DNA DSB repair phenotype of a class C mutant

A known suppressor of the MMS sensitivity of a number of *rad52* mutations is the *SRS2* helicase (Milne et al., 1995; Schild, 1995). Moreover, Srs2 has been shown to physically interact with Rad51 and to act as a negative regulator of HR by disrupting the Rad51 nucleoprotein filament (Krejci et al., 2003; Veaute et al., 2003). Interestingly, addition of Rad52 was shown to partially overcome the inhibitory effect of Srs2, suggesting that Srs2 and Rad52 antagonize each other in regulating HR (Krejci et al., 2003; Macris & Sung, 2005). To investigate if deletion of *srs2* could have an effect of the DNA DSB repair phenotype of the *rad52* class C mutants, we constructed double mutants, containing both *rad52-R70A* and *srs2*Δ, and analyzed there sensitivity to γ-irradiation in a spot assay. Surprisingly, deletion of *srs2* suppressed the sensitivity of the *rad52-R70A* class C mutant to irradiation (Figure 5.10). Similar results were obtained when sensitivity to MMS was analyzed (data not shown).

Most of the *rad52* mutations that have been reported to be suppressed by deletion of *srs2* affect the Rad51 binding domain of Rad52. Accordingly, these mutations were also suppressed by overexpression of *RAD51* (Milne et al., 1995; Schild, 1995). Although the Rad51 bind-

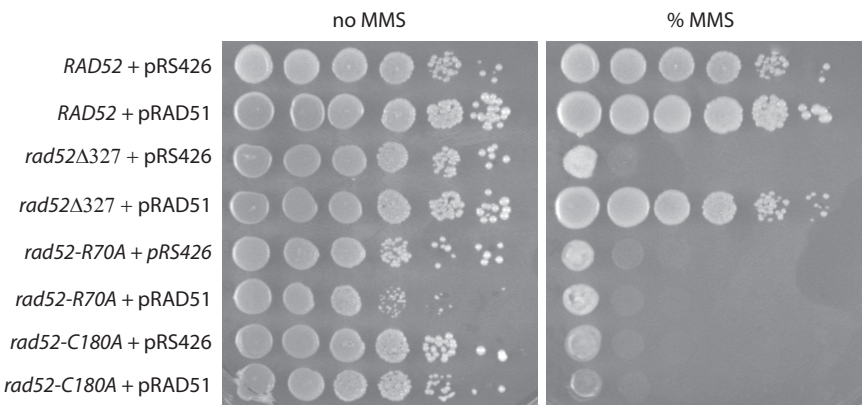

Figure 5.11. Effect of *RAD51* overexpression on the survival of *RAD52*, *rad52*Δ327, *rad52-R70A* and *rad52-C180A* strains to MMS. Strains were spotted on SC-Gal-URA medium containing the mentioned amounts of MMS. The *rad52*Δ327 was used as a positive control as its MMS sensitivity is suppressed by *RAD51* overexpression (Milne & Weaver, 1993; Asleson et al., 1999).

ing domain seems unaffected in the *rad52* class C mutants (see above and Lettier et al. (2006)), we investigated if overexpression of *RAD51* could suppress the MMS sensitivity in these strains. As showed in Figure 5.11, overexpression of *RAD51* did not suppress the DNA DSB repair phenotype of the *rad52-R70A* and *rad52-C180A* class C mutant strains. Accordingly, our results suggest that suppression of the DNA DSB repair phenotype of the *rad52* class C mutants by *srs2* may be independent of Rad51.

5.3.8 Deletion of *srs2* affects spontaneous foci formation but not the hyper-rec phenotype of a class C mutant

Intrigued by the fact that deletion of *srs2* suppresses the DNA DSB repair phenotype of the *rad52-R70A* mutant, we further investigated if this deletion had an effect on some of the other phenotypes observed in this mutant.

Recently, we observed that, in strains where the class C mutant Rad52 is tagged with YFP (yellow fluorescent protein), an abnormally high percentage of S/G2/M cells contain a spontaneous focus. Furthermore, we showed that such foci are longer-lived than those observed in wild-type strains (Lettier et al., 2006), but why this is the case remains unclear. One can hypothesize that the inefficient DNA binding of the class C mutant Rad52 hampers the DNA repair process, thus prolonging the need for Rad52 assembly at the site of the lesion. If Srs2 antagonizes Rad52 in this process, deleting *srs2* should have an effect on the spontaneous foci formation in the *rad52* class C mutant strains. As shown in Table 5.4, deletion of *srs2* reduced the number of

rad52-R70A cells containing a spontaneous focus to the level observed in wild-type strains, thus the spontaneous focus formation phenotype of the *rad52-R70A* mutants could also be suppressed by deletion of *srs2*.

Table 5.4. Effect of *srs2* deletion on Rad52-R70A spontaneous foci formation

Allele	Spontaneous Rad52-R70A focus (% Cells)	
	G1	S/G2/M
RAD52	0[a]	14[a]
rad52-R70A	0[a]	56[a]
*rad52-R70A srs2*Δ	0(205)	15(33)

a: From Lettier et al. (2006)

Given in parenthesis are the total number of cells counted.

Another characteristic phenotype of the *rad52* class C mutants is that they perform HR at wild-type or higher levels (Mortensen et al., 2002; Lettier et al., 2006). Considering the fact that these mutants are unable to repair DNA DSBs, we suggested that spontaneous HR was mainly triggered by lesions other than DNA DSBs (Lettier et al., 2006). Based on the results presented above, Srs2 appears to impair DNA DSBs repair by HR in the *rad52* class C mutants. However, one can envision that this effect is not limited to DNA DSB repair but concerns all Rad52-dependent HR. We therefore investigated the effect of combining the *srs2* deletion and the *rad52-R70A* mutation on mitotic HR. For these experiments, the simple *leu2* interchromosomal heteroallelic recombination assay, in which HR is measured between *leu2*Δ*EcoRI* and *leu2*Δ*BstEII* alleles in a diploid strain, was used (Smith & Rothstein, 1995). In agreement with previous findings (Aguilera & Klein, 1988), we found HR to be increased about 9-fold in the *RAD52 srs2*Δ strain compared to wild-type strains (Table 5.5). The HR rate observed in the *rad52-R70A srs2*Δ strain was about half of that observed in the *RAD52 srs2*Δ strain and this value was found not to be significantly different from the HR rate of the *rad52-R70A SRS2* strains. Accordingly, this shows that the *rad52-R70A* mutation is epistatic to *srs2*.

5.4 Discussion

Rad52 is a key protein involved in both DNA DSB repair and HR in *S. cerevisiae*. To date, two main activities of Rad52 have been described: its DNA binding/annealing activity and its recombination mediator activity.

The domain of Rad52 responsible for DNA binding is situated in the evolutionary conserved N-terminal part of the protein (Mortensen et al., 1996). Rad52 can bind both single- and double-stranded DNA and promotes annealing between complementary single-stranded DNA

Table 5.5. Effect of *srs2* deletion on interchromosomal recombination in *rad52-R70A* mutant strains

Allele	**Heteroallelic recombination** (Rate x 10^{-8})	**Fold increase** (compared to WT)
RAD52 SRS2	110 ± 30	1
*RAD52 srs2*Δ	944 ± 138[a,b]	8.6
rad52-R70A SRS2	370 ± 60[a]	3.4
*rad52-R70A srs2*Δ	480 ± 87[a,c]	4.4

a: $p < 0.05$ mutants versus wild-type

b: $p < 0.05$ *RAD52 srs2*Δ mutant versus *rad52-R70A* mutant

c: $p > 0.05$ *rad52-R70A srs2*Δ mutant versus *rad52-R70A* mutant

molecules in vitro (Mortensen et al., 1996; Reddy et al., 1997; Shinohara et al., 1998; Kagawa et al., 2001). Rad52 is also believed to mediate Rad51 filament assembly by removing RPA from the ssDNA while simultaneously replacing it by Rad51 (Song & Sung, 2000; Sugiyama & Kowalczykowski, 2002). This assumption is strongly backed-up by the fact that Rad52 can alleviate the inhibitory effect of RPA in strand exchange assays in vitro (Sung, 1997a; Benson et al., 1998; New et al., 1998; Shinohara & Ogawa, 1998). Moreover, Rad52 has been shown to bind both Rad51 (Milne & Weaver, 1993; Shen et al., 1996a; Shinohara & Ogawa, 1998) and RPA (Park et al., 1996; Hays et al., 1998; Shinohara et al., 1998). Importantly, both the DNA binding/annealing and the mediator activities of Rad52 have been described in several different organisms going from yeast to human thus suggesting that these activities are conserved.

When considering the Rad52 activities in the context of the classical DNA DSB repair models (Resnick & Martin, 1976; Szostak et al., 1983; Allers & Lichten, 2001) (reviewed in Haber et al. (2004)), the recombination mediator activity is generally associated with the strand invasion step. Indeed, after 5'-3' resection of the DNA DSB ends, the resulting 3' ssDNA tails, covered by RPA, need to engage in the repair process by invading a homologous template and priming for DNA synthesis. This requires prior removal of RPA and subsequent covering of the ssDNA tails by an active nucleoprotein filament of Rad51. As mentioned above, this step has been shown to be efficiently mediated by Rad52 in vitro thus leaving little doubt about the physiological relevance of the Rad52 mediator activity in this context. In contrast, the functionality of the DNA binding/annealing activity of Rad52 in vivo is still unclear. Several lines of evidence suggest however that this activity is biologically relevant. For example, single-strand annealing (SSA), a DNA repair pathway used to repair lesions between direct repeats by simple DNA annealing of the resected single-stranded complementary ends, has been shown to be impaired in the absence of Rad52 (Fishman-Lobell et al., 1992; Sugawara & Haber, 1992). Interestingly,

deletion of other proteins know to be important players of recombination such as *RAD51*, *RAD54*, *RAD55* and *RAD57* has no negative effect on SSA (Ivanov & Haber, 1995). Accordingly, Rad52 seems to be the key player of SSA thus suggesting that Rad52 can promote DNA annealing in vivo. In their study showing that Rad52 could promote the annealing of complementary ssDNA molecules in vitro, Mortensen et al. (1996) proposed that Rad52 DNA annealing could assist in homology search. Later, Shinohara et al. (1998) proposed that Rad52 could mediate Rad51-independent recombination through ssDNA annealing assisted by RPA as they observed that Rad52-RPA interaction enhanced annealing of complementary ssDNA molecules. A similar role of HsRad52 in the Rad51-independent recombination pathway was also proposed by Kagawa et al. (2001).

More recently, however, new findings have suggested a role for Rad52 DNA binding in Rad51-dependent recombination. Arai et al. (2005) proposed that Rad52 and Rad51 bind ssDNA as a complex and that this is required for the functional binding of the proteins-ssDNA complex to dsDNA in the strand invasion step. Importantly, they showed that this function of Rad52 was necessary even in the absence of RPA. Using immunofluorescence in vivo, Miyazaki et al. (2004) showed that Rad52 remained at the site of an HO-induced DNA DSB longer than Rad51 and the authors therefore suggested that Rad52 could have a postsynaptic role after dissociation of the Rad51 filament. In agreement with this, Sugiyama et al. (2006) showed that Rad52 promotes annealing of the ssDNA strand that is displaced by DNA strand exchange by Rad51 and RPA, to a second ssDNA strand in vitro. As this resembles the situation described by classical DNA DSB repair models as second strand capture, the authors suggest a role for Rad52 in this step.

Here, we present further evidence for the physiological importance of the Rad52 DNA binding/annealing activity in DNA DSB repair by characterizing *rad52* mutants that are impaired in this function.

5.4.1 DNA binding by Rad52 is required for second strand capture

In this study, we have used the separation of function *rad52* class C mutants described previously (Mortensen et al., 2002; Lettier et al., 2006), to investigate the physiological importance of the Rad52 DNA binding/annealing activity in DNA DSB repair. We have previously shown that these mutants are unable to repair even a defined DNA DSB on a chromosome (Lettier et al., 2006) and an analysis of four corresponding human Rad52 mutant species, in gel shift assays, have shown that these mutants have a decreased affinity for ssDNA (Kagawa et al., 2002; Lloyd et al., 2005). Accordingly, the Rad52 DNA binding activity appears to have a central role in the repair of DNA DSB in *S. cerevisiae*. In our previous analysis of these mutants, we showed that a class C Rad52 mutant protein tagged with YFP was able to

recruit to a defined DNA DSB and to recruit Rad51 to the site of the break (Lettier et al., 2006). Interestingly, this suggest that DNA binding by Rad52 is not required for the recruitment of the protein to the DNA DSB and that this recruitment must therefore be mediated by Rad52 interaction with proteins already present at the break such as the RPA complex. This has been suggested previously by Hays et al. (1998) (Model A) and by Lisby et al. (2004) who showed that Rfa1 is recruited to a DNA DSB before Rad52 and that Rad52 foci do not form in cells lacking Rfa1. Moreover, our laboratory has recently identified a region in the middle part of Rad52 that is responsible for foci formation (Plate, 2006). By yeast-two hybrid analysis, a Rad52 mutant lacking this region was shown to be unable to interact with Rfa1 (Swee H. Jensen, personal communication), thus suggesting that this interaction is important for Rad52 re-localization to the site of DNA damage.

The next step of the DNA DSB repair pathway that could potentially involve Rad52's DNA binding activity is strand invasion. However, using a strand invasion PCR assay (White & Haber, 1990; Aylon et al., 2003), we showed that the *rad52-R70A* mutant was able to perform strand invasion as efficiently as wild-type strains. Accordingly, the Rad52 DNA binding activity does not appear to be involved at this stage of the repair process. One can hypothesize that the role of Rad52 described by Arai et al. (2005) is mainly driven by Rad52's interaction with Rad51, a function that appears to be intact in the class C Rad52 mutants as they can recruit Rad51 to a DNA DSB (Lettier et al., 2006). Importantly, we show that although the *rad52* class C mutants seem proficient in strand invasion, they are still unable to repair the HO-induced DNA DSB that initiated the repair process as shown in Figure 5.15 (Supplementary materials). This suggests that the *rad52* class C mutants are impaired in a step downstream of strand invasion.

The last step of the DNA DSB repair that could require the Rad52 DNA binding/annealing activity is second strand capture and we suggest that this step is impaired in the *rad52* class C mutants. Specifically, in the SDSA model, this step consists in the displacement of the invading 3' end after DNA synthesis and the re-annealing of this end with the other single-stranded tail of the DSB. We envision that this process is promoted by the DNA binding/annealing activity of the N-terminal domain of Rad52. Supporting this view, we have previously shown that the *rad52* class C mutants are unable to repair a defined DNA DSB between direct repeats by SSA (Lettier et al., 2006), a mechanism that has been shown to mainly involve Rad52 (Ivanov & Haber, 1995). This suggests that the class C Rad52 mutant protein is impaired in its ability to bind and anneal two single-stranded DNA molecules in order to close the DSB. Accordingly we propose that this activity is required for second strand capture, thus suggesting an essential role of DNA binding/annealing by the N-terminal domain of Rad52 in this step of the DNA DSB repair process.

5.4.2 Quality control role of Srs2 in second strand capture

In order to investigate if inefficient DNA binding was the only cause in the *rad52* class C mutants' inability to repair DNA DSBs, we looked for suppressors of this phenotype. Among the known *rad52* suppressors tested, deletion of *srs2* was the only one that could suppress the DNA DSB repair phenotype of the *rad52* class C mutants. This was surprising as the *rad52* mutations previously reported to be suppressed by deletion of *srs2* affect the Rad51 DNA binding domain of Rad52 (Milne et al., 1995; Schild, 1995), which is not the case of our *rad52* mutants. Moreover, we showed that overexpression of *RAD51* does not suppress the MMS sensitivity of the *rad52* class C mutants, suggesting that the Rad52-Rad51 interaction is intact in these mutants. Accordingly, our results suggest that Srs2 impairs DNA DSB repair in the *rad52* class C mutants, and that this process is independent of Rad51. Moreover, we show that deletion of *srs2* complements the foci formation phenotype of the *rad52* class C mutant cells, suggesting that the spontaneous foci observed in *rad52-R70A* represent ongoing repair of spontaneous DNA DSBs. Indeed, in *rad52-R70A SRS2* strains, Srs2 may severely slow down DNA DSB repair (long-lasting foci) and unrepaired DSBs eventually lead to cell death (high sensitivity to MMS and γ-irradiation). However, in *rad52-R70A srs2*Δ strains, the negative effect of Srs2 is relieved, thus allowing for close to wild-type levels of spontaneous foci formation and DNA DSB repair.

In the context of second strand capture, we envision that Srs2 acts as a "quality controller" of the DNA binding/annealing step by removing Rad52 from ssDNA if annealing is weak. In our case, weak DNA annealing is due to the inability of the class C Rad52 mutant protein to efficiently bind DNA. However, in reality, weak annealing could be the sign that Rad52 is trying to anneal ss-stranded DNA molecules with low sequence identity that do not belong together. If this was allowed to happen, it would have severe consequences such as chromosomal translocations. Interestingly, this resembles Srs2's role in preventing untimely HR events by removing the Rad51 nucleoprotein filament from ssDNA (Krejci et al., 2003; Veaute et al., 2003) (reviewed in Macris & Sung (2005)). In fact, the inhibitory effect of Srs2 on the Rad51-mediated recombination reactions was found to be partially suppressed by addition of Rad52 and Krejci et al. (2002) suggested that Srs2 and Rad52 antagonize each other in the regulation of HR. In agreement with this view, Kaytor et al. (1995) found that overexpression of *SRS2* on a high copy plasmid increased the MMS sensitivity of *RAD52* wild-type strains. In our model (Figure 5.12), we propose that Srs2 acts to dissociate the paired ss-DNA ends and prevent repair if weak DNA annealing between these ends is detected. This can be achieved by Srs2's DNA helicase activity and/or removal of the Rad52 molecules promoting the annealing. However, the former hypothesis is preferred as no Rad52-Srs2 interaction has yet been reported. To our knowledge,

this describes a novel role of Srs2 in DNA DSB repair.

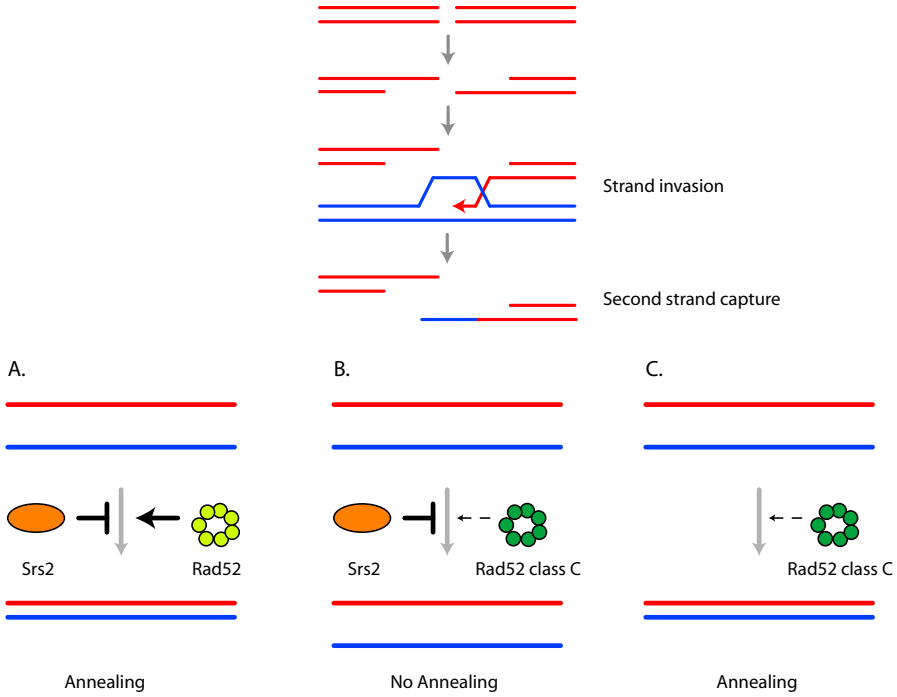

Figure 5.12. Rad52 and Srs2 antagonize each other in the second strand capture step of the DNA DSB repair pathway.

5.4.3 Is second strand capture required for spontaneous HR?

As previously reported, the *rad52* class C mutants are unable to repair DNA DSBs yet they perform mitotic HR at wild-type or higher levels (Mortensen et al., 2002; Lettier et al., 2006). In this study, we show that the spectrum of recombination events observed in the *rad52* class C mutants is similar to that observed in wild-type strain, suggesting HR occurs by the same pathways in these strains. However, higher rates of HR events associated with chromosome loss were observed in the *rad52-C180A* mutant strain and we suggest that this may represent the fraction of HR events that were initiated by a spontaneous DNA DSB. Indeed, as the *rad52-C180A* mutant is unable to repair such lesions, HR could result in the loss of the broken chromosome. If this is true, one can conclude that most HR events observed in this mutant must have been induced by lesions that are not DNA DSBs (Lettier et al., 2006).

We show that Srs2 impairs DNA DSB repair in these mutants and we propose a model where the DNA binding/annealing activity of Rad52 competes with the DNA helicase activity of Srs2 at the second strand capture step of the DNA DSB repair process. Interestingly, the ability of the *rad52* class C mutants to perform HR does not seem to be influenced by the presence or the absence of Srs2. Indeed, we

show that deletion of *srs2* in a *rad52-R70A* mutant does not significantly affect the mitotic HR rate in this strain. These results suggest that *rad52-R70A* is epistatic to *srs2*. One way to explain these results is to postulate that second strand capture is not required in the DNA repair process that drives spontaneous HR in *S.cerevisiae*. This would imply that the lesion that triggers spontaneous HR does not result in a physical separation of the DNA ends and is therefore not a DNA DSB (Figure 5.13). In our previous characterization of the *rad52* class C separation of function phenotype, we postulated that a DNA DSB was not the main lesion that triggers spontaneous HR in *S.cerevisiae* and proposed nicks or single-stranded DNA stretches as possible candidates (Lettier et al., 2006). The fact that second strand capture does not seem to be involved in the repair mechanism responsible for spontaneous HR only strengthens this hypothesis.

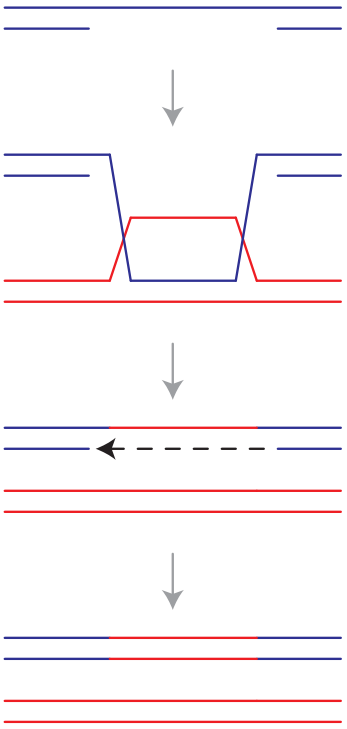

Figure 5.13. Model of single-stranded gap induced homologous recombination. The lesion that triggers spontaneous HR does not result in a physical separation of the DNA ends, thus its repair by HR does not require second strand capture.

5.5 Supplementary materials

Table 5.6. Strains used in this study

Strain	Genotype
UMR79-11	*Matα ade2Δ leu-ΔEcoRI::ADE2 trp1-1*
UM228-5C	*MAT***a** *ade2Δ leu-ΔBstEII::ade2-ΔAatII lys2Δ SPB1::kanMX TRX3::NAT1*
UM229-A	*MATα ade2Δ leu-ΔEcoRI::ADE2 trp1-1 rad52-C180A*
UM229-B	*MAT***a** *ade2Δ leu-ΔBstEII::ade2-ΔAatII lys2Δ SPB1::kanMX TRX3::NAT1 rad52-C180A*
UM237-A	*MATα ade2Δ leu-ΔEcoRI::ADE2 trp1-1 rad52Δ*
UM237-B	*MAT***a** *ade2Δ leu-ΔBstEII::ade2-ΔAatII lys2Δ SPB1::kanMX TRX3::NAT1 rad52Δ*
UM195-52D	*MATα trp1-1 ade2Δ leu2-ΔEcoRI::ADE2 SPB1::kanMX TRX3::NAT1 rad51Δ*
UM196-7D	*MATα trp1-1 ade2Δ leu2-ΔEcoRI::ADE2 SPB1::kanMX TRX3::NAT1 rad51Δ rad52-R70A*
UM197-8A	*MATα trp1-1 ade2Δ leu2-ΔEcoRI::ADE2 SPB1::kanMX TRX3::NAT1 rad51Δ rad52-C180A*
UM194-39A	*MAT***a** *ade2Δ lys2Δ leu2-ΔBstEII::ade2-ΔAatII rad51Δ*
UM199-4A	*MAT***a** *ade2Δ lys2Δ leu2-ΔBstEII::ade2-ΔAatII rad51Δ rad52-R70A*
UM200-1B	*MAT***a** *ade2Δ lys2Δ leu2-ΔBstEII::ade2-ΔAatII rad51Δ rad52-C180A*
W3847-7B	*MAT***a** ADE2 bar1::LEU2 leu2-3,112 trp1-1 YFP-RAD51 RAD52-CFP
UM204-37A	*MAT***a** *ADE2 bar1::LEU2 leu2-3,112 lys2Δ CFP-RAD51 rad52-R70A-YFP*
UM205-11D	*MAT***a** *ADE2 bar1::LEU2 leu2-3,112 lys2Δ YFP-RAD51 rad52-C180A-CFP*
UM225-11B	*MATα-inc ura3::HOcs lys2::ura3-HOcs-inc ade3::GALHO leu2-3,112 trp1-1 ade2-1*
UM225-8B	*MATα-inc ura3::HOcs lys2::ura3-HOcs-inc ade3::GALHO leu2-3,112 trp1-1 ade2-1 rad52-R70A*
W1588-4C	*MAT***a** *ade2-1 leu2-3,112 trp1 LYS2*
J786	*MAT***a** *ade2-1 leu2-3,112 trp1-1 rad52-C180A*
J788	*MAT***a** *ade2-1 leu2-3,112 trp1-1 rad52-R70A*
J883	*MAT***a** *ade2-1 leu2-3,112 trp1-1 rad52-Δ327*
W3800-35D	*MAT***a** *ade2-1 leu2-ΔBstEII trp1-1 rad52Δ*
UM268-22C	*MAT***a** *ade2-1 leu2-3,112 trp1-1 srs2::HIS3 rad52-R70A-YFP*
UM267-17B	*MAT***a** *ade2-1 leu2-ΔBstEII lys2Δ srs2::HIS3 rad52-R70A*
UM269-A	*MATα ade2-1 leu2-ΔEcoRI trp1-1 srs2::HIS3 rad52-R70A*
UM136-2C	*MATα ade2-1 leu2,3-112 trp1-1 srs2::HIS3*
UM267-47A	*MATα ade2-1 leu2,3-112 trp1-1 rad52-R70A*
UM267-55C	*MATα ade2-1 leu2,3-112 trp1-1 srs2::HIS3 rad52-R70A*
W1588-4A	*MATα ade2-1 leu2-3,112 trp1-1*

All strains are derivatives of W303 except that they are *RAD5*

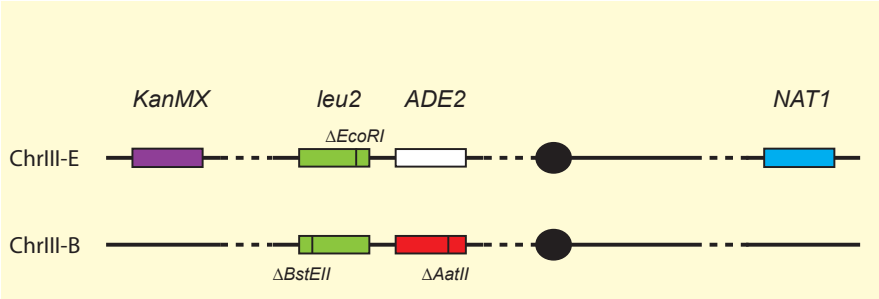

Figure 5.14. Representation of a variant of the heteroallelic recombination assay used in this study. For simplicity, only one chromatid of each chromosome is represented (black line). The centromeres and the different alleles are represented as black circles and colored boxes, respectively. Mutations present in some of the alleles are represented as vertical black lines.

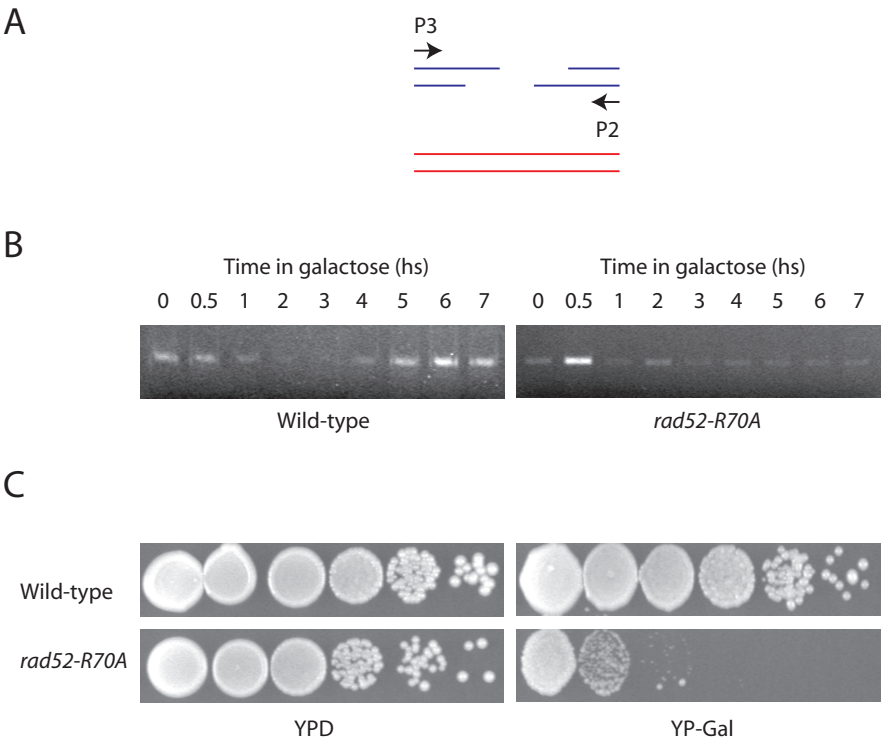

Figure 5.15. Quantitative measurement of intact chromosome V by PCR. (A) Primers P2 and P3 situated on each side HO cut site on chromosome V. (B) PCR products obtained in wild-type (left) and *rad52-R70A* mutant (right) strains. (C) Survival of wild-type and *rad52-R70A* mutant strains to an HO-induced DNA DSB on chromosome V. The HO-endonuclease, under the control of a GAL-promoter, is induced and cuts the HOcs on chromosome V when strains are plated on galactose containing plates.

Chapter 6

Homologous recombination in *Aspergillus nidulans*

6.1 *Aspergillus nidulans* as a model organism

Aspergillus nidulans is a filamentous fungus typically found in soil. As it primarily grows asexually, this fungus was first classified as a deuteromycete. However, in the 1960s, an analysis of the sexual fruiting bodies of a common soil ascomycete, *Emericella nidulans*, showed that its cleistothecia germinated into *A. nidulans* colonies. Accordingly, *A. nidulans* was reclassified as an ascomycete and renamed *E. nidulans*. This "taxonomically correct" name is however not commonly used. During the past fifty years, *A. nidulans* has been used as a model organism to study the physiology, biochemistry, genetics and molecular biology of multicellular eukaryotes. Several reasons can justify the status of this fungus as a model organism.

Firstly, it belongs to the genus *Aspergillus* which contains species that are important enzyme and food producers as well as human pathogenes and therefore have a daily impact on human life (Timberlake & Marshall, 1989). Secondly, it is relatively easy to handle as a laboratory organism. It grows rapidly on both solid and in liquid media under a variety of nutritional conditions (Pontecorvo et al., 1953; Clutterbuck, 1974). Unlike many industrially or medically relevant aspergilli such as *A. oryzae* and *A. fumigatus*, *A. nidulans* has a well-characterized sexual cycle. This is a strong advantage as it permits the generation of strains carrying new gene combinations in a relatively short amount of time. Moreover, the fact that the conidia produced during the asexual cell cycle are uninucleate provides a way of selecting for strains by simple replica-plating on selective media allowing large-scale screening for strains of interest. Additionally, these conidia are very stable structures that can be stored in dried or frozen state for long periods of time making the establishment of large fungal strain collections possible. Next, the recent release of its genome sequence (Galagan et al., 2005) and of those of several other aspergilli (Nierman et al., 2005b; Machida et al.,

2005; Pel et al., 2007), has given the possibility of understanding these organisms further by using comparative genomics (see 6.1.2). *A. nidulans* has more genes than *S. cerevisiae* and also contains more introns. It is a multicellular organism as septa divide the hyphae into compartments or cells. All in all, this places *A. nidulans* closer to higher eukaryotes than *S. cerevisiae* on the evolutionary ladder. Finally, the increasing amount of genetic tools and techniques being developed for *A. nidulans* has and will considerably ease the process of gene targeting in this organism thus opening an infinite amount of possibilities to generate new strains and acquire further knowledge of this organism, filamentous fungi and higher eukaryotes in general.

6.1.1 Life cycle of *A.nidulans*

The life cycle of *A. nidulans* is constituted of 3 cell cycles: an asexual, a sexual and a parasexual cycle as represented in Figure 6.1 (for reviews see Timberlake (1990) and Adams et al. (1998)).

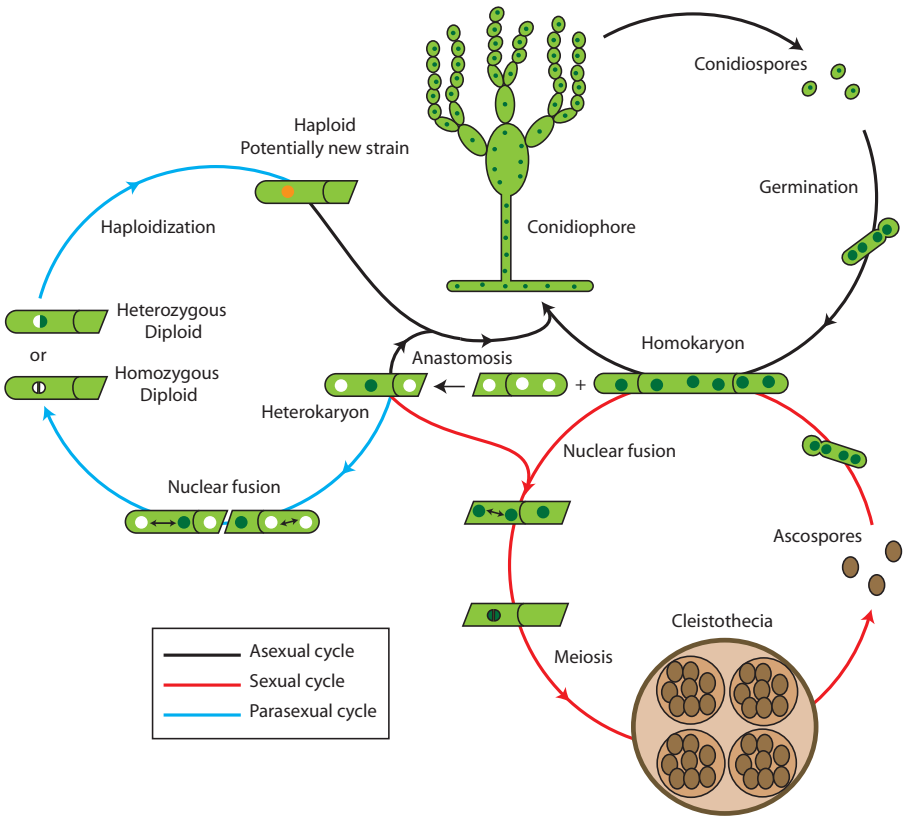

Figure 6.1. Life cycles of *A.nidulans*. Graphical representation of the asexual (black arrow), sexual (red arrows) and parasexual (blue arrows) life cycles of *A. nidulans*. Hyphae are represented as green tubes containing nuclei (coloured circles).

The asexual cycle (black arrows in Figure 6.1) is initiated by the germination of a mitotically derived conidiospore. This results in the formation of tubular hyphae that grow vegetatively to form a mycelium.

Hyphae are long, tube-like structures divided by walls, called septa, into compartments or cells. Each cell usually contains several nuclei sharing the same cytoplasm. Hyphal growth occurs both by apical extension and branching resulting in circular-shaped colonies on solid media (see Figure 6.2).

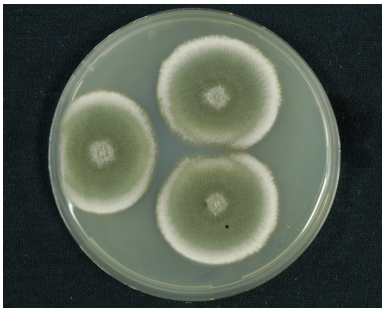

Figure 6.2. Picture of three colonies of *A.nidulans* strain IBT 27263 (*argB2, pyrG89, veA1*) growing on solid complete medium. A small amount of conidiospores was collected from a asexually growing colony using a sterile toothpick. Some conidiospores were then deposited at three different position on a plate by gently touching the surface of the medium with the toothpick. The colonies observed in this picture are approximately 4-5 days old, grow asexually and produce green conidiospores.

On solid media, fungal colonies that have reached a certain size will form specialized aerial structures called conidiophores. After several stages of development, these conidiophores bear several chains of conidiospores (Figure 6.3). When these chains are 4 to 5 conidiospores long, the spore at the end of the chain is fully matured and can therefore restart the asexual cycle when released from the conidiophore.

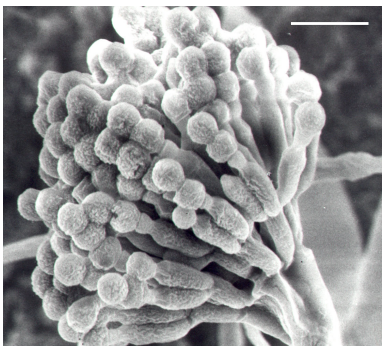

Figure 6.3. Picture of a conidiophore of *A.nidulans* obtained by scanning electron microscopy. This type of structure is produced during the asexual cell cycle and bears several chains of haploid conidia. The scale bar represents 5μm. Picture from work of Dr. Cavaliere, R. used with his permission.

The sexual cell cycle (red arrows in Figure 6.1) usually begins at the center of the colony where the oldest mycelium can be found. The signal(s) that triggers the entrance into this cycle remains unclear but could be hormone-related (Champe et al., 1987). The sexual cycle begins as two nuclei fuse to form a diploid nucleus and is characterized by the formation of cleistothecia or "fruiting bodies" imbedded

in specialized cells named Hülle cells. Within these structures, several rounds of meiosis and mitosis lead to the formation of hundreds of asci, each containing eight ascospores. In most cases, the two nuclei that fuse are identical thus meiosis will not result in genetically different strains. However, in some cases, genetically different nuclei can be present within the same hyphae. Indeed, two mycelia growing in proximity of each other are able to fuse or anastomose to form a heterokaryon (Figure 6.1). In this structure, two types of genetically different nuclei share a common cytoplasm within the hyphae. If two nuclei with different genotypes fuse (karyogamy), they will form a heterozygous diploid nucleus. When such a nucleus enters meiosis, meiotic recombination will produce ascospores with new genetic combinations (Hoffmann et al., 2001).

Another mechanism for the recombination of genetic information in *A. nidulans* is the parasexual cycle (blue arrows in Figure 6.1). In general, this cycle is considered as a laboratory phenomenon that very rarely occurs in nature. This cycle is initiated when two strains with complementing auxotrophies are mixed and anastomose to form a heterokaryon. Heterokaryons are unstable but can be maintained using selective medium where both genomes are required for growth (Pontecorvo et al., 1953). Eventually, two genetically different nuclei will fuse to produce a heterozygous diploid. When the diploid undergoes mitosis, mitotic recombination can take place leading to exchange of genetic markers. As diploids are unstable, haploidization will eventually occur creating a genetically new haploid strain (Figure 6.1). Haploidization can also be triggered by chemicals such as benomyl, which increases the frequency of non-disjunction of chromosomes during mitosis (Bignami et al., 1977). This often results in random chromosome loss thus also leading to the formation of new haploid strains.

6.1.2 The *A.nidulans* genome: an important tool for comparative genomics

In February 2003, the complete genome sequence of *A.nidulans* was released and available online (Ref: Aspergillus Sequencing Project. Broad Institute of MIT and Harvard (http://www.broad.mit.edu)). The data is regularly updated and additional releases containing new annotations and information have been made since 2003. Other important aspergilli have also been sequenced recently such as the human pathogen *A. fumigatus* (Nierman et al., 2005b), *A. oryzae* used in the production of sake, miso and soy sauce (Machida et al., 2005) and the enzyme and organic acid producer *A. niger* (Pel et al., 2007). Comparing the similarities and differences between these genomes permits the study of how these different aspergilli are related in evolution. This way, one can understand more about their physiology or get insight into aspects of genome evolution and gene regulation likely to be common to all eukaryotes. Moreover, sets of genes that are unique to each aspergillus species can bring information on specific characteristics such as pathogenicity in

the case of *A. fumigatus*.

A. nidulans has 8 chromosomes and its genome has a size of approximately 30 Mb containing about 9400 genes coding for proteins of over 100 amino acids. About 50% of the *A. nidulans* genome is coding and it has a gene density of about 1 gene per 3000bp (Galagan et al., 2005). In comparison, *A. fumigatus* and *A. oryzae* also have 8 chromosomes each and genome sizes of about 28 Mb and 37 Mb, respectively. The additional megabases of *A. oryzae* genome are mainly constituted of genes involved in the synthesis and transport of secondary metabolites and the authors suggest that these genes were transferred to *A. oryzae* from other species during evolution (Machida et al., 2005). In a comparative study of the *A. nidulans* genomes with the genomes of *A. oryzae* and *A. fumigatus*, Galagan et al. (2005) showed that their sequences are considerably different, similar to the differences observed between mammals and fish, which diverged approximately 450 millions years ago (Galagan et al., 2005). Interestingly, although extensive rearrangements were observed, conserved synteny blocks were found between the three species, suggesting similar genome evolution. Comparison between the three genomes also revealed that sexual reproduction could be possible in *A. oryzae* and *A. fumigatus*. Indeed, the presence of the HMG mating-type gene was confirmed in *A. fumigatus* (Poggeler, 2002; Galagan et al., 2005) while an alpha mating-type gene was reported in *A. oryzae* (Galagan et al., 2005). *A. nidulans* had previously been shown to contain both mating-type genes making it homothallic (or self-fertile) (Dyer et al., 2003). Interestingly, comparison between the mating-type systems of these three species revealed that these genes occupy nearly identical positions in their respective genomes and that conserved synteny was observed in the neighboring regions (Figure 6.4).

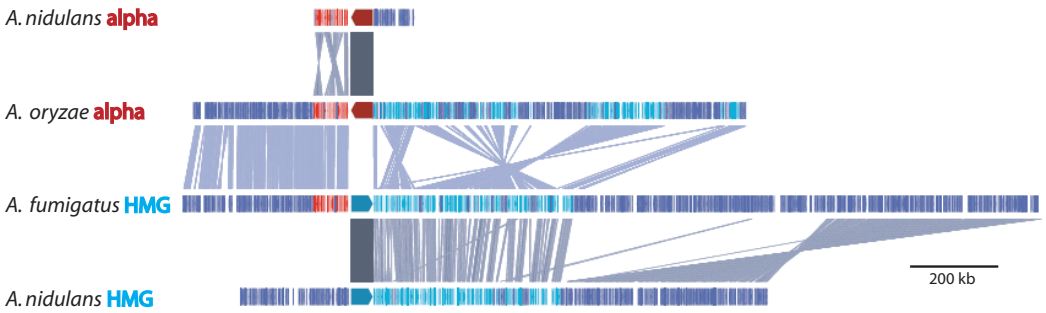

Figure 6.4. Comparison of MAT loci between *A. nidulans*, *A. oryzae* and *A. fumigatus*. Grey lines indicate predicted orthologs. Red genes indicate orthologs from the left flank of the *A. nidulans* alpha locus with the left flanks of the *A. fumigatus* and *A. oryzae* loci. Cyan genes indicate orthologs with the right flank of the *A. nidulans* HMG locus. Picture from (Galagan et al., 2005).

From these results, Galagan et al. (2005) proposed a model that predicts a common homothallic ancestor for all three species. Moreover, the authors concluded that the possible existence of mating in *A. oryzae* and *A. fumigatus* suggested by their results, can present

potential medical and industrial interest.

Using comparative genomics, high amounts of information can be retrieved that can permit us to understand the biology and evolution of different organisms. The sequencing of other *Aspergillus* genomes will surely provide data that will be the source of studies similar to that of Galagan et al. (2005) thus providing insight into how these organisms work. Such knowledge is of great interest for both the industrial and the medical fields; for example, understanding the mechanisms of pathogenicity in species that cause invasive aspergillosis could provide potential targets for drug development (Nierman et al., 2005a). Importantly, understanding these organisms better will make it possible to develop strategies to exploit their potentials at our advantage. This will increase the need for efficient genetics tools that will make specific strain engineering possible. As presented below, many research groups including ours, have already contributed to make this a reality.

6.2 From homologous recombination to gene targeting

Gene targeting is the method used to insert a DNA fragment into a specific genomic target site in an organism of interest. This specific integration is homology-driven as DNA fragment used contains sequences homologous to the genomic site that is being targeted. Two types of gene targeting events have been described depending on the configuration of the ends of the fragment when paired with the homologous target. When the ends of the fragment point towards each other the gene targeting event is defined as "ends-in" (Figure 6.5, A).

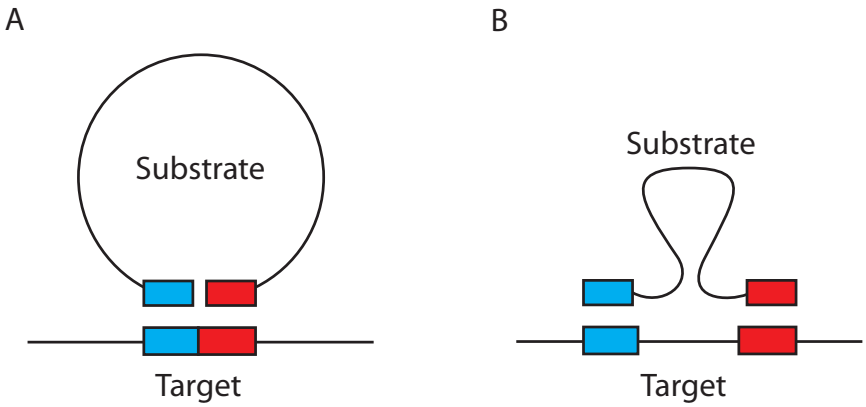

Figure 6.5. Gene targeting by (A) ends-in or (B) ends out recombination. Red and blue boxes represent homologous DNA sequences on the substrate and the target DNA.

On the other hand, if the ends of the fragment point away from each other, the gene targeting event is defined as "ends-out" (Figure 6.5, B) (Hastings et al., 1993). As the gene targeting method developed in

our lab and presented later in this chapter is based on "ends-out" gene targeting, the rest of this description will focus on this type of event. The mechanisms by which "ends-out" gene targeting takes place have been extensively studied and two main models have been proposed (see Figure 6.6). One model by Leung et al. (1997) suggests that gene replacement occurs by the formation of extensive heteroduplex DNA (hDNA) between the DNA fragment and the target region, that would span across the whole target region length. Accordingly the authors proposed that gene replacement occurs when one end of the DNA substrate invades the target duplex and is then assimilated. The resulting heteroduplex region and any potential mismatches are then acted upon by the mismatch repair system (see Figure 6.6, Panel A).

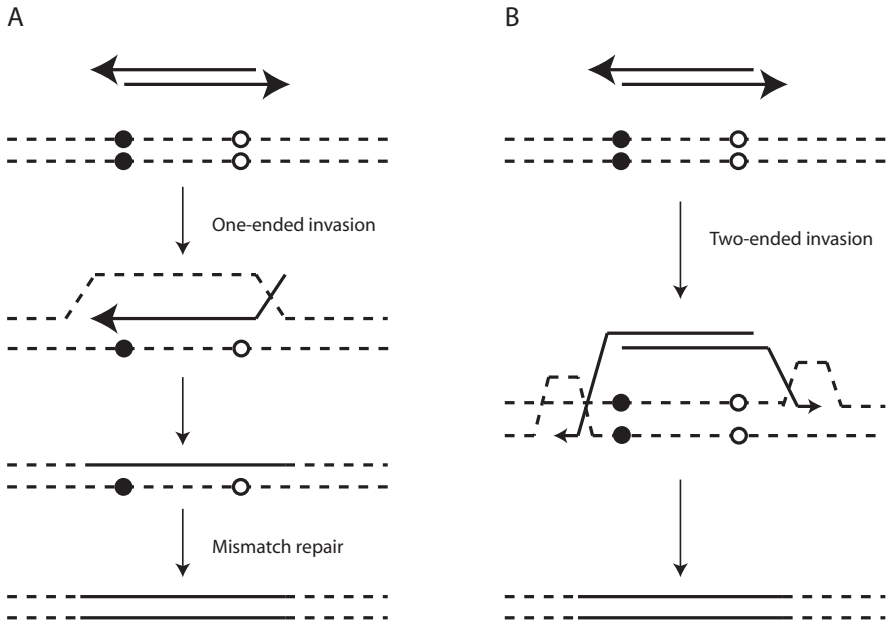

Figure 6.6. Graphical representation of the two main models of the mechanism of gene targeting. (A) One end of the DNA substrate invades the genomic target site thus forming a long stretch of hDNA. Mismatch repair correct any potential mismatches (white and black circles) within the heteroduplex. (B) Both ends of the DNA substrate invade the genomic target site leading to a crossover events at each end of the fragment. As both strands of the substrate are integrated at the target site, mismatch repair is not needed here. This figure is adapted from Leung et al. (1997).

Another model, proposed by Hastings et al. (1993), suggests that gene targeting occurs by separate crossovers at each of the two ends of the targeting fragment (see Figure 6.6, Panel B). This model is in agreement with the results of Li et al. (2001) in mammalian cells as they observed hDNA formation with both ends of the targeting substrate. In yeast, Langston & Symington (2004) showed that gene targeting is initiated by independent strand invasions at the two ends of the targeting substrate (see Figure 6.6, Panel B). They also showed that integration by the one-ended model (Figure 6.6, Panel A) occurs mainly when the mismatch repair system is impaired and therefore rarely in

wild-type cells.

As presented above, homologous recombination (HR) is the mechanism that allows gene targeting in vivo. In the yeast, *S. cerevisiae*, HR is the main pathway used for DNA repair making gene targeting relatively efficient in this organism. However, this is not the case in higher eukaryotes and gene targeting in these organisms is a much more difficult task. For this reason, development of efficient gene targeting methods in higher eukaryotes has been the goal of several research groups, including ours.

6.3 Increasing gene targeting in higher eukaryotes

The recent release of the genome sequence of *Aspergillus nidulans*, as well as several other aspergilli, has tremendously widened the possibilities of studying these industrially and medically relevant organisms. Indeed, the dream of creating fungal strain collections similar to those already existing for *S. cerevisiae*, e.g. Yeast Knockout (YKO) collection, Yeast GFP-clone collection, Yeast GST-fusion collection, etc, has now become realistic. Working towards this goal, several groups have developed gene targeting methods to enable and ease the creation of such strains in aspergilli (Bird & Bradshaw, 1997; Chaveroche et al., 2000; Yang et al., 2004; Yu et al., 2004; Zarrin et al., 2005; Forment et al., 2006; Nayak et al., 2006; Nielsen et al., 2006). Unfortunately, this process is often slowed down by the fact that gene targeting in filamentous fungi is far from being as efficient as in budding yeast. Indeed, the DNA substrates classically used for gene targeting in *S. cerevisiae* are relatively inefficient in filamentous fungi as they most often integrate randomly in the genome of these organisms. This is due to the fact that DNA DSB repair in these organisms mainly takes place by non-homologous end-joining (NHEJ), a mechanism by which two DNA ends are directly ligated without the need for a homologous template. Interestingly, this is similar to what is observed in higher eukaryotes where it poses limitations on the gene targeting possibilities in mouse and plants and for its use in human gene therapy. For these reasons, increasing the efficiency of gene targeting has been the goal of many research groups in the past few years.

One of the strategies used to increase gene targeting efficiency has been to delete the genes responsible for NHEJ. This way, DNA repair should mainly take place by HR thus increasing the amount of targeted genomic integration. In *A. nidulans*, Nayak et al. (2006) showed that gene targeting efficiency could be highly increased in a null strain of the human KU70 homolog, *nkuA*, as the frequency of non-homologous integrations was greatly reduced in such a strain. This strategy was also successfully used in several other fungi (Kooistra et al., 2004; Ninomiya et al., 2004; Krappmann et al., 2006; Poggeler & Kuck, 2006; Takahashi et al., 2006) but did not appear to work in mammalian cells

(Pierce et al., 2001; Dominguez-Bendala et al., 2006). The reason for this remains unclear but it could be due to the fact that the mammalian Ku proteins are involved in other cellular processes such as V(D)J recombination and that the deletion of the Ku genes could therefore have unexpected repercussions (Nussenzweig et al., 1996; Gu et al., 1997; Ouyang et al., 1997). Another explanation is the existence of alternative end-joining pathways independent of Ku (Feldmann et al., 2000; Ma et al., 2003; Wang et al., 2003; McVey et al., 2004).

Another attempted strategy to increase gene targeting efficiency has been to promote HR by over-expressing genes known to be involved in this repair pathway. One target of this strategy has been the *A. nidulans uvsC*, a homolog of the yeast *RAD51*. *uvsC* null mutants show high sensitivity to MMS, are defective in meiosis and deficient in gene targeting (Seong et al., 1997; Van Heemst et al., 1997; Ichioka et al., 2001). Natsume et al. (2004) investigated if an increase in the transcription of *uvsC* would increase gene targeting efficiency in *A. nidulans*. This was only a half success as gene targeting efficiency was increased several fold when *uvsC* transcription was high but these events were showed not to be linearly correlated. Accordingly, higher transcription levels of *uvsC* did not further increase gene targeting efficiency and had severe impacts on mycelial growth. These results are in agreement with those of Yanez & Porter (1999) who were able to increase gene targeting 2-to 3-fold by over-expressing human *RAD51* about 4-fold in human cells. Similarly to what was observed in *A. nidulans*, Flygare et al. (2001) later showed that a 10-fold over-expression of hRad51 had severe consequences as it suppressed cell proliferation in addition to other abnormal phenotypes. Over-expression of another HR protein, Rad52p, in human cells was not crowned with success either as it appeared to inhibit gene targeting Yanez & Porter (2002). However, expression of *S. cerevisiae* Rad52 in human cells did result in an increase in gene targeting by HR in these cells (Di Primio et al., 2005).

Following the idea of increasing gene targeting efficiency by promoting HR in the fungal cell, our research group developed an efficient PCR-based gene targeting method based on a strategy previously developed for *S. cerevisiae* (Erdeniz et al., 1997). In this method, the targeting substrate, called bipartite substrate, is constituted of two pieces of linear DNA each containing part of a selection marker. While integration of the classical DNA substrates used for "ends-out" gene targeting generally require one HR event at each end of the DNA substrate (two HR events in total) (Langston & Symington, 2004), integration of our substrate requires an additional HR event between the two fragments of the bipartite substrate. This event is essential as it reconstitutes the functional marker used for selection. Accordingly, we have investigated whether this additional requirement for an HR event within the substrate itself can channel the entire targeting substrate into the HR pathway thus promoting HR between the ends of the substrate and the targeted area in the genome. In the paper presented below, we show that this method increases gene targeting efficiency by reducing the

number of false positive transformants obtained. This is important as it minimizes the amount of screening required, an often tedious step in gene targeting experiments. Moreover, a higher number of positive integrants is obtained without having to disrupt the NHEJ pathway in the strains and organisms of interest which saves both work and risks of crosstalk between the NHEJ phenotype and the phenotype of interest. Also, our method presents the undeniable advantage of a recyclable marker. Indeed, once the genomic region of interest has been successfully targeted, the selectable marker, flanked by a direct repeat, can be excised via direct-repeat recombination. This allows multiple rounds of gene targeting to be performed in the same strain. Moreover, as the same marker is re-used each time, the vector serving as a template for the construction of the constant parts of the bipartite gene-targeting substrate can be used for every construction round. This is an advantage as the amount of available efficient selectable markers can become limiting if several rounds of gene targeting need to be performed and this applies to both NHEJ-proficient and -deficient strains.

My contribution to this work was to show that the bipartite method could be used to perform gene deletions. As I was interested in studying HR in *A. nidulans*, I created a deletion strain of the *S. cerevisiae RAD52* homolog, *radC*. How this strain was generated is presented in the following article and a characterization of the *A. nidulans radC* strain is presented in Chapter 7.

Available online at www.sciencedirect.com
SCIENCE DIRECT®
Fungal Genetics and Biology 43 (2006) 54–64
FUNGAL GENETICS AND BIOLOGY
www.elsevier.com/locate/yfgbi

Efficient PCR-based gene targeting with a recyclable marker for *Aspergillus nidulans*

Michael L. Nielsen, Line Albertsen, Gaëlle Lettier, Jakob B. Nielsen, Uffe H. Mortensen *

Center for Microbial Biotechnology, BioCentrum-DTU, Technical University of Denmark, Building 223, DK-2800 Kgs. Lyngby, Denmark

Received 20 July 2005; accepted 19 September 2005
Available online 11 November 2005

Abstract

The rapid accumulation of genomic sequences from a large number of eukaryotes, including numerous filamentous fungi, has created a tremendous scientific potential, which can only be realized if precise site-directed genome modifications, like gene deletions, promoter replacements, in-frame GFP fusions and specific point mutations can be made rapidly and reliably. The development of gene-targeting techniques in filamentous fungi and other higher eukaryotes has been hampered because foreign DNA is predominantly integrated randomly into the genome. For *Aspergillus nidulans*, we have developed a flexible method for gene-targeting employing a bipartite gene-targeting substrate. This substrate is made solely by PCR, which obviates the need for bacterial subcloning steps. The method reduces the number of false positives and can be used to produce virtually any genome alteration. A major advance of the method is that it allows multiple subsequent genome manipulations to be performed as the selectable marker is recycled.

Keywords: Gene targeting; Filamentous fungi; *Aspergillus nidulans*; Homologous recombination; Genome integration; Deletion; Point mutation

1. Introduction

In recent years, the complete genome sequences of a number of filamentous fungi, including that of the model fungus, *Aspergillus nidulans*, have become available (reviewed in Archer and Dyer, 2004). This has created a tremendous potential to obtain insight into many important aspects of fungal biology such as transcriptional regulation, secondary metabolite production, cellular differentiation, tissue specialization, hyphal growth, and pathogenicity. Experimentally, this potential can only be fully exploited if precise genome modifications like gene deletions, promoter replacements, in-frame GFP fusions and specific point mutations can be made. This has been demonstrated for the yeast, *Saccharomyces cerevisiae*, where the combination of a complete genome sequence and efficient gene-targeting methods has made this organism the genetically best characterized eukaryote. Moving from unicellular to multicellular model organisms, *A. nidulans* is a good choice since gene-targeting success rates are typically quite high, lying in the range of 10–50%, which is orders of magnitudes higher than for most other multicellular eukaryotes (Schaefer, 2001). Although, most types of genome manipulations have been reported for *A. nidulans*, the methods often employ several cumbersome *Escherichia coli* based cloning steps and therefore the development of a versatile cloning-free method is desirable. To avoid bacterial cloning, three similar PCR-based methods have recently been successfully used to perform gene deletions and promoter replacements in *A. nidulans* using a one-step gene replacement strategy (Yang et al., 2004; Yu et al., 2004; Zarrin et al., 2005). In all three methods, the final gene-targeting substrate is generated by combining three overlapping fragments in a subsequent PCR. A simpler and more flexible PCR-based method, which allows the selectable marker to be recycled, has previously been developed for *S. cerevisiae* (Erdeniz et al., 1997). The method employs PCR to generate two composite DNA fragments, here termed a bipartite gene-targeting substrate, that are fused in vivo by homologous

* Corresponding author. Fax: +45 4588 4148.
E-mail address: um@biocentrum.dtu.dk (U.H. Mortensen).

1087-1845/$ - see front matter © 2005 Elsevier Inc. All rights reserved.
doi:10.1016/j.fgb.2005.09.005

recombination (HR) to form the active gene-targeting substrate. In this method, the selectable marker is flanked by a direct repeat, which allows multiple rounds of gene targeting to be performed in the same strain as the marker can be excised via direct-repeat recombination. Furthermore, integration as well as direct-repeat recombination events are easily scored as a selectable/counter-selectable marker is used. This method has been used to create gene deletions, point mutations, allele replacements and GFP fusions (Erdeniz et al., 1997; Lisby et al., 2001; Reid et al., 2002a,b). The only prerequisite for each class of genome modification is a vector that serves as a template for constant parts of the bipartite gene-targeting substrate. In the present study, we demonstrate that this gene-targeting scheme can be adapted to *A. nidulans* to efficiently create gene deletions and point mutations. Furthermore, we show that the use of bipartite substrates results in a higher frequency of correct targeting events compared to that obtained with the corresponding continuous substrates.

2. Materials and methods

2.1. Strains, media, and plasmids

The *A. nidulans* strain, IBT 27263, (*argB2*, *pyrG89*, and *veA1*) was used for all gene-targeting experiments. The strain is derived from GO51 of the Glasgow strain collection. Solid and liquid media were made according to Clutterbuck (Clutterbuck, 1974). 5-fluoroorotic acid (5-FOA) was from Sigma. 5-FOA medium was made by adding filter-sterilized 5-FOA to a final concentration of 1.3 mg/ml to minimal medium supplemented with 10 mM uridine, 10 mM uracil, 4 mM L-arginine and 2% agar cooled to 50 °C after autoclavation. *E. coli* strain DH5α was used as host for plasmid construction. Plasmids pUC57 and pUC18 were obtained from Fermentas and New England Biolabs (NEB), respectively. Plasmid pDJB2 contains *pyr-4* of *Neurospora crassa* (Ballance and Turner, 1985) and pYA11 harbors both *argB* and *yA* of *A. nidulans* (Aleksenko and Ivanova, 1998).

2.2. Oligonucleotides, PCR, and cloning

A linker, d(pGGGTACCC) containing a *Kpn*I cut site was obtained from NEB. Oligonucleotides were supplied by MWG-Biotech AG and are listed in Table 1. PCR was performed using the Expand High Fidelity PCR kit from Roche according to manufacturer's recommendations. All PCR products were purified from agarose gels using a GFX purification kit (Amersham–Pharmacia). Plasmid construction was performed using standard methods (Sambrook and Russell, 2001) and all inserted PCR fragments were sequenced by MWG-Biotech AG.

pYA11-*Kpn*I served as PCR template for the mutant allele *yA*-*Kpn*I (see Section 2.3) and was constructed by ligating a phosphorylated *Kpn*I linker, see above, into the *Sma*I restriction site of pYA11. The *Kpn*I site is situated 401 bp downstream of the ATG of *yA* and causes a frameshift mutation.

Table 1
Oligonucleotides used in this study

Primer	Usage	Sequence
M1	Recyclable primers for gene targeting	catggcaattcccggggatc**GCCGGC** **AATTCTTTTTAGGTAGC**
M2		**CCAGAAGCAGTACACGGC**
M3		**GTTGTCTGCTTGCGCTTCTTC**
M4		catggtggtcagctggaat**TCCTCC** **GCCATTTCTTATTCCC**
R1		catggcaattcccggggatc**TGGAT** **AACCGTATTACCGCC**
R2		catggtggtcagctggaatt**TGCCAA** **GCTTAACGCGTACC**
D1	Deletion of *radC*	aattccagctgaccaccatg**CACTAT** **CGACCTCGTCTTATGC**
D2		**GGATACTCCTGAATCTCGAC**
U1		**CGCCTTCGGATCGATGAG**
U2		gatccccgggaattgccatgCGACTG CATCCGTACTAGCAGTCTGATGCG **TGTGATGCTTGCCGGGCC**
Y1	Mutagenesis in *yA*	aattccagctgaccaccatg**CAAA** **TGTTCTATCATGGGGGC**
Y2		gatccccgggaattgccatg**GGTTG** **ATTGGGAATATGTAGTTC**
O1	Cloning	cgctatattaccctgttatccctagc gtaact**CGGCAGATTTTCTGT** **GAAGAG**
O2		agttacgctagggataacagggtaat atagcg**CGAGCGAGGTCTCAA** **CAAC**
O3		ATCATTGCTGCAGCATCGAT **TCCTCCGCCATTTCTTA**
O4		TACTTCTAGAACCTAGG**GCCGGCAA** **TTCTTTTTAGGTAG**
O5		AGCAATGCATCTGGAGAATCGAT **AAATGTTCTATCATGGGGGC**
O6		GATGCATGCCTGGAGACTAGT**GGTT** **GATTGGGAATATGTAGTTC**
O7		ACCTGAAGCTTAACGCGTACCCGGGAA GATCT**CATGGTCATAGCTGTTTCCTG**
O8		ACTGGCATGCAGCGGCCGCAGCTAG CACAATTGAGGCGCGCC **GAGCTGATACCGCTCGCCGC**
O9	Probe P4	**TGGGTTGAACCGCTTACTCAG**
O10		**CAGCTGCAGCATGAAATCCAG**

All sequences are shown in 5′–3′ direction. Bases shown in bold capitals anneal to the template DNA. Sections of the oligonucleotides in lower case characters represent fusion tags.

pYA11-I-*Sce*I served as PCR template for the mutant allele *yA*-I-*Sce*I (see Section 2.3) and was constructed by inserting a *yA*-I-*Sce*I containing PCR fragment digested with *Mfe*I and *Nhe*I into a *Mfe*I–*Nhe*I vector fragment of pYA11. This PCR fragment was generated in two steps. First, two PCR fragments were made in separate reactions using primer pairs (Y1 and O1) and (Y2 and O2), respectively, and pYA11 as template. Second, these two fragments were fused via 32 bp I-*Sce*I sequences (Moure et al., 2003; Plessis et al., 1992) present in their ends using the primer pair Y1 and Y2 by PCR. In pYA11-I-*Sce*I, the 32 bp I-*Sce*I recognition sequence is located 1579 bp downstream of the ATG of *yA* and causes a frameshift mutation.

pRSub3 was used to produce targeting fragments described in Section 2.4 and was constructed in three steps. First, a 1.4 kb PCR fragment, which contained the entire *N. crassa pyr-4* marker, was generated by the primer pair O3 and O4 using pDJB2 as template. This fragment was digested with *Xba*I and *Pst*I and inserted into an *Xba*I–*Pst*I vector fragment of pUC57 to produce pRSub1. Next, a 2146 bp PCR fragment was generated by using the primer pair O5 and O6 and pYA11-*Kpn*I as template. This fragment, which contains the *yA-Kpn*I allele and a *Bpm*I recognition sequence just downstream of the *yA* locus, was digested with *Cla*I and *Sph*I and inserted into a *Cla*I–*Sph*I pRSub1 vector fragment to produce pRSub2. Finally, the 2146 bp PCR fragment obtained above was digested with *Nsi*I and *Spe*I to release a fragment containing the *yA-Kpn*I allele and a *Bpm*I recognition sequence just upstream of the *yA* locus. This fragment was inserted into an *Nsi*I–*Avr*II vector fragment of pRSub2 to produce pRSub3, see Fig. 1.

pDEL1 served as PCR template for the marker-containing fragments of the bipartite substrates for the *radC* deletion (see Section 2.3). The vector contains the *pyr-4* marker and a 290 bp direct repeat and was constructed in three steps. First, the *Xma*I site of pUC18 was destroyed by digesting the plasmid by *Xma*I, filling out the ends by Klenow polymerase (Large Fragment from NEB) followed by religation of the blunt ends to produce pJST1. Next, a 290 bp fragment, which was generated by PCR using the primer pair O7 and O8 and pJST1 as template, was digested by *Hin*dIII and *Sph*I and inserted into a *Hin*dIII–*Sph*I vector fragment of pJST1 to form pJSH1. Finally, an *Xba*I and *Pst*I fragment isolated from pRSub1, which contains the entire *pyr-4* gene, was inserted into an *Xba*I–*Pst*I vector fragment of pJSH1 to yield pDEL1.

2.3. PCR-based bipartite substrates for gene-targeting experiments

The two marker-containing fragments of the bipartite substrates were amplified by PCR using pDEL1 as template. Specifically, for creating deletions, the primer pairs (R1 and M3) and (M2 and R2) were used for the upstream and downstream fragments, respectively; and for making point mutations, primer pairs (M1 and M3) and (M2 and M4) were used for the upstream and downstream fragments, respectively.

To delete *radC* in the genome, the upstream (2088 bp) and downstream (2033 bp) specific targeting sequences flanking *radC* were PCR amplified from genomic DNA using the primer pairs (U1 and U2) and (D1 and D2), respectively. The 5′ flanking targeting sequence was fused to the upstream marker fragment (described above) by PCR using primers U1 and M3. The 3′ flanking sequence was fused to the downstream marker fragment by using primers M2 and D2.

For creating genomic point mutations in *yA*, mutant *yA* alleles were amplified from either pYA11-*Kpn*I or pYA11-I-*Sce*I using the primers, Y1 and Y2. In each case, the resulting fragment was fused to both the upstream and the downstream central marker fragment using primer pairs (Y1 and M3) and (M2 and Y2), respectively, in two independent reactions.

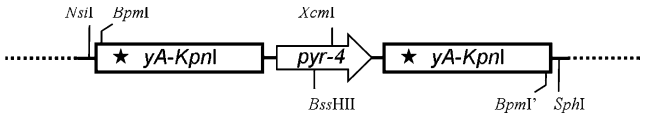

Fig. 1. A graphical representation showing the relevant features of pRSub3. The location of the *pyr-4* gene is given as an open arrow and the location of the *yA* targeting sequences as open boxes. The stars indicate the position of the new *Kpn*I site. The positions of relevant restriction enzyme cut sites are indicated. *Bpm*I and the enzyme pair *Nsi*I and *Sph*I are used to produce outer homologous and non-homologous substrate-ends, respectively. *Bpm*I recognizes an asymmetric sequence and the cuts produced from the sites with the orientations CTTGAG and CTCAAG are labeled *Bpm*I and *Bpm*I′, respectively. The actual *Bpm*I recognition sites are located outside the *yA* targeting sequences as this enzyme cuts 16 bp downstream of CTTGAG and 14 bp upstream of CTCAAG.

2.4. Gene-targeting substrates derived from pRSub3

pRSub3 is used as a source of both bipartite and complete gene-targeting substrates. Depending on the choice of restriction enzymes, substrates with homologous or non-homologous ends can be produced. Substrates with homologous ends were generated by exploiting the fact that the two asymmetric *Bpm*I recognition sites in pRSub3 are located so that *Bpm*I cuts inside the *yA* targeting sequence even though its recognition sequence is located outside the *yA* targeting sequence (see Fig. 1). Specifically, double digestions with *Bpm*I–*Xcm*I and *Bss*HII–*Bpm*I generated the 3.9 kb upstream and 3.7 kb downstream fragments of the bipartite substrate, respectively, while *Bpm*I digestion alone gives the 7.1 kb, continuous substrate. Substrates with non-homologous ends were generated by exploiting the fact that *Nsi*I and *Sph*I cleaves pRSub3 outside *yA* leaving 18 bp of non-homologous sequences in both ends of the substrate. Specifically, double digestions with *Nsi*I–*Xcm*I and *Bss*HII–*Sph*I were performed to yield the fragments of the bipartite substrate while a double digestion with *Nsi*I–*Sph*I was performed to generate the continuous substrate.

2.5. Transformation and selection of direct-repeat recombinants

Genetic transformation of *A. nidulans* protoplasts was preformed as previously described (Johnstone et al., 1985), except that protoplasting was achieved by using the enzyme, Glucanex, (Novozymes A/S), at a concentration of 40 mg/ml in protoplasting buffer. All transformations were performed with 10^7 protoplasts in 100 μl transformation buffer (Johnstone et al., 1985). For experiments using PCR derived fragments, 1–2 μg DNA was used unless otherwise indicated. In experiments where the efficiency of the two plasmid derived substrate types, continuous and bipartite, are compared, the same amount of DNA was used (in a range of 0.3–1 μg DNA).

Transformants were purified by streaking out spores to obtain single colonies on selective minimal medium. From these, direct-repeat recombinants were selected by plating approximately 10^6 spores on 5-FOA containing plates and incubated at 37 °C for 3–4 days. The resulting recombinants were further purified by streaking out spores on a fresh 5-FOA containing plate.

2.6. Southern blot hybridization

Genomic DNA from *A. nidulans* strains was isolated either as previously described (Blin and Stafford, 1976) or using the FastDNA spin kit from Qbiogene, Inc. For each sample, 2 μg genomic DNA was digested with appropriate restriction enzyme(s). Blotting was done as described by Sambrook and Russell (2001) using RapidHybe hybridization buffer (Amersham–Pharmacia) for probing. Probes for detecting the *radC* locus were: probe P1, a 2088 bp PCR fragment amplified from genomic DNA using primer pair U1 and U2 and Probe P2, a 2033 bp PCR fragment made using primer pair D1 and D2. Probes for detecting the *yA* locus were: Probe P3, a 1461 bp fragment of *yA*, generated from pRSub2 by *Bam*HI digestion and Probe P4, a 361 bp fragment, made by PCR from genomic DNA using the primer pair O9 and O10. All probes were radioactively labeled with [α-^{32}P]dCTP by random priming using Rediprime II kit (Amersham–Pharmacia).

3. Results

We were interested in developing a versatile PCR-based gene-targeting system for *A. nidulans*, where the selectable marker can be recycled. Such a system has previously been developed and successfully used to create genome modifications like gene deletions, point mutations and GFP fusions in *S. cerevisiae*. (Erdeniz et al., 1997; Reid et al., 2002a,b). The system is based on a bipartite gene-targeting substrate in which each of the two fragments carries a targeting sequence as well as a part of a selectable marker gene. None of the two individual fragments contain a functional marker, but if the fragments fuse by HR via overlapping marker sequences, a complete and functional marker is generated after co-transformation as shown in Figs. 2A and B. In addition, the bipartite substrate is designed so that a direct repeat is formed when it is integrated into the genome. This feature allows the marker to be eliminated in a subsequent direct-repeat recombination event, thereby permitting several rounds of gene targeting using the same marker. In *S. cerevisiae*, the *Kluyveromyces lactis URA3* gene is often used as the marker, since it only rarely recombines with the endogenous *URA3* gene (Bailis and Rothstein, 1990). Transformants can easily be selected on media lacking uracil, and direct-repeat recombinants can be identified by counter selecting on media containing 5-FOA. Similar advantages can be obtained for *A. nidulans* by using the *URA3* homolog, *pyr-4*, from *N. crassa* (Ballance and Turner, 1985). Accordingly, we tested the possibility of adapting the bipartite gene-targeting method to *A. nidulans* using *pyr-4* as a marker. Specifically, we tested whether it could be used to make gene deletions and point mutations. For this purpose, a general vector, pDEL1 containing *pyr-4* flanked by a 290 bp direct repeat was constructed, see Section 2 and Fig. 2C. pDEL1 serves as the template for all constant parts of the bipartite gene-targeting fragments. These fragments can be used in any gene-deletion or point-mutation experiment.

3.1. PCR generated bipartite gene-targeting substrates can be used for gene deletion

First, we tested the possibility of deleting a gene using a bipartite PCR derived gene-targeting substrate in *A. nidulans* by deleting *radC* (AN4407.2), a gene putatively involved in DNA repair (Goldman and Kafer, 2004). pDEL1 was used as a template in two independent PCR reactions to generate the constant segments of the bipartite substrate that contain the marker and the repetitive sequences (see, Fig. 2C). In parallel, two specific targeting fragments flanking *radC* were generated by PCR using genomic DNA as template. The bipartite gene-targeting substrate was completed in a second and final round of PCR. This was achieved by fusing the fragment containing the 2/3 upstream part of the *pyr-4* marker gene with the upstream *radC* targeting fragment. Similarly, the fragment containing the 2/3 downstream part of the *pyr-4* marker was fused to the downstream *radC* targeting fragment. A specific fusion of two PCR fragments was possible as the fragments contained identical sequences in their ends, see Fig. 2C. Such ends were generated by using primer pairs where one of the primers is an adaptamer, a chimeric oligonucleotide where the 3′-end acts as a normal PCR primer and the 5′-end contains a specific fusion-tag, see Fig. 2C and Erdeniz et al. (1997).

The bipartite gene-targeting substrate was transformed into *A. nidulans* and twelve transformants were obtained. In two of these transformants, *radC* was shown to be replaced by *pyr-4* as assessed by a PCR assay (data not shown). These two strains were transferred to media containing 5-FOA to select for direct-repeat recombinants. The 5-FOA treatment produced numerous candidates, which were purified and shown to be incapable of growth in the absence of uracil. After an initial PCR screen, one of the direct-repeat recombinants was selected for characterization by Southern blot hybridization. For the potential *radCΔ* strain, a single fragment was detected corresponding to the fragment size expected if a single repeat unit has replaced *radC*, see Fig. 3. We therefore conclude that both *radC* and the *pyr-4* marker had been successfully deleted from the genome. A biological characterization of the resulting *radCΔ* strain will be described elsewhere.

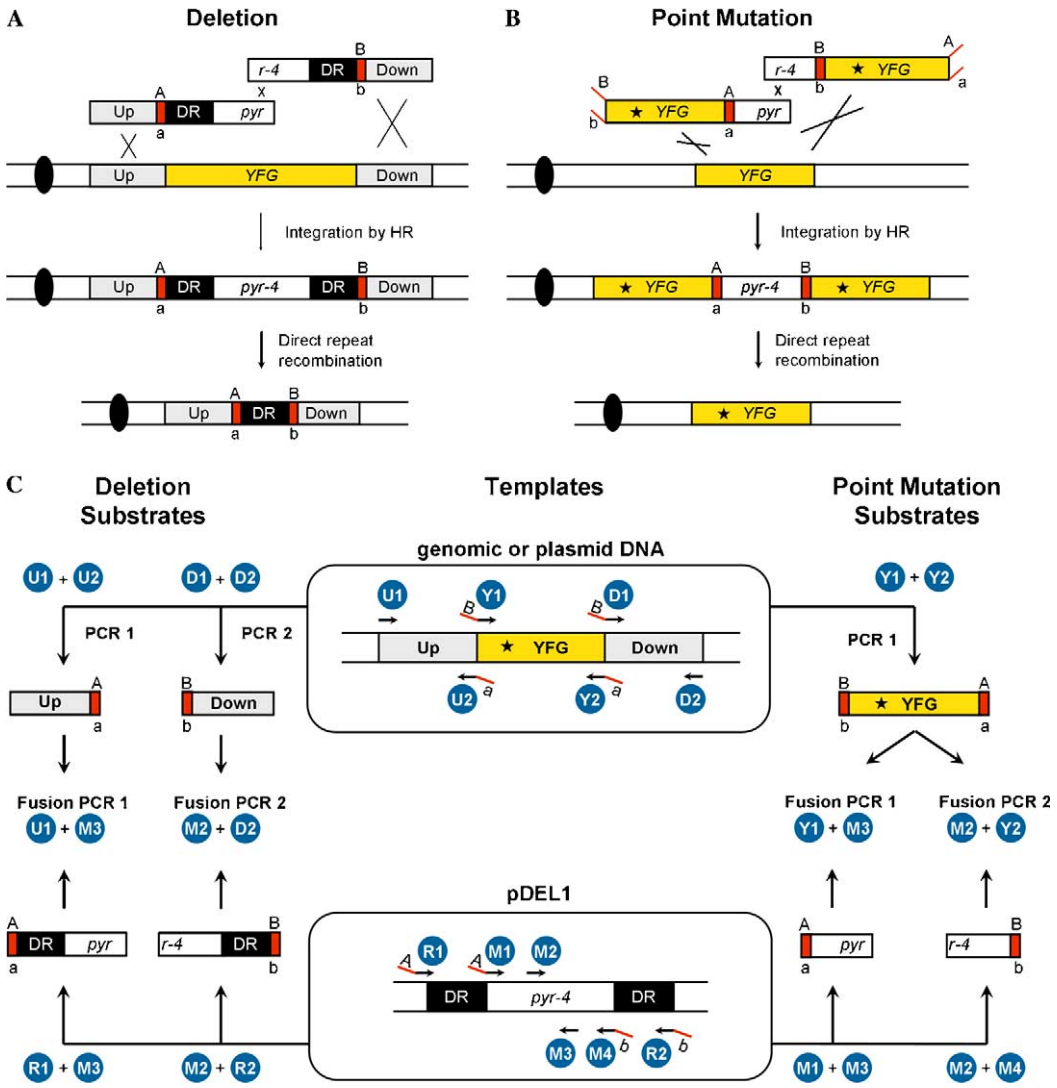

Fig. 2. Integration of bipartite gene-targeting substrates and subsequent direct-repeat recombination events to (A) delete your favorite gene, *YFG* (shown as an orange box), or (B) create a point mutation in the endogenous copy of *YFG*. In vivo recombination between two PCR fragments generates a functional, selectable *N. crassa pyr-4* gene. (A) Recombination between each fragment and the homologous chromosomal locus, via the two targeting sequences up and down (shown as grey boxes), results in deletion of *YFG* and insertion of *pyr-4*, shown as a white box, flanked by a direct repeat (shown as black boxes labeled DR). The chromosome is illustrated by two parallel fat lines with a solid black oval at the end, representing the centromere. After subsequent direct-repeat recombination, the *pyr-4* marker is excised leaving only a single DR sequence and the strain is ready for a new round of *pyr-4* based gene-targeting. Red boxes and lines are fusion tags, which are used during the construction of the gene-targeting substrate, see panel C. (B) Recombination between each fragment and the homologous chromosomal locus results in a duplication of *YFG* where both copies contain a point mutation depicted with an asterisk. During the integration, the two non-homologous fusion tags, **a**, and, **B**, are deleted from the ends of the fragments. After the subsequent direct-repeat recombination event, the point mutation is retained in the genome whereas the *pyr-4* marker is lost, thus, preparing the strain for a new round of *pyr-4* based gene-targeting. (C) Construction of bipartite gene-targeting substrates by two subsequent rounds of PCRs. The positions of individual primers are illustrated as arrows. Arrows with a red extension are adaptamers, see Section 2, and the red section illustrates the part of the primer that is used in a subsequent fusion PCR. In adaptamers, the sequence, **A**, is complementary to the sequence, **a**, and, **B**, is complementary to, **b**. Sequences, **A**, and, **B**, are not related. The names of primers are given in blue circles. In experiments designed to delete *YFG* (left side of the figure), the first round of PCR amplifies the two targeting sequences, Up and Down, in two individual PCRs using the primer pairs (U1 and U2) and (D1 and D2) and either genomic or plasmid DNA as template. Note that D1 and U2 are adaptamers. In parallel, two fragments containing *pyr-4* and repeat sequences are generated by using the primer pairs (R1 and M3) and (M2 and R2) with pDEL1 as template. Only the relevant part of pDEL1 is shown including the position of the direct repeats, DR, and the *pyr-4* marker gene. Note that R1 and R2 are adaptamers. In the second round of PCR, the fusion PCR, the appropriate PCR fragments are fused in two independent reactions that involve primer pairs (U1 and M3) and (M2 and D2) to complete construction of the bipartite gene-targeting substrate for deletion of *YFG*. In experiments designed to introduce a point mutation in *YFG* (right side of the figure), the first round of PCR amplifies the *YFG* open reading frame (or a section of *YFG* if the gene is not essential) that will act as the targeting sequence and, which contains the desired alteration. The YFG fragment is generated in a single PCR using the adaptamer pair Y1 and Y2 and either genomic or plasmid DNA as template. In parallel, two fragments containing *pyr-4* sequences are generated by using the primer pairs (M1 and M3) and (M2 and M4) and pDEL1 as template. Note that M1 and M4 are adaptamers. In the second round of PCR, the fusion PCR, the appropriate PCR fragments are fused in two independent reactions that involve primer pairs (Y1 and M3) and (M2 and Y2) to complete construction of a bipartite gene-targeting substrate designed to introduce a point mutation into *YFG*.

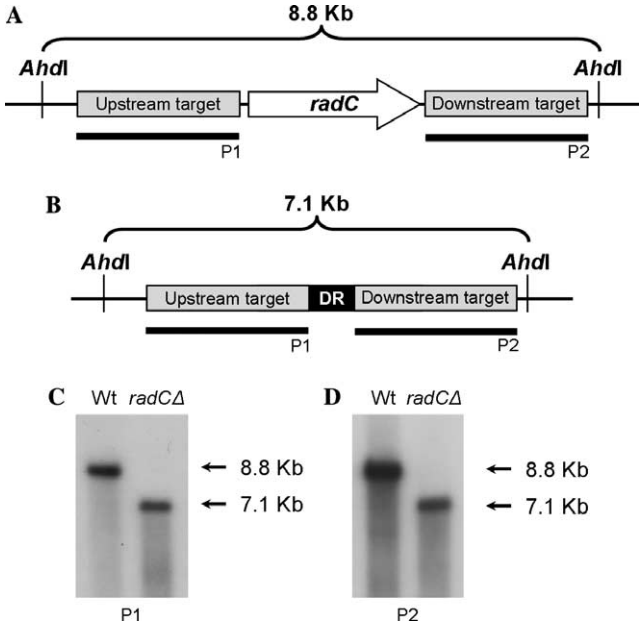

Fig. 3. Deletion of the *radC* locus. (A and B) Graphical representations of the *radC* locus before and after deletion of the *radC* open reading frame, respectively. In panel A, the *radC* open reading frame is illustrated as an open arrow and in panel B the repeat that remains after direct-repeat recombination is shown as a black box labeled DR. The up- and downstream targeting sequences are shown as grey boxes and the positions of relevant restriction enzyme cut sites and the predicted fragment size of a digest are indicated. The positions of the two probes, P1 and P2, are shown as thick black lines. (C and D) Southern blot analysis of the *radC* locus in a wild-type strain (lane marked Wt) and in a *radC* deletion strain (lane marked *radC*Δ). The probe used for a specific analysis is shown below each panel. Small arrows point to relevant fragment sizes.

3.2. PCR generated bipartite gene-targeting substrates can be used to create point mutations

An experiment was performed to investigate the versatility of the bipartite method by attempting to introduce point mutations into the genome. In the present study, we use the term "point mutation" in the broad sense as it covers introduction of restriction enzyme cut sites into the genome. The scheme for introducing point mutations into the genome is similar to the one described for gene deletions above, except that the direct repeat is now constituted by two identical targeting sequences, which contain the mutation (Figs. 2B and C). After transformation and integration of the bipartite substrate, the original allele is replaced by the selective marker flanked by a direct repeat of the mutant allele. In a subsequent direct-repeat recombination event, the marker and one repeat are excised from the genome, leaving a single copy of the mutant allele. However, integration of the gene-targeting substrate may also occur in such a way that only one of the two repeats contains the mutant allele. This has been observed in *S. cerevisiae*, especially when the mutation is located close to the outer end of the substrate (Erdeniz et al., 1997). If only one repeat contains the mutation, screening amongst the direct-repeat recombinants derived from the primary transformant is necessary to identify strains containing the desired genomic alteration.

Construction of the bipartite gene-targeting substrate for point mutations requires a total of three PCRs compared to the four needed to create the corresponding substrate for gene deletions. This is because only a single specific targeting fragment is required, which is generated in one PCR by using a single pair of adaptamers, Y1 and Y2 in Fig. 2C. The targeting fragment is then fused to both of the two fragments, which contain the overlapping parts of *pyr-4*, in two PCRs to complete formation of the bipartite substrate. In this case, the outer ends of the bipartite substrate contain adaptamer sequences that are not homologous to the target site (Fig. 2B). Such ends could potentially impede efficient homologous integration as they need to be removed by nucleases during the integration process. Alternatively, a bipartite substrate with homologous outer ends can be made if the targeting sequence is generated in two parallel PCR reactions by two primer pairs, where each pair consists of a regular primer and an adaptamer. Next, the resulting two fragments are fused to the *pyr-4* containing fragments in the same way as described for gene deletion substrates. However, in a large scale genome modification experiment, it may be important to limit costs by using as few primers and PCRs as possible. For this reason, we addressed the possibility of using bipartite substrates containing non-homologous adaptamer derived sequences in the outer ends.

To test the possibility of introducing specific point mutations into the genome by using a bipartite gene-targeting substrate we attempted to insert new restriction enzyme cut sites into the *yA* locus (AN6635.2). *yA* was selected for this analysis as a strain with a dysfunctional *yA* gene develops yellow, instead of the usual green conidiospores (O'Hara and Timberlake, 1989) allowing an easy way to score gene-targeting events. When the outcome of the targeting event produces a direct repeat where both copies contain a mutated *yA* allele, the transformants are yellow. In the cases, where only one of the repeats contains the mutation, transformants develop green conidia and cannot be distinguish from strains resulting from ectopic integration events. However, gene-targeted strains can easily be identified after the selection for direct-repeat recombinants since many yellow clones will develop. Accordingly, the ability of a transformant to produce yellow colonies after direct-repeat recombination was used to assess whether it was the result of a gene-targeting event.

Two different alleles of *yA*, *yA-Kpn*I, and *yA*-I-*Sce*I, were chosen for the point-mutation experiment. These alleles were amplified by PCR from the plasmids, pYA11-*Kpn*I and pYA11-I-*Sce*I. For each allele, the PCR product was fused to the two overlapping *pyr-4* containing fragments in two individual PCRs and the resulting bipartite gene-targeting substrates were co-transformed into *A. nidulans*. Only few of the primary transformants produced the yellow phenotype expected for events where the integration at *yA* contained the mutation in both repeats. Specifically,

Table 2
Introduction of restriction enzyme cut sites into *yA* using PCR generated bipartite gene-targeting substrates

Site introduced	Trial	Number of transformants		Gene-targeting efficiency (%)
		Total	Yellow on 5-FOA	
*Kpn*I	1	5 (0)[a]	3	60
	2	2 (0)	1	50
	Total	7 (0)	4	57
I-*Sce*I	1	3 (0)	1	33
	2	2 (1)	2	100
	3[b]	30 (9)	23	77
	Total	35 (10)	26	74

[a] The number of primary transformants producing yellow spores are shown in parenthesis.
[b] Four micrograms of substrate was used in this experiment.

with the *yA-Kpn*I substrate none of the seven primary transformants were yellow, and with the *yA*-I-*Sce*I substrates 10 out of 35 were yellow (Table 2). The remaining primary transformants were green. Next all transformants were plated on 5-FOA plates. As expected, yellow primary transformants produced only yellow direct-repeat recombinants. In addition, many of the green primary transformants were capable of producing yellow direct-repeat recombinants demonstrating that they were the result of a gene-targeting event. Of the 7 and 25 green transformants obtained with the *yA-Kpn*I and the *yA*-I-*Sce*I substrates, respectively, 4 and 16 could produce yellow colonies. In total, with bipartite substrates containing the *yA-Kpn*I and the *yA*-I-*Sce*I alleles, 57 and 74% of all primary transformants, respectively, were able to form yellow conidia, see Table 2. The remaining primary transformants (43 and 26%, respectively) never developed yellow conidia after 5-FOA treatment indicating that they were the result of an ectopic integration event. These results indicate that the *yA* locus had been targeted at a high frequency.

The status of the *yA* locus in four direct-repeat recombinants, two from each point mutation experiment, was analyzed by PCR. vIn all four cases, the size of the resulting *yA* fragment was identical to the one obtained from a wild-type strain, and subsequent digestion of the fragment by either *Kpn*I or I-*Sce*I indicated that the desired point mutation had been correctly created in the genome (data not shown). Next, the two potential *yA-Kpn*I strains were analyzed by Southern blot analysis to confirm that they were the result of successful gene-targeting events. Genomic DNA from each strain was either digested with *Hpa*I, which cuts outside the targeted area, or co-digested with *Hpa*I and *Kpn*I, where the latter only cleaves the *yA Hpa*I fragment if the *yA-Kpn*I allele is present (Fig. 4A). The blots were analyzed using two different probes. The first probe, P3, hybridizes to the *yA* specific targeting sequence of the bipartite substrate and therefore detects the *yA* locus as well as any additional ectopically integrated gene-targeting substrates (if any are present). On the other hand, the second probe, P4, detects only the *yA* locus as it hybridizes to a region of *yA* that is not included in the gene-targeting substrate. This experiment is designed to show whether the fragments detected in the previous experiment are generated from the *yA* locus. For the two mutant strains, probe P3 only detected a single fragment for *Hpa*I digested samples (Fig. 4B). The size of this fragment was identical to the fragment detected by probe P4 (Fig. 4C). As expected, these fragments were in the same

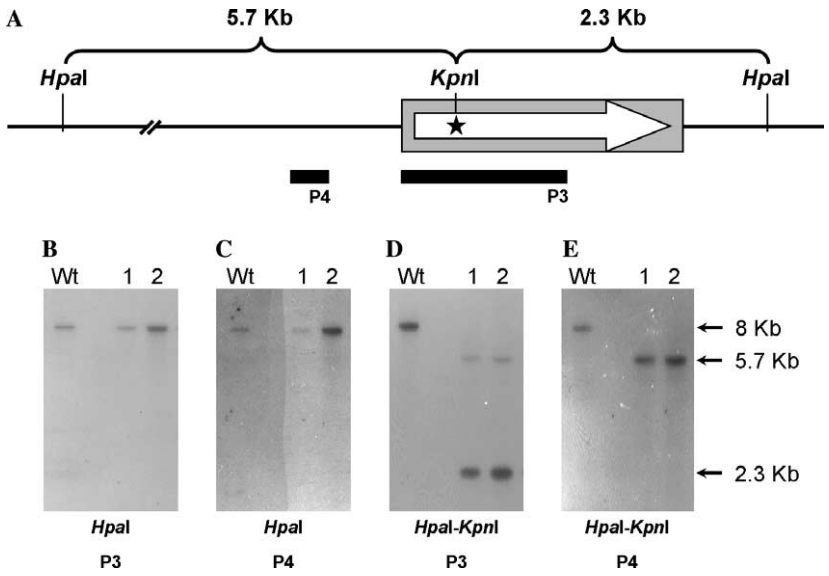

Fig. 4. Insertion of a novel *Kpn*I site in the endogenous *yA* by the use of a bipartite gene-targeting substrate generated by PCR. (A) Graphical representation of the *yA* locus. The *yA* open reading frame is illustrated as an open arrow, the location of the new *Kpn*I site as a star and the sequence used in the targeting substrate is shown as a grey box. The positions of relevant restriction enzyme cut sites and the predicted fragment sizes of a digest are indicated. The positions of the two probes, P3 and P4, used for Southern blot analysis are shown as thick black lines. (B, C, D, and E) Southern blot analysis of the *yA* locus in a wild-type strain (lane marked Wt) and in two mutated strains (lanes 1 and 2). The restriction enzyme(s) used for a specific analysis and the probe used to detect the relevant fragments are shown below each panel. Small arrows point to relevant fragment sizes.

position as the *yA* fragments detected in DNA from a wild-type strain by probes P3 and P4. This demonstrates that direct-repeat recombination was successfully achieved and rules out the possibility that integration of the bipartite substrate at the *yA* locus was accompanied by any additional ectopic integration events. Furthermore, for the *Hpa*I–*Kpn*I digested samples, hybridization with probes P3 and P4 showed that the *yA Hpa*I fragment from the mutant strains could be cleaved by *Kpn*I (Figs. 4D and E). Accordingly, the *yA-Kpn*I allele was successfully inserted into *yA* of both mutant strains. A similar Southern blot analysis was performed for the two potential *yA*-I-*Sce*I mutant strains. Likewise, the analysis confirmed that correct point mutations had been created in the two strains after direct-repeat recombination (data not shown). Overall these results show that bipartite PCR generated gene-targeting substrates can be successfully used to make point mutations in the genome of *A. nidulans*.

3.3. Bipartite gene-targeting substrates increase successful targeting compared to continuous gene-targeting substrates

Encouraged by the results above, a more careful analysis of the point-mutation gene-targeting method was performed to determine whether bipartite substrates were targeting the desired locus as efficiently as traditional continuous gene-targeting substrates. We also addressed whether the presence of non-homologous adaptamer sequences in the ends of point-mutation substrates reduced the gene-targeting efficiency. However, the targeting efficiencies of different PCR generated substrates are not easily comparable as they may contain different degrees of PCR generated errors. To solve this problem, a plasmid, pRSub3, was constructed from which all combinations of substrate fragments can be liberated, including versions where the outer substrate-ends are either homologous or non-homologous to the target site (Fig. 1 and Section 2).

Transformation of *A. nidulans*, with the four different substrate types rarely produced yellow primary transformants. In fact only one out of a total of 42 primary transformants obtained was initially yellow. This is similar to the result obtained by the PCR derived *yA-Kpn*I bipartite substrate (see Section 3.2). Transformation with substrates containing non-homologous ends produced slightly lower numbers of transformants compared to the numbers achieved by substrates containing homologous ends. However, the gene-targeting efficiencies determined for the two substrate types were identical, Table 3. We then compared the gene-targeting efficiencies obtained with bipartite substrates with those obtained with continuous substrates. The numbers of transformants obtained using bipartite substrates were reduced approximately twofold compared to those obtained with the corresponding continuous substrates (Table 3). In contrast, the gene-targeting efficiencies obtained with bipartite substrates were two- to threefold higher compared to those obtained with the continuous substrates (Table 3). The average gene-targeting efficiency for integrating the *yA-Kpn*I allele using a bipartite gene-targeting plasmid (pRSub3) derived substrate was 62%. This is similar to the efficiencies obtained when PCR derived bipartite substrates were used to create *yA-Kpn*I strains (57%) and *y*A-I-*Sce*I strains (74%), compare Table 2 and 3.

Table 3
Introduction of a *Kpn*I site into endogenous *yA* by gene-targeting. Comparison of the efficiency obtained by bipartite- and continuous gene-targeting substrates derived from pRSub3

Substrate	End-types	Number of transformants	Yellow on 5-FOA	Gene targeting efficiency (%)
Bipartite	H[a]	5 (1)[b]	3	60
	NH	8 (0)	5	63
	Total	13 (1)	8	62
Continuous	H	17 (0)	5	30
	NH	12 (0)	2	17
	Total	29 (0)	7	24

[a] H are homologous- and NH are non-homologous ends.
[b] The number of primary transformants producing yellow spores are shown in parenthesis.

To confirm that all yellow direct-repeat recombinants presented in Table 3 were due to correct targeting of *yA*, all transformants were analyzed by Southern blot analysis. First, we investigated the status of the *yA* locus before direct-repeat recombination. In this case, a 12.2 kb *Hpa*I fragment is expected if the substrate is integrated at *yA* by HR, see Fig. 5A. In transformants obtained with continuous as well as with bipartite gene-targeting substrates, *Hpa*I fragments larger than 12.2 kb were often observed indicating that additional DNA was inserted at the *yA* locus, Fig. 5B. The larger fragments may be due to polymerization of gene-targeting fragments by non-homologous end-joining. If this happens prior to integration at *yA* by HR, several gene-targeting fragments can simultaneously be integrated at the *yA* locus. However, after integration at *yA*, the polymer will always contain an outer direct repeat. Accordingly, the desired genomic alteration may still be obtained from such transformants by direct-repeat recombination. To test this possibility, one randomly selected yellow colony from each of the 15 yellow direct-repeat recombinants presented in Table 3 was subjected to Southern blot analysis. In all cases, only the desired genomic alteration was left in the genome (Figs. 6A, B, C, and data not shown). Apparently, direct-repeat recombination generally results in complete removal of all additional sequences that integrated at the locus. Based on these results, we conclude that non-homologous ends in the gene-targeting substrate do not adversely affect the gene-targeting efficiency nor do they result in any unwanted ectopic co-integration events.

4. Discussion

With the increasing availability of fully sequenced fungal genomes, the demand for efficient gene-targeting methods for filamentous fungi has increased. In the present

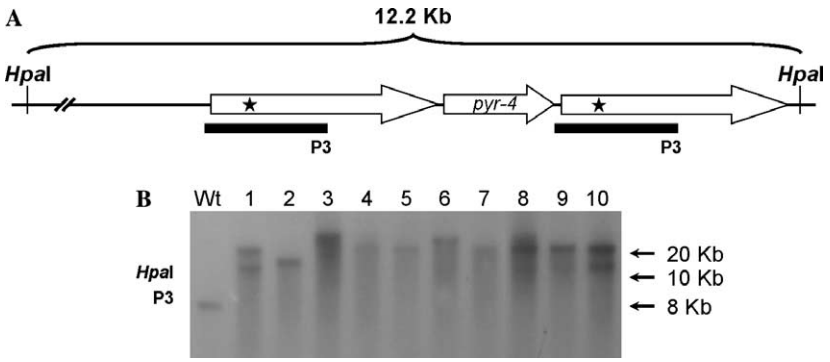

Fig. 5. Analysis of the *yA* locus after transformation with a plasmid derived bipartite gene-targeting substrate. (A) A graphical representation of the structure of the *yA* locus after integration of the bipartite gene-targeting substrate by mechanisms that only involve HR. The two *yA* open reading frames are illustrated by large open arrows, the *pyr-4* marker gene is shown as a small open arrow and the location of the new *Kpn*I site as a star. The position of *Hpa*I cut sites and the predicted fragment size of the digest is indicated. The positions of the probe, P3, used for Southern blot analysis are shown as thick black lines. (B) Southern blot analyses of the *yA* locus in 10 transformed strains. The wild-type locus is included for comparison (lane marked Wt). The analyses of DNA from transformants obtained by continuous and bipartite substrates containing homologous ends are shown in lane 1 and lanes 2–4, respectively; and by continuous and bipartite substrates containing non-homologous ends are shown in lanes 5–8 and 9–10, respectively. For each lane the genomic DNA was *Hpa*I digested and probed with P3. Small arrows to the right of each panel point to relevant fragment sizes.

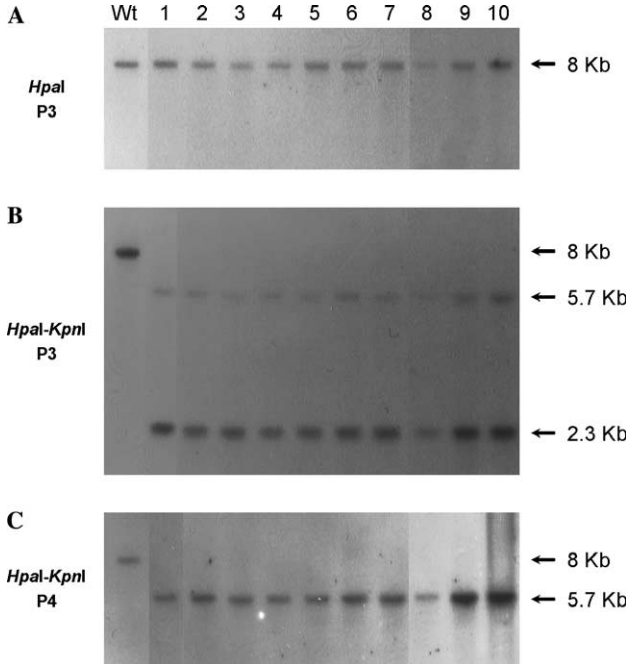

Fig. 6. Analysis of the *yA* locus after transformation with a plasmid derived bipartite gene-targeting substrate and after elimination of the *pyr-4* marker by subsequent direct-repeat recombination. For a graphical representation of the *yA* locus after direct-repeat recombination including the positions of the probes, P3 and P4, and predicted fragment sizes of relevant digests, see Fig. 4A. (A, B, and C) Southern blot analyses of the *yA* locus in 10 transformed strains after selection for direct-repeat recombinants. The wild-type locus is included for comparison (lane marked Wt). The analyses of DNA from transformants obtained by continuous and bipartite substrates containing homologous ends are shown in lane 1 and lanes 2–4, respectively; and by continuous and bipartite substrates containing non-homologous ends are shown in lanes 5–8 and 9–10, respectively. The restriction enzyme(s) used for a specific analysis and the probe used to detect the relevant fragments are shown to the left of each panel. Small arrows to the right of each panel point to relevant fragment sizes.

study, we have adapted a PCR-based gene-targeting method from *S. cerevisiae*, which can be used to create virtually any genome modification, in *A. nidulans* and demonstrated that it works efficiently for creating gene deletions and point mutations. The ability to create specific point mutations allows for a more detailed analysis of enzymatic activities e.g., by construction of separation of function mutants or construction of genes encoding a mutant protein where the capacity for a posttranslational modification has been altered. Even essential genes can be manipulated this way if the resulting point mutation is not lethal. In this case, it is important to note that the direct repeat used to introduce the mutation needs to cover the entire open reading frame of the gene of interest. This way, one repeat unit consisting of the entire mutated open reading frame will be in the normal position with respect to the original promoter of the gene.

After integration of the gene-targeting substrate, the selective marker will be flanked by a direct repeat. This is an important feature of the method and it provides three main advantages. First, since the marker can be eliminated by direct-repeat recombination, it allows iterative gene-targeting experiments to be performed as the marker can be recycled. Hence, the genome of a progenitor strain can be manipulated an unlimited number of times. Second, in the scheme used to introduce a deletion, one of the direct-repeat sequences remains in the genome after the procedure is completed. It is therefore easy to adjust the procedure to allow construction of fusion genes, e.g., to tag proteins with GFP or to allow promoter swapping. The only requirement is a vector where the *pyr-4* marker is flanked by the relevant sequence as a direct repeat, e.g., by the sequence encoding GFP or by the promoter sequence of choice. Third, in methods, where the selective marker gene remains at the target locus after integration, transcription from the marker gene may influence the state of the chromatin structure at the targeted region. Accordingly, the phenotype of a given mutation inserted by such a method could be influenced by this effect as the regulation of neighbor genes may be affected. This problem is minimized in the method presented here as the marker is eliminated by direct-repeat recombination.

In the method, gene-targeting is achieved by co-transformation with a bipartite gene-targeting substrate. This allows PCR construction of substrates where the marker is flanked by large targeting sequences that help to increase the efficiency of the directed integration process (Bird and Bradshaw, 1997). The bipartite substrate is made via two successive PCRs. In contrast, construction of the corresponding continuous substrate generally requires three successive PCRs or a second reaction where three PCR fragments are fused simultaneously. Since DNA polymerases are not error free, an additional round of PCR increases the possibility of the final targeting substrate containing unwanted mutations. More importantly, PCR amplification of a large continuous fragment that contains a direct repeat is difficult and often results in production of a small byproduct, which results from PCR recombination between the repetitive sequences (Meyerhans et al., 1990). The bipartite method circumvents this problem because each repeat is amplified in separate reactions.

A successful gene-targeting event using a bipartite gene-targeting substrate requires that three HR events take place. At first glance, this hardly seems favorable given that in *A. nidulans* non-homologous end-joining rather than HR is the predominant process for integration of recombinant DNA (Goldman et al., 2002). However, since bipartite substrates only produce transformants if the marker is reconstituted by HR it may be envisioned that this HR event may channel the entire substrate into the HR pathway. Mechanistically this is feasible since in organisms ranging from *S. cerevisiae* to mammals DNA double strand breaks, DSBs, are repaired in large protein structures termed repair centers (reviewed in Lisby and Rothstein, 2005) Importantly, when multiple DNA DSBs are introduced in *S. cerevisiae*, the resulting DNA ends are typically localized in a single repair center (Lisby et al., 2003). Therefore, when the bipartite substrate is fused in the cell by HR in a DNA repair center, the two outer ends of the substrate may likely be embedded in the same center, which is specialized for HR. If so, the entire substrate may preferentially proceed in the HR pathway and integrate at the desired location. In agreement with this view, the gene-targeting efficiency determined for bipartite substrates is threefold higher compared to the efficiency obtained by the corresponding continuous gene-targeting substrate. A higher ratio of correctly to ectopically integrated transformants means less cumbersome screening to identify desired transformants. At the same time, we note that the overall transformation efficiency obtained with bipartite substrates is reduced compared to the efficiency obtained with continuous substrates. This may be due to the fact that ectopic integration of the individual fragments of a bipartite substrate cannot produce viable transformants. Thus, the increased gene-targeting efficiency obtained with bipartite substrates may simply reflect a reduced number of ectopic integrants.

The activity of the non-homologous end-joining pathway may be visible in some of the integrations at the *yA* locus. In the Southern blot analyses in Fig. 5B showing the configuration of the *yA* locus after transformation, it was interesting to note that in lanes 1, 3, 8, 9, and 10 the *yA* specific probe hybridizes to two restriction fragments, when only a single band was expected. This would typically be interpreted as a result of ectopic integration. However, given that the subsequent Southern blot analyses (Figs. 6A, B, and C) of the same strains after elimination of the *pyr-4* marker in all cases fail to show any evidence of ectopic integration, it is highly unlikely that ectopic integration could account for the additional band in the transformants. Perhaps, they may be explained as the result of different degrees of repeat loss, caused by the instability of large tandem repeats during shake flask growth of mycelia prior to genomic DNA isolation.

In genome-wide gene-modification projects, it may be important to reduce costs for primers and PCR. The use of adaptamers is well suited for this purpose as previously described for *S. cerevisiae* (Reid et al., 2002a,b). For example, in a gene deletion project the number of targeting fragments can be reduced by 50% if entire intergenic regions are amplified by adaptamers and used as targeting sequences. This is possible as the same fragment can be used to target the upstream gene as well as the down stream gene. Similarly, in projects where only one specific targeting sequence is needed, like in substrates for making point mutations, the targeting fragment can be created using a single adaptamer pair to reduce costs as two primers and one PCR can be saved for every point mutation strain to be created. A consequence of using adaptamer pairs to generate targeting sequences is that the final gene-targeting substrate will contain short adaptamer derived sequences in the outer ends, which are not homologous to the genomic target sequence. In *S. cerevisiae* such ends are efficiently removed by the Rad1/Rad10 endonuclease (Sung et al., 1993; Tomkinson et al., 1993; Ivanov and Haber, 1995). Since a *RAD1* homolog (AN3620.1) is present in the *A. nidulans* genome (Goldman and Kafer, 2004), we reasoned that a similar activity would be present in *A. nidulans*. In agreement with this, we show that the presence of non-homologous ends does not seem to influence the gene-targeting efficiency. We conclude that it is possible to take advantage of adaptamers for making gene-targeting substrates for *A. nidulans*.

The bipartite method presented here is extremely flexible and can easily be adapted to perform genome manipulations like promoter replacements and GFP tagging. It is suitable for large scale genome alteration projects since the substrates are PCR based and the method reduces the screening required to find correct integrants. Recently, key genes, *mus-51* (a *KU70* homolog) and *mus-52* (a *KU80* homolog), in the non-homologous end-joining repair pathway have been deleted in *N. crassa*. Such strains have shown gene-targeting efficiencies approaching 100% (Ninomiya et al., 2004). If similar mutant strains were available for *A. nidulans*, the bipartite method could easily be adapted to a high throughput gene-targeting scheme. In addition, it may eliminate polymerization of gene-targeting substrates and thereby eliminate

the need to verify that unwanted sequences are left at the target locus after direct-repeat recombination.

Acknowledgments

This work was supported by the Danish Research Agency to UHM and the Danish Biotech Research Academy, FOBI to G.L. The Technical University of Denmark for Ph.D. grants to G.L. and J.B.N. We thank Jesper Storm and Maya Pedersen for skilful technical assistance, and Gerald Hofmann and Iben Plate for critically reviewing this manuscript.

References

Aleksenko, A., Ivanova, L., 1998. In vivo linearization and autonomous replication of plasmids containing human telomeric DNA in *Aspergillus nidulans*. Mol. Gen. Genet. 260, 159–164.

Archer, D.B., Dyer, P.S., 2004. From genomics to post-genomics in *Aspergillus*. Curr. Opin. Microbiol. 7, 499–504.

Bailis, A.M., Rothstein, R., 1990. A defect in mismatch repair in *Saccharomyces cerevisiae* stimulates ectopic recombination between homeologous genes by an excision repair dependent process. Genetics 126, 535–547.

Ballance, D.J., Turner, G., 1985. Development of a high-frequency transforming vector for *Aspergillus nidulans*. Gene 36, 321–331.

Bird, D., Bradshaw, R., 1997. Gene targeting is locus dependent in the filamentous fungus *Aspergillus nidulans*. Mol. Gen. Genet. 255, 219–225.

Blin, N., Stafford, D.W., 1976. A general method for isolation of high molecular weight DNA from eukaryotes. Nucleic Acids Res. 3, 2303–2308.

Clutterbuck, A.J., 1974. In: King, R.C. (Ed.), Handbook of Genetics. Plenum Press, New York, NY, pp. 447–510.

Erdeniz, N., Mortensen, U.H., Rothstein, R., 1997. Cloning-free PCR-based allele replacement methods. Genome Res. 7, 1174–1183.

Goldman, G.H., McGuire, S.L., Harris, S.D., 2002. The DNA damage response in filamentous fungi. Fungal Genet. Biol. 35, 183–195.

Goldman, G.H., Kafer, E., 2004. *Aspergillus nidulans* as a model system to characterize the DNA damage response in eukaryotes. Fungal Genet. Biol. 41, 428–442.

Ivanov, E.L., Haber, J.E., 1995. RAD1 and RAD10, but not other excision repair genes, are required for double-strand break-induced recombination in *Saccharomyces cerevisiae*. Mol. Cell. Biol. 15, 2245–2251.

Johnstone, I.L., Hughes, S.G., Clutterbuck, A.J., 1985. Cloning an *Aspergillus nidulans* developmental gene by transformation. EMBO J. 4, 1307–1311.

Lisby, M., Mortensen, U.H., Rothstein, R., 2003. Colocalization of multiple DNA double-strand breaks at a single Rad52 repair centre. Nat. Cell Biol. 5, 572–577.

Lisby, M., Rothstein, R., Mortensen, U.H., 2001. Rad52 forms DNA repair and recombination centers during S phase. Proc. Natl. Acad. Sci. USA 98, 8276–8282.

Lisby, M., Rothstein, R., 2005. Localization of checkpoint and repair proteins in eukaryotes. Biochimie 87, 579–589.

Meyerhans, A., Vartanian, J.P., Wain-Hobson, S., 1990. DNA recombination during PCR. Nucleic Acids Res. 18, 1687–1691.

Moure, C.M., Gimble, F.S., Quiocho, F.A., 2003. The crystal structure of the gene targeting homing endonuclease I-*Sce*I reveals the origins of its target site specificity. J. Mol. Biol. 5, 685–695.

Ninomiya, Y., Suzuki, K., Ishii, C., Inoue, H., 2004. Highly efficient gene replacements in *Neurospora* strains deficient for nonhomologous end-joining. Proc. Natl. Acad. Sci. USA 101, 12248–12253.

O'Hara, E.B., Timberlake, W.E., 1989. Molecular characterization of the *Aspergillus nidulans yA* locus. Genetics 121, 249–254.

Plessis, A., Perrin, A., Haber, J.E., Dujon, B., 1992. Site-specific recombination determined by I-*Sce*I, a mitochondrial group I intron-encoded endonuclease expressed in the yeast nucleus. Genetics 130, 451–460.

Reid, R.J., Lisby, M., Rothstein, R., 2002a. Cloning-free genome alterations in *Saccharomyces cerevisiae* using adaptamer-mediated PCR. Methods Enzymol. 350, 258–277.

Reid, R.J., Sunjevaric, I., Keddache, M., Rothstein, R., 2002b. Efficient PCR-based gene disruption in *Saccharomyces* strains using intergenic primers. Yeast 19, 319–328.

Sambrook, J., Russell, D.W., 2001. Molecular Cloning A Laboratory Manual. Cold Spring Harbor Laboratory Press, Cold Spring Harbor, NY.

Schaefer, D.G., 2001. Gene targeting in *Physcomitrella patens*. Curr. Opin. Plant. Biol. 4, 143–150.

Sung, P., Reynolds, P., Prakash, L., Prakash, S., 1993. Purification and characterization of the *Saccharomyces cerevisiae* RAD1/RAD10 endonuclease. J. Biol. Chem. 268, 26391–26399.

Tomkinson, A.E., Bardwell, A.J., Bardwell, L., Tappe, N.J., Friedberg, E.C., 1993. Yeast DNA repair and recombination proteins Rad1 and Rad10 constitute a single-stranded-DNA endonuclease. Nature 362, 860–862.

Yang, L., Ukil, L., Osmani, A., Nahm, F., Davies, J., De Souza, C.P., Dou, X., Perez-Balaguer, A., Osmani, S.A., 2004. Rapid production of gene replacement constructs and generation of a green fluorescent protein-tagged centromeric marker in *Aspergillus nidulans*. Eukaryot. Cell 3, 1359–1362.

Yu, J.H., Hamari, Z., Han, K.H., Seo, J.A., Reyes-Dominguez, Y., Scazzocchio, C., 2004. Double-joint PCR: a PCR-based molecular tool for gene manipulations in filamentous fungi. Fungal Genet. Biol. 41, 973–981.

Zarrin, M., Leeder, A.C., Turner, G., 2005. A rapid method for promoter exchange in *Aspergillus nidulans* using recombinant PCR. Fungal Genet. Biol. 42, 1–8.

Chapter 7

Characterization of a deletion strain of the *Aspergillus nidulans radC*, a homolog of the double-strand break repair gene *RAD52*

7.1 Introduction

The Rad52 protein of the yeast *S. cerevisiae* plays a key role in the repair of DNA double-strand breaks (DSBs) and homologous recombination (HR). Accordingly, deletion of *RAD52* in budding yeast results in severe recombination and DSB repair phenotypes. Δ*rad52* mutants have growth and sporulation defects, are extremely sensitivity to DNA damaging agents and are deficient in mating-type switching as well as in mitotic and meiotic recombination (reviewed by Krogh & Symington (2004)). The N-terminal of Rad52 is evolutionary conserved and contains the DNA binding as well as the self-association domains of the protein. Importantly, several studies have shown that these functions are also present and active in Rad52 of higher eukaryotes (Shen et al., 1996b; Mortensen et al., 1996, 2002). The central region of Rad52 contains the RPA binding domain. Again, Rad52 has been shown to interact with RPA in both yeast and human suggesting that this function is also conserved (Park et al., 1996; Hays et al., 1998; Shinohara et al., 1998). Finally, the C-terminal part of the protein contains the Rad51 binding (Milne & Weaver, 1993; Shen et al., 1996a; Shinohara & Ogawa, 1998; Krejci et al., 2002) and the multimer formation domains Ranatunga et al. (2001). Although this region of Rad52 is less conserved at the amino acid residue level, several studies have shown that the Rad51 binding ability of Rad52 through this domain seems to be conserved from yeast to human (Milne & Weaver, 1993; Shen et al., 1996a; Shinohara & Ogawa, 1998; Krejci et al., 2002).

Homologs of Sc*RAD52* have been isolated from various other organisms such as fungi, fish, chicken, mouse and human, underlining its

importance (Sakuraba et al., 2000; Ostermann et al., 1993; van den Bosch et al., 2001; Takahashi & Dawid, 2005; Bezzubova et al., 1993; Bendixen et al., 1994; Muris et al., 1994; Shen et al., 1995). Surprisingly, mouse cell lines lacking *RAD52* are not hypersensitive to DNA-damaging agents such as γ-irradiation or MMS. *MmRad52*$^{-/-}$ mice are both viable and fertile and show no gross abnormalities. However, gene targeting experiments in *MmRad52*$^{-/-}$ ES cells demonstrated a reduced frequency of targeted integration in these cells (Rijkers et al., 1998). Similar results were obtained in *RAD52*$^{-/-}$ mutants of the chicken B-cell line DT40 (Yamaguchi-Iwai et al., 1998). Altogether, these results suggest that although the structure and biochemical activities of Rad52 have been conserved during evolution, its roles in recombination and repair of DNA lesions have evolved from yeast to higher eukaryotes. While ScRad52 is required for both mitotic and meiotic recombination as well as for the repair of DNA DSBs in yeast, the mammalian Rad52 species do not seem to play a major role in these processes. One hypothesis to explain these phenotypic differences is that functional homologs of Rad52 could have developed during evolution. In fact, in *S.cerevisiae*, Rad59 has been described as a ScRad52 paralog and the two proteins have been shown to have overlapping functions (Bai & Symington, 1996; Bai et al., 1999; Wu et al., 2006b; Feng et al., 2007). Moreover, two Rad52 homologs, Rad22A (Rad22) and Rad22B (Rti1), have been identified in the fission yeast *Schizosaccharomyces pombe*. Interestingly, *rad22A* and *rad22B* deletion mutants have different phenotypes where *rad22A* mutants behave similarly to the *S. cerevisiae rad52* mutants with respect to recombination and radiation sensitivity while *rad22B* mutants have a much milder phenotype (Suto et al., 1999; van den Bosch et al., 2001; Doe et al., 2004). To date, no Rad52 functional homologs have been described in mammalian cells. However, proteins that appear to have overlapping function with the latter have been described. For example, work by Fujimori et al. (2001) in chicken DT40 cells revealed that double mutant cells of *rad52* and *xrcc3*, one of the mammalian *RAD51* paralogs, are inviable whereas each of the single mutants grows normally. These results suggest that XRCC3 and Rad52 have overlapping functions in chicken cells. Recently, results obtained by Saeki et al. (2006) implied that a key role of the tumor suppressor BRCA2 in vivo is to deliver Rad51 to ssDNA which is one of the roles of Rad52 in budding yeast (Song & Sung, 2000; Sugiyama & Kowalczykowski, 2002). Moreover, a functional homolog of BRCA2, the *Caenorhabditis elegans* CeBRC-2 (Martin et al., 2005), has recently been shown to promote Rad51 mediated D-loop formation, a function directly dependant on CeBRC-2's ability to bind both Rad51 and DNA. In this study, CeBRC-2 was also shown to mediate DNA single-strand annealing and the authors therefore suggested that CeBRC-2 could have replaced the role of Rad52, which is absent from *C. elegans* (Petalcorin et al., 2006).

In order to investigate the role of Rad52 in filamentous fungi and further understand how this protein has evolved, we have characterized

a deletion strain of the *A.nidulans radC*, a homolog of the *S. cerevisiae RAD52*. Our results show that the *radC*Δ strain is highly sensitive to MMS but surprisingly resistant to γ-ray induced DNA damage. Sexual crosses between *radC*Δ mutants are sterile suggesting a role of RadC in meiosis. Moreover, the *radC*Δ strain is deficient in both gene targeting and gap repair implying a role of RadC in recombination in *A. nidulans*. This suggests that, as Rad52, RadC is a multi-functional protein involved in DNA repair and HR in *A. nidulans*. Moreover, our results show that some aspects of the phenotype observed in the *A. nidulans radC*Δ strain resemble those observed in *S. cerevisiae rad52*Δ strains while other aspects are closer to what is observed in the mammalian $RAD52^{-/-}$ cells. Accordingly, our results strengthen the hypothesis that the roles of Rad52 in DNA DSB repair and HR have changed throughout evolution.

7.2 Materials and Methods

7.2.1 Strains, media and plasmids

All experiments were performed using the *A. nidulans* strain, IBT 27263, (*argB2*, *pyrG89*, and *veA1*) as reference strain. All the strains used in this study are presented in Table 7.1. The *A. nidulans radC*Δ strain, IBT 28010, was generated using a bipartite substrate-based gene targeting method and confirmed by Southern analysis as described previously (Nielsen et al., 2006). Solid and liquid media were made according to Clutterbuck (Clutterbuck, 1974). Minimal and complete media were supplemented with 10mM uridine, 10mM uracil and 4mM L-arginine if not stated otherwise. MMS or HU complete media were made by adding MMS or HU to complete media containing 2% agar and cooled down to 50°C after autoclavation. Plasmid pYA1 contains *argB*, *yA* and *AMA1* of *A. nidulans* (Aleksenko & Ivanova, 1998). Plasmid pYA1-I-*Sce*I carries a *yA* allele in which an I-*Sce*I restriction site has been inserted thus causing a frameshift mutation (Nielsen et al., 2006). In the rest of this article, this allele will be referred to as yA-I-*Sce*I. Plasmid pYA-Icegap1 was used as a substrate for the gap repair experiments. Plasmid pRSUB3 contains the entire *N. crassa pyr4* gene flanked by directly repeated sequences of a *yA-Kpn*I allele. In this allele, the KpnI site has been inserted 401 bp downstream of the ATG of *yA* thus causing a frameshift mutation (Nielsen et al., 2006).

7.2.2 Cloning

pYA-Icegap1, used for the gap repair experiments, was constructed by inserting a yA-I-*Sce*I containing fragment, cut out of pYA1-I-*Sce*I using *Mfe*I and *Nhe*I, into a *Mfe*I-*Nhe*I vector fragment of pYA1.

Table 7.1. Strains used in this study

Strain	Genotype	Source/Reference
IBT 27263	*argB2, pyrG89, veA1*	IBT
IBT 28010	*argB2, pyrG89, veA1, radC*Δ	Nielsen et al., 2006
IBT 27266	*argB2, pyrG89, veA1, yA-KpnI*	This study
IBT 28539	*argB2, pantoA10, veA1, radC*Δ*, yA-KpnI*	This study
IBT 26166	*biA1, veA1*	IBT*
IBT 26134	*pantoA10, veA1*	IBT*
IBT 28540	*pantoA10, veA1, yA-KpnI*	This study
IBT 28538	*argB2, pyrG89, veA1, radC*Δ*, yA-KpnI*	This study

* IBT, Instituttet for Bioteknologi Strain Collection (Lyngby, Denmark)

7.2.3 Transformation of *A. nidulans*

Genetic transformation of *A. nidulans* protoplasts was performed as previously described (Johnstone et al., 1985) except that protoplasting was achieved by using the enzyme, Glucanex, (Novozymes A/S), at a concentration of 40 mg/ml in protoplasting buffer. All transformations were performed with 10^7 protoplasts in 100 μl transformation buffer. For experiments using PCR derived fragments, 1-2 μg DNA was used unless otherwise indicated.

7.2.4 cDNA analysis

The *radC* mRNA transcript was analyzed using the SMART RACE cDNA amplification kit (Clontech Laboratories Inc., Mountain View USA.) that allows reverse transcription and PCR amplification of both 5' and 3' ends of a given mRNA. Briefly, cDNA for both 5' and 3' amplification was prepared according to manufacturer recommendations from total RNA extracted from exponentially growing mycelia in minimal medium. 5' cDNA was generated by PCR using a single *radC* internal reverse primer (5'-GAGGAAGCTGCTGCCCTTCAAGCAC-3') and the universal primer mix supplied with the kit. The PCR product was inserted into the pGEM-T vector system (Promega Corp., Madison, USA.), and propagated in *E. coli*. The inserts from several clones were sequenced. Cloned 3' end cDNA fragments were acquired in a similar manner using *radC* specific primers (5'-ATCGCCAGAAACCCGTTT-GAGGAAGCC-3' and 5'-AACGCGCTCTGCGGAACTTCGGC-3').

7.2.5 Spot assay

Sensitivity to MMS and hydroxyurea (HU) was tested by spotting conidial suspensions on complete medium containing various concentrations of these chemicals. Specifically, a series of 10-fold dilutions of conidial suspensions containing 10^8 cells per ml were made and 5 μl of each dilution was then spotted on chemical-containing medium. To test for

sensitivity to UV and γ-irradiation, conidial suspensions were spotted as described above on complete medium. Plates were then irradiated with different doses of UV or γ irradiation. UV irradiation was performed by using a Stratalinker 2400 UV Crosslinker from Stratagene (La Jolla, California, USA). γ-irradiation was performed using a γ-irradiator at the Radiation Research Department at Risø National Laboratory (Roskilde, Denmark). After UV irradiation, plates were wrapped into aluminium foil to avoid repair by photolyase. All plates were incubated at 37°C for 2-3 days before being examined and photographed.

7.2.6 Gene targeting assay

The continuous substrate used for the gene targeting experiment was cut out of pRSub3 using *Bpm*I as described previously (Nielsen et al., 2006). Cutting with *Bpm*I generates a 7.1 kb fragment containing the *pyr4* gene flanked by two direct repeats of yA-*Kpn*I. This fragment was used to investigate gene targeting efficiency at the *yA* locus in the *radC*Δ strain.

7.2.7 Gap repair assay

To evaluate the gap-repair frequency, *radC* strain IBT 27266 and *radC*Δ strain IBT 28538, carrying a non-functional yA-*Kpn*I allele, were transformed with a gapped pYA-Icegap1 plasmid. This substrate was made by cutting a 900 bp fragment out of the yA-I-*Sce*I marker of pYA-Icegap1 using the restriction enzymes *Nhe*I and *Mfe*I. When the plasmid is repaired by HR using the genomic yA-*Kpn*I allele, a functional *yA* gene is reconstituted on the plasmid and the colonies obtained produce green conidia. In contrast, if the plasmid is repaired by NHEJ, no functional *yA* is produced and colonies obtained will have yellow conidia. After transformation, protoplasts were plated on minimal media supplemented with uracil and uridine and incubated for 2-3 days before observation. Gap repair efficiency was calculated as the total number of green colonies divided by the total number of yellow colonies obtained after transformation with the gapped fragment.

7.2.8 Analysis of the meiotic phenotype of the *radc*Δ strain

Meiosis was investigated by sexual crossing of *A. nidulans* strains. This was performed by plating 10^6 conidia of each parental strain in the central part (about 3.5 cm diameter) of a minimal media plate. In cases where the two parental strains had a common auxotrophy (for example, *argB2*), the minimal medium was supplemented accordingly. Ideally, none of the parental strain are able to grow on minimal media and a 0.5 cm^3 cube of solid complete media was therefore placed in the center of the plate to allow initial germination and growth. The high density of

germinating conidia promotes heterokaryon formation and conidiation. After 2-3 days incubation at 37°C , the plates were sealed with two layers of parafilm, wrapped in aluminium foil to induce meiosis and incubated for and additional 14 days. Plates were then examined for number and size of the cleistothecia formed. The ascospore content of the cleistothecia was determined visually using microscopy and viability was assessed by plating the spores on complete media.

7.3 Results

7.3.1 Sequence and cDNA analysis of the *radC* gene

The present annotation of the *A.nidulans radC* (AN4407.1) (Aspergillus Sequencing Project, Broad Institute of MIT and Harvard (http://www.broad.mit.edu)), describes an ORF of 2001 bp interrupted by 4 introns, encoding a protein of 582 amino acids. Interestingly, this is approximately 100-150 amino acid residues longer than for example *S. cerevisiae* or human Rad52 and this may prove to be significant for the functions of RadC. The predicted coding sequence based on conceptual translation of genomic DNA has previously been available online from NCBI (Accession: AY032591 & XM_656919). To confirm these predictions, mRNA was isolated from *A. nidulans* strain, IBT 26166, and sequenced by 5' and 3' RACE (rapid amplification of cDNA ends) (see Figure 7.1).

In order to locate the transcription start site of the *radC* mRNA transcript, five individual subcloned 5' cDNA fragments were sequenced. The five independent fragments started at four different points located within a 25 nucleotide region of the 5'. Thus, initiation of transcription is expected to occur between -93 and -67 bp of the start codon. Unexpectedly, the 5' sequencing revealed the presence of a novel 68 nucleotide intron not determined in previous conceptual translations. At first, it was thought that the intron was located in the 5' untranslated region of the transcript, but closer examination revealed that the intron interrupted a novel open reading frame (ORF), which was in frame with the conceptual translations and thus added 16 novel amino acid residues to RadC. Sequence comparison with *radC* homologs from several fungal strains showed that these 16 amino acid residues and the position of the intron are conserved. Sequencing of the 3' cDNA revealed that the final intron of *radC* is three nucleotides larger than previously annotated from conceptual translations, resulting in one aa less. The polyadenine splice signal, occurs 344 nucleotides downstream of the TAA stop codon.

7.3.2 The *radC* mutant is highly sensitive to MMS but not to IR

As mentioned earlier, deletion of *rad52* in *S.cerevisiae* results in mutants that are highly sensitive to ionizing radiation (Resnick, 1975;

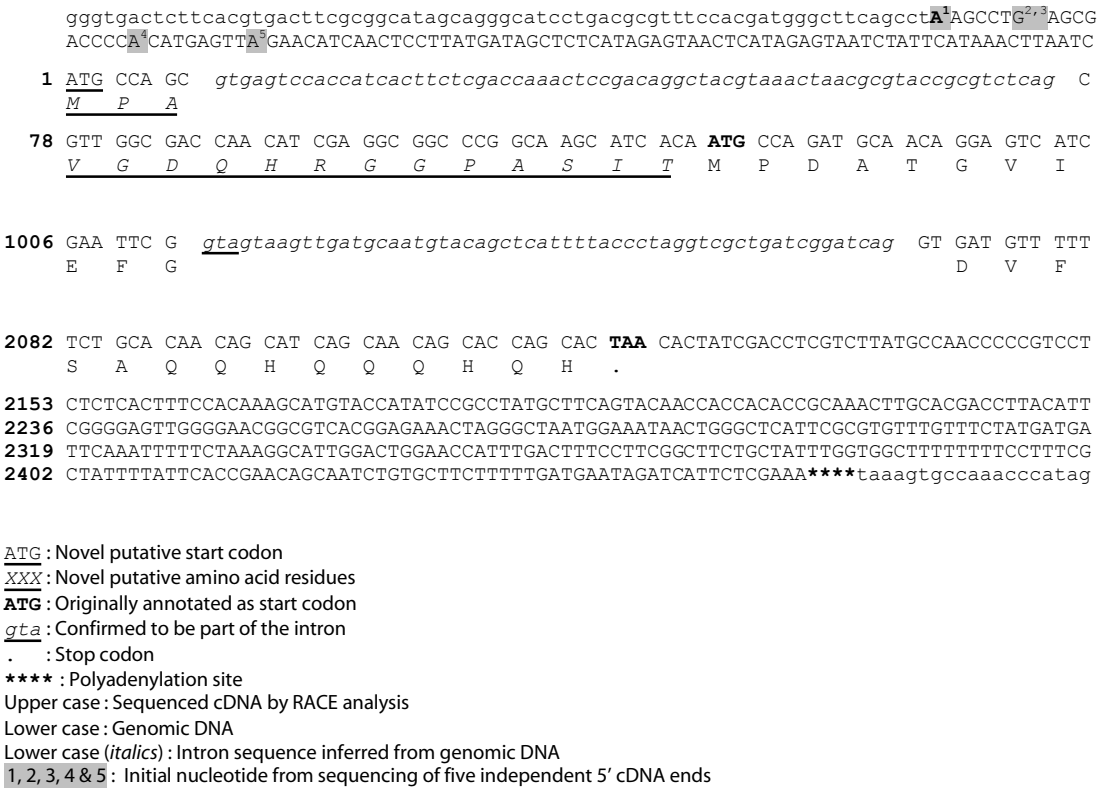

Figure 7.1. Results of the cDNA sequencing of *radC*.

Resnick & Martin, 1976). In contrast, this severe phenotype is not observed in *rad52* mammalian cells (Rijkers et al., 1998; Yamaguchi-Iwai et al., 1998). γ-irradiation is known to mainly kill cells by induction of DNA DSBs, but also causes a variety of DNA modifications such as clustered base-modifications, abasic sites, nicks, as well as DNA-DNA and DNA-protein crosslinks (Ward, 2000; Jenner et al., 2001; Bjelland & Seeberg, 2003; Cadet et al., 2004). The ability of the *A.nidulans radC*Δ mutant to survive such lesions was investigated by testing the sensitivity of the mutant to γ-irradiation by spot assay. For control and comparison, serial dilutions of *S. cerevisiae RAD52* wild-type and *rad52*Δ strains were also spotted. For each dose tested, the *A. nidulans* and the *S. cerevisiae* containing plates were irradiated together so that both types of cells would receive the same amount of irradiation. The results obtained are presented in Figure 7.2.

As expected the *S. cerevisiae rad52*Δ strain was extremely sensitive to IR while the wild-type strain was practically unaffected. In contrast to the *S. cerevisiae rad52*Δ strain, the *radC*Δ mutant strain was not highly sensitive to γ-irradiation. In fact, both *A. nidulans radC* and *radC*Δ strains were equally resistant showing that deletion of *radC* had no effect on strain survival after IR. These results suggest that the *A. nidulans* RadC is not involved in the repair of DNA DSBs in somatic cells, similar to what is observed for *rad52* mutants in mammalian cells.

As the *radC*Δ mutant was not sensitive to γ-ray induced DNA

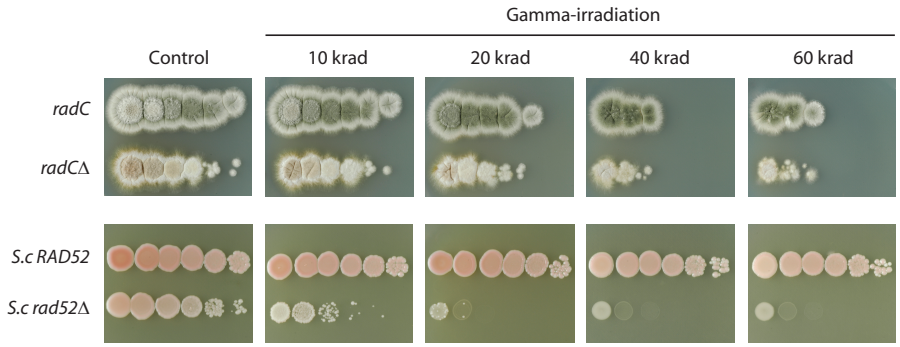

Figure 7.2. (Top panel) Survival spot assay of *radC*Δ mutant after different doses of γ-irradiation. (Bottom panel) Survival spot assay of *S. cerevisiae* wild-type and *rad52*Δ strains after the same doses of γ-irradiation showing the extreme sensitivity of the *rad52* mutant. *A. nidulans* spores and *S. cerevisiae* cells were plated on CM and YPD medium respectively.

DSBs, we then investigated the sensitivity of this mutant to other known genotoxins such as UV, MMS and HU. While UV induces pyrimidine dimers and photoproducts that are primarly repaired by Rad52-independent pathways (Sinha & Hader, 2002), MMS and HU have both been shown to induce lesions that can interfere with replication forks (Lundin et al., 2002; Michel et al., 2004; Lundin et al., 2005). The results obtained are presented in Figure 7.3 and show that the *radC* and *radC*Δ strains were equally resistant to UV irradiation although the *radC*Δ mutant seemed to be slightly more sensitive at high doses. Interestingly, a striking difference was observed between the two strains after treatment with MMS and HU. Indeed, survival of the *radC*Δ mutant strain was severely affected by both compounds while only a low level of sensitivity was observed in the *radC* strain. These results suggest that RadC has an important role in the repair of DNA lesions that involve the replication machinery.

7.3.3 Gene targeting and gap repair efficiencies are severely reduced in the *radC*Δ strain

In *S. cerevisiae*, Rad52 is essential for HR. To investigate whether the *A. nidulans* RadC protein is also involved in HR, a gene-targeting experiment was performed at the *A. nidulans yA* locus (AN6635.2) as described previously (Nielsen et al., 2006). *yA* was selected for this analysis as a strain with a dysfunctional *yA* gene develops yellow, instead of the usual green conidiospores (O'Hara & Timberlake, 1989), thus providing an easy way to score gene targeting events. The gene targeting substrate used for this experiment is the same as the plasmid-derived continuous substrate previously used by Nielsen et al. (2006) to introduce a *Kpn*I point mutation in *yA*. Here, we used the fragment containing ends homologous to the target site which has previously been shown to result in a gene-targeting efficiency of about 30% in the wild-type strain (Nielsen et al., 2006). In comparison, no yellow trans-

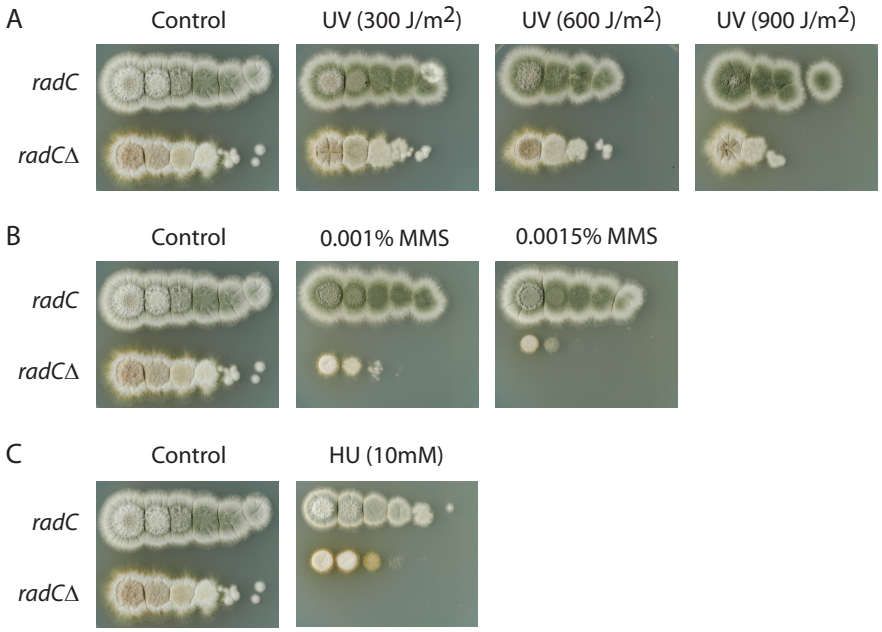

Figure 7.3. Survival spot assay of *radC*Δ mutant using different types of genotoxins: (A) UV irradiation, (B) MMS and (C) HU. *A. nidulans* spores were plated on CM medium.

formants were obtained when we transformed this substrate into the *radC*Δ strain, suggesting that gene targeting is impaired in this strain. We also investigated the ability of the *radC*Δ strain to repair a defined DNA DSB on a plasmid by HR. To do this, we used a gap-repair assay where a gapped plasmid can be re-circularized by HR with a genomic homologous target sequence or simple ligation by NHEJ. Again, the *A.nidulans yA* was used as a reporter as repair of the plasmid occurs by using the *yA* gene as donor. In agreement with the results obtained in the gene targeting experiment, the *radC*Δ strain was unable to repair the gapped plasmid by HR as no green transformants were ever obtained (see Table 7.2). In comparison, the *radC* strain was able to repair the gapped plasmid using HR with an efficiency of 0.6%. Although the repair efficiency of the *radC* strain is low, one would have expected to obtain about 7 ($1159 \times 0.6\%$) yellow *radC*Δ transformants if the repair efficiency in the *radC*Δ strain was identical to that of the *radC* strain. All in all, these results show that repair by HR is severely reduced, if not impaired, in the *radC*Δ strain and suggest that the RadC protein plays an important role in HR in *A. nidulans*.

7.3.4 Meiotic phenotype of the *radC*Δ mutant

In *S. cerevisiae* and most sexually reproducing eukaryotes, recombination is very frequent during meiosis where it ensures the correct pairing and segregation of homologous chromosomes during meiotic division I. Meiotic recombination is a well-regulated event of the meiotic cell cycle as it is initiated genome-wide by the specific formation of multiple

Table 7.2. Plasmid gap repair efficiency in the *A. nidulans radC*Δ strain

Trial	*radC*		*radC*Δ	
	yellow	green	yellow	green
1	245	1	97	0
2	170	1	62	0
3	550	15	240	0
4	2	0	123	0
5	3329	10	637	0
Total	4296	27	1159	0

DNA DSBs at chromosomal hot spots, a process involving the topoisomerase type II-like protein, Spo11 (for recent review see Keeney & Neale (2006)). In *S. cerevisiae*, *rad52* null strains are unable to repair these DSBs and are defective in meiosis (Krogh & Symington, 2004). This shows that ScRad52 has a key role in the repair of the Spo11-induced DNA DSBs by HR in budding yeast. Spo11 is widely conserved (Keeney & Neale, 2006) and *A. nidulans* also contains a Spo11 homolog (AN8259.1) (Goldman & Kafer, 2004). In this study, we show that the *radC*Δ mutant is not sensitive to γ-irradiation, suggesting that the many DNA DSBs induced are repaired through a RadC-independent pathway. As many DNA DSBs are produced during meiosis, we investigated if these lesions could also be repaired in the absence of RadC by studying the meiotic phenotype of the *radC*Δ mutant strain.

First, a self-mating sexual cross was set up using the *radC*Δ strain, IBT 28010. A similar cross using the reference strain IBT 27263 was set up as a control. Conidiospores were plated in the middle of a minimal media plate supplemented with uracil, uridine and arginine and the plate was processed as described in Materials and methods. For the *radC*Δ strain, the cleistothecia formed on the plates after 14 days of incubation in the dark were extremely small (more than 100 times smaller than what is normally observed) and contained no ascospores. Curiously, the cleistothecia produced with the reference strain were also small but these contained viable ascospores. From these results, we concluded that deletion of *radC* seemed to affect meiosis. However, an inherent problem of self-mating sexual crosses is that it is impossible to select for the formation of the nuclear fusion (homo-dikaryon), thus the appropriate starvation conditions supposed to promote meiosis are difficult to control experimentally. This may explain the unexpected low yield and small size of the cleistothecia produced in our self-mating experiments. To avoid this problem, we decided to investigate cleistothecia arising from a forced cross between two *radC*Δ strains (Figure 7.4).

To do this, we first introduced a new marker combination into the *radC*Δ background by crossing the *radC*Δ strain IBT 28010 to the *radC* strain, IBT 28540. This cross proceeded normally and the cleistothe-

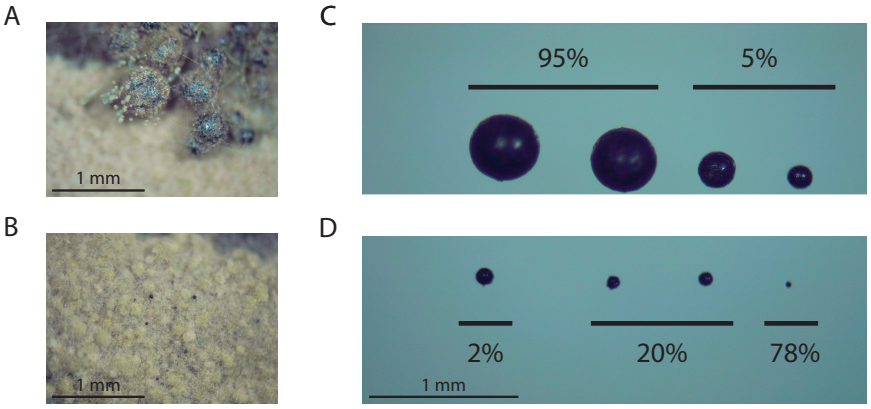

Figure 7.4. Effect of the deletion of *radC* on cleistothecia formation. (A) Cleistothecia from a forced cross between two *radC* strains. (B) Cleistothecia from a forced cross between two *radC*Δ strains. (C) Representation of the population of cleistothecia obtained from a forced cross between two *radC* strains. (D) Representation of the population of cleistothecia obtained from a forced cross between two *radC*Δ strains. Percentages for each type of cleistothecia are given.

cia were both normal in size and ascospore content. The ascospores from this cross were isolated and cultured and a haploid strain, IBT 28539, was obtained. This strain was subsequently crossed with the *radC*Δ strain IBT 28010, using the *pantoA10* and *pyrG89* markers to force the cross. Similarly to was observed for the self-mating cross, the cleistothecia that originated from the forced cross were very scarce and abnormally small (Figure 7.4). Furthermore, out of 30 cleistothecia examined, none contained ascospores. These results show that the deletion of *radC* has a severe effect on the formation of fruiting bodies and suggest that RadC is required in meiosis in a step prior to ascospore formation.

7.4 Discussion

Deletion of *RAD52* in *S. cerevisiae* and vertebrates results in cells with very different phenotypes going from extremely severe DNA DSB repair and HR defects in the budding yeast to only reduced HR in mammalian cells Symington (2002); Rijkers et al. (1998); Yamaguchi-Iwai et al. (1998). These results indicate that the role of Rad52 has changed during evolution and that functional homologs or proteins having overlapping functions with Rad52 have evolved. If this is true, investigating Rad52 functions in lower and higher eukaryotes, may give further insight into how the roles of Rad52 have changed with time. In this study, we have investigated the role of the *A. nidulans* homolog of *ScRAD52*, *radC*, in the repair of different types of induced DNA damage, in homologous recombination as well as in meiosis. We showed that, similarly to what has previously been observed in *S.cerevisiae rad52* null strains,

the *radC*Δ strain is highly sensitive to the DNA damaging agents MMS and HU but not to UV. Moreover, the *radC*Δ strain is defective in meiosis, as it fails to produces viable ascospores, and in HR, measured by its inability to perform gene targeting and plasmid gap repair. Interestingly, the *radC* deletion strain resembled the $RAD52^{-/-}$ mammalian cells in their ability to survive γ-irradiation, which suggests that RadC is not involved in the repair of γ-ray induced lesions.

7.4.1 *A. nidulans* RadC is not involved in the repair of γ-ray induced DNA DSBs

In this study, we show that the *radC*Δ mutant is not sensitive to γ-ray induced DNA damage. Several explanations are possible to account for this result. One hypothesis is that γ-ray induced DNA DSBs are not repaired via the HR pathway in *A.nidulans* as it is the case in *S. cerevisiae*. A second pathway known to be involved in DNA DSB repair in higher eukaryotes is the NHEJ pathway (for recent review see Burma et al. (2006)). Indeed, NHEJ has been shown to play an important role in the repair of DNA DSBs in vertebrates as cells defective in either Ku70 and Ku80, two of the key proteins in NHEJ, are sensitive to IR (Smider et al., 1994; Gu et al., 1997; Nussenzweig et al., 1997; Ouyang et al., 1997). Moreover, although HR is the pathway of choice for the repair of DNA DSBs in *S. cerevisiae*, work by Siede et al. (1996) showed that the NHEJ pathway is involved in the repair of some γ-ray induced DSBs in an HR-deficient background. To our knowledge, although Ku deletion strains have been constructed in several fungi (Kooistra et al., 2004; Ninomiya et al., 2004; Krappmann et al., 2006; Poggeler & Kuck, 2006; Takahashi et al., 2006), their sensitivity to IR has not be reported and it is therefore difficult to assess the role of NHEJ in repair of γ-ray induced DNA DSBs in these organisms. Most recently however, (Meyer et al., 2007) showed that the *A. niger kus*A mutant was 10 times more sensitive to γ-ray than wild-type strains. This suggests that γ-ray induced DNA lesions are mainly repaired by the NHEJ pathway in filamentous fungi. As this pathway is intact in the *radC*Δ mutant, this can explain why this strain is resistant to γ-irradiation.

A second hypothesis is that the repair of γ-ray induced DNA lesions does occur via HR in *A.nidulans*, but that the key proteins involved in this process are different from those of *S. cerevisiae*. Interestingly, this hypothesis has previously been proposed to explain why no severe phenotype was observed in $RAD52^{-/-}$ mammalian cells (Rijkers et al., 1998; Yamaguchi-Iwai et al., 1998). These results suggested that, in vertebrates, proteins having overlapping functions with Rad52 have evolved. Supporting this idea, a *rad52 xrcc3* DT40 chicken cell line was shown to be inviable while each of the single mutants can proliferate normally (Fujimori et al., 2001). These results suggest that XRCC3 may have overlapping functions with Rad52 and that both proteins can substitute for one another in HR. A clear advantage of evolving proteins with overlapping functions is the fact that mechanisms that

are important for the cell, such as HR, can be maintained in case the functions of one of these proteins is impaired. Accordingly, the existence of yet undescribed functional homologs of RadC in *A. nidulans* may explain that γ-ray induced DNA lesions can be repaired by HR in the absence of RadC.

Finally, one can postulate that *A. nidulans* RadC is involved in the repair of γ-ray induced DNA DSBs in a cell cycle-dependent or a cell type-dependent manner. Indeed, the conclusions drawn here are based on data from resting conidia and it has been shown that some discrepancy can be observe between data from resting and germinating conidia (Babudri et al., 1998). Moreover, studies in both chicken and mouse showed that HR and NHEJ are differentially involved in the repair of γ-ray induced DNA damage. Specifically, $MmRAD54^{-/-}$ deficient mice are hypersensitive to IR at the embryonic but not at the adult stage (Essers et al., 2000). Similarly, when DNA DSB repair was observed in γ-irradiated cells of the DT40 chicken B-cell line, NHEJ was the preferred repair pathway during G1-early S phase whereas HR took over in late S-G2 phase (Takata et al., 1998). HR has also been shown to be the DNA DSB repair pathway of choice during S-phase in human cells (Saleh-Gohari & Helleday, 2004). Based on these results, it appears that both HR and NHEJ are active DNA repair pathways in higher eukaryotes and have more specialized roles than what is observed in budding yeast where NHEJ is mostly only required when HR is defective. The fact that the *radC* deletion strain is not sensitive to γ-ray induced DNA DSBs may reflect that, at the conidial stage, NHEJ is the dominant repair pathway.

7.4.2 *A. nidulans* RadC is involved in HR

In this study, we showed that gene targeting and gap repair efficiencies were severely reduced in the *radC*Δ strain. Both these processes have been shown to be impaired in *S. cerevisiae rad52*Δ strains which suggests that integration of the gene targeting substrate and repair of the gapped plasmid occurs by Rad52-dependent HR. In fact, using a similar assay in *S. cerevisiae*, we have previously shown that a gapped plasmid was always repaired by HR in *RAD52* strains but predominantly repaired by NHEJ in *rad52*Δ strains (Lettier et al., 2006). In the assay used in this study, the high number of yellow colonies recovered suggests that repair of the gapped plasmid occurs primarily by NHEJ in the wild-type *radC* strain. Indeed, less than 1% of the transformants obtained with this strain were green thus contained a plasmid that had been repaired by HR. Nevertheless, in the *rad52*Δ, no green transformants were obtained and together with the fact that no recombinants were obtained in the gene targeting experiment in this strain either, we conclude that HR is severely reduced if not impaired in the absence of RadC in *A. nidulans*. Accordingly, similar to the role of Rad52 in *S. cerevisiae*, RadC appears to have a key role in HR in *A. nidulans*.

7.4.3 *A. nidulans* RadC is required after replication arrest

Our results show that the *radC*Δ strain is hypersensitive to both MMS and HU which suggests a direct role of RadC in the repair of the lesions induced by these two genotoxins. At first glance, these results can seem in contradiction with the fact that RadC does not appear to be involved in the repair of DNA DSBs. Indeed, MMS has been used for many years as an IR mimetic agent and HU has been shown to induce replication arrest and to generate the formation of DNA DSBs at newly replicated DNA (Lundin et al., 2002). However, recent data obtained after the treatment of mammalian cells with MMS and HU have given new insight into the mode of action of these chemicals.

MMS is an alkylating agent that has been shown to induce randomly distributed heat-labile DNA lesions in vivo (Lundin et al., 2005). Although this compound does not create DNA DSBs, both HR-deficient *S. cerevisiae* and mammalian cells have been shown to be hypersensitive to MMS treatment (Symington, 2002; Lundin et al., 2005). One possible explanation for this is that stalled replication forks formed at alkylated sites trigger the formation of lesions that require HR to be repaired (Michel et al., 2004). HU has been shown to inhibit DNA replication by blocking DNA synthesis and preventing the dNTP pool expansion normally occurring at G1/S (Koc et al., 2004). Hence, HU treatment leads to stalled replication fork and has been shown to induce the formation of DNA DSBs at newly replicated DNA in mammalian cells (Lundin et al., 2002). As for MMS, both HR-deficient *S. cerevisiae* and mammalian cells have been shown to be hypersensitive to HU treatment (Symington, 2002; Lundin et al., 2002). In a study of DNA repair after replication arrest, Lundin et al. (2002) showed that both HR and non homologous end-joining (NHEJ) were required for survival after HU treatment. In the same study, cells were treated with thymidine which only slows down the replication fork but does not induce DNA DSB formation. Interestingly, only HR was required to survive thymidine treatment suggesting that NHEJ is only involved in DNA repair at stalled replication forks in the presence of DNA DSBs. Accordingly, other types of lesions or substrates produced at stalled replication forks were triggering the need for HR.

Altogether these results suggest that DNA DSBs are not the cause of death of HR-deficient cells after MMS or HU treatment. For this reason, the fact that the *radC* deletion strain is sensitive to MMS and HU but not to γ-irradiation is not contradictory. A common characteristic of MMS and HU is that they both promote replication fork arrest. Several models have been proposed to explain what takes place at stalled replication fork and suggest the formation of DNA structures, e.g. chicken foot structures, including Holliday junctions (Postow et al., 2001; McGlynn & Lloyd, 2001; Sogo et al., 2002; Michel et al., 2004) which potentially require the HR pathway to be repaired. Supporting this view are results obtained in prokaryotes in which replication

restart is extensively studied. Several studies suggest that the recombination machinery is crucial in the reactivation of stalled replication forks as it enables the repair or bypass of blocking lesions in an error-free way (for recent review see Heller & Marians (2006)). One example is the recombination-dependent replication (RDR) pathway where recombination is believed to generate DNA structures, such as D-loops, onto which the PriA helicase can reload the replication machinery thus re-starting replication (Liu et al., 1999; Liu & Marians, 1999; Xu & Marians, 2003). Accordingly, the fact that deletion of *radC* induced high sensitivity to both HU and MMS suggests that the *A. nidulans* RadC is involve in the repair of lesions at stalled replication forks. Keeping this in mind, one can argue that the *radC*Δ strain does not seem sensitive to UV-irradiation although it has been shown to induce lesions that distort the DNA helix and inhibit the progression of the DNA and RNA polymerases thus interfering with replication and transcription (Sinha & Hader, 2002). One explanation for this is that UV lesions are mainly repaired in a RadC-independent manner. Indeed, in *S. cerevisiae*, UV lesions are mainly repaired by the nucleotide excision repair (NER) pathway which does not involve Rad52 (Prakash & Prakash, 2000).

All in all, our results suggest that RadC plays an important role in the repair of lesions that induce replication fork arrest in *A. nidulans*. This most probably reflects the need for RadC-dependent HR in the process of replication fork restart.

7.5 Concluding remarks

In this study we have presented an initial characterization of a deletion strain of the *Aspergillus nidulans radC*, a homolog of the double-strand break repair gene *RAD52*. We find that the *radC*Δ strain is resistant to γ-ray induced DNA damage, suggesting that RadC is not involved in the repair of DNA DSB in mitotic cells. Interestingly, this is similar to what is observed in *RAD52*$^{-/-}$ in higher eukaryotes. Furthermore, we show that the *radC*Δ is highly sensitive to MMS and HU, suggesting the involvement of RadC in the repair of replication-related DNA lesions by HR. Supporting the view that RadC is important for HR in *A. nidulans*, we show that the *radC*Δ is deficient in gene targeting and plasmid gap repair. Lastly, analysis of meiotic crosses of *radC*Δ strains show that such crosses are sterile, suggesting an essential role of RadC in meiosis in *A. nidulans*. Interestingly, both the A. nidulans HR and meiotic phenotypes resemble the phenotypes observed in *rad52*Δ *S. cerevisiae* strains. In conclusion, the phenotype of this deletion strain appears to be intermediate between that of yeast and that of human cells and we propose that *A. nidulans* may serve as an interesting model system to investigate how new repair pathways have developed in higher eukaryotes.

Bibliography

Aboussekhra, A., Chanet, R., Adjiri, A. & Fabre, F. (1992). Semidominant suppressors of srs2 helicase mutations of saccharomyces cerevisiae map in the rad51 gene, whose sequence predicts a protein with similarities to procaryotic reca proteins, *Mol Cell Biol* **12**: 3224–3234.

Aboussekhra, A., Chanet, R., Zgaga, Z., Cassier-Chauvat, C., Heude, M. & Fabre, F. (1989). Radh, a gene of saccharomyces cerevisiae encoding a putative dna helicase involved in dna repair. characteristics of radh mutants and sequence of the gene, *Nucleic Acids Res* **17**: 7211–7219.

Adams, T., Wieser, J. & Yu, J. (1998). Asexual sporulation in aspergillus nidulans, *Microbiol Mol Biol Rev* **62**: 35–54.

Adzuma, K. (1992). Stable synapsis of homologous dna molecules mediated by the escherichia coli reca protein involves local exchange of dna strands, *Genes Dev* **6**: 1679–1694.

Adzuma, K. (1998). No sliding during homology search by reca protein, *J Biol Chem* **273**: 31565–31573.

Adzuma, K., Ogawa, T. & Ogawa, H. (1984). Primary structure of the rad52 gene in saccharomyces cerevisiae, *Mol Cell Biol* **4**: 2735–2744.

Aguilera, A. & Klein, H. (1988). Genetic control of intrachromosomal recombination in saccharomyces cerevisiae. i. isolation and genetic characterization of hyper-recombination mutations, *Genetics* **119**: 779–790.

Aguilera, A. & Klein, H. (1989). Yeast intrachromosomal recombination: long gene conversion tracts are preferentially associated with reciprocal exchange and require the rad1 and rad3 gene products, *Genetics* **123**: 683–694.

Aihara, H., Ito, Y., Kurumizaka, H., Yokoyama, S. & Shibata, T. (1999). The n-terminal domain of the human rad51 protein binds dna: structure and a dna binding surface as revealed by nmr, *J Mol Biol* **290**: 495–504.

Ajimura, M., Leem, S. & Ogawa, H. (1993). Identification of new genes required for meiotic recombination in saccharomyces cerevisiae, *Genetics* **133**: 51–66.

Alani, E., Padmore, R. & Kleckner, N. (1990). Analysis of wild-type and rad50 mutants of yeast suggests an intimate relationship between meiotic chromosome synapsis and recombination, *Cell* **61**: 419–436.

Alani, E., Subbiah, S. & Kleckner, N. (1989). The yeast rad50 gene encodes a predicted 153-kd protein containing a purine nucleotide-binding domain and two large heptad-repeat regions, *Genetics* **122**: 47–57.

Aleksenko, A. & Ivanova, L. (1998). In vivo linearization and autonomous replication of plasmids containing human telomeric dna in aspergillus nidulans, *Mol Gen Genet* **260**: 159–164.

Alexeev, A., Mazin, A. & Kowalczykowski, S. (2003). Rad54 protein possesses chromatin-remodeling activity stimulated by the rad51-ssdna nucleoprotein filament, *Nat Struct Biol* **10**: 182–186.

Allers, T. & Lichten, M. (2001). Intermediates of yeast meiotic recombination contain heteroduplex dna, *Mol.* **8**: 225–231.

Anderson, D., Trujillo, K., Sung, P. & Erickson, H. (2001). Structure of the rad50 x mre11 dna repair complex from saccharomyces cerevisiae by electron microscopy, *J Biol Chem* **276**: 37027–37033.

Antunez de Mayolo, A., Lisby, M., Erdeniz, N., Thybo, T., Mortensen, U. & Rothstein, R. (2006). Multiple start codons and phosphorylation result in discrete rad52 protein species, *Nucleic Acids Res* **34**: 2587–2597.

Arai, N., Ito, D., Inoue, T., Shibata, T. & Takahashi, H. (2005). Heteroduplex joint formation by a stoichiometric complex of rad51 and rad52 of saccharomyces cerevisiae, *J Biol Chem* **280**: 32218–32229.

Asleson, E., Okagaki, R. & Livingston, D. (1999). A core activity associated with the n terminus of the yeast rad52 protein is revealed by rad51 overexpression suppression of c-terminal rad52 truncation alleles, *Genetics* **153**: 681–692.

Aylon, Y., Liefshitz, B., Bitan-Banin, G. & Kupiec, M. (2003). Molecular dissection of mitotic recombination in the yeast saccharomyces cerevisiae, *Mol. Cell Biol.* **23**: 1403–1417.

Babudri, N., Marini, A., Matmati, N. & Morpurgo, G. (1998). The uvsc and uvse genes of aspergillus nidulans are not required for the mutagenic repair of uv damage, *Mol Gen Genet* **259**: 130–132.

Bai, Y., Davis, A. & Symington, L. (1999). A novel allele of rad52 that causes severe dna repair and recombination deficiencies only in the absence of rad51 or rad59, *Genetics* **153**: 1117–1130.

Bai, Y. & Symington, L. (1996). A rad52 homolog is required for rad51-independent mitotic recombination in saccharomyces cerevisiae, *Genes Dev.* **10**: 2025–2037.

Bailly, V., Lamb, J., Sung, P., Prakash, S. & Prakash, L. (1994). Specific complex formation between yeast rad6 and rad18 proteins: a potential mechanism for targeting rad6 ubiquitin-conjugating activity to dna damage sites, *Genes Dev* **8**: 811–820.

Bailly, V., Lauder, S., Prakash, S. & Prakash, L. (1997). Yeast dna repair proteins rad6 and rad18 form a heterodimer that has ubiquitin conjugating, dna binding, and atp hydrolytic activities, *J Biol Chem* **272**: 23360–23365.

Basile, G., Aker, M. & Mortimer, R. (1992). Nucleotide sequence and transcriptional regulation of the yeast recombinational repair gene rad51, *Mol Cell Biol* **12**: 3235–3246.

Bendixen, C., Gangloff, S. & Rothstein, R. (1994). A yeast mating-selection scheme for detection of protein-protein interactions, *Nucleic Acids Res* **22**: 1778–1779.

Benson, F., Baumann, P. & West, S. (1998). Synergistic actions of rad51 and rad52 in recombination and dna repair, *Nature* **391**: 401–404.

Beranek, D. (1990). Distribution of methyl and ethyl adducts following alkylation with monofunctional alkylating agents, *Mutat Res* **231**: 11–30.

Bezzubova, O., Schmidt, H., Ostermann, K., Heyer, W. & Buerstedde, J. (1993). Identification of a chicken rad52 homologue suggests conservation of the rad52 recombination pathway throughout the evolution of higher eukaryotes, *Nucleic Acids Res* **21**: 5945–5949.

Bi, B., Rybalchenko, N., Golub, E. & Radding, C. (2004). Human and yeast rad52 proteins promote dna strand exchange, *Proc Natl Acad Sci U S A* **101**: 9568–9572.

Bignami, M., Aulicino, F., Velcich, A., Carere, A. & Morpurgo, G. (1977). Mutagenic and recombinogenic action of pesticides in aspergillus nidulans, *Mutat Res* **46**: 395–402.

Bird, D. & Bradshaw, R. (1997). Gene targeting is locus dependent in the filamentous fungus aspergillus nidulans, *Mol Gen Genet* **255**: 219–225.

Bjelland, S. & Seeberg, E. (2003). Mutagenicity, toxicity and repair of dna base damage induced by oxidation, *Mutat Res* **531**: 37–80.

Boiteux, S. & Guillet, M. (2004). Abasic sites in dna: repair and biological consequences in saccharomyces cerevisiae, *DNA Repair (Amst)* **3**: 1–12.

Bosco, G. & Haber, J. (1998). Chromosome break-induced dna replication leads to nonreciprocal translocations and telomere capture, *Genetics* **150**: 1037–1047.

Boundy-Mills, K. & Livingston, D. (1993). A saccharomyces cerevisiae rad52 allele expressing a c-terminal truncation protein: activities and intragenic complementation of missense mutations, *Genetics* **133**: 39–49.

Bressan, D., Baxter, B. & Petrini, J. (1999). The mre11-rad50-xrs2 protein complex facilitates homologous recombination-based double-strand break repair in saccharomyces cerevisiae, *Mol. Cell Biol.* **19**: 7681–7687.

Brill, S. & Stillman, B. (1991). Replication factor-a from saccharomyces cerevisiae is encoded by three essential genes coordinately expressed at s phase, *Genes Dev* **5**: 1589–1600.

Burma, S., Chen, B. & Chen, D. (2006). Role of non-homologous end joining (nhej) in maintaining genomic integrity, *DNA Repair (Amst)* **5**: 1042–1048.

Cadet, J., Bellon, S., Douki, T., Frelon, S., Gasparutto, D., Muller, E., Pouget, J., Ravanat, J., Romieu, A. & Sauvaigo, S. (2004). Radiation-induced dna damage: formation, measurement, and biochemical features, *J Environ Pathol Toxicol Oncol* **23**: 33–43.

Cai, L., Marquardt, U., Zhang, Z., Taisey, M. & Chen, J. (2001). Topological testing of the mechanism of homology search promoted by reca protein, *Nucleic Acids Res* **29**: 1389–1398.

Campbell, D. & Fogel, S. (1977). Association of chromosome loss with centromere-adjacent mitotic recombination in a yeast disomic haploid, *Genetics* **85**: 573–585.

Campbell, D., Fogel, S. & Lusnak, K. (1975). Mitotic chromosome loss in a disomic haploid of saccharomyces cerevisiae, *Genetics* **79**: 383–396.

Champe, S., Rao, P. & Chang, A. (1987). An endogenous inducer of sexual development in aspergillus nidulans, *J Gen Microbiol* **133**: 1383–1387.

Chaveroche, M., Ghigo, J. & d'Enfert, C. (2000). A rapid method for efficient gene replacement in the filamentous fungus aspergillus nidulans, *Nucleic Acids Res.* **28**: E97.

Chen, L., Trujillo, K., Ramos, W., Sung, P. & Tomkinson, A. (2001). Promotion of dnl4-catalyzed dna end-joining by the rad50/mre11/xrs2 and hdf1/hdf2 complexes, *Mol Cell* **8**: 1105–1115.

Clutterbuck, A. (1974). *Handbook of Genetics*, Plenum Press, pp. 447–510.

Conway, A., Lynch, T., Zhang, Y., Fortin, G., Fung, C., Symington, L. & Rice, P. (2004). Crystal structure of a rad51 filament, *Nat Struct Mol Biol* **11**: 791–796.

Cortes-Ledesma, F., Malagon, F. & Aguilera, A. (2004). A novel yeast mutation, rad52-l89f, causes a specific defect in rad51-independent recombination that correlates with a reduced ability of rad52-l89f to interact with rad59, *Genetics* **168**: 553–557.

Cunningham, R., Shibata, T., DasGupta, C. & Radding, C. (1979). Single strands induce reca protein to unwind duplex dna for homologous pairing, *Nature* **281**: 191–195.

Davis, A. & Symington, L. (2001). The yeast recombinational repair protein rad59 interacts with rad52 and stimulates single-strand annealing, *Genetics* **159**: 515–525.

Davis, A. & Symington, L. (2003). The rad52-rad59 complex interacts with rad51 and replication protein a, *DNA Repair (Amst)* **2**: 1127–1134.

Davis, A. & Symington, L. (2004). Rad51-dependent break-induced replication in yeast, *Mol. Cell Biol.* **24**: 2344–2351.

de Jager, M., van Noort, J., van Gent, D., Dekker, C., Kanaar, R. & Wyman, C. (2001). Human rad50/mre11 is a flexible complex that can tether dna ends, *Mol Cell* **8**: 1129–1135.

De Zutter, J. & Knight, K. (1999). The hrad51 and reca proteins show significant differences in cooperative binding to single-stranded dna, *J Mol Biol* **293**: 769–780.

Di Primio, C., Galli, A., Cervelli, T., Zoppe, M. & Rainaldi, G. (2005). Potentiation of gene targeting in human cells by expression of saccharomyces cerevisiae rad52, *Nucleic Acids Res* **33**: 4639–4648.

Dianov, G., O'Neill, P. & Goodhead, D. (2001). Securing genome stability by orchestrating dna repair: removal of radiation-induced clustered lesions in dna, *Bioessays* **23**: 745–749.

Doe, C., Osman, F., Dixon, J. & Whitby, M. (2004). Dna repair by a rad22-mus81-dependent pathway that is independent of rhp51, *Nucleic Acids Res.* **32**: 5570–5581.

Dominguez-Bendala, J., Masutani, M. & McWhir, J. (2006). Down-regulation of parp-1, but not of ku80 or dna-pkcs', results in higher gene targeting efficiency, *Cell Biol Int* **30**: 389–393.

Dyer, P., Paoletti, M. & Archer, D. (2003). Genomics reveals sexual secrets of aspergillus, *Microbiology* **149**: 2301–2303.

Ellouze, C., Norden, B. & Takahashi, M. (1997). Dissociation of non-complementary second dna from reca filament without atp hydrolysis: mechanism of search for homologous dna, *J Biochem (Tokyo)* **121**: 1070–1075.

Erdeniz, N., Mortensen, U. & Rothstein, R. (1997). Cloning-free pcr-based allele replacement methods, *Genome Res* **7**: 1174–1183.

Esposito, M. (1978). Evidence that spontaneous mitotic recombination occurs at the two-strand stage, *Proc Natl Acad Sci U S A* **75**: 4436–4440.

Essers, J., van Steeg, H., de Wit, J., Swagemakers, S., Vermeij, M., Hoeijmakers, J. & Kanaar, R. (2000). Homologous and non-homologous recombination differentially affect dna damage repair in mice, *EMBO J* **19**: 1703–1710.

Fabre, F., Chan, A., Heyer, W. & Gangloff, S. (2002). Alternate pathways involving sgs1/top3, mus81/ mms4, and srs2 prevent formation of toxic recombination intermediates from single-stranded gaps created by dna replication, *Proc. Natl. Acad. Sci. U. S.* **99**: 16887–16892.

Fan, H., Cheng, K. & Klein, H. (1996). Mutations in the rna polymerase ii transcription machinery suppress the hyperrecombination mutant hpr1 delta of saccharomyces cerevisiae, *Genetics* **142**: 749–759.

Feldmann, E., Schmiemann, V., Goedecke, W., Reichenberger, S. & Pfeiffer, P. (2000). Dna double-strand break repair in cell-free extracts from ku80-deficient cells: implications for ku serving as an alignment factor in non-homologous dna end joining, *Nucleic Acids Res* **28**: 2585–2596.

Feng, Q., During, L., Antunez de Mayolo, A., Lettier, G., Lisby, M., Erdeniz, N., Mortensen, U. & Rothstein, R. (2007). Rad52 and rad59 exhibit both overlapping and distinct functions, *DNA Repair (Amst)* **6**: 27–37.

Fiorentini, P., Huang, K., Tishkoff, D., Kolodner, R. & Symington, L. (1997). Exonuclease i of saccharomyces cerevisiae functions in mitotic recombination in vivo and in vitro, *Mol Cell Biol* **17**: 2764–2773.

Fishman-Lobell, J., Rudin, N. & Haber, J. (1992). Two alternative pathways of double-strand break repair that are kinetically separable and independently modulated, *Mol Cell Biol* **12**: 1292–1303.

Flygare, J., Falt, S., Ottervald, J., Castro, J., Hellgren, D. & Wennborg, A. (2001). Effects of hsrad51 overexpression on cell proliferation, cell cycle progression, and apoptosis, *Exp Cell Res* **268**: 61–69.

Fogel, S. & Mortimer, R. (1969). Informational transfer in meiotic gene conversion, *Proc Natl Acad Sci U S A* **62**: 96–103.

Forment, J., Ramon, D. & Maccabe, A. (2006). Consecutive gene deletions in aspergillus nidulans: application of the cre/loxp system, *Curr Genet* **50**: 217–224.

Fortin, G. & Symington, L. (2002). Mutations in yeast rad51 that partially bypass the requirement for rad55 and rad57 in dna repair by increasing the stability of rad51-dna complexes, *EMBO J* **21**: 3160–3170.

Fujimori, A., Tachiiri, S., Sonoda, E., Thompson, L., Dhar, P., Hiraoka, M., Takeda, S., Zhang, Y., Reth, M. & Takata, M. (2001). Rad52 partially substitutes for the rad51 paralog xrcc3 in maintaining chromosomal integrity in vertebrate cells, *EMBO J* **20**: 5513–5520.

Furuse, M., Nagase, Y., Tsubouchi, H., Murakami-Murofushi, K., Shibata, T. & Ohta, K. (1998). Distinct roles of two separable in vitro activities of yeast mre11 in mitotic and meiotic recombination, *EMBO J* **17**: 6412–6425.

Galagan, J., Calvo, S., Cuomo, C., Ma, L., Wortman, J., Batzoglou, S., Lee, S., Basturkmen, M., Spevak, C., Clutterbuck, J., Kapitonov, V., Jurka, J., Scazzocchio, C. & Farman, M. (2005). Sequencing of aspergillus nidulans and comparative analysis with a. fumigatus and a. oryzae, *Nature* **438**: 1105–1115.

Game, J. & Mortimer, R. (1974). A genetic study of x-ray sensitive mutants in yeast, *Mutat Res* **24**: 281–292.

Gangloff, S., Soustelle, C. & Fabre, F. (2000). Homologous recombination is responsible for cell death in the absence of the sgs1 and srs2 helicases, *Nat Genet* **25**: 192–194.

Gasior, S., Wong, A., Kora, Y., Shinohara, A. & Bishop, D. (1998). Rad52 associates with rpa and functions with rad55 and rad57 to assemble meiotic recombination complexes, *Genes Dev* **12**: 2208–2221.

Godar, D. (2005). Uv doses worldwide, *Photochem Photobiol* **81**: 736–749.

Goedecke, W., Eijpe, M., Offenberg, H., van Aalderen, M. & Heyting, C. (1999). Mre11 and ku70 interact in somatic cells, but are differentially expressed in early meiosis, *Nat Genet* **23**: 194–198.

Goldman, G. & Kafer, E. (2004). Aspergillus nidulans as a model system to characterize the dna damage response in eukaryotes, *Fungal Genet Biol* **41**: 428–442.

Golin, J. & Esposito, M. (1984). Coincident gene conversion during mitosis in saccharomyces, *Genetics* **107**: 355–365.

Goodman, M. (2002). Error-prone repair dna polymerases in prokaryotes and eukaryotes, *Annu Rev Biochem* **71**: 17–50.

Gu, Y., Jin, S., Gao, Y., Weaver, D. & Alt, F. (1997). Ku70-deficient embryonic stem cells have increased ionizing radiosensitivity, defective dna end-binding activity, and inability to support v(d)j recombination, *Proc Natl Acad Sci U S A* **94**: 8076–8081.

Haber, J. & Hearn, M. (1985). Rad52-independent mitotic gene conversion in saccharomyces cerevisiae frequently results in chromosomal loss, *Genetics* **111**: 7–22.

Haber, J., Ira, G., Malkova, A. & Sugawara, N. (2004). Repairing a double-strand chromosome break by homologous recombination: revisiting robin holliday's model, *Philos Trans R Soc Lond B Biol Sci* **359**: 79–86.

Halliwell, B. (2007). Oxidative stress and cancer: have we moved forward?, *Biochem J* **401**: 1–11.

Harlow, E. & Lane, D. (1988). *Antibodies: A Laboratory Manual*, Cold Spring Harbor: Cold Spring Harbor Laboratory.

Hastings, P., McGill, C., Shafer, B. & Strathern, J. (1993). Ends-in vs. ends-out recombination in yeast, *Genetics* **135**: 973–980.

Hays, S., Firmenich, A. & Berg, P. (1995). Complex formation in yeast double-strand break repair: participation of rad51, rad52, rad55, and rad57 proteins, *Proc Natl Acad Sci U S A* **92**: 6925–6929.

Hays, S., Firmenich, A., Massey, P., Banerjee, R. & Berg, P. (1998). Studies of the interaction between rad52 protein and the yeast single-stranded dna binding protein rpa, *Mol Cell Biol* **18**: 4400–4406.

Hefferin, M. & Tomkinson, A. (2005). Mechanism of dna double-strand break repair by non-homologous end joining, *DNA Repair (Amst)* **4**: 639–648.

Heller, R. & Marians, K. (2006). Replisome assembly and the direct restart of stalled replication forks, *Nat Rev Mol Cell Biol* **7**: 932–943.

Heyer, W., Rao, M., Erdile, L., Kelly, T. & Kolodner, R. (1990). An essential saccharomyces cerevisiae single-stranded dna binding protein is homologous to the large subunit of human rp-a, *EMBO J* **9**: 2321–2329.

Hickson, I. (2003). Recq helicases: caretakers of the genome, *Nat Rev Cancer* **3**: 169–178.

Hoffmann, B., Eckert, S., Krappmann, S. & Braus, G. (2001). Sexual diploids of aspergillus nidulans do not form by random fusion of nuclei in the heterokaryon, *Genetics* **157**: 141–147.

Holliday, R. (1964). A mechanism for gene conversion in fungi, *Genet. Res.* **5**: 282–304.

Honigberg, S., Rao, B. & Radding, C. (1986). Ability of reca protein to promote a search for rare sequences in duplex dna, *Proc Natl Acad Sci U S A* **83**: 9586–9590.

Hopfner, K., Craig, L., Moncalian, G., Zinkel, R., Usui, T., Owen, B., Karcher, A., Henderson, B., Bodmer, J., McMurray, C., Carney, J., Petrini, J. & Tainer, J. (2002). The rad50 zinc-hook is a structure joining mre11 complexes in dna recombination and repair, *Nature* **418**: 562–566.

Hopfner, K., Karcher, A., Craig, L., Woo, T., Carney, J. & Tainer, J. (2001). Structural biochemistry and interaction architecture of the dna double-strand break repair mre11 nuclease and rad50-atpase, *Cell* **105**: 473–485.

Hsieh, P., Camerini-Otero, C. & Camerini-Otero, R. (1990). Pairing of homologous dna sequences by proteins: evidence for three-stranded dna, *Genes Dev* **4**: 1951–1963.

Hurst, D., Fogel, S. & Mortimer, R. (1972). Conversion-associated recombination in yeast (hybrids-meiosis-tetrads-marker loci-models), *Proc Natl Acad Sci U S A* **69**: 101–105.

Ichioka, D., Itoh, T. & Itoh, Y. (2001). An aspergillus nidulans uvsc null mutant is deficient in homologous dna integration, *Mol Gen Genet* **264**: 709–715.

Ira, G. & Haber, J. (2002). Characterization of rad51-independent break-induced replication that acts preferentially with short homologous sequences, *Mol Cell Biol* **22**: 6384–6392.

Ira, G., Malkova, A., Liberi, G., Foiani, M. & Haber, J. (2003). Srs2 and sgs1-top3 suppress crossovers during double-strand break repair in yeast, *Cell* **115**: 401–411.

Ira, G., Satory, D. & Haber, J. (2006). Conservative inheritance of newly synthesized dna in double-strand break-induced gene conversion, *Mol Cell Biol* **26**: 9424–9429.

Ivanov, E. & Haber, J. (1995). Rad1 and rad10, but not other excision repair genes, are required for double-strand break-induced recombination in saccharomyces cerevisiae, *Mol Cell Biol* **15**: 2245–2251.

Ivanov, E., Korolev, V. & Fabre, F. (1992). Xrs2, a dna repair gene of saccharomyces cerevisiae, is needed for meiotic recombination, *Genetics* **132**: 651–664.

Ivanov, E., Sugawara, N., White, C., Fabre, F. & Haber, J. (1994). Mutations in xrs2 and rad50 delay but do not prevent mating-type switching in saccharomyces cerevisiae, *Mol Cell Biol* **14**: 3414–3425.

Jasin, M. (2002). Homologous repair of dna damage and tumorigenesis: the brca connection, *Oncogene* **21**: 8981–8993.

Jenner, T., Fulford, J. & O'Neill, P. (2001). Contribution of base lesions to radiation-induced clustered dna damage: implication for models of radiation response, *Radiat Res* **156**: 590–593.

Jiang, H., Xie, Y., Houston, P., Stemke-Hale, K., Mortensen, U., Rothstein, R. & Kodadek, T. (1996). Direct association between the yeast rad51 and rad54 recombination proteins, *J. Biol. Chem.* **271**: 33181–33186.

Johnson, R. & Symington, L. (1995). Functional differences and interactions among the putative reca homologs rad51, rad55, and rad57, *Mol Cell Biol* **15**: 4843–4850.

Johnstone, I., Hughes, S. & Clutterbuck, A. (1985). Cloning an aspergillus nidulans developmental gene by transformation, *EMBO J* **4**: 1307–1311.

Johzuka, K. & Ogawa, H. (1995). Interaction of mre11 and rad50: two proteins required for dna repair and meiosis-specific double-strand break formation in saccharomyces cerevisiae, *Genetics* **139**: 1521–1532.

Kadyrov, F., Dzantiev, L., Constantin, N. & Modrich, P. (2006). Endonucleolytic function of mutlalpha in human mismatch repair, *Cell* **126**: 297–308.

Kagawa, W., Kurumizaka, H., Ikawa, S., Yokoyama, S. & Shibata, T. (2001). Homologous pairing promoted by the human rad52 protein, *J Biol Chem* **276**: 35201–35208.

Kagawa, W., Kurumizaka, H., Ishitani, R., Fukai, S., Nureki, O., Shibata, T. & Yokoyama, S. (2002). Crystal structure of the homologous-pairing domain from the human rad52 recombinase in the undecameric form, *Mol.* **10**: 359–371.

Kasai, H. & Nishimura, S. (1984). Hydroxylation of deoxyguanosine at the c-8 position by ascorbic acid and other reducing agents, *Nucleic Acids Res* **12**: 2137–2145.

Kaytor, M. & Livingston, D. (1994). Saccharomyces cerevisiae rad52 alleles temperature-sensitive for the repair of dna double-strand breaks, *Genetics* **137**: 933–944.

Kaytor, M., Nguyen, M. & Livingston, D. (1995). The complexity of the interaction between rad52 and srs2, *Genetics* **140**: 1441–1442.

Keeney, S., Giroux, C. & Kleckner, N. (1997). Meiosis-specific dna double-strand breaks are catalyzed by spo11, a member of a widely conserved protein family, *Cell* **88**: 375–384.

Keeney, S. & Neale, M. (2006). Initiation of meiotic recombination by formation of dna double-strand breaks: mechanism and regulation, *Biochem Soc Trans* **34**: 523–525.

Kennedy, R. & D'Andrea, A. (2005). The fanconi anemia/brca pathway: new faces in the crowd, *Genes Dev* **19**: 2925–2940.

Kiianitsa, K., Solinger, J. & Heyer, W. (2002). Rad54 protein exerts diverse modes of atpase activity on duplex dna partially and fully covered with rad51 protein, *J Biol Chem* **277**: 46205–46215.

Kiianitsa, K., Solinger, J. & Heyer, W. (2006). Terminal association of rad54 protein with the rad51-dsdna filament, *Proc Natl Acad Sci U S A* **103**: 9767–9772.

Koc, A., Wheeler, L., Mathews, C. & Merrill, G. (2004). Hydroxyurea arrests dna replication by a mechanism that preserves basal dntp pools, *J Biol Chem* **279**: 223–230.

Kolodner, R. & Marsischky, G. (1999). Eukaryotic dna mismatch repair, *Curr Opin Genet Dev* **9**: 89–96.

Kooistra, R., Hooykaas, P. & Steensma, H. (2004). Efficient gene targeting in kluyveromyces lactis, *Yeast* **21**: 781–792.

Kostriken, R., Strathern, J., Klar, A., Hicks, J. & Heffron, F. (1983). A site-specific endonuclease essential for mating-type switching in saccharomyces cerevisiae, *Cell* **35**: 167–174.

Krappmann, S., Sasse, C. & Braus, G. (2006). Gene targeting in aspergillus fumigatus by homologous recombination is facilitated in a nonhomologous end- joining-deficient genetic background, *Eukaryot Cell* **5**: 212–215.

Krejci, L., Damborsky, J., Thomsen, B., Duno, M. & Bendixen, C. (2001). Molecular dissection of interactions between rad51 and members of the recombination-repair group, *Mol Cell Biol* **21**: 966–976.

Krejci, L., Macris, M., Li, Y., Van Komen, S., Villemain, J., Ellenberger, T., Klein, H. & Sung, P. (2004). Role of atp hydrolysis in the antirecombinase function of saccharomyces cerevisiae srs2 protein, *J Biol Chem* **279**: 23193–23199.

Krejci, L., Song, B., Bussen, W., Rothstein, R., Mortensen, U. & Sung, P. (2002). Interaction with rad51 is indispensable for recombination mediator function of rad52, *J. Biol. Chem.* **277**: 40132–40141.

Krejci, L., Van, K., Li, Y., Villemain, J., Reddy, M., Klein, H., Ellenberger, T. & Sung, P. (2003). Dna helicase srs2 disrupts the rad51 presynaptic filament, *Nature* **423**: 305–309.

Krogh, B. & Symington, L. (2004). Recombination proteins in yeast, *Annu Rev Genet* **38**: 233–271.

Kumar, J. & Gupta, R. (2004). Strand exchange activity of human recombination protein rad52, *Proc Natl Acad Sci U S A* **101**: 9562–9567.

Kupiec, M. (2000). Damage-induced recombination in the yeast saccharomyces cerevisiae, *Mutat Res* **451**: 91–105.

Kupiec, M. & Petes, T. (1988). Allelic and ectopic recombination between ty elements in yeast, *Genetics* **119**: 549–559.

Lambert, S., Watson, A., Sheedy, D., Martin, B. & Carr, A. (2005). Gross chromosomal rearrangements and elevated recombination at an inducible site-specific replication fork barrier, *Cell* **121**: 689–702.

Langston, L. & Symington, L. (2004). Gene targeting in yeast is initiated by two independent strand invasions, *Proc Natl Acad Sci U S A* **101**: 15392–15397.

Lawrence, C. & Christensen, R. (1979). Metabolic suppressors of trimethoprim and ultraviolet light sensitivities of saccharomyces cerevisiae rad6 mutants, *J Bacteriol* **139**: 866–876.

Le, S., Moore, J., Haber, J. & Greider, C. (1999). Rad50 and rad51 define two pathways that collaborate to maintain telomeres in the absence of telomerase, *Genetics* **152**: 143–152.

Lea, D. & Coulson, C. (1949). The distribution in the numbers of mutants in bacterial populations, *J Genet* **49**: 264–285.

Lee, G., Neiditch, M., Salus, S. & Roth, D. (2004). Rag proteins shepherd double-strand breaks to a specific pathway, suppressing error-prone repair, but rag nicking initiates homologous recombination, *Cell* **117**: 171–184.

Lettier, G., Feng, Q., Antunez de Mayolo, A., Erdeniz, N., Reid, R., Lisby, M., Mortensen, U. & Rothstein, R. (2006). The role of dna double-strand breaks in spontaneous homologous recombination in s. cerevisiae, *PLoS Genet* **2**.

Leung, W., Malkova, A. & Haber, J. (1997). Gene targeting by linear duplex dna frequently occurs by assimilation of a single strand that is subject to preferential mismatch correction, *Proc Natl Acad Sci U S A* **94**: 6851–6856.

Lewis, L., Karthikeyan, G., Westmoreland, J. & Resnick, M. (2002). Differential suppression of dna repair deficiencies of yeast rad50, mre11 and xrs2 mutants by exo1 and tlc1 (the rna component of telomerase), *Genetics* **160**: 49–62.

Li, J., Read, L. & Baker, M. (2001). The mechanism of mammalian gene replacement is consistent with the formation of long regions of heteroduplex dna associated with two crossing-over events, *Mol Cell Biol* **21**: 501–510.

Lin, F., Sperle, K. & Sternberg, N. (1984). Model for homologous recombination during transfer of dna into mouse l cells: role for dna ends in the recombination process, *Mol Cell Biol* **4**: 1020–1034.

Lindahl, T. (1993). Instability and decay of the primary structure of dna, *Nature* **362**: 709–715.

Lindahl, T. & Nyberg, B. (1972). Rate of depurination of native deoxyribonucleic acid, *Biochemistry* **11**: 3610–3618.

Lisby, M., Barlow, J., Burgess, R. & Rothstein, R. (2004). Choreography of the dna damage response: spatiotemporal relationships among checkpoint and repair proteins, *Cell* **118**: 699–713.

Lisby, M., Rothstein, R. & Mortensen, U. (2001). Rad52 forms dna repair and recombination centers during s phase, *Proc. Natl. Acad. Sci. U. S.* **98**: 8276–8282.

Liu, J. & Marians, K. (1999). Pria-directed assembly of a primosome on d loop dna, *J Biol Chem* **274**: 25033–25041.

Liu, J., Xu, L., Sandler, S. & Marians, K. (1999). Replication fork assembly at recombination intermediates is required for bacterial growth, *Proc Natl Acad Sci U S A* **96**: 3552–3555.

Lloyd, J., McGrew, D. & Knight, K. (2005). Identification of residues important for dna binding in the full-length human rad52 protein, *J. Mol. Biol.* **345**: 239–249.

Lo, Y., Paffett, K., Amit, O., Clikeman, J., Sterk, R., Brenneman, M. & Nickoloff, J. (2006). Sgs1 regulates gene conversion tract lengths and crossovers independently of its helicase activity, *Mol Cell Biol* **26**: 4086–4094.

Lundin, C., Erixon, K., Arnaudeau, C., Schultz, N., Jenssen, D., Meuth, M. & Helleday, T. (2002). Different roles for nonhomologous end joining and homologous recombination following replication arrest in mammalian cells, *Mol Cell Biol* **22**: 5869–5878.

Lundin, C., North, M., Erixon, K., Walters, K., Jenssen, D., Goldman, A. & Helleday, T. (2005). Methyl methanesulfonate (mms) produces heat-labile dna damage but no detectable in vivo dna double-strand breaks, *Nucleic Acids Res* **33**: 3799–3811.

Ma, J., Kim, E., Haber, J. & Lee, S. (2003). Yeast mre11 and rad1 proteins define a ku-independent mechanism to repair double-strand breaks lacking overlapping end sequences, *Mol Cell Biol* **23**: 8820–8828.

Machida, M., Asai, K., Sano, M., Tanaka, T., Kumagai, T., Terai, G., Kusumoto, K., Arima, T., Akita, O., Kashiwagi, Y., Abe, K., Gomi, K., Horiuchi, H., Kitamoto, K. & Kobayashi, T. (2005). Genome sequencing and analysis of aspergillus oryzae, *Nature* **438**: 1157–1161.

Macris, M. & Sung, P. (2005). Multifaceted role of the saccharomyces cerevisiae srs2 helicase in homologous recombination regulation, *Biochem Soc Trans* **33**: 1447–1450.

Malkova, A., Ivanov, E. & Haber, J. (1996). Double-strand break repair in the absence of rad51 in yeast: a possible role for break-induced dna replication, *Proc. Natl. Acad. Sci. U. S.* **93**: 7131–7136.

Malkova, A., Signon, L., Schaefer, C., Naylor, M., Theis, J., Newlon, C. & Haber, J. (2001). Rad51-independent break-induced replication to repair a broken chromosome depends on a distant enhancer site, *Genes Dev.* **15**: 1055–1060.

Malone, R. & Esposito, R. (1980). The rad52 gene is required for homothallic interconversion of mating types and spontaneous mitotic recombination in yeast, *Proc Natl Acad Sci U S A* **77**: 503–507.

Malone, R., Montelone, B., Edwards, C., Carney, K. & Hoekstra, M. (1988). A reexamination of the role of the rad52 gene in spontaneous mitotic recombination, *Curr. Genet.* **14**: 211–223.

Martin, J., Winkelmann, N., Petalcorin, M., McIlwraith, M. & Boulton, S. (2005). Rad-51-dependent and -independent roles of a caenorhabditis elegans brca2-related protein during dna double-strand break repair, *Mol Cell Biol* **25**: 3127–3139.

Mazin, A., Alexeev, A. & Kowalczykowski, S. (2003). A novel function of rad54 protein. stabilization of the rad51 nucleoprotein filament, *J Biol Chem* **278**: 14029–14036.

Mazin, A., Zaitseva, E., Sung, P. & Kowalczykowski, S. (2000). Tailed duplex dna is the preferred substrate for rad51 protein-mediated homologous pairing, *EMBO J* **19**: 1148–1156.

McDonald, J., Levine, A. & Woodgate, R. (1997). The saccharomyces cerevisiae rad30 gene, a homologue of escherichia coli dinb and umuc, is dna damage inducible and functions in a novel error-free postreplication repair mechanism, *Genetics* **147**: 1557–1568.

McGlynn, P. & Lloyd, R. (2001). Rescue of stalled replication forks by recg: simultaneous translocation on the leading and lagging strand templates supports an active dna unwinding model of fork reversal and holliday junction formation, *Proc Natl Acad Sci U S A* **98**: 8227–8234.

McGlynn, P. & Lloyd, R. (2002). Recombinational repair and restart of damaged replication forks, *Nat. Rev. Mol. Cell Biol.* **3**: 859–870.

McVey, M., Radut, D. & Sekelsky, J. (2004). End-joining repair of double-strand breaks in drosophila melanogaster is largely dna ligase iv independent, *Genetics* **168**: 2067–2076.

Meselson, M. & Radding, C. (1975). A general model for genetic recombination, *Proc Natl Acad Sci U S A* **72**: 358–361.

Meyer, V., Arentshorst, M., El-Ghezal, A., Drews, A., Kooistra, R., van den Hondel, C. & Ram, A. (2007). Highly efficient gene targeting in the aspergillus niger kusa mutant, *J Biotechnol* .

Michel, B., Grompone, G., Flores, M. & Bidnenko, V. (2004). Multiple pathways process stalled replication forks, *Proc. Natl. Acad. Sci. U. S.* **101**: 12783–12788.

Milne, G., Ho, T. & Weaver, D. (1995). Modulation of saccharomyces cerevisiae dna double-strand break repair by srs2 and rad51, *Genetics* **139**: 1189–1199.

Milne, G. & Weaver, D. (1993). Dominant negative alleles of rad52 reveal a dna repair/recombination complex including rad51 and rad52, *Genes Dev* **7**: 1755–1765.

Miyazaki, T., Bressan, D., Shinohara, M., Haber, J. & Shinohara, A. (2004). In vivo assembly and disassembly of rad51 and rad52 complexes during double-strand break repair, *EMBO J.* **23**: 939–949.

Modrich, P. (2006). Mechanisms in eukaryotic mismatch repair, *J Biol Chem* **281**: 30305–30309.

Moreau, S., Morgan, E. & Symington, L. (2001). Overlapping functions of the saccharomyces cerevisiae mre11, exo1 and rad27 nucleases in dna metabolism, *Genetics* **159**: 1423–1433.

Morrow, D., Connelly, C. & Hieter, P. (1997). Break copy duplication: a model for chromosome fragment formation in saccharomyces cerevisiae, *Genetics* **147**: 371–382.

Mortensen, U., Bendixen, C., Sunjevaric, I. & Rothstein, R. (1996). Dna strand annealing is promoted by the yeast rad52 protein, *Proc. Natl. Acad. Sci. U. S.* **93**: 10729–10734.

Mortensen, U., Erdeniz, N., Feng, Q. & Rothstein, R. (2002). A molecular genetic dissection of the evolutionarily conserved n terminus of yeast rad52, *Genetics* **161**: 549–562.

Muris, D., Bezzubova, O., Buerstedde, J., Vreeken, K., Balajee, A., Osgood, C., Troelstra, C., Hoeijmakers, J., Ostermann, K. & Schmidt, H. (1994). Cloning of human and mouse genes homologous to rad52, a yeast gene involved in dna repair and recombination, *Mutat Res* **315**: 295–305.

Nassif, N., Penney, J., Pal, S., Engels, W. & Gloor, G. (1994). Efficient copying of nonhomologous sequences from ectopic sites via p-element-induced gap repair, *Mol Cell Biol* **14**: 1613–1625.

Natsume, T., Egusa, M., Kodama, M., Johnson, R., Itoh, T. & Itoh, Y. (2004). An appropriate increase in the transcription of aspergillus nidulans uvsc improved gene targeting efficiency, *Biosci. Biotechnol. Biochem.* **68**: 1649–1656.

Nayak, T., Szewczyk, E., Oakley, C., Osmani, A., Ukil, L., Murray, S., Hynes, M., Osmani, S. & Oakley, B. (2006). A versatile and efficient gene-targeting system for aspergillus nidulans, *Genetics* **172**: 1557–1566.

New, J., Sugiyama, T., Zaitseva, E. & Kowalczykowski, S. (1998). Rad52 protein stimulates dna strand exchange by rad51 and replication protein a, *Nature* **391**: 407–410.

Nielsen, M., Albertsen, L., Lettier, G., Nielsen, J. & Mortensen, U. (2006). Efficient pcr-based gene targeting with a recyclable marker for aspergillus nidulans, *Fungal Genet Biol* **43**: 54–64.

Nierman, W., May, G., Kim, H., Anderson, M., Chen, D. & Denning, D. (2005a). What the aspergillus genomes have told us, *Med Mycol* **43 Suppl 1**: S3–5.

Nierman, W., Pain, A., Anderson, M., Wortman, J., Kim, H., Arroyo, J., Berriman, M., Abe, K., Archer, D., Bermejo, C., Bennett, J., Bowyer, P., Chen, D., Collins, M. & Coulsen, R. (2005b). Genomic sequence of the pathogenic and allergenic filamentous fungus aspergillus fumigatus, *Nature* **438**: 1151–1156.

Ninomiya, Y., Suzuki, K., Ishii, C. & Inoue, H. (2004). Highly efficient gene replacements in neurospora strains deficient for nonhomologous end-joining, *Proc. Natl. Acad. Sci. U. S.* **101**: 12248–12253.

Nishinaka, T., Shinohara, A., Ito, Y., Yokoyama, S. & Shibata, T. (1998). Base pair switching by interconversion of sugar puckers in dna extended by proteins of reca-family: a model for homology search in homologous genetic recombination, *Proc Natl Acad Sci U S A* **95**: 11071–11076.

Nussenzweig, A., Chen, C., da Costa Soares, V., Sanchez, M., Sokol, K., Nussenzweig, M. & Li, G. (1996). Requirement for ku80 in growth and immunoglobulin v(d)j recombination, *Nature* **382**: 551–555.

Nussenzweig, A., Sokol, K., Burgman, P., Li, L. & Li, G. (1997). Hypersensitivity of ku80-deficient cell lines and mice to dna damage: the effects of ionizing radiation on growth, survival, and development, *Proc Natl Acad Sci U S A* **94**: 13588–13593.

Ogawa, T., Yu, X., Shinohara, A. & Egelman, E. (1993). Similarity of the yeast rad51 filament to the bacterial reca filament, *Science* **259**: 1896–1899.

O'Hara, E. & Timberlake, W. (1989). Molecular characterization of the aspergillus nidulans ya locus, *Genetics* **121**: 249–254.

Ostermann, K., Lorentz, A. & Schmidt, H. (1993). The fission yeast rad22 gene, having a function in mating-type switching and repair of dna damages, encodes a protein homolog to rad52 of saccharomyces cerevisiae, *Nucleic Acids Res* **21**: 5940–5944.

Ouyang, H., Nussenzweig, A., Kurimasa, A., Soares, V., Li, X., Cordon-Cardo, C., Li, W., Cheong, N., Nussenzweig, M., Iliakis, G., Chen, D. & Li, G. (1997). Ku70 is required for dna repair but not for t cell antigen receptor gene recombination in vivo, *J Exp Med* **186**: 921–929.

Ozenberger, B. & Roeder, G. (1991). A unique pathway of double-strand break repair operates in tandemly repeated genes, *Mol Cell Biol* **11**: 1222–1231.

Papouli, E., Chen, S., Davies, A., Huttner, D., Krejci, L., Sung, P. & Ulrich, H. (2005). Crosstalk between sumo and ubiquitin on pcna is mediated by recruitment of the helicase srs2p, *Mol Cell* **19**: 123–133.

Paques, F. & Haber, J. (1999). Multiple pathways of recombination induced by double-strand breaks in saccharomyces cerevisiae, *Microbiol. Mol. Biol. Rev.* **63**: 349–404.

Parekh-Olmedo, H., Ferrara, L., Brachman, E. & Kmiec, E. (2005). Gene therapy progress and prospects: targeted gene repair, *Gene Ther* **12**: 639–646.

Park, M., Ludwig, D., Stigger, E. & Lee, S. (1996). Physical interaction between human rad52 and rpa is required for homologous recombination in mammalian cells, *J Biol Chem* **271**: 18996–19000.

Paull, T. & Gellert, M. (1998). The 3' to 5' exonuclease activity of mre 11 facilitates repair of dna double-strand breaks, *Mol Cell* **1**: 969–979.

Pel, H., de Winde, J., Archer, D., Dyer, P., Hofmann, G., Schaap, P., Turner, G., de Vries, R., Albang, R., Albermann, K., Andersen, M., Bendtsen, J. & Benen, J. (2007). Genome sequencing and analysis of the versatile cell factory aspergillus niger cbs 513.88, *Nat Biotechnol* **25**: 221–231.

Petalcorin, M., Sandall, J., Wigley, D. & Boulton, S. (2006). Cebrc-2 stimulates d-loop formation by rad-51 and promotes dna single-strand annealing, *J Mol Biol* **361**: 231–242.

Petukhova, G., Stratton, S. & Sung, P. (1998). Catalysis of homologous dna pairing by yeast rad51 and rad54 proteins, *Nature* **393**: 91–94.

Petukhova, G., Stratton, S. & Sung, P. (1999a). Single strand dna binding and annealing activities in the yeast recombination factor rad59, *J Biol Chem* **274**: 33839–33842.

Petukhova, G., Sung, P. & Klein, H. (2000). Promotion of rad51-dependent d-loop formation by yeast recombination factor rdh54/tid1, *Genes Dev* **14**: 2206–2215.

Petukhova, G., Van Komen, S., Vergano, S., Klein, H. & Sung, P. (1999b). Yeast rad54 promotes rad51-dependent homologous dna pairing via atp hydrolysis-driven change in dna double helix conformation, *J Biol Chem* **274**: 29453–29462.

Pfander, B., Moldovan, G., Sacher, M., Hoege, C. & Jentsch, S. (2005). Sumo-modified pcna recruits srs2 to prevent recombination during s phase, *Nature* **436**: 428–433.

Pierce, A., Stark, J., Araujo, F., Moynahan, M., Berwick, M. & Jasin, M. (2001). Double-strand breaks and tumorigenesis, *Trends Cell Biol.* **11**: S52–S59.

Pinsince, J. & Griffith, J. (1992). Early stages in reca protein-catalyzed pairing. analysis of coaggregate formation and non-homologous dna contacts, *J Mol Biol* **228**: 409–420.

Plate, I. (2006). *Identification of novel functional domains of Rad52 in Saccharomyces cerevisiae*, PhD thesis, Technical University of Denmark.

Poggeler, S. (2002). Genomic evidence for mating abilities in the asexual pathogen aspergillus fumigatus, *Curr Genet* **42**: 153–160.

Poggeler, S. & Kuck, U. (2006). Highly efficient generation of signal transduction knockout mutants using a fungal strain deficient in the mammalian ku70 ortholog, *Gene* **378**: 1–10.

Pontecorvo, G., Roper, J., Hemmons, L., Macdonald, K. & Bufton, A. (1953). The genetics of aspergillus nidulans, *Adv Genet* **5**: 141–238.

Postow, L., Ullsperger, C., Keller, R., Bustamante, C., Vologodskii, A. & Cozzarelli, N. (2001). Positive torsional strain causes the formation of a four-way junction at replication forks, *J Biol Chem* **276**: 2790–2796.

Prakash, L. & Prakash, S. (1977). Isolation and characterization of mms-sensitive mutants of saccharomyces cerevisiae, *Genetics* **86**: 33–55.

Prakash, S., Johnson, R. & Prakash, L. (2005). Eukaryotic translesion synthesis dna polymerases: specificity of structure and function, *Annu Rev Biochem* **74**: 317–353.

Prakash, S. & Prakash, L. (2000). Nucleotide excision repair in yeast, *Mutat Res* **451**: 13–24.

Radding, C. (1982). Homologous pairing and strand exchange in genetic recombination, *Annu Rev Genet* **16**: 405–437.

Ralf, C., Hickson, I. & Wu, L. (2006). The bloom's syndrome helicase can promote the regression of a model replication fork, *J Biol Chem* **281**: 22839–22846.

Ranatunga, W., Jackson, D., Lloyd, J., Forget, A., Knight, K. & Borgstahl, G. (2001). Human rad52 exhibits two modes of self-association, *J. Biol. Chem.* **276**: 15876–15880.

Rao, B. & Radding, C. (1993). Homologous recognition promoted by reca protein via non-watson-crick bonds between identical dna strands, *Proc Natl Acad Sci U S A* **90**: 6646–6650.

Rattray, A. & Strathern, J. (2003). Error-prone dna polymerases: when making a mistake is the only way to get ahead, *Annu Rev Genet* **37**: 31–66.

Raynard, S., Bussen, W. & Sung, P. (2006). A double holliday junction dissolvasome comprising blm, topoisomerase iiialpha, and blap75, *J Biol Chem* **281**: 13861–13864.

Reddy, G., Golub, E. & Radding, C. (1997). Human rad52 protein promotes single-strand dna annealing followed by branch migration, *Mutat Res* **377**: 53–59.

Resnick, M. (1975). The repair of double-strand breaks in chromosomal dna of yeast, *Basic Life Sci* **5B**: 549–556.

Resnick, M. & Martin, P. (1976). The repair of double-strand breaks in the nuclear dna of saccharomyces cerevisiae and its genetic control, *Mol Gen Genet* **143**: 119–129.

Resnick, M., Nitiss, J., Edwards, C. & Malone, R. (1986). Meiosis can induce recombination in rad52 mutants of saccharomyces cerevisiae, *Genetics* **113**: 531–550.

Rijkers, T., Van Den Ouweland, J., Morolli, B., Rolink, A., Baarends, W., Van Sloun, P., Lohman, P. & Pastink, A. (1998). Targeted inactivation of mouse rad52 reduces homologous recombination but not resistance to ionizing radiation, *Mol Cell Biol* **18**: 6423–6429.

Roman, H. & Fabre, F. (1983). Gene conversion and associated reciprocal recombination are separable events in vegetative cells of saccharomyces cerevisiae, *Proc Natl Acad Sci U S A* **80**: 6912–6916.

Rong, L., Palladino, F., Aguilera, A. & Klein, H. (1991). The hyper-gene conversion hpr5-1 mutation of saccharomyces cerevisiae is an allele of the srs2/radh gene, *Genetics* **127**: 75–85.

Rothkamm, K. & Lobrich, M. (2003). Evidence for a lack of dna double-strand break repair in human cells exposed to very low x-ray doses, *Proc. Natl. Acad. Sci. U. S.* **100**: 5057–5062.

Rould, E., Muniyappa, K. & Radding, C. (1992). Unwinding of heterologous dna by reca protein during the search for homologous sequences, *J Mol Biol* **226**: 127–139.

Saeki, H., Siaud, N., Christ, N., Wiegant, W., van Buul, P., Han, M., Zdzienicka, M., Stark, J. & Jasin, M. (2006). Suppression of the dna repair defects of brca2-deficient cells with heterologous protein fusions, *Proc Natl Acad Sci U S A* **103**: 8768–8773.

Sagi, D., Tlusty, T. & Stavans, J. (2006). High fidelity of reca-catalyzed recombination: a watchdog of genetic diversity, *Nucleic Acids Res* **34**: 5021–5031.

Sakuraba, Y., Schroeder, A., Ishii, C. & Inoue, H. (2000). A neurospora double-strand-break repair gene, mus-11, encodes a rad52 homologue and is inducible by mutagens, *Mol. Gen. Genet.* **264**: 392–401.

Saleh-Gohari, N., Bryant, H., Schultz, N., Parker, K., Cassel, T. & Helleday, T. (2005). Spontaneous homologous recombination is induced by collapsed replication forks that are caused by endogenous dna single-strand breaks, *Mol Cell Biol* **25**: 7158–7169.

Saleh-Gohari, N. & Helleday, T. (2004). Conservative homologous recombination preferentially repairs dna double-strand breaks in the s phase of the cell cycle in human cells, *Nucleic Acids Res* **32**: 3683–3688.

Sancar, G. (2000). Enzymatic photoreactivation: 50 years and counting, *Mutat Res* **451**: 25–37.

Sauvageau, S., Stasiak, A., Banville, I., Ploquin, M., Stasiak, A. & Masson, J. (2005). Fission yeast rad51 and dmc1, two efficient dna recombinases forming helical nucleoprotein filaments, *Mol Cell Biol* **25**: 4377–4387.

Schiestl, R., Prakash, S. & Prakash, L. (1990). The srs2 suppressor of rad6 mutations of saccharomyces cerevisiae acts by channeling dna lesions into the rad52 dna repair pathway, *Genetics* **124**: 817–831.

Schild, D. (1995). Suppression of a new allele of the yeast rad52 gene by overexpression of rad51, mutations in srs2 and ccr4, or mating-type heterozygosity, *Genetics* **140**: 115–127.

Schwacha, A. & Kleckner, N. (1994). Identification of joint molecules that form frequently between homologs but rarely between sister chromatids during yeast meiosis, *Cell* **76**: 51–63.

Schwacha, A. & Kleckner, N. (1995). Identification of double holliday junctions as intermediates in meiotic recombination, *Cell* **83**: 783–791.

Schwacha, A. & Kleckner, N. (1997). Interhomolog bias during meiotic recombination: meiotic functions promote a highly differentiated interhomolog-only pathway, *Cell* **90**: 1123–1135.

Seong, K., Chae, S. & Kang, H. (1997). Cloning of an e. coli reca and yeast rad51 homolog, rada, an allele of the uvsc in aspergillus nidulans and its mutator effects, *Mol Cells* **7**: 284–289.

Shen, Z., Cloud, K., Chen, D. & Park, M. (1996a). Specific interactions between the human rad51 and rad52 proteins, *J Biol Chem* **271**: 148–152.

Shen, Z., Denison, K., Lobb, R., Gatewood, J. & Chen, D. (1995). The human and mouse homologs of the yeast rad52 gene: cdna cloning, sequence analysis, assignment to human chromosome 12p12.2-p13, and mrna expression in mouse tissues, *Genomics* **25**: 199–206.

Shen, Z., Peterson, S., Comeaux, J., Zastrow, D., Moyzis, R., Bradbury, E. & Chen, D. (1996b). Self-association of human rad52 protein, *Mutat Res* **364**: 81–89.

Sherman, F., Fink, G. & Hicks, J. (1989). *Methods in yeast genetics*, Cold Spring Harbor Laboratory Press.

Shibata, T., Cunningham, R., DasGupta, C. & Radding, C. (1979). Homologous pairing in genetic recombination: complexes of reca protein and dna, *Proc Natl Acad Sci U S A* **76**: 5100–5104.

Shibutani, S., Takeshita, M. & Grollman, A. (1991). Insertion of specific bases during dna synthesis past the oxidation-damaged base 8-oxodg, *Nature* **349**: 431–434.

Shin, D., Pellegrini, L., Daniels, D., Yelent, B., Craig, L., Bates, D., Yu, D., Shivji, M., Hitomi, C., Arvai, A., Volkmann, N., Tsuruta, H., Blundell, T., Venkitaraman, A. & Tainer, J. (2003). Full-length archaeal rad51 structure and mutants: mechanisms for rad51 assembly and control by brca2, *EMBO J* **22**: 4566–4576.

Shinohara, A., Ogawa, H. & Ogawa, T. (1992). Rad51 protein involved in repair and recombination in s. cerevisiae is a reca-like protein, *Cell* **69**: 457–470.

Shinohara, A. & Ogawa, T. (1998). Stimulation by rad52 of yeast rad51-mediated recombination, *Nature* **391**: 404–407.

Shinohara, A., Shinohara, M., Ohta, T., Matsuda, S. & Ogawa, T. (1998). Rad52 forms ring structures and co-operates with rpa in single-strand dna annealing, *Genes Cells* **3**: 145–156.

Siede, W., Friedl, A., Dianova, I., Eckardt-Schupp, F. & Friedberg, E. (1996). The saccharomyces cerevisiae ku autoantigen homologue affects radiosensitivity only in the absence of homologous recombination, *Genetics* **142**: 91–102.

Signon, L., Malkova, A., Naylor, M., Klein, H. & Haber, J. (2001). Genetic requirements for r, *Mol. Cell Biol.* **21**: 2048–2056.

Sigurdsson, S., Van Komen, S., Petukhova, G. & Sung, P. (2002). Homologous dna pairing by human recombination factors rad51 and rad54, *J Biol Chem* **277**: 42790–42794.

Sikorski, R. & Hieter, P. (1989). A system of shuttle vectors and yeast host strains designed for efficient manipulation of dna in saccharomyces cerevisiae, *Genetics* **122**: 19–27.

Singleton, M., Wentzell, L., Liu, Y., West, S. & Wigley, D. (2002). Structure of the single-strand annealing domain of human rad52 protein, *Proc. Natl. Acad. Sci. U. S.* **99**: 13492–13497.

Sinha, R. & Hader, D. (2002). Uv-induced dna damage and repair: a review, *Photochem Photobiol Sci* **1**: 225–236.

Slupphaug, G., Kavli, B. & Krokan, H. (2003). The interacting pathways for prevention and repair of oxidative dna damage, *Mutat Res* **531**: 231–251.

Smider, V., Rathmell, W., Lieber, M. & Chu, G. (1994). Restoration of x-ray resistance and v(d)j recombination in mutant cells by ku cdna, *Science* **266**: 288–291.

Smith, G. (2004). How homologous recombination is initiated: unexpected evidence for single-strand nicks from v(d)j site-specific recombination, *Cell* **117**: 146–148.

Smith, J. & Rothstein, R. (1995). A mutation in the gene encoding the saccharomyces cerevisiae single-stranded dna-binding protein rfa1 stimulates a rad52-independent pathway for direct-repeat recombination, *Mol. Cell Biol.* **15**: 1632–1641.

Smith, J. & Rothstein, R. (1999). An allele of rfa1 suppresses rad52-dependent double-strand break repair in saccharomyces cerevisiae, *Genetics* **151**: 447–458.

Sogo, J., Lopes, M. & Foiani, M. (2002). Fork reversal and ssdna accumulation at stalled replication forks owing to checkpoint defects, *Science* **297**: 599–602.

Solinger, J. & Heyer, W. (2001). Rad54 protein stimulates the postsynaptic phase of rad51 protein-mediated dna strand exchange, *Proc Natl Acad Sci U S A* **98**: 8447–8453.

Solinger, J., Kiianitsa, K. & Heyer, W. (2002). Rad54, a swi2/snf2-like recombinational repair protein, disassembles rad51:dsdna filaments, *Mol Cell* **10**: 1175–1188.

Solinger, J., Lutz, G., Sugiyama, T., Kowalczykowski, S. & Heyer, W. (2001). Rad54 protein stimulates heteroduplex dna formation in the synaptic phase of dna strand exchange via specific interactions with the presynaptic rad51 nucleoprotein filament, *J Mol Biol* **307**: 1207–1221.

Song, B. & Sung, P. (2000). Functional interactions among yeast rad51 recombinase, rad52 mediator, and replication protein a in dna strand exchange, *J Biol Chem* **275**: 15895–15904.

Spell, R. & Jinks-Robertson, S. (2003). Role of mismatch repair in the fidelity of rad51- and rad59-dependent recombination in saccharomyces cerevisiae, *Genetics* **165**: 1733–1744.

Stasiak, A., Larquet, E., Stasiak, A., Muller, S., Engel, A., Van Dyck, E., West, S. & Egelman, E. (2000). The human rad52 protein exists as a heptameric ring, *Curr Biol* **10**: 337–340.

Strathern, J., Klar, A., Hicks, J., Abraham, J., Ivy, J., Nasmyth, K. & McGill, C. (1982). Homothallic switching of yeast mating type cassettes is initiated by a double-stranded cut in the mat locus, *Cell* **31**: 183–192.

Sugawara, N. & Haber, J. (1992). Characterization of double-strand break-induced recombination: homology requirements and single-stranded dna formation, *Mol. Cell Biol.* **12**: 563–575.

Sugawara, N., Ira, G. & Haber, J. (2000). Dna length dependence of the single-strand annealing pathway and the role of saccharomyces cerevisiae rad59 in double-strand break repair, *Mol Cell Biol* **20**: 5300–5309.

Sugawara, N., Wang, X. & Haber, J. (2003). In vivo roles of rad52, rad54, and rad55 proteins in rad51-mediated recombination, *Mol.* **12**: 209–219.

Sugiyama, T., Kantake, N., Wu, Y. & Kowalczykowski, S. (2006). Rad52-mediated dna annealing after rad51-mediated dna strand exchange promotes second ssdna capture, *EMBO J* **25**: 5539–5548.

Sugiyama, T. & Kowalczykowski, S. (2002). Rad52 protein associates with replication protein a (rpa)-single-stranded dna to accelerate rad51-mediated displacement of rpa and presynaptic complex formation, *J Biol Chem* **277**: 31663–31672.

Sugiyama, T., New, J. & Kowalczykowski, S. (1998). Dna annealing by rad52 protein is stimulated by specific interaction with the complex of replication protein a and single-stranded dna, *Proc. Natl. Acad. Sci. U. S.* **95**: 6049–6054.

Sun, H., Treco, D. & Szostak, J. (1991). Extensive 3'-overhanging, single-stranded dna associated with the meiosis-specific double-strand breaks at the arg4 recombination initiation site, *Cell* **64**: 1155–1161.

Sung, P. (1994). Catalysis of atp-dependent homologous dna pairing and strand exchange by yeast rad51 protein, *Science* **265**: 1241–1243.

Sung, P. (1997a). Function of yeast rad52 protein as a mediator between replication protein a and the rad51 recombinase, *J Biol Chem* **272**: 28194–28197.

Sung, P. (1997b). Yeast rad55 and rad57 proteins form a heterodimer that functions with replication protein a to promote dna strand exchange by rad51 recombinase, *Genes Dev* **11**: 1111–1121.

Sung, P., Krejci, L., Van Komen, S. & Sehorn, M. (2003). Rad51 recombinase and recombination mediators, *J Biol Chem* **278**: 42729–42732.

Sung, P. & Robberson, D. (1995). Dna strand exchange mediated by a rad51-ssdna nucleoprotein filament with polarity opposite to that of reca, *Cell* **82**: 453–461.

Suto, K., Nagata, A., Murakami, H. & Okayama, H. (1999). A double-strand break repair component is essential for s phase completion in fission yeast cell cycling, *Mol Biol Cell* **10**: 3331–3343.

Symington, L. (2002). Role of rad52 epistasis group genes in homologous recombination and double-strand break repair, *Microbiol Mol Biol Rev* **66**: 630–70.

Szostak, J., Orr-Weaver, T., Rothstein, R. & Stahl, F. (1983). The double-strand-break repair model for recombination, *Cell* **33**: 25–35.

Takahashi, N. & Dawid, I. (2005). Characterization of zebrafish rad52 and replication protein a for oligonucleotide-mediated mutagenesis, *Nucleic Acids Res.* **33**: e120.

Takahashi, T., Masuda, T. & Koyama, Y. (2006). Enhanced gene targeting frequency in ku70 and ku80 disruption mutants of aspergillus sojae and aspergillus oryzae, *Mol Genet Genomics* **275**: 460–470.

Takata, M., Sasaki, M., Sonoda, E., Morrison, C., Hashimoto, M., Utsumi, H., Yamaguchi-Iwai, Y., Shinohara, A. & Takeda, S. (1998). Homologous recombination and non-homologous end-joining pathways of dna double-strand break repair have overlapping roles in the maintenance of chromosomal integrity in vertebrate cells, *EMBO J* **17**: 5497–5508.

Thomas, B. & Rothstein, R. (1989). Elevated recombination rates in transcriptionally active dna, *Cell* **56**: 619–630.

Timberlake, W. (1990). Molecular genetics of aspergillus development, *Annu Rev Genet* **24**: 5–36.

Timberlake, W. & Marshall, M. (1989). Genetic engineering of filamentous fungi, *Science* **244**: 1313–1317.

Trujillo, K. & Sung, P. (2001). Dna structure-specific nuclease activities in the saccharomyces cerevisiae rad50*mre11 complex, *J Biol Chem* **276**: 35458–35464.

Trujillo, K., Yuan, S., Lee, E. & Sung, P. (1998). Nuclease activities in a complex of human recombination and dna repair factors rad50, mre11, and p95, *J Biol Chem* **273**: 21447–21450.

Tsubouchi, H. & Ogawa, H. (1998). A novel mre11 mutation impairs processing of double-strand breaks of dna during both mitosis and meiosis, *Mol Cell Biol* **18**: 260–268.

Ulrich, H. (2005). The rad6 pathway: control of dna damage bypass and mutagenesis by ubiquitin and sumo, *Chembiochem* **6**: 1735–1743.

Usui, T., Ohta, T., Oshiumi, H., Tomizawa, J., Ogawa, H. & Ogawa, T. (1998). Complex formation and functional versatility of mre11 of budding yeast in recombination, *Cell* **95**: 705–716.

van den Bosch, M., Vreeken, K., Zonneveld, J., Brandsma, J., Lombaerts, M., Murray, J., Lohman, P. & Pastink, A. (2001). Characterization of rad52 homologs in the fission yeast schizosaccharomyces pombe, *Mutat Res* **461**: 311–323.

Van Dyck, E., Hajibagheri, N., Stasiak, A. & West, S. (1998). Visualisation of human rad52 protein and its complexes with hrad51 and dna, *J Mol Biol* **284**: 1027–1038.

Van Dyck, E., Stasiak, A., Stasiak, A. & West, S. (2001). Visualization of recombination intermediates produced by rad52-mediated single-strand annealing, *EMBO Rep* **2**: 905–909.

Van Heemst, D., Swart, K., Holub, E., R, v., Offenberg, H., Goosen, T., HW, v. & Heyting, C. (1997). Cloning, sequencing, disruption and phenotypic analysis of uvsc, an aspergillus nidulans homologue of yeast rad51, *Mol Gen Genet* **254**: 654–664.

Van Komen, S., Petukhova, G., Sigurdsson, S., Stratton, S. & Sung, P. (2000). Superhelicity-driven homologous dna pairing by yeast recombination factors rad51 and rad54, *Mol Cell* **6**: 563–572.

van Veelen, L., Essers, J., van de Rakt, M., Odijk, H., Pastink, A., Zdzienicka, M., Paulusma, C. & Kanaar, R. (2005). Ionizing radiation-induced foci formation of mammalian rad51 and rad54 depends on the rad51 paralogs, but not on rad52, *Mutat Res* **574**: 34–49.

Veaute, X., Jeusset, J., Soustelle, C., Kowalczykowski, S., Le Cam, E. & Fabre, F. (2003). The srs2 helicase prevents recombination by disrupting rad51 nucleoprotein filaments, *Nature* **423**: 309–312.

Voelkel-Meiman, K. & Roeder, G. (1990). Gene conversion tracts stimulated by hot1-promoted transcription are long and continuous, *Genetics* **126**: 851–867.

Walsh, C. & Xu, G. (2006). Cytosine methylation and dna repair, *Curr Top Microbiol Immunol* **301**: 283–315.

Wang, H., Perrault, A., Takeda, Y., Qin, W., Wang, H. & Iliakis, G. (2003). Biochemical evidence for ku-independent backup pathways of nhej, *Nucleic Acids Res* **31**: 5377–5388.

Ward, J. (2000). Complexity of damage produced by ionizing radiation, *Cold Spring Harb Symp Quant Biol* **65**: 377–382.

Weitzman, S., Turk, P., Milkowski, D. & Kozlowski, K. (1994). Free radical adducts induce alterations in dna cytosine methylation, *Proc Natl Acad Sci U S A* **91**: 1261–1264.

White, C. & Haber, J. (1990). Intermediates of recombination during mating type switching in saccharomyces cerevisiae, *EMBO J.* **9**: 663–673.

Wolner, B., Van, K., Sung, P. & Peterson, C. (2003). Recruitment of the recombinational repair machinery to a dna double-strand break in yeast, *Mol.* **12**: 221–232.

Wu, L. & Hickson, I. (2003). The bloom's syndrome helicase suppresses crossing over during homologous recombination, *Nature* **426**: 870–874.

Wu, Y., Siino, J., Sugiyama, T. & Kowalczykowski, S. (2006a). The dna binding preference of rad52 and rad59 proteins: implications for rad52 and rad59 protein function in homologous recombination, *J Biol Chem* **281**: 40001–40009.

Wu, Y., Sugiyama, T. & Kowalczykowski, S. (2006b). Dna annealing mediated by rad52 and rad59 proteins, *J Biol Chem* **281**: 15441–15449.

Xu, L. & Marians, K. (2003). Pria mediates dna replication pathway choice at recombination intermediates, *Mol Cell* **11**: 817–826.

Yamaguchi-Iwai, Y., Sonoda, E., Buerstedde, J., Bezzubova, O., Morrison, C., Takata, M., Shinohara, A. & Takeda, S. (1998). Homologous recombination, but not dna repair, is reduced in vertebrate cells deficient in rad52, *Mol Cell Biol* **18**: 6430–6435.

Yanez, R. & Porter, A. (1999). Gene targeting is enhanced in human cells overexpressing hrad51, *Gene Ther* **6**: 1282–1290.

Yanez, R. & Porter, A. (2002). Differential effects of rad52p overexpression on gene targeting and extrachromosomal homologous recombination in a human cell line, *Nucleic Acids Res* **30**: 740–748.

Yang, L., Ukil, L., Osmani, A., Nahm, F., Davies, J., CP, D., Dou, X., Perez-Balaguer, A. & Osmani, S. (2004). Rapid production of gene replacement constructs and generation of a green fluorescent protein-tagged centromeric marker in aspergillus nidulans, *Eukaryot Cell* **3**: 1359–1362.

Yang, S., Yu, X., Seitz, E., Kowalczykowski, S. & Egelman, E. (2001). Archaeal rada protein binds dna as both helical filaments and octameric rings, *J Mol Biol* **314**: 1077–1085.

Yang, W. (2003). Damage repair dna polymerases y, *Curr Opin Struct Biol* **13**: 23–30.

Yu, J., Hamari, Z., Han, K., Seo, J., Reyes-Dominguez, Y. & Scazzocchio, C. (2004). Double-joint pcr: a pcr-based molecular tool for gene manipulations in filamentous fungi, *Fungal. Genet. Biol.* **41**: 973–981.

Zarrin, M., Leeder, A. & Turner, G. (2005). A rapid method for promoter exchange in aspergillus nidulans using recombinant pcr, *Fungal Genet Biol* **42**: 1–8.

Zhang, X., Lee, K., Solinger, J., Kiianitsa, K. & Heyer, W. (2005). Gly-103 in the n-terminal domain of saccharomyces cerevisiae rad51 protein is critical for dna binding, *J Biol Chem* **280**: 26303–26311.

Zou, H. & Rothstein, R. (1997). Holliday junctions accumulate in replication mutants via a reca homolog-independent mechanism, *Cell* **90**: 87–96.